

Coagulation Factor XIII A: Clinical and Biological Significance in Epithelial Ovarian Cancer

Elmena Mohamed Osman Ahmed Elfaki

Submitted in accordance with the requirements for the degree of
Doctor of Philosophy

The University of Leeds
Faculty of Medicine and Health
School of Medicine
Leeds Institute of Medical Research at St James

July, 2021

The candidate confirms that the work submitted is her own, and that appropriate credit has been given within the thesis where reference has been made to the work of others.

This copy has been supplied on the understanding that it is copyright material and that no quotation from the thesis may be published without proper acknowledgement.

Assertion of moral rights:

The right of Elmena Elfaki to be identified as Author of this work has been asserted by her in accordance with the Copyright, Designs and Patents Act 1988.

© 2021 The University of Leeds and Elmena Elfaki

Acknowledgements

All praise to ALLAH, the Almighty, for providing me with the blessings, the strength and the opportunity to complete this PhD study.

I would like to express my grateful thanks to my supervisors: Dr Rashida Anwar, Dr Aruna Asipu, Professor Tim Perren and Professor Sir Alexander Markham for their time, guidance and support throughout this PhD project. I would like to acknowledge with great gratitude Dr. Rashida for her help, guidance, valuable advice and scientific remarks throughout my candidature. Thank you Rashida for your great supervision and mentorship, I am forever grateful. Thank you to Professor Tim for your support, clinical discussions, and continuous encouragement. Thank you to Dr Aruna for her encouragement and protein expertise.

I would like to acknowledge with great gratitude Professor Sir Alexander Markham, as this work could not have been completed without his funding of this project. Thank you Alex for your generosity.

I would like to acknowledge the women whose blood and tissue samples were used in this study - thank you.

Thank you to all my colleagues at level 9 WTBB, and the Anwar research group. It has been a pleasure to work with you all. Special thanks to Dr Kathryn Hutchinson and Dr Laura Rice.

I am greatly indebted to my devoted husband Salih, my wonderful parents, and my lovely children Mohamed, Yousra and Ahmed who have supported me throughout my journey.

Abstract

Epithelial ovarian cancer (EOC) is a heterogeneous group of malignant neoplasms that are usually detected at metastatic advance stages, leading to difficulty in its management. Abnormal hemostasis including hyper coagulation and increased fibrinolysis, as well as their clinical complications, are common in epithelial ovarian cancer. High levels of cross-linked fibrin degradation products (FDPs) have been found in epithelial ovarian cancer ascites. Coagulation factor XIIIa gene variants affect enzyme activity and properties of the cross-linked substrate structure.

In this PhD study, plasma FXIII activity, plasma levels of its A-subunit, selected *F13A1* genotypes, FXIIIa protein expression in tumour tissues, and plasma levels of stable FDP as determined by D-Dimer levels were concurrently explored for the first time in EOC (patients entered into the translational cohort of the ICON7 trial, n=91). The associations between these variables and EOC prognostic factors, survival outcome and the effect of treatment received were evaluated. High plasma FXIII activity was associated with EOC progression. Plasma FXIIIa levels was associated with serous high-grade disease. The haplotype 1951A_1954C, was significantly associated with low plasma FXIII activity. FXIIIa expression in tumour tissues was associated with the grade of disease.

The functional capability of FXIIIa protein variants was assessed on substrates important in EOC fibrinogen, fibronectin, vitronectin and collagen. The data showed that the FXIIIa V34L variant produced an increased level of FXIIIa specific activity on fibronectin, fibrinogen, and vitronectin compared to the wildtype. These substrates were then examined for their cross-linking ability by a range of FXIIIa variants. The highest level of FXIIIa substrate cross-linking was seen in fibronectin, followed by fibrinogen, vitronectin and the lowest cross-links were observed on collagen. As FXIIIa cross-links substrates involved in cell adhesion, FXIIIa-mediated cross-linking of fibrinogen, fibronectin, and vitronectin was explored and found to result in an increased EOC cell adhesion. The activated FXIIIa variants have significantly inhibited EOC cell migration in cross-linked matrices and in the growth medium. In conclusion, the data presented in this thesis suggest that FXIIIa may aid EOC development and dissemination.

Table of Contents

Acknowledgements	iii	
Abstract	iv	
Table of Contents	v	
List of Tables	xii	
List of Figures	xiv	
List of Abbreviations	xvi	
Chapter 1	Introduction	1
1.1	Ovarian cancer	1
1.1.1	Pathogenesis of EOC	1
1.1.2	Histological and molecular subtypes of EOC	4
1.1.3	Grading of EOC	8
1.1.4	TNM and FIGO staging	8
1.1.5	Diagnosis of ovarian cancer	10
1.1.6	Management of EOC	12
	1.1.6.1 Management of early (FIGO stage I-II) EOC	12
	1.1.6.2 Management of advanced (FIGO stage III-IV) EOC	13
	1.1.6.3 Management of recurrent EOC.....	17
	1.1.6.4 Management of BRCA1/2 mutations carriers	18
1.1.7	Ovarian tumour microenvironment	18
1.2	Cancer and coagulation.....	20
1.2.1	Coagulation complications in cancer	20
1.2.2	The effect of cancer in coagulation.....	20
1.2.3	Role of coagulation factors in cancer	21
1.3	Coagulation factor XIIIa.....	22
1.3.1	FXIIIa gene and polymorphisms	23
1.3.2	Structure of FXIII	24
1.3.3	Activation and function of FXIIIa	26
1.3.4	FXIIIa Substrates	28
	1.3.4.1 Fibrinogen.....	28
	1.3.4.2 Fibronectin	28
	1.3.4.3 Vitronectin.....	29
	1.3.4.4 Collagen-1	29
1.3.5	FXIIIa in different malignancies	30
	1.3.5.1 F13A1 gene polymorphisms in cancer	30
	1.3.5.2 Plasma FXIIIa levels in cancer	30

	1.3.5.3	FXIIIa activity in cancer	31
	1.3.5.4	FXIIIa expression in cancer tissues.....	31
	1.3.5.5	FXIIIa in OC.....	32
	1.4	Research project	35
Chapter 2		Materials and Methods.....	36
	2.1	Patients' samples	36
	2.1.1	ICON7 plasma samples.....	36
	2.1.2	ICON7 tissue microarrays	36
	2.2	Recombinant FXIIIa expression	36
	2.2.1	Expression vector	37
	2.3	DNA techniques.....	38
	2.3.1	Restriction endonuclease digestion.....	38
	2.3.2	Polymerase Chain Reaction (PCR).....	38
	2.3.3	Agarose gel electrophoresis	39
	2.3.4	Plasmid DNA quantification	40
	2.3.5	Transformation into E-Coli cells.....	40
	2.3.6	Plasmid DNA mini-preps	40
	2.3.7	Plasmid DNA maxi-prep	41
	2.3.8	Sanger sequencing.....	41
	2.3.9	Site-directed mutagenesis	41
	2.3.10	Generation of FXIIIa negative control construct.....	45
	2.4	Construction of AH22 yeast recombinant clones.....	48
	2.4.1	AH22 yeast strain growth curve.....	48
	2.4.2	Preparation and storage of AH22 competent cells	48
	2.4.3	Transformation of AH22 yeast strain	49
	2.4.3.1	Transformation of AH22 yeast strain by Lithium acetate (LiAc), PEG and SS carrier DNA	49
	2.5	Expression of F13A cDNA.....	50
	2.5.1	Growth pattern of AH22 recombinant cells.....	50
	2.5.2	Expression of recombinant FXIIIa protein	50
	2.5.3	Production of yeast cell lysates	51
	2.6	Generation of heterozygous model of FXIIIa V34L variant .	51
	2.7	Protein techniques.....	52
	2.7.1	Purification of recombinant FXIIIa protein variants	52
	2.7.2	De-salting of FXIIIa purified protein.....	53
	2.7.3	SDS-PAGE	53
	2.7.4	Western Blot.....	54
	2.7.5	Coomassie brilliant blue R-250 staining	54

2.7.6	Factor XIIIa activity assay	55
2.7.6.1	Protocol.....	55
2.7.6.2	Quantification.....	56
2.7.6.3	Validation	56
2.7.7	ELISA for recombinant FXIIIa	56
2.7.7.1	Protocol.....	56
2.7.7.2	Quantification.....	57
2.7.8	ELISA for plasma FXIII	58
2.7.8.1	Protocol.....	58
2.7.9	ELISA for plasma D-Dimer	59
2.8	Tissue culture techniques.....	60
2.8.1	Mammalian cell lines	60
2.8.2	Cell culture chemicals and reagents.....	60
2.8.3	Sub-culture of cell lines	60
2.8.4	Storage and resuscitation of cell lines	62
2.8.5	Cell lysate preparation from cell lines and protein quantification	62
2.8.6	MTT assay.....	63
2.8.6.1	MTT standard response curves for OVCA cell lines 63	
2.8.6.2	Determination of seeding density for growth experiments	64
2.8.7	EOC cell proliferation assay	65
2.8.8	Scratch wound assay	66
2.8.9	Cell adhesion assay	67
2.9	Genetic analysis techniques.....	67
2.9.1	Extraction of genomic deoxyribonucleic acid (gDNA).....	67
2.9.2	Isolation of ribonucleic acid (RNA)	68
2.9.3	Synthesis of complementary deoxyribonucleic acid (cDNA) 68	
2.9.4	Genotyping ovarian cancer cell lines for F13A1 SNPs.....	68
2.10	Immunofluorescence on cultured OVCA cells	70
2.11	Data analysis	71
2.11.1	Transformation efficiency	71
2.11.2	ICON7 clinical cohort and survival analysis.....	71
2.11.3	Cell biology work	71
2.11.4	Calculations of Linkage Disequilibrium (LD).....	72
Chapter 3	Coagulation Factor XIIIa in Epithelial Ovarian Cancer	73
3.1	Introduction.....	73

3.2	ICON7 prospective cohort	76
3.2.1	Characteristics of the ICON7 plasma cohort	76
3.3	Plasma FXIII	80
3.3.1	Plasma FXIII activity	80
3.3.2	Plasma FXIIIa levels	81
3.3.3	Correlation between plasma FXIII activity and plasma FXIIIa levels	81
3.3.4	Summary	81
3.4	Plasma D-Dimer levels	82
3.4.1	Correlation between plasma D-Dimer levels and plasma FXIII	83
3.4.2	Summary	83
3.5	<i>F13A1</i> genotypes	84
3.5.1	Hardy Weinberg Equilibrium for ICON7 <i>F13A1</i> genotypes	84
3.5.2	Comparison between allele frequencies in ICON7 patients and normal population	84
3.5.3	Linkage Disequilibrium	84
3.5.4	Summary	85
3.6	Plasma FXIII, plasma D-Dimer and <i>F13A1</i> genotypes	87
3.6.1	Plasma FXIII activity and <i>F13A1</i> genotypes	87
3.6.2	FXIIIa subunit levels and <i>F13A1</i> genotypes	87
3.6.3	Plasma D-Dimers levels and <i>F13A1</i> genotypes	88
3.6.4	Summary	88
3.7	Plasma FXIII, plasma D-Dimer levels, <i>F13A1</i> genotypes and EOC prognostic factors	94
3.7.1	FXIII activity	94
3.7.2	FXIIIa levels	94
3.7.3	D-Dimer levels	95
3.7.4	<i>F13A1</i> genotypes	95
3.7.5	Summary	95
3.8	FXIIIa tissue expression	100
3.8.1	Expression site	100
3.8.2	Plasma FXIIIa subunit	100
3.8.3	<i>F13A1</i> genotypes	100
3.8.4	FXIIIa tissue expression and EOC prognostic factors	101
3.8.5	101
3.8.6	Summary	101
3.9	Survival analysis	105

3.9.1	Univariate analysis	105
3.9.1.1	Overall Survival.....	105
3.9.1.2	Progression-Free Survival	106
3.9.1.3	Survival Post-Progression	106
3.9.2	Sub-group analysis.....	116
3.9.2.1	Treatment received.....	116
3.9.2.2	FIGO stage	116
3.9.2.3	Histology	116
3.9.2.4	Grade of disease	117
3.9.2.5	Risk of disease progression.....	117
3.9.3	Multivariate analysis	119
3.9.3.1	Overall Survival.....	119
3.9.3.2	Progression-Free survival.....	119
3.9.3.3	Survival Post-Progression	120
3.9.4	122
3.9.5	Summary	125
3.10	Key findings:	126
3.11	Discussion	127
3.11.1	Plasma FXIII activity and subunit A levels.....	127
3.11.2	Plasma D-Dimer	131
3.11.3	Prognostic factors.....	132
3.11.4	Tissue expression.....	134
3.11.5	Survival.....	135
Chapter 4	Influence of Recombinant FXIII A Variants on Epithelial Ovarian Cancer Cell Behaviour	138
4.1	Introduction.....	138
4.2	Construction of plasmids encoding the human FXIII A variants	140
4.2.1	Expression of recombinant FXIII A protein variants	140
4.2.2	Pooled yeast lysates.....	142
4.2.3	Purification of recombinant FXIII A variants	143
4.2.4	Stability of purified FXIII A variants on storage.....	146
4.2.5	Summary	146
4.3	Functional studies on recombinant FXIII A variants	147
4.3.1	Optimising yeast lysate dilution for FXIII A activity assays	147
4.3.2	Levels of FXIII A expression in pooled yeast lysates	148
4.3.3	Differences in cross-linking between FXIII A substrates .	149

4.3.4	Relative comparative assessment of FXIII A protein variants	152
4.3.5	Summary	155
4.4	Characterisation of ovarian cancer cell lines	156
4.4.1	Genotyping OVCA cell lines for F13A1 SNPs	156
4.4.2	FXIII A protein expression	157
4.4.3	Localisation of N-(γ -glutamyl)- ϵ -lysine isopeptide bond in OC cell lines in situ	159
4.4.4	Reverse Transcription- Polymerase Chain Reaction (RT-PCR)	161
4.4.5	Summary	161
4.5	Assessment of FXIII A variants on EOC cell behaviour	163
4.5.1	FXIII A-mediated cross-linked substrates significantly increase EOC cell adhesion	164
4.5.2	FXIII A purified protein variants affect EOC cell growth differentially	169
4.5.3	FXIII A variants have a differential effect on EOC cell migration	171
4.5.4	Summary	171
4.6	Key findings	174
4.7	Discussion	175
4.7.1	Production and purification of recombinant FXIII A protein	175
4.7.2	Variations in cross-linking of different substrates	176
4.7.3	Variations in cross-linking by different FXIII A variants ...	177
4.7.4	TG activity in OC cell lines	177
4.7.5	FXIII A-mediated cross-linked substrates and EOC cell adhesion	178
4.7.6	FXIII A variants and EOC cell proliferation	179
4.7.7	FXIII A variants and EOC cell migration	179
Chapter 5	General Discussion and Future Work	181
5.1	Summary of thesis results	181
5.2	Plasma FXIII activity may aid EOC dissemination	182
5.3	Plasma FXIII activity may influence the prognosis in advanced-stage EOC and response to therapy	182
5.4	<i>F13A1</i> genotypes are associated with plasma FXIII activity and differentially affect EOC prognosis	183
5.5	FXIII A levels in plasma and tumour tissues may be used as predictive biomarkers for high grade EOC	184
5.6	FXIII A variants demonstrate functional differences for substrates important in EOC microenvironment	185
5.7	FXIII A variants may influence EOC cell behaviour	186

5.8	Limitations and future work.....	186
5.8.1	ICON7 cohort.....	186
5.8.2	ICON7 tissue microarrays	187
5.8.3	EOC expression levels of FXIII A, fibrinogen, fibronectin, and vitronectin	188
5.8.4	Growth, migration and invasion experiments	189
5.9	Conclusions	191
	Appendix I Text Map of pYF13_PCS 650I_651Q.....	192
	Appendix II OVCA cell line authentication	200
	Appendix III Examples of the IHC for the different core types, staining intensity and positive and negative controls.....	202
	List of References	204

List of Tables

Table 1-1: TNM and FIGO staging systems of Ovarian, Fallopian tube, and Primary peritoneal carcinoma	9
Table 1-2: SNPs in <i>F13A1</i> coding region included in this thesis	23
Table 1-3: FXIIIA substrates	29
Table 1-4: Factor XIIIA in different malignancies	34
Table 2-1: Primer sequences used for <i>F13A1</i> and <i>TG2</i> exons amplification ..	39
Table 2-2: PCR Reaction Procedures.....	39
Table 2-3: Plasmid Constructs required for the project.....	42
Table 2-4: Primer sequences used for mutagenesis	43
Table 2-5: Sequences of primers used to amplify <i>F13A1</i> cDNAs.....	43
Table 2-6: Primers used for colony PCR	46
Table 2-7: Antibodies used in ELISA	59
Table 2-8: Mammalian cell lines	61
Table 2-9: Mammalian cell lines medium.....	61
Table 2-10: Primers used to amplify <i>F13A1</i> exons	68
Table 3-1: Characteristics of study subjects of the full ICON7 translational cohort and the study-cohort	79
Table 3-2: Test of correlation between plasma D-Dimer levels and plasma FXIII	83
Table 3-3: Normal <i>F13A1</i> polymorphisms at codons 34, 650 and 651	85
Table 3-4: Distribution of <i>F13A1</i> genotypes in ICON7 study-cohort.....	85
Table 3-5: Difference in allele frequencies between ICON7 study cohort and a European population	86
Table 3-6: Pairwise Linkage Disequilibrium for three <i>F13A1</i> loci	86
Table 3-7: Variations in plasma FXIII activity for <i>F13A1</i> polymorphisms	88
Table 3-8: Variations of FXIIIA levels for <i>F13A1</i> polymorphisms.....	89
Table 3-9: Results of one-way ANOVA for associations between <i>F13A1</i> SNPs, plasma FXIII and D-Dimer levels.....	89
Table 3-10: Results of Chi-squared test for association between the clinical variables in ICON7 study-cohort	96
Table 3-11: Results of one-way ANOVA for association between EOC prognostic factors, plasma FXIII and D-Dimer levels	97
Table 3-12: Results of Chi-squared test for association between <i>F13A1</i> genotypes and EOC prognostic factors	97
Table 3-13: Descriptive statistics for FXIIIA stained ICON7 TMAs	102
Table 3-14: Tests of correlation between FXIIIA tissue expression and plasma FXIIIA subunit levels in EOC ICON7 tissue microarrays	103
Table 3-15: Results of Chi-squared tests for association between FXIIIA positive stained ICON7 tissue microarrays and <i>F13A1</i> genotypes.....	103

Table 3-16: Results of one-way ANOVA tests for association between FXIIIa protein expression in EOC tumour types and EOC prognostic factors	104
Table 3-17: Univariate analysis of <i>F13A1</i> SNPs for OS	113
Table 3-18: Univariate analysis of <i>F13A1</i> SNPs for PFS	114
Table 3-19: Univariate analysis of <i>F13A1</i> SNPs for SPP	115
Table 3-20: Multivariate Cox Proportional Hazard Regression Model for OS	121
Table 3-21: Multivariate Cox Proportional Hazard Regression Model for PFS	122
Table 3-22: Multivariate Cox Proportional Hazard Regression Model for SPP	123
Table 4-1: Activity of purified FXIIIa variants stored at 4°C at different time intervals	146
Table 4-2: Yeast lysate dilution factor for FXIIIa activity assays	147
Table 4-3: Variations in cross-linking among FXIIIa substrates	151
Table 4-4: FXIIIa specific activity	153
Table 4-5: Summary of OVCA cells <i>F13A1</i> genotypes	157
Table 4-6: Summary of transglutaminase activity in OVCA cell line lysates and conditioned medium	158

List of Figures

Figure 1-1: Classification of malignant ovarian neoplasms	7
Figure 1-2: Pathway of care for detecting ovarian cancer	11
Figure 1-3: Gene, location of SNPs included in this study, mRNA, polypeptide and X-Ray structure of FXIIIa	25
Figure 1-4: Activation of FXIII	27
Figure 2-1: The original map of plasmid pYF13AH.....	37
Figure 2-2: Schematic representation of vector pYF13AH_PCS	38
Figure 2-3: Plasmid constructs sequence confirmation	44
Figure 2-4: Schematic representation of FXIIIa negative control vector	47
Figure 2-5: FXIIIa NC restriction mapping.....	47
Figure 2-6: MTT standard response curves	64
Figure 2-7: Mammalian cell lines growth curves	65
Figure 2-8: Genotypes of OVCA cell lines	69
Figure 3-1: FXIII activity in ICON7 plasma samples.....	80
Figure 3-2: FXIIIa subunit level in ICON7 plasma samples	81
Figure 3-3: D-Dimer levels in ICON7 plasma samples.....	82
Figure 3-4: 34L carriers demonstrate higher activity than the WT.....	90
Figure 3-5: 650I_651Q (⁶⁵⁰ ATT_ ⁶⁵¹ CAG) alleles demonstrate significantly lower activity.....	91
Figure 3-6: 651Q carriers show significantly lower activity.....	92
Figure 3-7: 650I carriers show significantly lower activity	93
Figure 3-8: Plasma FXIII activity is significantly lower in EOC stage IV than in stage III.....	98
Figure 3-9: Plasma FXIIIa levels is significantly lower in SerousHighGrade (Type II) EOC	98
Figure 3-10: Higher D-Dimer levels observed with increasing EOC stage.....	99
Figure 3-11: Level of staining of FXIIIa in ICON7 TMAs.....	102
Figure 3-12: FXIIIa expression in tumour tissue is significantly lower in poorly differentiated disease	104
Figure 3-13: Kaplan-Meier Curves for EOC Prognostic Factors For Overall Survival	107
Figure 3-14: Kaplan-Meier Curves for EOC Prognostic Factors and Progression-Free Survival	108
Figure 3-15: Kaplan-Meier Curves for EOC Prognostic Factors and Survival Post Progression	109
Figure 3-16: Kaplan-Meier Curves for Survival Intervals for Plasma XIII Activity and Plasma FXIIIa Levels.....	110
Figure 3-17: Kaplan-Meier Curves for Survival Intervals for Plasma D-Dimer Levels.....	111

Figure 3-18: Kaplan-Meier Curves for Survival Intervals for Treatment Received	112
Figure 3-19: Kaplan-Meier Curves for Plasma FXIII Activity and EOC Prognostic Factors for Survival Post Progression.....	118
Figure 3-20: Independent Prognostic Indicators for Survival Identified by Cox Proportional Hazard Models	124
Figure 4-1: Presence of recombinant FXIIIa variants in yeast lysates	141
Figure 4-2: Western Blot to confirm detection of FXIIIa protein on pooled yeast lysates.....	142
Figure 4-3: SDS-PAGE of purified recombinant FXIIIa variants.....	144
Figure 4-4: Western blot of purified FXIIIa variants	145
Figure 4-5: FXIIIa antigen concentration.....	148
Figure 4-6: FXIIIa substrates are being cross-linked differently by FXIIIa protein variants	151
Figure 4-7: Comparison of FXIIIa variants specific activity for FXIIIa substrates.....	154
Figure 4-8: <i>In-situ</i> localization of isopeptide bonds in OVCA cell lines	160
Figure 4-9: OVCA433 and SKOV3 do not express <i>F13A1</i> mRNA, nor FXIIIa protein.....	162
Figure 4-10: Cross-linked FXIIIa substrates significantly increase OVCA433 cell adhesion	165
Figure 4-11: Representative images of OVCA433 cells adhered to FXIIIa substrates.....	166
Figure 4-12: Cross-linked FXIIIa substrates significantly increase SKOV3 cell adhesion	167
Figure 4-13: Representative images of SKOV3 cells adhered to FXIIIa substrates.....	168
Figure 4-14: The presence of FXIIIa purified protein variants in the medium has a differential effect on EOC cell growth.....	170
Figure 4-15: Activated FXIIIa variants significantly reduced EOC cell migration in growth medium.....	172
Figure 4-16: Activated FXIIIa variants significantly reduced EOC cell migration in Matrigel.....	173

List of Abbreviations

~	Approximately
$\alpha_v\beta_3$	Alpha-v beta-3 integrin
β -hCG	Beta-human chorionic gonadotrophin
AFP	Alpha fetoprotein
ALL	Acute lymphoblastic leukaemia
AML	Acute myeloid leukaemia
AP	Activation peptide
APL	Acute promyelocytic leukaemia
ATCC	American Type Culture Collection
AUC	Area under the curve
BAPA	5-(Biotinamido) pentylamine
<i>BRCA1</i>	Breast cancer gene 1
<i>BRCA2</i>	Breast cancer gene 2
BSA	Bovine serum albumin
CA125	Cancer Antigen 125
CRUK	Cancer Research UK
CT	Computed tomography
CV	Coefficient of Variation
°C	Degrees Celsius
dH ₂ O	Deionised water
DIC	Disseminated intravascular coagulation
DM	Double mutant
DMSO	Dimethyl sulfoxide
DPBS	Dulbecco's Phosphate Buffered Saline
DSBs	Double-stranded breaks
DTT	1,4-Dithiothreitol
ECM	Extra Cellular Matrix
EDTA	Ethylenediaminetetraacetic acid
EOC	Epithelial Ovarian Cancer
<i>F13A1</i>	The gene for FXIIIA
FDPs	Fibrin degradation products
FFPE	Formalin-fixed paraffin-embedded
FIGO	International Federation of Gynecology and Obstetrics
FGN	Fibrinogen
FN	Fibronectin
FSH	Follicle stimulating hormone

FXIIIA	Coagulation factor XIII A subunit
Gln	Glutamine (Amino Acid)
Glu	Glutamic acid (Amino Acid)
HBOC	Hereditary breast and ovarian cancer
HGSC	High grade serous carcinoma
HNPCC	Hereditary non polyposis colorectal cancer
HRP	Horseradish peroxidase
Ht	Heterozygous
ICON7	International Collaboration on Ovarian Neoplasms 7
Ile	Isoleucine (Amino Acid)
IU	International Unit
KM	Kaplan-Meier
≤	Less than or equals to
LiAc	Lithium acetate
LB	Lennox Broth
LBA	Lennox Broth Agar
LGSC	Low grade serous carcinoma
LH	Luteinizing hormone
mcg	Microgram
MDT	Multidisciplinary team
μL	microliters
mL	millilitres
mg/m ²	milligram per square meter of body-surface area
mg/kg	milligram per kilogram of body weight
MMPs	Matrix metalloproteinases
MRI	Magnetic resonance imaging
NAC	Neoadjuvant chemotherapy
NCBI	National Centre for Biotechnology Information
NFDM	Non-fat dried milk
NHS	National Health Service
NIBSC	National Institute for Biological Standards and Control
NICE	National Institute for Health and Care Excellence
Ni-NTA	Nickel-Nitrilotriacetic acid
NP-40	Nonyl phenoxy polyethoxy ethanol
NSCLC	Non-small cell lung cancer
OC	Ovarian cancer
OS	Overall Survival

O/N	Overnight
OSCC	Oral Squamous Cell Carcinoma
OSE	Ovarian surface epithelium
PARP	Poly-ADP ribose polymerase
PCR	Polymerase Chain Reaction
PCOS	Polycystic ovary syndrome
PEG	Poly ethylene glycol
PET-CT	Positron emission tomography-computed tomography
PFS	Progression-Free Survival
PMSF	Phenylmethylsulphonylfluoride
PVDF	Polyvinylidene-difluoride
rFXIIIa	Recombinant FXIIIa protein
RIPA	Radio-Immunoprecipitation Assay
RPMI	Roswell Park Memorial Institute
RT-PCR	Reverse Transcriptase - Polymerase Chain Reaction
RT	Room temperature
SD	Standard deviation
SDS-PAGE	Sodium dodecyl sulphate polyacrylamide gel electrophoresis
SNP	Single nucleotide polymorphism
SPP	Survival post-progression
SSBs	Single-stranded breaks
STR	Short Tandem Repeats
TB	Terrific Broth
TBS	Tris buffered saline
TCGA	The Cancer Genome Atlas
TF	Tissue Factor
TG-2	Transglutaminase- 2
TG-3	Transglutaminase -3
TME	Tumour microenvironment
UTR	Untranslated region
Val	Valine (Amino Acid)
VEGF	Vascular endothelial growth factor
VEGFR-2	Vascular endothelial growth factor receptor-2
VTN	Vitronectin
VTE	Venous thromboembolism
WHO	World Health Organization
YPD	Yeast Extract – Peptone – Dextrose medium

Chapter 1 Introduction

1.1 Ovarian cancer

Ovarian cancer (OC) is a heterogeneous group of malignant neoplasms found in the ovary. OC is currently the seventh most common cancer in women worldwide, and the third most common gynaecological malignancy – after cervical and uterine. It has continued to be the most lethal of all the gynaecological malignancies for several reasons: firstly, early stages of the disease, with good prognosis, are asymptomatic. Secondly, recognised symptoms for later destructive stages, such as bloating, abdominal pain and loss of appetite are nonspecific; therefore, most women present at an advanced stage when the tumour has already spread outside the ovaries (Maringe et al., 2012). Thirdly, failure of standard chemotherapy and the development of recurrent chemoresistance disease reduce the chances of a successful therapeutic outcome. In 2018, an estimated 295,414 cases were newly diagnosed with OC, representing about 3.4% of all cancer cases in women globally, and 184,799 women died from the disease accounting for 4.4% of all cancer-related deaths among females (Ferlay et al., 2019). In the UK it is the sixth most common cancer in women after breast, colorectal, lung, cervical and uterine. The lifetime risk is about 2% in England and Wales and its incidence is rising (NICE clinical guideline 122, issued: April 2011), with 7,470 new cases between 2014 and 2016, and around 4,100 deaths in 2017 (CRUK).

1.1.1 Pathogenesis of EOC

The aetiology of epithelial OC (EOC) is unknown, although various risk factors are known to increase the likelihood of developing the condition, such as old age, post-menopausal status, increased Body-Mass Index (BMI), nulliparity and family history of the disease. Further investigations have revealed that inhibition of ovulation by pregnancy, breast feeding, and the use of hormonal contraceptive methods such as oral contraceptive pills reduce the OC risk (Whittmore et al., 1992, Cancer, 2008, Tsilidis et al., 2011, Havrilesky et al., 2013). Nevertheless, patients with polycystic ovary syndrome (PCOS), which is associated with reduced ovulation, have increased OC risk (Schildkraut et al., 1996, Gottschau et al., 2015). A thorough review detailing the epidemiology and risk factors in OC has recently become available (Momenimovahed et al., 2019).

While the bulk of OC cases are known to be sporadic, up to 20% reflecting high grade serous OC patients with *BRCA* mutations (George et al., 2017). Familial genetic

syndromes are mainly caused by germline mutations in cancer susceptibility genes. The Hereditary breast and ovarian cancer (HBOC) syndrome, caused by mutations in the *BRCA1* or *BRCA2* genes accounts for about 90% of cases, and the mismatch repair genes, associated with hereditary non-polyposis colorectal cancer (HNPCC); Lynch syndrome accounts for up to 10% of these cases (Russo et al., 2009). Compared to a 1–2% risk for women in general population, the lifetime risk of developing EOC in women with *BRCA1* mutations is 39–63%, and/or 17–27% with *BRCA2* mutations carriers (Petruccioli et al., 2016).

Traditionally, OC was thought to originate from the ovarian surface epithelium (OSE) as highlighted by the incessant ovulation theory, or the repeated rupture and repair of the OSE and the exposure to the oestrogen-rich environment during the process of ovulation leading to malignant transformation. It was assumed that, this repetition enhances epithelial proliferation for repair, the occurrence of DNA mutations, and the formation of ovarian inclusion cysts which subsequently invaginate through the OSE into the surrounding ovarian stroma, developing tumours. In addition, observations from comparative animal studies indicate that decreased ovulation is associated with a decrease in tumour formation (Fathalla, 1971).

During ovulation, normal, non-malignant fallopian tube epithelial cells may detach and insert on the OSE when the fimbriated end of the tube is in close proximity to the ovary, forming inclusion cysts. Following insertion and exposure to the ovarian microenvironment including hormones stimulate proliferation and differentiation, the cysts may then undergo metaplasia forming proliferative borderline tumours (with cystic appearance), and subsequently malignant transformation (Cho and Shih, 2009, Kurman and Shih, 2010).

Another theory proposed that the surge of gonadotrophic hormones (LH and FSH) during ovulation, which leads to an increased proliferation, ultimately transforms the entrapped epithelium into cancer (Cramer and Welch, 1983). The majority of risk factors conventionally linked to EOC (e.g. early menarche, late menopause, nulliparity, and lack of oral contraceptive use) support both theories, as they link OC development with increased lifetime ovulation. However, the main critique of these two theories is that the OSE as a monolayered squamous-to-cuboidal mesothelium does not resemble the serous, endometrioid, mucinous, clear cell or transitional cell histology. OSE differs from the other epithelium, as the ovaries originate from the urogenital ridge, whereas, the fallopian tubes, endometrium and the cervix are derived separately from the müllerian ducts. As an alternative theory, it was suggested that EOC starts from müllerian-originated tissue and not the mesothelium

(Kurman and Shih, 2010). While some EOCs may originate in the ovaries, given the convincing evidence that there was no precursor lesion identified from or in the ovaries, it is possible that some EOCs arise from the fallopian tubes and consequently metastasise to the ovary (Kurman and Shih, 2011, Karst and Drapkin, 2011).

There is realistic evidence which supports the theory that some cases of EOC develop from the fallopian tubes, as lesions of tubal intraepithelial carcinoma (TIC). Serous tubal intraepithelial carcinoma (STIC) have been discovered in tissues from high-risk women with a family history of OC, breast cancer, or *BRCA1* or *BRCA2* gene mutations, undergoing prophylactic risk-reducing surgery (salpingo-oophorectomies) (Leeper et al., 2002, Piek et al., 2003, Cass et al., 2005, Callahan et al., 2007, Erickson et al., 2013).

Gene expression analysis from EOC cases of different histology has revealed close correlation with normal fallopian tube epithelium patterns (Marquez et al., 2005, O'Shannessy et al., 2013). Another study has linked TIC and consequently STIC with OC, as they have found that these changes are present in around 70% of patients with sporadic OC, non-hereditary, and peritoneal high-grade serous carcinoma (HGSC) (Kindelberger et al., 2007).

Mutations of *TP53* and p53 protein are detected in high percentages of STICs and HGSCs lesions (Soussi et al., 2006, Zhang et al., 2016). In addition, the *TP53* mutations in STICs lesions were found to be identical in around 93% of metastatic EOC patients, indicating that the paired lesions are likely to initiate from the same clone (Kuhn et al., 2012). This finding supports the assumption that TIC/STICs lesions within the fallopian tube epithelium are considered to be a precursor lesion for the HGSC subtype of EOC; as malignant cells from these lesions at the fimbriated end of the fallopian tube may drop and embed on the OSE during the ovulation, and progress to form HGSCs. Nevertheless, TIC/STIC lesions are not found in every single HGSC case (Erickson et al., 2013), nor in mucinous or endometrioid EOC subtypes (Lee et al., 2006, Przybycin et al., 2010). Therefore, the cell of origin of HGSC remains to be identified.

Low-grade serous carcinoma (LGSC) is assumed to arise from serous cystadenoma or adenofibroma and progress to an atypical proliferative serous tumour (APST). APSTs are typical serous borderline tumours, which subsequently progress to non-invasive micropapillary serous borderline tumours (MPSCs), and then invasive MPSCs in a gradual stepwise pattern. After an MPSC becomes invasive, it is classified as an LGSC (Vang et al., 2009).

Clear cell and endometrioid carcinomas are highly associated with endometriosis (Kaku et al., 2003), and considered to develop from endometriotic cysts, which are believed to be the consequence of endometrial tissue implanted on the ovaries. Therefore, endometriosis is a recognised risk factor for EOC (Schottenfeld and Fraumeni Jr, 2006).

The precursor lesions of transitional cell tumours (Brenner) and mucinous tumours are not ascertained. It has been suggested that these tumours may arise from transitional cell nests detected in paraovarian locations, in the transitional epithelium between the peritoneum and the fallopian tube (Walthard nests). Additionally, It is assumed that transitional cell and mucinous tumours share the same molecular pathway of carcinogenesis (Kurman and Shih, 2010).

Increased pro-inflammatory mediators, for instance, cytokines, reactive oxygen intermediates and prostaglandins have been reported to be associated with OC proliferation, invasion and progression (Sethi et al., 2012). They have also been considered to influence genetic and epigenetic changes and consequently lead to OC development. The role of inflammation and inflammatory molecules in OC development, progression and chemoresistance has been thoroughly reviewed (Savant et al., 2018). In addition, a full review of OC development, progression and cellular origin has been published (Cardenas et al., 2016).

1.1.2 Histological and molecular subtypes of EOC

The histological classification of OC is complex, with a large number of subtypes. It depends on the histogenesis of the normal ovary, which groups OCs according to their cell of origin into three main categories: epithelial ovarian cancer (EOC), originates from coelomic epithelial cells (cells covering the ovarian surface); stromal tumours originate from mesenchyme (the stroma and the sex cord); and germ cell tumours originate in the germ cells.

EOC represents the vast majority of malignant ovarian tumours accounting for approximately 90% of cases, and it is the main focus of this thesis. Each of the other non-epithelial types account for 5% of ovarian malignancies, and as they are outside the scope of this thesis, they will not be discussed. Detailed information about these uncommon subtypes has been published (Foulkes et al., 2016, Ray-Coquard et al., 2018).

Primary peritoneal carcinoma and primary fallopian tube carcinoma are both classified and treated similarly to EOC (Prat and Oncology, 2014).

EOC comprises a heterogeneous group of neoplasms with different morphology and biological behaviour. Serous neoplasms are the most common subtype of EOC. Other histological subtypes consist of: mucinous, squamous, endometrioid, clear cell, transitional cell tumours (Brenner tumours), carcinosarcoma, mixed epithelial tumours, undifferentiated carcinomas, and others. Recent studies have supported more subdivisions of EOC into distinct groups, depending on a combination of histopathological, morphological, immunohistochemical and molecular characteristics (McCluggage, 2011). Each subtype has unique, underlying molecular mechanisms that have an effect on response to chemotherapy, pattern of metastasis, prognosis and chances of survival (Kurman and Shih, 2011, Banerjee and Kaye, 2013).

EOC has been further sub-divided into two groups (type I and type II) according to the carcinogenesis pathways suggested by Shih and Kurman (2004). Type I originates from borderline tumours, presents at an early stage, is genetically stable, has a better prognosis, and includes: LGSC, mucinous, endometrioid, malignant Brenner tumours, and clear cell carcinomas. Type II presents at advanced stages, has a poorer prognosis, is genetically unstable, and its development is not clearly understood, hence it was named '*de novo*' and includes: HGSC, malignant mixed mesodermal tumours (carcinosarcoma) and undifferentiated carcinoma.

LGSC and HGSC are distinct entities, and progression from LGSC to HGSC is rare (Kurman and Shih, 2016). Type I and type II molecular characteristics differ substantially. *BRAF*, *KRAS*, *PTEN*, β -catenin, TGF- β RII mutations are mainly seen in type I, whereas, mutations of *TP53*, overexpression of *HER2/neu* gene, *AKT2* gene, and inactivation of *p16* gene are identified in type II (Figure 1-1). *BRAF* and *KRAS* oncogenes are altered in EOC. They are involved in cell signalling, cell growth, cell maturation and apoptosis. Mutations in these genes give rise to the increased growth and spread of cancer cells.

The recent advances in molecular biology techniques – especially gene expression profiling – has facilitated further sub-division of EOC into distinctive groups according to the specific molecular alterations discovered. A total of six molecular subtypes

were identified in a study conducted on 285 serous and endometrioid EOCs, primary peritoneal and fallopian tube invasive cancers and linked to clinical outcome. Two of these molecular subtypes are low-grade tumours, tumours with low malignant potential, and early-stage endometrioid EOC; four of the subtypes represent high-grade tumours (Tothill et al., 2008).

The project of The Cancer Genome Atlas (TCGA) analysed 489 HGSC cases and showed that *TP53* mutations were present in 96% of the cohort; in addition, the project confirmed the existence of the four HGSC molecular subtypes identified by Tothill et al. (2008) and named them: 'proliferative', 'mesenchymal', 'immunoreactive', and 'differentiated', according to their gene content (Network, 2011). The catalogue of TCGA was used to develop a prognostic model to estimate the effect on survival by combination of molecular subtype and survival gene expression signatures termed: 'Classification of Ovarian Cancer' (CLOVAR) (Verhaak et al., 2012).

Konecny et al. (2014) confirmed the presence of the four HGSC molecular subtypes previously described by TCGA and others (Tothill et al., 2008) on 174 HGSCs. Furthermore, they established that the immunoreactive subtype is associated with the longest survival, whereas the mesenchymal presented the shortest survival.

Wang C. et al. (2017), in a pooled cohort of over 2,100 patients, confirmed the four subtypes classified by TCGA and, in addition, identified a new subtype – 'anti-mesenchymal' – which originated from the differentiated subtype as a result of downregulation of mesenchymal signature genes. These five subtypes were found to be significantly associated with the size of the residual tumour following debulking surgery, as well as overall survival.

Despite accumulating information about molecular subtypes of HGSCs, they have not so far been implemented into routine clinical practice. Platinum-refractory HGSCs have not been accurately identified using the current molecular subtype prognostic signatures (Wang C. et al., 2017). However, gene expression signatures may have a future role in deciding which HGSC patients would be most suitable to receive neoadjuvant therapy. This target could be achieved by performing more research to assess the influence of these subtypes on therapeutic response, and subsequently validation of which molecular subtype could be suitable to exclude or select patients for specified treatment.

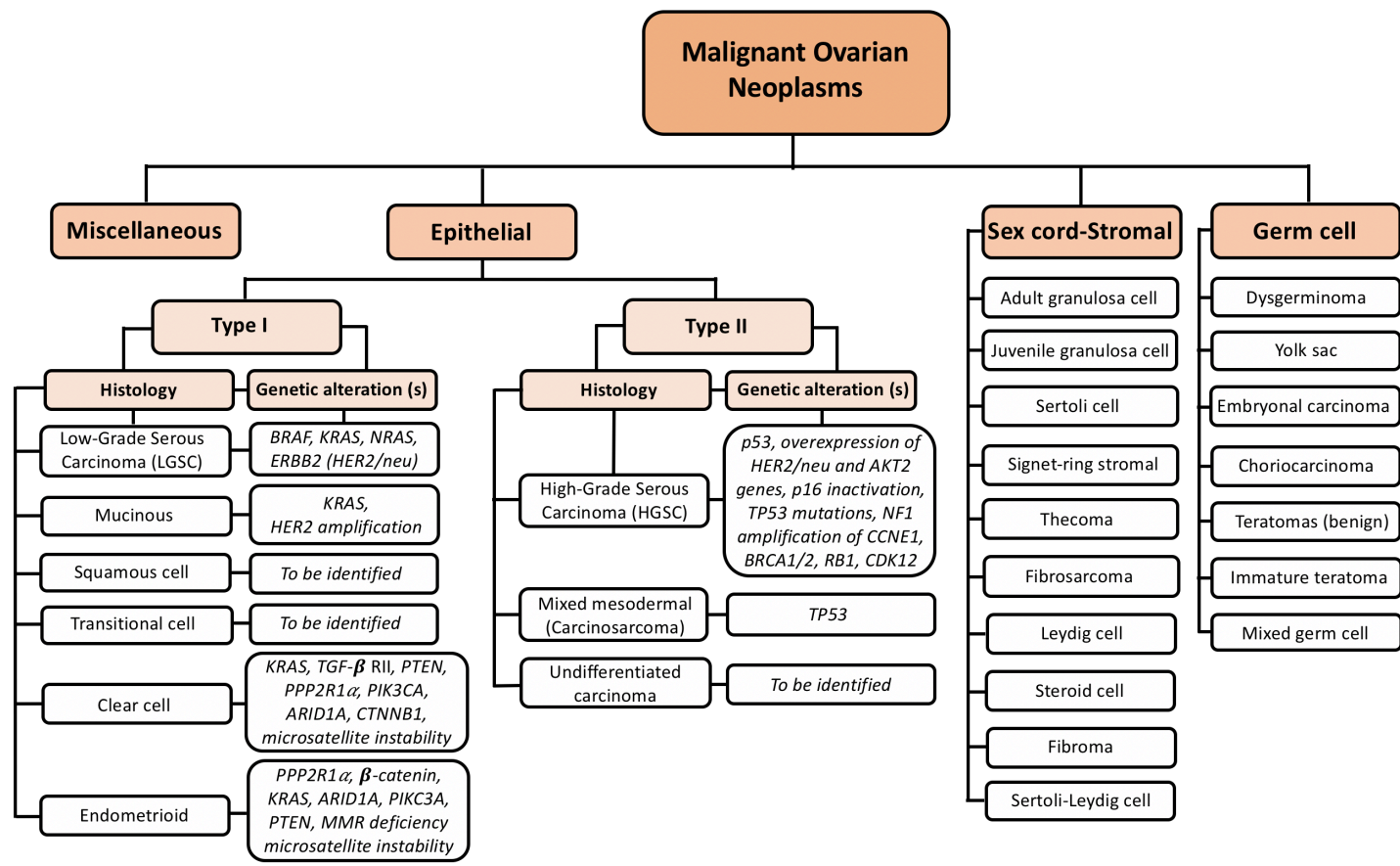


Figure 1-1: Classification of malignant ovarian neoplasms

The histological subtypes of the ovary, adapted from the 2020 WHO Classification of Tumours, *Female Genital Tumours*, 5th Edition, available online from: <https://tumourclassification.iarc.who.int/>. This figure also includes molecular characteristics of EOC subtypes summarised from tables produced by Shih and Kurman (2004) and Banerjee and Kaye (2013).

1.1.3 Grading of EOC

There are several universal grading systems available which describe tumours according to the degree of differentiation. Tumour grade is an important prognostic indicator of tumour progression and outcome, as higher grade cancers are poorly differentiated and have worse prognosis than well-differentiated cancers. The most frequently used systems are those defined by the International Federation of Gynaecology and Obstetrics (Prat and Oncology), which grades tumours according to architectural criteria. The World Health Organization (WHO), uses both architectural and cytological characteristics; and the Gynaecologic and Obstetrics Group (GOG), classifies different tumour grades based on histology (Cho and Shih, 2009). Current clinical practice in the UK recommends employing various grading systems according to histological subtype. In addition, the preliminary biopsies before chemotherapy should be used for grading tumours to avoid possible morphological changes induced by this treatment (Wilkinson et al., 2019). Serous carcinomas as two unique entities – HGSC and LGSC – are graded using a two-tier system. Endometrioid carcinoma is graded based on the International Federation of Gynecology and Obstetrics (FIGO) grading system, whereas, clear cell carcinoma, undifferentiated carcinoma and carcinosarcoma are considered as high grade (Wilkinson et al., 2019).

1.1.4 TNM and FIGO staging

FIGO staging criteria are based primarily on findings observed during surgical exploration. The staging rules are applicable to malignant ovarian tumours including neoplasms of low malignant potential, or borderline malignancy, fallopian tube and primary peritoneal carcinoma (Berek et al., 2018). The TNM staging system is based on clinical and/or pathological classification. Tumours are categorised based on the clinical assessment of the primary tumour (T), involvement of regional lymph nodes (N), and the occurrence or absence of distant metastasis (M). Clinical examination for TNM staging can be achieved through physical examination, imaging modalities and surgical exploration (laparoscopy/laparotomy), while pathological categorisation is determined via microscopic examination of the tumour. A summary of FIGO staging and the corresponding TNM classifications is presented in Table 1-1.

Table 1-1: TNM and FIGO staging systems of ovarian, fallopian tube, and primary peritoneal carcinoma

T	N	M	FIGO	Classification
Tx	N0	M0		Primary tumour cannot be assessed
T0	N0	M0		No evidence of primary tumour
T1	N0	M0	I	Tumour limited to the ovaries (one or both) or fallopian tube(s)
T1a	N0	M0	IA	Tumour limited to one ovary or fallopian tube; capsule intact, no tumour on ovarian surface or fallopian tube surface; no malignant cells in ascites or peritoneal washings
T1b	N0	M0	IB	Tumour limited to both ovaries or fallopian tubes; capsule intact, no tumour on ovarian surface or fallopian tube surface; no malignant cells in ascites or peritoneal washings
T1c	N0	M0	IC	Tumour limited to one or both ovaries or fallopian tubes with any of the following subcategories (IC1-3) below:
T1c1	N0	M0	IC1	Surgical spill
T1c1	N0	M0	IC2	Capsule rupture before surgery or tumour on ovarian or fallopian tube surface
T1c3	N0	M0	IC3	Malignant cells in ascites or peritoneal washings
T2	N0	M0	II	Tumour involves one or both ovaries or fallopian tubes with pelvic extension (below the pelvic brim) or primary peritoneal cancer
T2a	N0	M0	IIA	Extension and/or implants on uterus and/or fallopian tube(s) and/or ovar(ies)
T2b	N0	M0	IIB	Extension and/or implants to other pelvic tissue
T3	And/or N1	M0	III	Tumour involves one or both ovaries or fallopian tubes with microscopically confirmed peritoneal metastasis outside the pelvis and/or retroperitoneal LNs involvement; liver capsule involvement
T3	N1	M0	IIIA1	Positive (histologically confirmed) retroperitoneal LNs
T3	N1a	M0	IIIA1i	LN metastasis ≤ 10 mm in greatest dimension
T3	N1b	M0	IIIA1ii	LN metastasis > 10 mm in greatest dimension
T3a	N0/N1	M0	IIIA2	Microscopic peritoneal metastasis beyond the pelvis with or without positive retroperitoneal LNs
T3b	N0/N1	M0	IIIB	Macroscopic peritoneal metastasis beyond the pelvis ≤ 2 cm in greatest dimension with or without positive retroperitoneal LNs
T3c	N0/N1	M0	IIIC	Macroscopic peritoneal metastasis beyond the pelvis > 2 cm in greatest dimension including extension to liver capsule or spleen without parenchymal involvement of those organs and with or without positive retroperitoneal LNs
Any T	Any N	M1	IV	Distant metastasis excluding peritoneal metastasis and including liver or splenic parenchymal involvement
Any T	Any N	M1a	IVA	Pleural effusion with positive cytology
Any T	Any N	M1b	IVB	Parenchymal metastasis and metastasis to extra abdominal organs (including inguinal LNs and LNs outside the abdominal cavity); transmural involvement of intestine

This table presents information published in the 2017 TNM classification of malignant tumours, eighth edition [295,2790], in association with the Union for International Cancer Control © 2017(UICC) (Brierley et al., 2017). This table also includes combined FIGO staging of ovarian, fallopian tube, primary peritoneal cancers revised in 2014 (Berek et al., 2018). N0= no regional LN involvement; M0= no distant metastasis.

1.1.5 Diagnosis of ovarian cancer

Bloating, early satiety, loss of appetite, changes in bowel habit, urinary urgency and/or frequency, and pelvic or abdominal pain are the most common presenting symptoms of OC. The initial key assessment tests include serum CA125 and ultrasound scan, and in combination with menopausal status, the risk of malignancy index (RMI) is calculated (Jacobs et al., 1990) (Figure 1-2). OC is highly suspected if RMI is greater than 250 (NICE., 2011). In women under 40, besides CA125, other tumour markers frequently measured include levels of alpha fetoprotein (AFP) and beta-human chorionic gonadotrophin (β -hCG) to exclude or detect ovarian germ cell tumours or sex cord-stromal tumours. Other investigations include: computed tomography (CT) of the abdomen, pelvis and thorax, magnetic resonance imaging (MRI) and positron emission tomography-computed tomography (PET-CT) for early staging, detection of recurrence, or precise surgical management planning, and follow-up (Qayyum et al., 2005, Lenhard et al., 2008, Iyer and Lee, 2010).

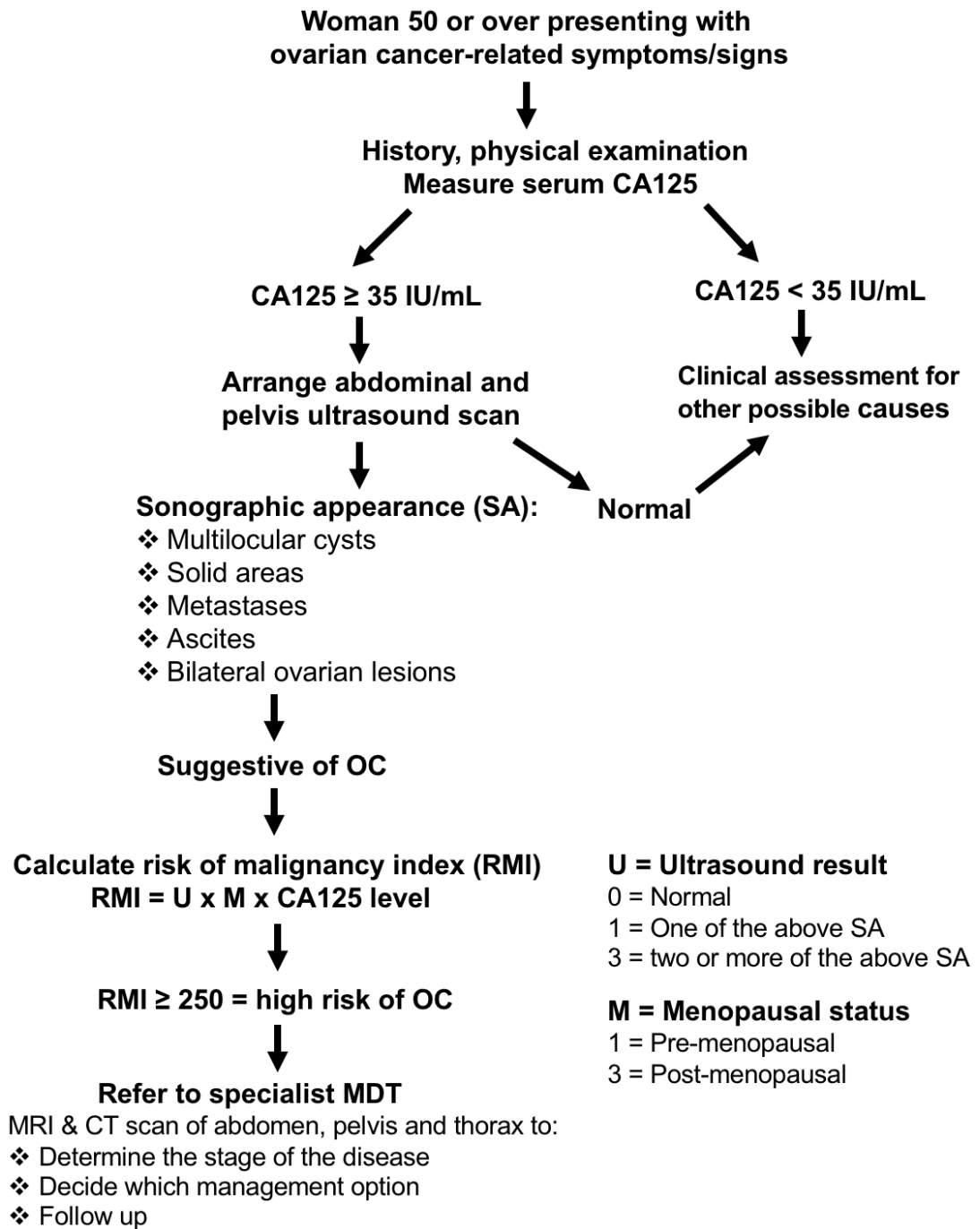


Figure 1-2: Pathway of care for detecting ovarian cancer

This flowchart presents the pathway of care for women with symptoms and/or signs suggestive of OC as detailed in NICE guideline (NICE., 2011). The risk of malignancy index (Eckert et al.) is calculated by multiplying the value of CA125 by ultrasound score by the menopausal status. All women with an RMI > 250 are referred to specialist multidisciplinary team (MDT) for further management.

1.1.6 Management of EOC

Several studies have established that care for women with EOC by a multidisciplinary team with a gynaecologic oncologist on-site at specialised institutions is associated with improved survival compared to general hospitals (Fotopoulou et al., 2017, Minig et al., 2017).

1.1.6.1 Management of early (FIGO stage I-II) EOC

Initial surgical treatment for women with suspected EOC confined to the ovaries includes total abdominal hysterectomy, bilateral salpingo-oophorectomy, infracolic omentectomy and biopsies from the following regions: pelvic and para-aortic LNs, ascites if found, cytologic brushing/washings of the diaphragm, both paracolic gutters, and abdominal and pelvic peritoneum. Appendectomy may be performed in women with mucinous subtype or right-sided OC (Timofeev et al., 2010). Patients with disease limited to one ovary may wish to undergo fertility-sparing surgery by removing the affected ovary and the ipsilateral fallopian tube with preservation of the uterus and contralateral ovary (Park et al., 2008).

Adjuvant chemotherapy may not be required as part of the initial management in women with early-stage OC (grade 1 and 2, FIGO stage IA and IB) who underwent optimal cytoreduction surgery. Nevertheless, adjuvant chemotherapy, comprising six cycles of carboplatin, is considered in women with high-risk stage I OC (grade 3, FIGO stage IC) (NICE., 2011). Furthermore, two randomised prospective clinical trials the (Adjuvant ChemoTherapy In Ovarian Neoplasm (ACTION) and International Collaborative Ovarian Neoplasm trial 1 [ICON1] have evaluated the use of platinum-based adjuvant chemotherapy (PBAC) following surgery in women with early-stage OC (grade 2 and 3 stage IA and IB; and all stage IC and IIA). Initial analysis was performed at a median follow-up of four years, and demonstrated that this treatment significantly improved the recurrent-free survival (RFS) and overall survival (OS) (Trimbos et al., 2003, Colombo et al., 2003). A Cochrane meta-analysis of five clinical trials including ACTION and ICON1, has established the effectiveness of post-operative PBAC in patients with early-stage OC (FIGO stage I/IIA), however, subgroup analysis showed that it may be withheld depending on grade and histological subtype (encapsulated unilateral grade 1 stage IA, stage IB, and well/moderately differentiated grade 1/2 OC) (Winter-Roach et al., 2009, Winter-Roach et al., 2012). An updated analysis on the review first published in the Cochrane database in 2009, which took into account mature data (10 years follow-up from ICON1), confirmed that

PBAC improved OS in FIGO stage I/IIA cases, but there was not sufficient evidence to ascertain the beneficial effect of this treatment in women with low/intermediate risk of early-stage OC. Therefore, consideration of this treatment for this group should be tailored to their individual circumstances (Lawrie et al., 2015).

1.1.6.2 Management of advanced (FIGO stage III-IV) EOC

The standard first-line chemotherapy for women with EOC is based around platinum drugs – this was initially with cisplatin and subsequently with carboplatin. A standard of care in the early 1990s in the USA was cisplatin given in combination with cyclophosphamide, or in combination with cyclophosphamide and doxorubicin.

The second International Collaborative Ovarian Neoplasm trial (ICON2) of 1526 patients confirmed that CAP combination chemotherapy: (cyclophosphamide 500 mg/m², doxorubicin 50 mg/m², cisplatin 50mg/m²) three-weekly for six months resulted in no statistical improvement in progression-free survival (PFS) or OS in women with EOC when compared with the much simpler and better tolerated full-dose single-agent carboplatin (AUC 5) chemotherapy (Collaborators, 1998).

However, cisplatin remained the standard of care in the USA, and when paclitaxel was introduced it was initially investigated by the GOG in the GOG-111 trial, which compared cisplatin + paclitaxel with cisplatin + cyclophosphamide in women with advanced EOC. The data from this trial showed significant improvement of PFS and OS in patients treated with cisplatin and paclitaxel (McGuire et al., 1996). The benefit of paclitaxel therapy on PFS and OS was then confirmed by another international phase III trial, the European-Canadian Intergroup trial (OV-10) (Piccart et al., 2000). As a result of these trials, paclitaxel, given alongside platinum, has replaced the alkylating agents in treatment of EOC.

The GOG-158 trial compared the combination of paclitaxel and carboplatin with the then standard combination of paclitaxel and cisplatin in women with FIGO stage III EOC and residual disease < 1 cm. PFS and OS were shown to be very similar (Ozols et al., 2003). However, women treated with the cisplatin regimen experienced significantly more severe side-effects than women treated with carboplatin (Ozols et al., 2003). Consequently, carboplatin has replaced cisplatin due to its serious side-effects.

The benefits from the addition of paclitaxel to platinum were not, however, universal. The third International Collaborative Ovarian Neoplasm trial ICON3 of 2,074 patients, evaluated the combination of paclitaxel + carboplatin vs full dose single-agent carboplatin or the CAP regimen as first-line treatment in advanced EOC. ICON3 found no significant difference in PFS or OS between the groups (Group, 2002). Furthermore, due to severe side-effects associated with combination chemotherapy, usage of single-agent carboplatin as first-line treatment was recommended (Group, 2002).

The UK National Institute for Health and Care Excellence (NICE) has weighed the data, and in the TA55 guidance on the use of paclitaxel in the treatment of OC, stated that “The choice of treatment [between single-agent platinum or a combination of platinum and paclitaxel for first-line chemotherapy for ovarian cancer should be made after discussion between the responsible clinician and the patient about the risks and benefits of the options available” (NICE., 2003).

The platinum-based cytotoxic agents – cisplatin and its derivative, carboplatin – induce tumour cell death and necrosis by triggering DNA damage. DNA monoadducts are formed by the interaction of both drugs with purine bases Adenine and Guanine, which subsequently binds to another nucleotide to form intra/inter-strand di-adducts (Hah et al., 2006, Sousa et al., 2014). These platinum-DNA adducts inhibit DNA replication, prevent RNA transcription, and activate several signalling pathways leading to apoptosis (Siddik, 2003, Shen D. W. et al., 2012).

Paclitaxel is a powerful antimitotic drug. It exerts this effect by promoting microtubule polymerisation and stabilisation, hindering disassembly of microtubule polymer and blocking normal spindle formation at the metaphase, leading to mitosis arrest at the G2M phase (Horwitz, 1994). Additionally, disruption of microtubules stimulates Raf-1 activation and Bcl-2 phosphorylation, leading to cytotoxicity following DNA damage (Kamazawa et al., 2002).

In advanced EOC, several prospective and retrospective clinical trials have shown that primary optimal cytoreduction surgery with complete resection or to minimal

residual disease have significantly improved PFS and OS (Du Bois et al., 2009, Vergote et al., 2010). Women with advanced-stage EOC (FIGO stage III-IV) who received chemotherapy following optimal cytoreduction surgery with complete removal of all macroscopically visible tumours have better PFS and OS than patients with minimal residual disease (Minig et al., 2017).

Traditional management for women with advanced-stage EOC has been primary debulking surgery followed by optimal chemotherapy. However, for women presenting with widespread disease and severe co-morbidities, neoadjuvant chemotherapy (NAC) with interval debulking surgery (two to four cycles of chemotherapy followed by surgery) is recommended. Advantages of NAC include improved resection of disseminated tumour and fewer intra-operative and post-operative surgical complications (Zheng and Gao, 2012). The randomised clinical trial by the Gynaecological Cancer Cooperative Group of the European Organisation for Research and Treatment of Cancer (EORTC) has evaluated the influence of NAC on OS (Van Der Burg et al., 1995). The results of this trial, the very similar phase III, an open-label, randomised, controlled, non-inferiority trial (CHORUS) of 552 patients (Kehoe et al., 2015), the following meta-analysis on pooled data for 1,220 patients from the EORTC and CHORUS trials (Vergote et al., 2018), and the follow-on Cochrane review revealed no difference in PFS or OS between treatment arms. However, interval debulking surgery was found to be beneficial to patients who had less extensive initial surgery (Tangjitgamol et al., 2016).

The addition of modern, targeted therapies, such as anti-angiogenics, to the current standard chemotherapy regimen has been investigated by GOG in the GOG-0218 trial and in the seventh International Collaborative Ovarian Neoplasm (ICON7).

Bevacizumab (Avastin[®], Roche), is a humanised monoclonal antibody that neutralises all isoforms of VEGF-A, leading to inhibition of VEGF binding to its receptors on cell surface (Ferrara et al., 2005). Following this inhibition, the microvascular growth of tumour blood vessels is reduced, limiting the blood supply to tumour tissue (Kazazi-Hyseni et al., 2010, Keating, 2014).

GOG-0218, a phase III, double-blind, placebo-controlled trial of 1,873 patients, investigated the use of bevacizumab in first-line chemotherapy in women newly diagnosed with advanced EOC (stage III [macroscopic minimal residual disease or

completely resected disease following initial debulking surgery] or stage IV) (Burger et al., 2011). Eligible women were randomly enrolled into three treatment arms. These treatments arms compared standard chemotherapy regimen (carboplatin (AUC 6) + paclitaxel (175 mg/m²) given three-weekly for 22 cycles) to bevacizumab at a dose of 15 mg/kg added to the standard chemotherapy from the second treatment cycle, for 22 cycles, or bevacizumab 15 mg/kg added to the standard chemotherapy from the second to the sixth treatment cycles only, with addition of a placebo from the seventh cycle, for 22 cycles. The outcome of this trial indicated that the addition of bevacizumab has improved the median PFS in women with advanced EOC (Burger et al., 2011). ICON7 was a phase III international trial led by the UK Medical Research Council Clinical Trial Unit (MRC CTU) (Perren et al., 2011). In this trial, 1,528 women newly diagnosed with epithelial ovarian, primary peritoneal, or fallopian tube cancers (high-risk early FIGO stage I or IIA [grade III or clear cell histology], or advanced FIGO stage IIB-IV [all grades, all histology]), were randomised into two treatment groups. The first group was given the standard chemotherapy regimen: carboplatin (AUC 5/6) + paclitaxel (175 mg/m²) given three-weekly for five or six cycles. The second group received bevacizumab (7.5 mg/kg), added to the standard regimen and given three-weekly for six cycles, followed by a continuation of bevacizumab for 12 further cycles or until progression occurred.

The results showed significant improvement of 1.7 months in the median PFS in women who received bevacizumab in addition to standard chemotherapy (HR= 0.81, 95% CI: 0.70-0.94, p=0.004). Women at high risk for progression benefited from the bevacizumab in terms of median PFS by 5.4 months, compared with standard chemotherapy alone (HR=0.68, 95% CI: 0.55-0.85, p<0.001) (Perren et al., 2011). Further analysis of completed ICON7 trial data by Oza and colleagues found that no OS benefit was observed for the whole trial population. However, the addition of bevacizumab significantly improved median OS in high-risk patients (restricted mean survival time 39.3 vs 34.5 months [p=0.03]). (Oza et al., 2015). The results of this trial showed that bevacizumab significantly improved PFS in all sub-groups analysed, with greater benefit for patients at high-risk of progression (Perren et al., 2011). However, the benefit of bevacizumab on OS from the whole cohort was seen only in patients with poor prognosis (Oza et al., 2015). These results have led to the integration of bevacizumab into the standard first-line management of EOC patients with poorer prognoses globally.

Trials have also been conducted to examine the scheduling of carboplatin and paclitaxel in first-line chemotherapy. For instance, a randomised controlled trial led by the Japanese GOG (JGOG3016) showed that weekly dense paclitaxel, in

combination with three-weekly carboplatin, significantly improved PFS and OS in patients with ovarian, fallopian tube and primary peritoneal cancers (Katsumata et al., 2013). Nevertheless, this association was not seen in data from the European (MITO-7) trial, although weekly paclitaxel + three-weekly carboplatin was associated with lower toxic side-effects and improved patients' quality of life (Pignata et al., 2014). This result was partially attributed to the lower dose of paclitaxel used in this trial compared to JGOG3016 (60 mg/m² vs 80 mg/m² weekly). The ICON8 international trial has subsequently compared two dense-dose regimens to the standard three-weekly regimen in 1566 patients randomised to three treatment arms. This trial has established that a weekly dense-dose regimen has not significantly improved the PFS nor the OS in women with newly diagnosed OC (Clamp et al., 2019).

1.1.6.3 Management of recurrent EOC

Approximately 70–80% of patients with EOC respond to initial chemotherapeutic treatment. Nevertheless, among responding individuals, the estimated relapse rate during the first two years following treatment completion varies between 55 and 75% (Edwards et al., 2015). The length of time during and after treatment without disease progression is around 18 months, while progression ultimately occurs in approximately 80% of patients (Luvero et al., 2014). The time from the end of the first-line platinum-based chemotherapy to recurrence of EOC is a key in determining subsequent management options. Patients with disease progression during treatment, or up to one month following their last chemotherapy dose, are considered to have 'platinum-refractory' disease. Whereas, 'platinum-resistance' disease is defined as cancer progression within six months of completion of treatment. Patients who have responded to initial platinum-based therapy, and have been off treatment for over 12 months before presenting with active recurrent EOC, are experiencing 'platinum-sensitive' disease. 'Partially platinum-sensitive' disease occurs in patients whose disease has progressed between six and 12 months (Stuart et al., 2011).

Several second-line chemotherapeutic options which are alternatives to platinum compounds are available, such as: liposomal doxorubicin, topotecan, gemcitabine, and etoposide. Generally, patients with platinum-sensitive disease are treated with further platinum-based regimens. For instance, carboplatin or cisplatin as a single agent, docetaxel + carboplatin, gemcitabine + carboplatin (Markman and Bookman, 2000, Edwards et al., 2015).

Essential considerations in the selection of best management options for recurrent advanced EOC are the toxicity profile for the chosen agent to reduce complications, and the level of improvement in the patient's quality of life.

1.1.6.4 Management of *BRCA1/2* mutations carriers

BRCA1 and *BRCA2* are important proteins in repairing DNA double-stranded breaks (DSBs) damage via error-free homologous repair pathway. In women with *BRCA1* and *BRCA2* mutations, DSBs cannot be efficiently repaired due to errors in DNA-repair mechanism, and may ultimately lead to the development of cancer. Poly (ADP-ribose) polymerase 1 (PARP1) protein is one of the essential enzymes in repairing DNA single-stranded breaks (SSBs) damage. Persistent SSBs may cause DSBs, therefore, inhibition of PARP triggers formation of multiple DSBs. In OC cases with *BRCA1/2* mutations, failure to repair these DNA aberrations leads to tumour cell death (Ashworth, 2008). PARP inhibitors are DNA-repair targeted therapy especially beneficial in treatment of cancers induced by *BRCA1/2* mutations which are mostly hereditary, but also may emerge as *BRCA1* somatic mutations in OC (Merajver et al., 1995). PARP inhibitors such as Olaparib, Niraparib and Rucaparib have been shown to be effective in patients with relapsed, platinum-sensitive OC who have *BRCA1/2* mutations (Ledermann and Pujade-Lauraine, 2019). In addition, they are associated with improved PFS in patients who suffer recurrent platinum-sensitive EOC (Wiggins et al., 2015).

More recently, Niraparib was found to significantly improve PFS in women newly diagnosed with EOC after initial treatment with standard chemotherapy (González-Martín et al., 2019). In addition, after first-line platinum-based chemotherapy and bevacizumab, Olaparib was used as a maintenance treatment in combination with bevacizumab in women with advanced EOC, resulting in a significant increase in PFS (Ray-Coquard et al., 2019).

Risk-reducing surgical management of women carrying *BRCA1/2* mutations comprises of bilateral mastectomy, bilateral salpingo-oophorectomy, or both. Several studies have shown that prophylactic, risk-reducing bilateral salpingo-oophorectomy is associated with reduced EOC risk and OC related mortality in *BRCA1/2* mutation carriers while the risk of peritoneal cancer is still present (Domchek et al., 2010).

1.1.7 Ovarian tumour microenvironment

The tumour microenvironment (TME) is a complex, dynamic niche that comprised of cancer cells, cancer stem cells and various types of non-cancer stromal cells such as: fibroblasts and adipocytes, endothelial cells and pericytes, neuroendocrine cells, different types of immune cells, in addition to signalling molecules and extracellular matrices (ECMs). Many of the hallmarks of cancer described by Hanahan and Weinberg are affected by the various cellular and non-cellular components of TME (Hanahan and Weinberg, 2011). It has been established that TME influences the process of cancer development and spread (Wang M. et al., 2017). Currently, the ovarian TME is increasingly used for therapy, due to accumulating evidence from various genomic, transcriptomic and proteomic studies of its fundamental role in carcinogenesis (Yang et al., 2020) and sensitivity to therapy (Östman, 2012). The ECM is a critically important component of TME. It regulates a variety of cell functions including cell growth, adhesion and migration (Ricciardelli and Rodgers, 2006, Lu et al., 2012). It also strongly influence the effectiveness of cancer treatment (Henke et al., 2020). There is an established role played by the Matrix metalloproteinases (MMPs) in regulating TME, reviewed in detail by (Kessenbrock et al., 2010). It has been demonstrated that, MMP-2 increases OC cell metastasis by cleaving fibronectin and vitronectin, and enhancing OC cell attachment to these cleaved fragments via $\alpha_v\beta_1$ and $\alpha_v\beta_3$ integrins (Kenny et al., 2008). Ovarian ECM is composed of two layers, the interstitial matrix, predominantly composed of fibrillar collagen I and III (Cho et al., 2015, Ricciardelli and Rodgers, 2006), and the basal lamina (basement membrane) which is composed of collagen IV and laminin (Ricciardelli and Rodgers, 2006).

Previous *in vitro* studies and reviews have described the EOC microenvironment and its involvement in tumour development and dissemination as a very complex process that involves a wide range of molecules, as well as several different cell types (Freedman et al., 2004, Lengyel, 2010, Thibault et al., 2014, Satpathy et al., 2009).

1.2 Cancer and coagulation

1.2.1 Coagulation complications in cancer

Coagulation abnormalities are well recognised in patients with malignant neoplasms, especially those undergoing chemotherapeutic treatment (Arnout et al., 2003). Thromboembolism, both arterial and venous, is considered the most frequent coagulation complication affecting cancer patients (Khorana, 2012), leading to recurrent clinically symptomatic episodes and the potential for increased risk of bleeding during prolonged anticoagulation therapy (Prandoni et al., 2002), all of which is associated with reduced survival (Letai and Kuter, 1999, Khorana, 2010).

Haemorrhagic complications represent the other side of haemostatic abnormalities in patients with malignant tumours, and present a recognised cause of death in those patients (Falanga et al., 2013). For instance, disseminated intravascular coagulation (DIC) is a serious hemostatic disorder characterised by a contradictory clinical presentation of thrombosis and bleeding. In DIC, entry of procoagulant substances to the blood stream trigger systemic activation of intravascular coagulation system simultaneously leading to deposition of fibrin-platelets thrombi. The abnormal acceleration of the coagulation cascade results in thrombosis. The coagulation factors and platelets are consumed at a high rate, exceeding the capacity of the synthetic ability of liver and bone marrow . The continuous reduction of clotting factors and platelets, with the activation of fibrinolysis, results in haemorrhage and contributes to diminished blood supply to different organs and eventually multi-organ failure. Severe DIC has been described in acute leukaemias, leading to intractable bleeding (Falanga et al., 2013).

1.2.2 The effect of cancer in coagulation

Malignant tumours have been shown to cause considerable disruption of Virchow's classical triad of thromboembolic disease components: change of blood flow, injury to endothelial cells and increase of procoagulants (Letai and Kuter, 1999). Blood flow in the vessels adjacent to the tumour growth is affected by venous stasis due to external mechanical compression, sepsis and formation of new complex vascular plexus (angiogenesis), leading to abnormal blood viscosity and blood flow disturbances (Arnout et al., 2003). It has been reported that, damage to the vascular endothelial cells can occur directly by cancer growth or chemotherapy, for example, some tumours particularly renal cell carcinoma, were able to cause inferior vena cava thrombosis by direct invasion (Letai and Kuter, 1999). In addition, malignant cells

were found to be capable of activation of the intrinsic clotting system via different intracellular signalling mechanisms including platelet activation, generation of thrombin (Arnout et al., 2003) and expression of procoagulants such as tissue factor (Konecny et al.) (Sampson and Kakkar, 2002).

1.2.3 Role of coagulation factors in cancer

It has been demonstrated that levels of several circulating clotting factors are increased in patients with cancer including: fibrinogen, fibrinogen/fibrin degradation products (FDPs), factor V, factor VIII, factor IX and factor X (Lima and Monteiro, 2013). Furthermore, previous research has established that the presence of the coagulation factors within the TME plays a key role in tumour progression (Lima and Monteiro, 2013). Factor VII is expressed in hepatocellular carcinoma cells, bladder cancer, OC and laryngeal carcinoma tissue. In addition, the combination of tissue factor and activated factor VII (TF:FVIIa complex) is thought to be involved in angiogenesis, migration and invasion (Unlu and Versteeg, 2014). The importance of the role of FXIIIA in cancer is increasingly recognised. Besides its role in haemostasis, FXIIIA plays important roles in localised tissue remodelling and wound healing, angiogenesis and stimulation of cell proliferation, migration and inhibition of apoptosis (Schroeder and Kohler, 2013) – all these functions are potentially related to tumour progression. It has been shown that FXIIIA-mediated cross-linked fibrin was used by the cancer cells to form invadopodia (Malik et al., 2010). In addition, the cross-linked matrix in the TME, provided a scaffold for cancer metastasis (Porrello et al., 2018). Factor XIIIA will be the main focus of this thesis. Previous findings for this enzyme in cancer will be discussed in section 1.3.5.

1.3 Coagulation factor XIII A

The first observation of the stabilisation of the fibrin clot in weak acids, made in the presence of Ca^{2+} , was identified by (Barkan and Gaspar, 1923). Twenty years later, it had been recognised that a “serum factor” is essential to make the clot insoluble in weak acids (Robbins, 1944). Follow-on research has shown that the serum factor was non-dialyzable and thermolabile, and was named Fibrin Stabilising Factor (FSF) (Laki and Lóránd, 1948, Lóránd, 1948), and linked to fibrin (Lóránd, 1950). The serum factor was purified and the enzymatic nature was determined by Loewy and colleagues (Loewy et al., 1957, Loewy et al., 1961). The international committee on blood clotting factors then declared FSF as a coagulation factor XIII, in 1963. Factor XIII was found to be a zymogen (Lóránd, 1977).

Plasma coagulation factor XIII (FXIII) is a heterotetramer (320 kDa) composed of two A and two B-subunits (FXIII-A₂B₂). FXIII, as a heterotetramer, circulates in the blood bound to fibrinogen (Greenberg and Shuman, 1982), at a concentration of 21.6 $\mu\text{g}/\text{mL}$ (Yorifuji et al., 1988). The A-subunit is synthesised by the resident macrophages (Beckers et al., 2017) and exists intracellularly in dermal dendritic cells, astrocytes, macrophages, fibroblasts, chondrocytes, monocytes, osteocytes, and osteoblasts as a homodimer of two A-subunits, and extracellularly in plasma, the cytoplasm of platelets, the placenta, synovial fluid, the heart and the eyes, as part of heterotetrameric factor XIII (Muszbek et al., 2011). The A-subunit is also expressed in adipose tissue, skin, soft tissues, testis, and placenta (The Human Protein Atlas). The B-subunit is synthesised in hepatocytes and secreted into the plasma where it could be found as a non-compound form or complexed with A-subunits. The main focus of this thesis will be on the A-subunit.

Factor XIII A (FXIII A) belongs to the transglutaminase (TG) family of proteins (EC 2.3.2.13) (Facchiano and Facchiano, 2009). This family consists of nine members including: TG1 Keratinocyte transglutaminase, TG2 tissue transglutaminase, TG3 epidermal transglutaminase, TG4 prostate transglutaminase, TG5, TG6, TG7, Erythrocyte membrane protein band 4.2 and FXIII A (Eckert et al., 2014). The structure of all TGs is composed of a β -sandwich at the N-terminus, α/β catalytic core, two β -barrel domains at the C-terminus (Iismaa et al., 2009), additionally, FXIII A contains an N-terminal 37-amino acid activation peptide (AP). These enzymes modify other proteins by catalysing the Ca^{+2} dependent formation of N- γ -(glutamyl)- ϵ -lysyl covalent bonds (isopeptide bonds) (Eckert et al., 2014).

1.3.1 FXIII gene and polymorphisms

The gene encoding the coagulation factor XIIIa subunit, *F13A1*, is located on chromosome 6 (6p24-p25.1), and contains 15 exons and 14 introns (Ichinose and Davie, 1988). The mRNA is 3.86 kb (NCBI Reference Sequence: NM_000129.3) producing a polypeptide comprising 731 amino acids (731 plus starter methionine) (Figure 1-3). FXIIIa is known to be highly polymorphic, with multiple (SNPs) in *F13A1* gene coding region. More details are available from the Genome Aggregation Database (gnomAD), available at: <https://gnomad.broadinstitute.org/>. There are five SNPs frequently explored for their effect on the enzyme biological functions and involvements in complex diseases: 103G>T (Val34Leu), 614A>T (Tyr204Phe), 1694C>T (Leu564Pro), 1951G>A (Val650Ile) and 1954G>C (Glu651Gln). In this thesis, the focus will be on Val34Leu, Val650Ile, and Glu651Gln variants, which are summarised in Table 1-2. There are also two silent polymorphisms, in codons 331 and 567 (Anwar et al., 1995). In addition, two further polymorphisms, -246G>A transition and (AAAG)_n around 800-900 bp away from the transcription site, were described in the promoter region (Arnout et al., 2003). Moreover, a rare SNP, T1766A (L588Q) is also reported in exon 13 (Gemmati et al., 2016). There are a further 480 SNPs, but these do not result in amino acid changes (dbSNP NCBI). The influence of the FXIIIa SNPs on the enzyme activity, level and specific activity (SA) has been reported (Anwar et al., 1999, Gallivan et al., 1999b). FXIIIa Leu34, Tyr204, and Leu564 variants were found to be linked with high FXIII SA, whereas, Ile650 and Gln651 SNPs have shown minimal to normal FXIII SA (Anwar et al., 1999). Carriage of homozygous Leu564 polymorphism was significantly associated with low plasma FXIII level (Gallivan et al., 1999b). It has been reported that, the Val34Leu variant is associated with increased cross-linking activity (Kohler et al., 1998). The observed increase in activity could be attributed to the fact that, carriers of this variant were found to have rapid cleavage of FXIII by thrombin (Ariëns et al., 2000, Wartiovaara et al., 2000b). Furthermore, linkage and association tests of six FXIIIa SNPs were performed in 201 dizygotic twin pairs females, and have identified the Val34Leu to be the main functional variant affecting FXIII activation (de Lange et al., 2006).

Table 1-2: SNPs in *F13A1* coding region included in this thesis

<i>F13A1</i> SNP	rs number	<i>F13A1</i> Exon	Codon (nucleotide substitution)	Change in amino acid
103G>T	rs5985	II	GTT > TTT (G > T)	Val34Leu (V34L)
1951G>A	rs5987	XIV	GTT > ATT (G > A)	Val650Ile (V650I)
1954G>C	rs5988	XIV	GAG > CAG (G > C)	Glu651Gln (E651Q)

1.3.2 Structure of FXIII

The three-dimensional X-ray crystallographic structure of the recombinant FXIII_A subunit produced in yeast found that the A-subunit comprised of four main domains: the β -sandwich (residues 38–184), the catalytic core region (residues 185–515), β -barrel 1 (residues 516–628) and β -barrel 2 (residues 629–731), plus an NH₂-terminal AP (residues 1–37) (Yee et al., 1994, Yee et al., 1996, Weiss et al., 1998) (Figure 1-3). The crystal structure of activated recombinant FXIII_A has been produced and effectively used to generate data about the active site of the enzyme, allowing scientists to design molecules that could target this active site and provide the basis of new anticoagulant medications (Stieler et al., 2013). Recently, the structure of plasma FXIII concentrate (Fibrogammin-P) was revealed using the mass spectroscopy (MS) technique (Singh et al., 2019b).

The structure of the A-subunit is globular, but the B-subunit is a glycoprotein composed of 10 sushi domains (kinked, thin, flexible strands), each stabilised by a pair of disulphide bridges (Komaromi et al., 2011) with 8.5% carbohydrates of total weight. The A-subunits exert its TG activity via the catalytic triad (Cysteine314, Histidine373 and Asparagine396). Meanwhile, the B-subunits have no enzymatic activity and functions as a carrier for the A-subunits, preventing their proteolytic degradation within the plasma (and prolonging the A-subunit's half-life in the circulation). Other roles of the B-subunit include acceleration of fibrin cross-linking (Souri et al., 2015), participation in underlying mechanisms of FXIII activation and function (Gupta et al., 2016b) and involvement in bleeding diathesis (Singh et al., 2019a).

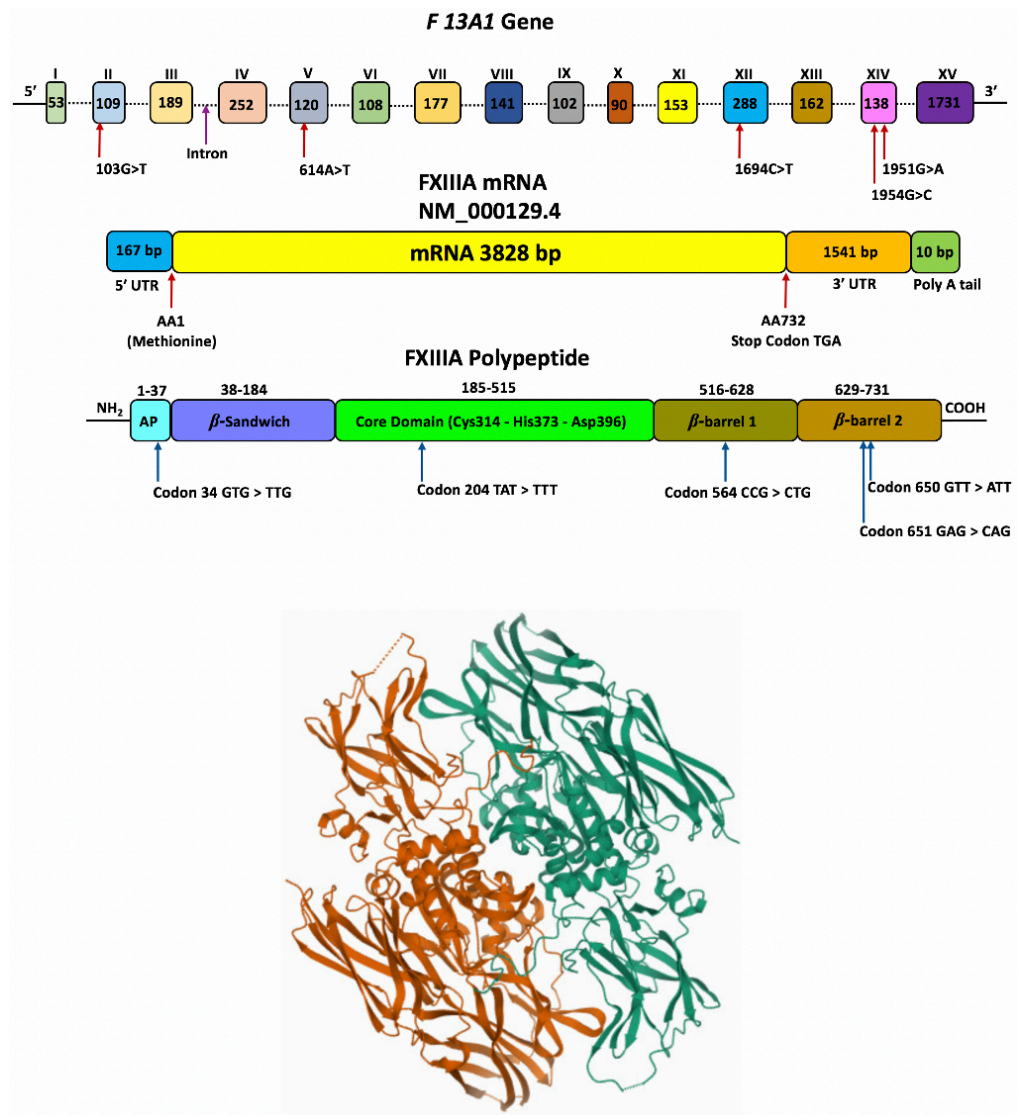


Figure 1-3: Gene, location of SNPs included in this study, mRNA, polypeptide and X-Ray structure of FXIIIa

Top: Sequential arrangement of the FXIII A-subunit polypeptide, mRNA and the corresponding cDNA presenting the position of the exons which are indicated by Roman numbers and the sizes of the exons are specified in base pairs, adapted from (Anwar and Miloszewski, 1999). The AP and the four domains including β - sandwich, core domain, β -barrel 1, and β -barrel 2 are marked on the linear polypeptide, along with their amino acid residues indicated on top. The core domain includes the residues involved in construction of the catalytic triad (Cysteine314, Histidine373, and Asparagine396) that interact with each other through a hydrogen bonding network (Pedersen et al., 1994). The AP is cleaved by thrombin in the presence of Ca^{+2} between Arg37 and Gly38. The calcium binding site is located in the core domain (Fox et al., 1999). This schematic representation also displays the location of SNPs in relation to exons, and the protein domains. UTR= Untranslated region.

Bottom: R-ray crystallography structure of recombinant FXIIIa homodimer. The two subunits are displayed in orange and green colures (deposited on the Protein Data Bank, <https://www.rcsb.org/structure/1F13>) by Weiss, M.S., Hilgenfeld, R. (Weiss et al., 1998).

1.3.3 Activation and function of FXIIIa

Factor XIIIa is the last enzyme to be activated as part of the coagulation cascade. Several different mechanisms lead to FXIIIa activation. FXIIIa is primarily activated by thrombin cleavage of the AP at the NH₂ terminus by hydrolysis of Arg37-Gly38 bond, and in the presence of Ca²⁺, the protective B-subunits dissociate, facilitating conformational change to produce active FXIIIa (Figure 1-4). It can also be activated by high Ca²⁺ concentrations (>100 mM) without proteolysis in some non-physiological conditions (Muszbek et al., 2011). It is reported that high Ca²⁺ stimulates the detachment of B-subunits to activate FXIIIa. Intracellular FXIIIa dimer is activated by thrombin and Ca²⁺ as well, and in the absence of B-subunits, activation can occur by Ca²⁺ only. Unlike plasma FXIIIa, low Ca²⁺ concentration is required to activate cellular FXIIIa leading to the exposure of the active site for the substrates (Muszbek et al., 2011, Schroeder and Kohler, 2013).

During the final stages of the coagulation cascade, fibrinogen is cleaved by thrombin into fibrin. Activated factor FXIIIa binds to amino acid residues 241 to 247 in the α C-domain of fibrin (Procyk et al., 1993) to form γ - γ fibrin cross linking first, then α - α cross-links and occasionally α - γ cross-linking when the reaction has continued for a while between the fibrin chains of two aligned molecules (Ariëns et al., 2002). Consequently, it strengthens the fibrin clot by converting the loose fibrin polymers into a firm and stable fibre network that is able to withstand mechanical stress and resist clot rupture and so remains firmly attached to the site of the wound (Anwar and Miloszewski, 1999). Furthermore, it also cross-links antifibrinolytic proteins such as α -2 antiplasmin, a plasmin inhibitor, into the fibrin clot. This contributes to a significant increase in clot stability and serves to protect the clot from proteolytic degradation by plasmin, the main fibrinolytic protease (Fraser et al., 2011).

In addition to fibrin, activated FXIIIa also cross-links a wide range of substrates including fibronectin, vitronectin, thrombospondin, and collagen etc. (Nikolajsen et al., 2014). FXIIIa is also involved in many different physiological and pathophysiological processes outside haemostasis and coagulation such as wound healing, angiogenesis, osteoblast differentiation, inflammation, and maintenance of pregnancy (Muszbek et al., 2011, Shi and Wang, 2017). FXIIIa also has vital roles in stimulation of connective tissue cells and tumour matrix formation (Adany and Bardos, 2003). During wound healing, FXIIIa facilitated platelets adhesion by integrins α _{IIb} β ₃ and α _v β ₃ on the surface of platelets through a tyrosine-kinase-dependent mechanism, unrelated to its TG activity (Magwenzi et al., 2011).

Congenital FXIII deficiency is an autosomal recessive disorder, characterised by severe bleeding, impaired wound healing and recurrent miscarriages (Duckert et al., 1960, Anwar and Miloszewski, 1999). Data from FXIII^A knockout mice studies showed that they presented with diminished angiogenesis, inability to maintain pregnancy and a decrease in clot retraction (Koseki-Kuno et al., 2003, Kasahara et al., 2010).

Previous studies have shown that recombinant FXIII^A expressed in the *Saccharomyces Cerevisiae* yeast strain (Bishop et al., 1990) has the same function as platelet FXIII (Hornyak et al., 1989). This recombinant FXIII^A was used successfully in clinical trials as medication for FXIII deficiency (Reynolds et al., 2005, Abdel-Samad, 2017). No severe side-effects or anaphylaxis response have been reported following administration (Visich et al., 2005).

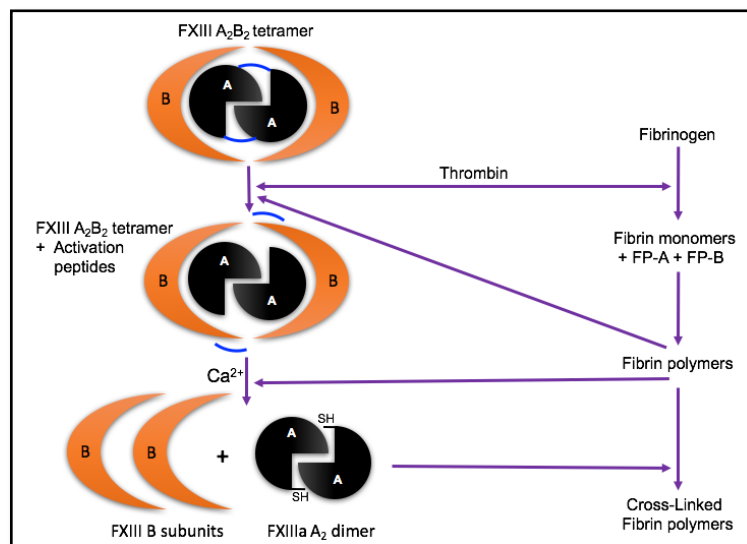


Figure 1-4: Activation of FXIII

Plasma FXIII is a heterotetrameric of A₂ and B₂-subunits. The thrombin cleaves the AP from subunits-A, revealing the enzyme active site, then the B-subunits dissociates in the presence of Ca²⁺. Both fibrin polymerisation and Ca²⁺ enhances cleavage of AP and dissociation of B-subunit as well. Abbreviations: FP-A= Fibrinopeptide A; FP-B= Fibrinopeptide B; SH= Active thiol. Adapted from (Ariëns et al., 2002).

1.3.4 FXIIIa Substrates

FXIIIa is distributed ubiquitously and documented to cross-link a range of protein molecules found both intracellularly and in the plasma. These protein molecules can be categorised into different groups based on the biological process they are involved in e.g. coagulation, wound healing, angiogenesis, immune system processes, proteolysis, cell adhesion, and extracellular matrix (ECM) organisation (Nikolajsen et al., 2014). Several of the FXIIIa substrates identified to date are reported to be important in ovarian cancer growth and metastasis. These include molecules that are important in cell adhesion and ECM organisation, for example those listed by Richardson et al (Richardson et al., 2013): Fibrinogen, Collagen; (Ueki et al., 1996): Fibronectin, Vitronectin, $\alpha_v\beta_3$ and β_1 family integrins; (Thibault et al., 2014): Extracellular matrix protein-1, Transforming Growth Factor- β (TGF- β), Secreted protein acidic and rich in cysteine (SPARC) and Monocyte differentiation antigen CD14.

In a study that identified 147 FXIIIa substrates, the research group has shown the ability of activated FXIIIa (FXIIIa) to cross-link around 48 structural proteins to the fibrin clot. Many of these proteins cross-talk with cell surface receptors and are able to influence cell adhesion, proliferation, and metastasis (Nikolajsen et al., 2014). The following sections provide a brief summary of the molecular structure and function of FXIIIa substrates which will be examined in this thesis. In addition, their cross-linking sites and roles are shown in Table 1-3.

1.3.4.1 Fibrinogen

Fibrinogen (FGN) is a large glycoprotein with a molecular weight of 340 kDa synthesised primarily by hepatocytes and secreted into the plasma. Its structure is dimeric, composed of two $A\alpha$, two $B\beta$, and two γ chains containing 610, 461, and 411 amino acids respectively (Henschen et al., 1983).

1.3.4.2 Fibronectin

Fibronectin (FN) is a multifunctional glycoprotein present in the ECM and body fluids. It occurs as a dimer with two subunits of about 250 kDa that are substantially similar. It promotes cell adhesion, migration and differentiation primarily through cytoskeletal structure changes mediated by integrins (Akiyama, 1996). Cellular fibronectin (cFN) and plasma fibronectin (pFN) are two distinct types of fibronectin. cFN is insoluble, and found throughout the body and is predominantly produced by fibroblasts. pFN, is soluble, produced only by hepatocytes, and found in plasma and body fluids.

1.3.4.3 Vitronectin

Vitronectin (VTN) is a glycoprotein that can be found in large concentrations in the blood, extracellular matrix, and bone. It has three structural domains: an N-terminus somatomedin B domain that binds to plasminogen activator inhibitor 1 (PAI-1); a central domain; and a C-terminus domain. Vitronectin also has an RGD sequence that interacts to integrin receptors $\alpha_v\beta_1$ and $\alpha_v\beta_3$ (Ständker et al., 1996). It binds to the urokinase receptor (uPAR, also known as CD87) via the somatomedin B domain (Madsen et al., 2007).

1.3.4.4 Collagen-1

Each collagen molecule is made up of three α chains. Collagen-1 is encoded by two genes, COL1A1 and COL1A2, with two 1 α chains and one 2 α chain forming the fibrillar collagens' unique triple helix shape (Leitinger and Hohenester, 2007).

Table 1-3: FXIIIA substrates

Substrate	Site of cross-linking	Cross-linked with	Role	Reference
Fibrinogen γ-chain	Gln398, Gln399, and Lys406	Itself and α -chain	Stabilization of clot	(Weisel et al., 1993) (Purves et al., 1987) (Spraggon et al., 1997)
Fibrinogen α-chain	Gln221, Gln237, Gln328, Gln366, Gln223-Lys508, Gln223-Lys539, Gln237-Lys418, Gln237-Lys508, Gln237-Lys539, Gln237-Lys556, Gln366-Lys539	Itself and γ -chain	Stabilization of clot	(Fretto et al., 1978) (Cottrell et al., 1979) (Matsuka et al., 1996) (Sobel and Gawinowicz, 1996) (Lorand, 2001) (Wang, 2011)
Fibronectin	Gln3	Itself, fibrin, and collagen	Wound healing; Migration of cells into the clot	(Mosher and Schad, 1979) (Procyk et al., 1985)
Collagen-1	-	Fibrin, fibronectin	Stabilization of ECM	(Mosher and Schad, 1979)
Vitronectin	Gln93	-		(Sane et al., 1988) (Skorstengaard et al., 1990)

This table displays FXIIIA substrates, their site of cross-linking, proteins cross-linked with, and their roles. Table adapted from (Ariëns et al., 2002).

1.3.5 FXIII A in different malignancies

Previous research has provided important information on FXIII A and its association with cancer on the basis of its polymorphisms, plasma levels and activity, and tumour tissue expression. The following sections provide an overview of the literature relating to FXIII A influence on cancer development, metastases, and prognosis, which is summarised in Table 1-4. There is inconsistency in the literature with regards to the influence of FXIII A on cancer. These varying effects indicate that FXIII A may have diverse functions depending on the type of cancer being studied.

1.3.5.1 F13A1 gene polymorphisms in cancer

Polymorphisms in genes of coagulation factors including *F13A1* are found to be associated with cancer risk (Tinholt et al., 2016). It has been shown that, *F13A1* gene is up-regulated in the peritoneum and stroma of malignant, but not benign, ovarian tumours (Wang E. et al., 2005). Individuals carrying heterozygous FXIII A Val34Leu polymorphism have a 15% decreased risk of colorectal cancer (Vossen et al., 2011). In contrast, a three-fold increased risk of oral squamous cell carcinoma was observed for Leu/Leu homozygous for FXIII A Val34Leu, vs two-fold greater risk associated with the heterozygous of the variant (Val/Leu) compared to healthy controls (Vairaktaris et al., 2007). FXIII A Val34Leu polymorphism wildtype (Kenny et al., 2014) and heterozygous for the variant have been shown to have a protective effect on uterine fibroid (Leiomyoma) development, a benign heterogeneous tumour originating from the myometrium (Ahmadi, 2016).

1.3.5.2 Plasma FXIII A levels in cancer

It has been reported that plasma FXIII A levels diminished progressively with tumour progression in mice with plasmacytoma, indicating that FXIII A was taken up by malignant plasma cells (Eipe et al., 1977). Plasma FXIII A levels were significantly decreased in women with metastatic gynaecological malignancies compared to women who had malignancies without metastases and those with benign tumours, suggesting utilisation of FXIII A for cross-linking proteins in the process of the tumour matrix formation. This decline in FXIII A level was also attributed to local nonspecific proteolysis within the TME (van Wersch et al., 1994). However, in the same study, plasma FXIII A levels were significantly increased in women with benign and non-metastasised gynaecological tumours compared to healthy women, which was explained by the possibility that FXIII A might be released within tumour tissues (van Wersch et al., 1994). However, this study was based on a relatively small sample

size. In addition, low plasma FXIIIa levels were also seen in acute promyelocytic leukaemia (Goncalves et al., 2012).

1.3.5.3 FXIIIa activity in cancer

Reduced plasma FXIIIa activity was reported in gynaecological cancers, with the lowest level of 33.8–51% in advanced stages (Seki, 1986). In addition, reduced FXIIIa activity was also found in precursor B acute lymphoblastic leukaemia (ALL) (Funato et al., 2011). Furthermore, the lack of FXIIIa activity was significantly associated with decreased LLC^{GFP} (Lewis Lung Carcinoma cells) experimental metastases to the lungs in immunocompetent FXIIIa deficient mice (FXIIIa^{-/-}), indicating that FXIIIa was detrimental for pulmonary metastases (Palumbo et al., 2008). Nevertheless, FXIIIa activity levels were found to be significantly increased in patients with advanced-stage non-small cell lung cancer (NSCLC) compared to patients in the early-stage of the disease and the healthy control group (Lee et al., 2013).

1.3.5.4 FXIIIa expression in cancer tissues

Positive immunohistochemical staining for FXIIIa was found in benign and fibro-histiocytic tumours, as well as focal positive staining in fibrosarcoma and embryonic sarcoma (Reid et al., 1986). Another study also revealed positive staining of FXIIIa in malignant histiocytes (neoplastic cells within malignant histiocytosis cases) and in tumour-associated macrophages. In this same study, FXIIIa expression was associated with the phagocytic activation of histiocytic cells in cases of true histiocytic lymphoma (THL), supporting the notion that FXIIIa is deemed as a marker for mature phagocytic histiocytes and assisting in the identification of THL phenotype (Nemes and Thomazy, 1988). FXIIIa has been used along with CD34 as a tool to distinguish between dermatofibrosarcoma protuberans and benign fibrous histiocytoma (dermatofibroma) (Goldblum and Tuthill, 1997).

FXIIIa expression was also detected within the stromal cells of invasive ductal carcinoma of the breast, and in colorectal cancer in all of the specimens cores examined, and especially in the invasive margin, suggesting that FXIIIa may play an important role in facilitating cancer invasion (Turnock et al., 1990). Another study reported a significant decrease in FXIIIa levels in breast cancer tissues compared with normal mammary tissues (Jiang et al., 2003).

The A-subunit of FXIII was found within the connective tissue stroma of fresh frozen sections of metastatic malignant melanoma (Wojtukiewicz et al., 1990), as well as

the adenocarcinoma of pancreas (Wojtukiewicz et al., 2001). Moreover, it has been established that, FXIIIa protein levels were significantly higher in bone metastases compared to liver and lymph node secondaries from primary prostate cancer (Morrissey et al., 2008).

Conversely, FXIIIa was found to be expressed in the cytoplasm of B-cell lineage ALL (Kiss et al., 2006), and was significantly associated with improved event-free survival (Burke MA) and OS, suggesting FXIIIa as a potential prognostic indicator in children with B-cell precursor ALL (Kárai et al., 2018). Previous studies exploring other types of leukaemias confirmed that FXIIIa is an intracytoplasmic marker for monocytic and megakaryocytic acute myeloid leukaemia (AML) and for chronic myelomonocytic leukaemia (CMML) (Kappelmayer et al., 2005, Kiss et al., 2008), however, most of these studies were limited by the lack of information on the role of FXIIIa on OS and prognostic implications for these types of haematological malignancies. Additionally, it has been demonstrated that FXIIIa is expressed in acute leukaemic promyelocytes, a common form of *de novo* AML M3 (Simon et al., 2012).

1.3.5.5 FXIIIa in OC

Van Wersch et al. (1994) showed that Factor XIII may have a role in metastatic ovarian cancer. They found that plasma levels of FXIIIa were lower in metastatic ovarian cancer than in non-metastatic disease. Surprisingly, very little research has been done on OC and FXIII, particularly following this study.

In a recent study which set out to assess the role of factor XIII in surgical treatment of patients with EOC FIGO stage III and IV, data from 347 patients showed that increased ascites formation, histology (SerousHighGrade vs others), low albumin, and increased CA125 were all linked to low FXIII levels. Moreover, in a multivariate model, low FXIII levels were found to be strongly predictive of severe post-operative complications (Yazdian et al., 2020).

A multicentre study of patients with EOC (n=629) was carried out by the Anwar laboratory between April 1999 and September 2002. In this study, the researchers looked at the links between FXIIIa genetic polymorphisms, the biological phenotype of EOC, and OS in individuals with EOC. The analysis of this cross-sectional data showed significant links between OS and *F13A1* genotypes. The *F13A1* 1951G>A polymorphism was found to be a significant predictor of patient death in EOC with shorter OS, while the 1954G>C variant was an independent prognostic factor (Anwar et al., Unpublished work). Recently, the analysis of long-term mature follow-up survival data of the study by Anwar *et al.* (>20 years, n=252) has confirmed these

associations (Hutchinson, 2019). In addition, what stands out in this research is that heterozygous carriers of V34L polymorphism showed improved survival post-progression and OS in a newly diagnosed EOC patients cohort (Hutchinson, 2019). Since FXIII A variants are reported in EOC, this suggests that FXIII A may play a role in this cancer progression and prognosis. The basis for these *F13A1* gene variants' effects on OS, however, has yet to be determined.

Table 1-4: Factor XIIIa in different malignancies

F13A1 gene polymorphisms		
No	Effect in tumour	Reference
1	Val/Leu and Leu/Leu of V34L had 2 to 3-fold greater risk of oral cancer development	(Vairaktaris et al., 2007)
2	Val/Leu carriers of V34L had decreased risk of colorectal cancer	(Vossen et al., 2011)
3	Carriage of V allele (Val/Val and Val/Leu) of V34L is protective in uterine fibroids	(Ahmadi, 2016)
Plasma factor XIIIa levels		
1	Plasma levels are lower in plasmacytoma	(Eipe et al., 1977)
2	Plasma levels are higher in patients with benign ovarian tumours than healthy women	(van Wersch et al., 1994)
3	Plasma levels are lower in metastatic OC than benign ovarian tumour	(van Wersch et al., 1994)
4	Plasma levels are lower in acute promyelocytic leukaemia	(Goncalves et al., 2012)
Factor XIIIa enzymatic activity		
1	Activity is lower in gynaecological cancers	(Seki, 1986)
2	The absence of FXIIIa catalytic activity impaired the development of experimental pulmonary metastases	(Palumbo et al., 2008)
3	Activity is lower in precursor B acute lymphoblastic leukemia	(Funato et al., 2011)
4	Activity is higher in advanced stage NSCLC patients	(Lee et al., 2013)
Factor XIIIa expression in cancer tissues		
1	Expression is decreased in malignant melanoma	(Wojtukiewicz et al., 1990)
2	Used in conjunction with CD34 to differentiate between dermatofibrosarcoma protuberans and dermatofibroma	(Goldblum and Tuthill, 1997)
3	Expression is decreased in breast cancer	(Jiang et al., 2003)
4	Expression is increased in bone metastases	(Morrissey et al., 2008)
5	Expression in B-cell acute leukaemic lymphoblasts linked with improved OS	(Kiss et al., 2006) (Kárai et al., 2018)
6	Used as a marker for the monocytic, megakaryocytic leukemias and chronic myelomonocytic leukaemia	(Kappelmayer et al., 2005) (Kiss et al., 2008)

This table summarises previous research findings on coagulation FXIIIa and cancer. There is no general agreement on how FXIIIa affects cancer, and the contradicting data suggests that FXIIIa may play diverse roles depending on the type of cancer and how this protein is measured, such as plasma levels, activity, or tissue expression.

1.4 Research project

The previous research findings presented in section 1.3.5 offer contradictory and inconsistent outcomes for FXIIIa in cancer. Nevertheless, there are various important reasons to study FXIII in EOC. Plasma factor XIIIa levels are significantly lower in metastatic ovarian cancer compared to benign ovarian tumours. This could mean that FXIIIa was used during cancer spread, as shown by low plasma levels. There is a notable paucity of studies investigating FXIIIa in EOC. No previous study has investigated F13A genotype, levels and activity in the same sample set. Therefore, further research is required to gain better understanding of the different mechanisms underlying FXIIIa's role in EOC. This study seeks to obtain data which will help to address these research gaps.

The main aim was to examine factor XIIIa and its major substrate fibrinogen in epithelial ovarian cancer, and then to use *in vitro* studies to confirm or further explore any findings. This aim was achieved through analysing:

- Factor XIIIa function, expression in plasma and tumour tissue, and relationships with prognostic factors and survival intervals in EOC patients;
- Factor 13A genotypes and their relationships with enzyme function and expression levels, and prognostic factors in EOC patients;
- Fibrinogen expression in plasma and tumour tissue, and D-Dimer levels and relationships with prognostic factors and survival intervals in EOC patients and
- Recombinant expression of FXIIIa variants, identified as important in the above work, for *in vitro* functional analyses and investigating their influence on cell adhesion, migration and growth using cell lines.

Chapter 2 Materials and Methods

2.1 Patients' samples

2.1.1 *ICON7 plasma samples*

Plasma samples from the ICON7 translational cohort were obtained from the MRC, ICON7 Biorepository (n=91, plasma samples) at the University College London. The ICON7 translational cohort is the group of women who kindly gave consent for using their samples and clinical data in translational research programmes. The ICON7 patient enrolment, study design and outcome were published by Perren *et al.* (2011). Ethical approval for the use of the ICON7 plasma samples in translational research and access to associated anonymised clinical data was granted as part of the ethical approval process for the trial (MREC Approval Number: 06/MRE02/52, ISTCTN: 91273375, 21/09/2006 v1). The ICON7 committee approved this project prior to sample release.

2.1.2 *ICON7 tissue microarrays*

The Medical Research Council, ICON7 Biorepository generously provided genomic DNA and tumour and stroma tissue microarrays as well. At the University of Cambridge, tumour and stroma microarrays were produced by processing 4 µm sections onto SuperFrost Plus glass slides (Thermo Scientific, Fisher Scientific). A histopathologist at the University of Cambridge assembled the tissues into tissue microarrays, and three different kinds of microarrays were created: tumour, tumour mixed with stroma, and stroma.

2.2 Recombinant FXIIIa expression

Recombinant FXIIIa protein variants were expressed in the yeast strain *Saccharomyces Cerevisiae* AH22, which was obtained by Dr Anwar from collaborators in Australia (Professor Board, Molecular Genetics Group, John Curtin School of Medical Research, Australian National University, Canberra, Australia): *Saccharomyces cerevisiae* Meyen ex E.C. Hansen, Strain Designations: AH22 [NRRL Y-12843] (ATCC® 38626™). Genotype: MATa leu2-3 leu2-112 his4-519 can1 [KIL-o], form I rDNA. The purification was performed by the affinity of Ni-NTA to their His-tags. The integrity and functionality of this recombinant FXIIIa protein were then assessed using a variety of techniques including WB, ELISA and activity assays.

2.2.1 Expression vector

The plasmid pYF13AH carrying a 2.3kb *Pst*I+*Hind*III fragment encoding the F13A cDNA was also kindly offered by Professor Board from Australian National University, Canberra, Australia. This plasmid is 6.8kb, carries a His tag at the 3'-end of the F13A cDNA, and the F13A expression is regulated by the *GAL*I promoter (Figure 2-1). This expression system had been shown to produce active FXIIIa protein in Professor Board's laboratory (Kangsadalampai and Board, 1998b). Since some of the FXIIIa variants included in this study are near the C-terminus, and the effect of the His tag on FXIIIa polymorphisms was unknown at the time, a thrombin cleavage site was introduced between the end of the F13A cDNA and the His tag in Dr Anwar's laboratory (Figure 2-2). Thus, the His tag would be removed during the activation of the recombinant FXIIIa produced by this plasmid to prevent any interference from the His tag (FXIIIa is activated by thrombin; section 1.3.3). This new construct was named pYF13AH_PCS, and forms the basis of the work presented in this thesis. DNA restriction and nucleotide sequence analysis confirmed the *F13A1* cDNA to be the correct expected size and sequence.

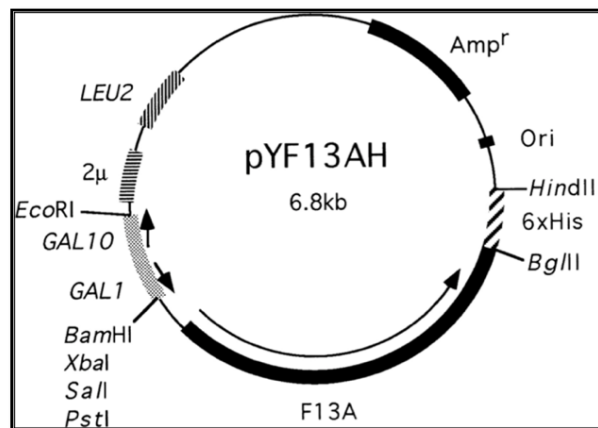


Figure 2-1: The original map of plasmid pYF13AH

A diagram illustrating the structure of the original plasmid. The F13A cDNA is shown with an extension of six histidine residues at the C-terminus. F13A cDNA expression is under the control of the *GAL*I promoter. The plasmid can be selected in bacteria using Ampicillin resistance, and in yeast via the *LEU2* auxotrophic marker, taken from (Kangsadalampai and Board, 1998b).

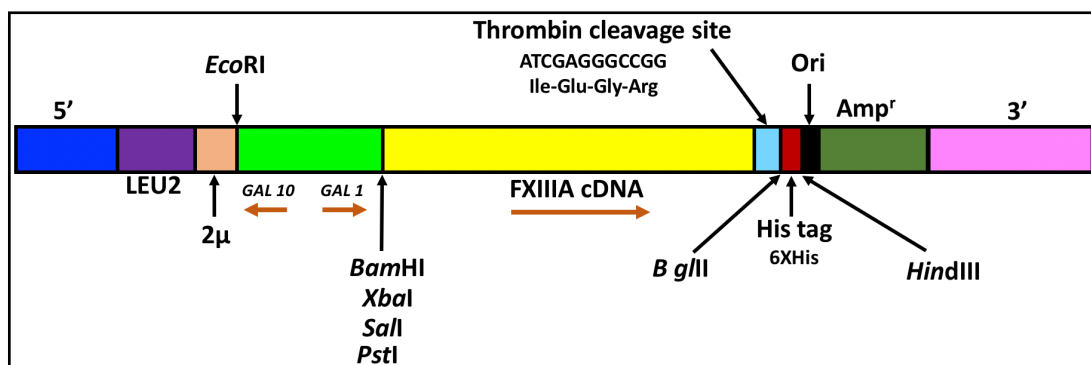


Figure 2-2: Schematic representation of vector pYF13AH_PCS

A thrombin cleavage site was inserted just prior to the His tag by Dr Anwar's laboratory, so that the His tag could be removed during the activation of recombinant FXIIIa protein variants by thrombin. The direction of transcription is given by the orange arrows.

2.3 DNA techniques

2.3.1 Restriction endonuclease digestion

The DNA substrate was cut as follows: 0.5–1.0 μg plasmid DNA, 1 unit of restriction enzyme and 1x appropriate buffer (supplied with the enzyme) were made up to final volume of 10 μL in sterile deionised water (dH₂O), and incubated at 37°C for 60 minutes. The digestion products were separated by molecular weight using 1% agarose gel electrophoresis. All enzymes and buffers were purchased from Promega, Madison, USA unless otherwise stated.

2.3.2 Polymerase Chain Reaction (PCR)

All primers were purchased from Sigma-Aldrich and prepared to a final concentration of 100 mM using nuclease-free water (Ambion, Cat No. AM9937, Fisher Scientific). Table 2-1 lists primers used in PCR. A 5x primers mastermix was prepared by adding: 10 μL of 100 mM Forward primer, 10 μL of 100 mM Reverse primer, and 180 μL of nuclease free water and stored at –20°C. PCR reaction was performed in a total volume of 10 μL by adding 5 μL of HotShot Diamond PCR Mastermix (Clontech Life Science, Stourbridge, UK), 2 μL of 5x primers mastermix and 3 μL of plasmid DNA template or OC cell lines cDNA (30 ng per reaction). PTC-200 Thermal Cycler (MJ Research, DNA Engine, Ramsey, USA) was used to perform the PCR reactions as shown in Table 2-2. On completion of PCR amplification, agarose gel electrophoresis was used to visualise PCR products (section 2.3.3). Depending on the size of the PCR product produced, agarose concentrations ranged from 1.5 to 3%.

Table 2-1: Primer sequences used for *F13A1* and *TG2* exons amplification

Oligo Name	Sequence 5'– 3'	length (bp)	Tm°	PCR Product size (bp)
<i>F13A1_</i> Ex13_ F	CAAGCCGGCGAGTACATGG	19	62	402
<i>F13A1_</i> Ex15_ R	CACGTCCAGCTCGCCATAC	19	62	
<i>TG2_</i> Ex8_ F	CGTGACCAACTACAACCTCGG	20	62	202
<i>TG2_</i> Ex9_ R	CTCTTCTCCTGGGGCGTTG	19	62	

Table 2-2: PCR Reaction Procedures

Step	Temperature	Time
1. Hot start	96°C	6 minutes
2. Denaturation	92°C	2 minutes
3. Annealing	62°C	1 minute
4. Elongation	72°C	2 minutes
Steps 2-4 were repeated 39x cycles		
Final cycle for 2 minutes at 92°C, 1 minutes at the annealing temperature		
Final extension	72°C	10 minutes
Hold	4 – 15°C	15 minutes

2.3.3 Agarose gel electrophoresis

Agarose gels were made by mixing molecular-grade agarose (Seakem LG Agarose, Cat No: 50004, Lonza, Basel, Switzerland) in 1x Tris-acetate EDTA (TAE) buffer (10 mM Tris-HCl pH 8.0, 0.1 mM EDTA) final concentration. The fluorescent intercalating dye, EtBr (0.5 µg/mL) was added to the melted agarose and poured into a mould with an appropriate comb to create the wells. 6X DNA loading buffer (Life Technologies, Paisley, UK) was added to the DNA samples at final 1x concentration and loaded onto the gel. GeneRuler™ 1 kb or 100 bp ladders were used as molecular weight marker. Samples were run at 100–120V for 30–45 minutes. Following electrophoresis, the DNA bands were visualised under ultraviolet-transillumination at 302 nm using the BioRad, GelDoc System.

2.3.4 Plasmid DNA quantification

The NanoDrop Spectrophotometer (Labtech International, UK) was used to read the absorbance at $A_{260\text{nm}}$ and $A_{280\text{nm}}$, using 2 μL of DNA sample. The absorbance at $A_{260\text{nm}}$ was multiplied by 50 for calculating the DNA concentration. DNA samples indicating high concentrations were diluted in $T_{10}E_1$ (10mM Tris-HCl pH 7.5, 1mM EDTA) to approximately 0.2 $\mu\text{g}/\text{mL}$, and the absorbance was read again. This was because the NanoDrop was found to give more consistent readings at lower concentrations compared to using highly concentrated DNA. The purity of the DNA was evaluated based on the ratio of absorbance at 260 nm and A 280 nm. A ratio of 1.8 indicates pure DNA; whereas, samples contaminated with proteins have a lower ratio.

2.3.5 Transformation into E-Coli cells

E.coli strain DH5 α chemically competent cells product code. 500173 (Genotype: F Φ 80/*lacZ* Δ M15 Δ (*lacZYA-argF*) U169 *recA1 endA1 hsdR17*(r_k^- , m_k^+) *phoA supE44 thi-1 gyrA96 relA1* λ^-) were transformed with the desired plasmid according to the manufacturer's instructions (Life Technologies Ltd, Paisley, Scotland, UK). Briefly, competent cells were thawed on ice and 20 ng of plasmid DNA was added to 50 μL of cells followed by incubation on ice for 30 minutes. Cells were heat shocked at 42°C for 20 seconds to enable the uptake of plasmid DNA and incubated on ice for 2 minutes. Pre-warmed 950 μL of SOC media (0.5% Yeast extract, 2% Tryptone, 10 mM NaCl, 2.5 mM KCl, 10 mM MgCl_2 , 10 mM MgSO_4 , 20 mM Glucose) was added to the mix. The tubes were incubated at 37°C, 200 rpm for 60 minutes. 100–200 μL of the transformed cells were plated on LB agar containing ampicillin (100 $\mu\text{L}/\text{mL}$). Plates were incubated at 37°C overnight (O/N). Colonies were counted the next day and transformation efficiencies were determined (section 2.17.3).

2.3.6 Plasmid DNA mini-preps

Single colonies of recombinant *E.coli* cells were inoculated in 10 mL of Terrific Broth (Al-Jallad et al.) medium (1.2% Tryptone, 2.4% Yeast extract, 0.4% Glycerol, 0.17 mM KH_2PO_4 monobasic, 0.72 mM K_2HPO_4 dibasic) plus Ampicillin (100 $\mu\text{g}/\text{mL}$ final concentration) and grown in an orbital shaker at 37°C, 200 rpm overnight. 5 mL of the starter culture was used to prepare plasmid DNA using the Sigma GenElute™ plasmid mini-prep kit (Sigma-Aldrich Company Ltd, Gillingham, UK) according to the manufacturer's instructions. Plasmid DNA was quantified using the NanoDrop Spectrophotometer (section 2.3.4). The quality of the mini-prep was assessed by

restriction digestion of 0.5 µg of the prepared plasmid and analyses by agarose gel electrophoresis (section 2.3.1 and section 2.3.3) respectively.

2.3.7 Plasmid DNA maxi-prep

A 10 mL starter culture of recombinant *E.coli* cells was grown overnight as described for a mini-prep (section 2.3.6). 5 mL of this culture was added to 400 mL of TB medium containing Ampicillin (100 µg/mL final concentration) in a 2-litre flask to ensure good aeration and grown overnight at 37°C, shaking at 200 rpm. Cells were harvested and plasmid DNA purified using the Qiagen Maxi plasmid prep kit (Qiagen, Manchester, UK) according to the protocol in the kit manual. Purified plasmid DNA was quantified and analysed as for the plasmid mini-preps.

2.3.8 Sanger sequencing

The sanger sequencing service provided by Source Bioscience was employed to check the constructs (SourceBioscience, 2021). Plasmid DNAs and primers (Table 2-5) were supplied to Source Bioscience at the required concentrations. Following the processing of the samples the data was returned as electropherograms, and then analysed using 4Peaks software (Figure 2-3).

2.3.9 Site-directed mutagenesis

The plasmid constructs essential for this study are displayed in Table 2-3. The Wildtype (WT), 34L, 650I and 651Q single mutants were already available in the laboratory, however, the double mutant (DM) 650I_651Q needed to be made. The plasmid pYF13AH_PCS_651Q was used as a template to make the DM plasmid (pYF13AH_PCS_650I_651Q). This plasmid has already contained *F13A1* gene polymorphism (CAG) at codon 651, therefore, substitution was only required for 650 codon. In order to substitute F13A cDNA 650GTT for 650ATT, relevant nucleotide within F13A cDNA was mutated (G>A) using site-directed mutagenesis. 50 ng of pYF13AH_PCS_651Q plasmid DNA containing F13A cDNA template target for mutation was first amplified with mutagenic primers listed in Table 2-4 at 100 pm/µL each, 5 µL reaction buffer (Q5 NEB No B927G 5x), 1 µL of deoxynucleotide triphosphate (dNTP) mix, 2 units of Q5 High-Fidelity DNA polymerase (NEB No M0491G 2,000 U/mL), and molecular-grade dH₂O up to a final volume of 50 µL in a PCR reaction tube. 15 amplification cycles were performed (95°C for 0.5 minute, 55°C for 1 minute, 68°C for 7 minutes) followed by a single extension cycle at 68°C

for 10 minutes. This has led to the mutagenic primers being extended, copying the DNA template, resulting in nicked circular strands. After the completion of PCR, the mixture containing the methylated, non-mutated parental DNA template was digested using 10 units of *DpnI* (Promega, Southampton, UK) at 37°C for 60 minutes, as this restriction enzyme is specific for methylated DNA. The digested PCR mixture was stored at 4°C until transformation into *E.coli* DH5α cells (section 2.3.5). Following the transformation, four colonies were cultured for plasmid mini-preps as detailed in Section 2.3.6. Following the plasmids maxi-preps (section 2.3.7), Sanger sequencing analysis (section 2.3.8) was performed using primers that generated a sequence covering the whole F13A cDNA, in both orientation where possible in each of the vectors used in the project to ascertain each clone only carried the desired sequence (Figure 2-3).

Table 2-3: Plasmid Constructs required for the project

F13A1 Gene Variant (amino acid number)	Codon	Amino acid
1. Wildtype (³⁴Val_⁶⁵⁰Val_⁶⁵¹Glu)	³⁴ GTT_ ⁶⁵⁰ GTT_ ⁶⁵¹ GAG	34V_650V_651E
2. V34L (³⁴Leu_⁶⁵⁰Val_⁶⁵¹Glu)	³⁴ TTG	34L
3. V650I (³⁴Val_⁶⁵⁰Ile_⁶⁵¹Glu)	⁶⁵⁰ ATT	650I
4. E651Q (³⁴Val_⁶⁵⁰Val_⁶⁵¹Gln)	⁶⁵¹ CAG	651Q
5. 650I_651Q Double Mutant (³⁴Val_⁶⁵⁰Ile_⁶⁵¹Gln)	⁶⁵⁰ ATT_ ⁶⁵¹ CAG	650I_651Q

This table displays the plasmid constructs required for this study. The WT, V34L, V650I and E651Q variants were already available in the laboratory, but the F13A cDNA sequences in these clones was verified for reassurance. *E.coli* DH5α cells were transformed with each of these plasmids, and maxi plasmid DNAs prepared as described under Methods (section 2.3.5). Sanger sequencing was performed using primers that generated sequence covering the whole F13A cDNA, in both orientation where possible. Results obtained are detailed in section 2.4.

Table 2-4: Primer sequences used for mutagenesis

Oligo Name	Sequence 5'– 3'	Length (bp)	Tm°
F13A 650 + 651 F	GACTGTGACAATTCAGTTTACCAA	24	64
F13A 650 + 651 R	TTGGTAAACTGAATTGTCACAGTC	24	66

This table shows the forward and reverse primers used for generating the DM plasmid are listed with their 5'–3' sequence. Abbreviations: F: Forward, R: Reverse, (bp): base pairs length, and (Tm°): Annealing temperature.

Table 2-5: Sequences of primers used to amplify F13A1 cDNAs

Oligo Name	Sequence 5' – 3'	Length (bp)	Tm°
G8928 C1	AACGTGAATTCCAAACTCACCA	22	62
G8929 C2	CTTCTTGAATTCTGCCTTCAGG	22	64
G8930 D1	CCAACGTCGACATGGACTTTGAAG	24	70
G8933 A2	AGCTCAAGCTTCTGGTCTTGATGT	24	64
G8934 B1	AACCAGTCGACACCCAGAAACAGA	24	72
G8935 B2	GTCCAAAGCTTGCCAGCCTCCAAA	24	74
H0518 A1ii	AAGTCAAAAATGTCAGAAACTTCC	24	58
RA1	TCGGGAAACCTGTCGTGCCA	20	64
RA2	GAAGTCTCTTCTGCCTCCAA	21	64
RA3	AGCACATCCCCCTTTCGCCA	20	62
RA4	TAAGGGATTTTGGTCATGAGA	21	58
RA5	AGCGTTGATGATTCTTCATTGG	22	60
RA6	TCCAGTTCGATGTAACCCACTC	22	66
RA7	CTTCCTTCAGCACTACCCTTT	21	60
RA8	GGTGCTGCTATCGATGCTAC	20	62

This table shows the forward and reverse F13A cDNA specific primers and 'walk out' primers used for sequencing plasmid constructs F13AH_PCS listed with their 5'–3' Sequence. Abbreviations: (bp): base pairs length, and (Tm°): Annealing temperature.

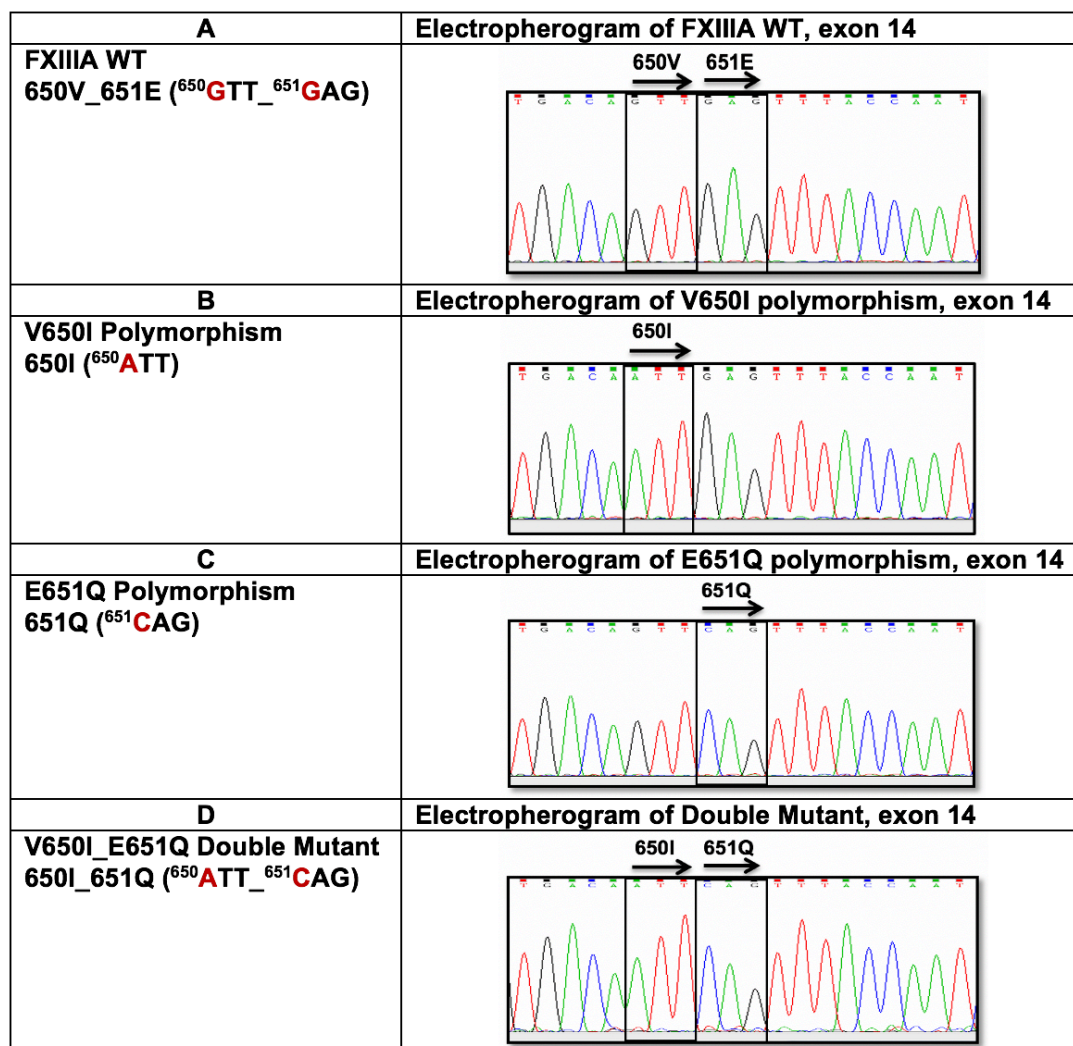


Figure 2-3: Plasmid constructs sequence confirmation

Representative electropherograms of *F13A1* exon 14 sequencing traces for FXIII A plasmid DNA constructs which were created using 4Peaks software. **A)** The electropherogram obtained for pYF13AH_PCS WT plasmid DNA clearly shows the codon sequences at positions 650_651 to be **GTT_GAG**. **B)** The electropherogram obtained for pYF13AH_PCS_650 plasmid DNA clearly shows the codon sequences at position 650 to be **ATT**. **C)** The electropherogram obtained for pYF13AH_PCS_651 plasmid DNA clearly shows the codon sequences at position 651 to be **CAG**. **D)** The electropherogram obtained for pYF13AH_PCS 650_651 DM plasmid DNA clearly shows the codon sequences at positions 650_651 to be **ATT_CAG**.

2.3.10 Generation of FXIII A negative control construct

FXIII A negative control vector (FXIII A NC) was generated as a control for the *in vitro* cell biology work. pYF13AH_PCS WT⁶⁵⁰GTT⁶⁵¹GAG was the parental plasmid. *Bam*HI restriction enzyme was chosen because it cuts within F13A cDNA coding region at 4307 bp and outside the coding region at 3434, just 41 bp before the start of the open reading frame (ORF) which spans from 3475 bp to 5703 bp (Appendix I). Once the plasmid is cut, the ORF will be incorrect, since it will be missing an 832 bp fragment from the start. The length of the fragment cut by *Bam*HI is 873 bp from the whole plasmid (Figure 2-4). The *GAL*I promoter (2980 bp to 3430 bp) has been incorporated 45 bp upstream of the ORF in the pYF13AH plasmid. It controls the transcription of the plasmid in transformed cells. Following digestion with *Bam*HI, the transcription initiation site will be missing, therefore F13A cDNA will not be transcribed.

20 U of *Bam*HI was used to cut F13A cDNA at 3434 bp and 4307 bp sites producing two fragments with size of 7765 bp and 873 bp respectively (Figure 2-5). Following the standard electrophoresis procedure, a minimal area containing the 7765 bp DNA fragments was cut from the agarose gel using a clean scalpel. The excised fragments were then rapidly and efficiently purified using the PureLink™ Quick Gel Extraction Kit (ThermoFisher Scientific, Cat No: K210012) as per the manufacturer's instructions. After purification, the DNA was quantified by NanoDrop (Section 2.3.4). 2.46 µg DNA was obtained from 3.6 µg band in agarose pieces, therefore the yield was 68.3%. T4 DNA ligase (Promega, USA, Cat. No: M180A) was used to ligate the purified DNA. 135.5 ng of DNA template, 1.5 µL of T4 DNA ligase, 1 µL of 10x T4 buffer (supplied with enzyme) were made up to final volume of 10 µL in sterile dH₂O and incubated O/N at 4°C. The next day the quality of purified ligated DNA was checked on 1% agarose gel. 3 volumes of 100% ethanol and 0.1 volume of 2 M Sodium acetate pH 5 were added to 100 µL diluted T4 DNA ligase and DNA mix. The sample was mixed well by vortexing and precipitated O/N at -20°C. Following incubation, the DNA was pelleted by centrifugation at 12000g, 4°C for 15 minutes. The pellet was washed twice with ice-cold 75% ethanol, followed by spinning at 4°C for 10 minutes each. This step was followed by quick spin at full speed, 4°C for 10 seconds to remove ethanol. DNA pellet was air-dried and resuspended in 10 µL of T₁₀E_{0.1} (10 mM Tris-HCl pH 7.5, 0.1 mM EDTA) buffer. The next day, the DNA was transformed into DH5α cells according to protocol (Section 2.3.5). Clones containing the desired DNA fragments were identified by colony PCR using primers designed to target this region with complementary sequence (Table 2-6). A single bacterial colony was taken from

an ampicillin selection plate using a sterile pipette tip and gently dabbed onto fresh plate, then the same tip was mixed into a 10 μ L final volume reaction mix used to amplify DNA. PCR setup and protocol as detailed in Section 2.3.2. Nucleotide sequence analysis confirmed the new construct is lacking 873 bp fragment including the transcription initiation site; therefore, FXIII A protein will not be produced.

Table 2-6: Primers used for colony PCR

Oligo Name	Sequence 5' - 3'	Length (bp)	T_m[°]
Neg Plasmid _F	AGTAACCTGGCCCCACAAAC	20	62
Neg Plasmid _R	TTGCGGGTATTCCAAGGCAT	20	60

This table shows the forward and reverse primers used for colony PCR listed with their 5'–3' sequence. Abbreviations: F: Forward, R: Reverse, (bp): base pairs length, and (T_m[°]): Annealing temperature.

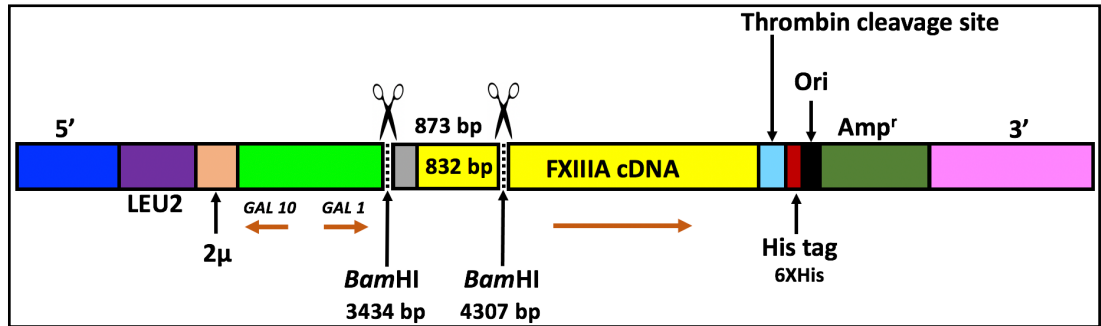


Figure 2-4: Schematic representation of FXIII A negative control vector

*Bam*HI restriction digestion was used to remove 873 bp fragment from pYF13A_PCS WT plasmid to generate FXIII A NC vector. FXIII A protein will not be produced by the new construct since the removed fragment contains the transcription initiation site and the beginning of the FXIII A ORF. The direction of transcription is given by the orange arrows.

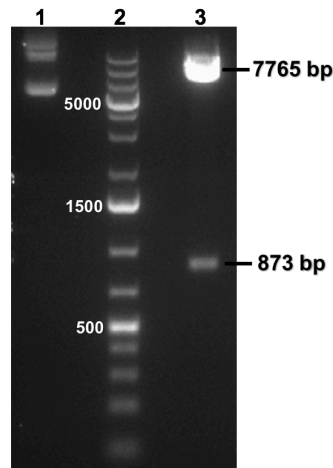


Figure 2-5: FXIII A NC restriction mapping

10 μ g of pYF13AH_PCS WT plasmid was digested with *Bam*HI, the restriction products analysed on a 1% agarose gel against 1kb DNA ladder (GeneRuler™). Lane 1, pYF13AH_PCS WT uncut; Lane 2, molecular weight marker, 1kb DNA ladder; Lane 3, pYF13AH_PCS WT plasmid DNA cut with *Bam*HI producing two fragments 7765 bp and 873 bp respectively, as expected.

2.4 Construction of AH22 yeast recombinant clones

The development of a method for preparing yeast competent cells and transforming these cells requires an in-depth understanding of the AH22 yeast strain's growth properties (Becker and Guarente, 1991). Hence, a yeast growth curve experiment was designed to determine the optimal growth phase for yeast competent cells, as well as the proper optical density at a suitable time.

2.4.1 AH22 yeast strain growth curve

It has been reported that the initial yeast cell concentration influences the growth pattern of *Saccharomyces Cerevisiae* (Asaduzzaman, 2007). Therefore, it was important to establish an optimal protocol for culture of yeast cells prior to performing a growth curve experiment that can ultimately be influenced by the starting culture. Consequently, two experiments were conducted to determine an appropriate growth curve experiment. The results of these experiments showed that starting with an O/N culture diluted to an OD₆₀₀ of 0.4 offered useful data, with all three phases of the growth curve were visible. A growth curve for AH22 was then performed in triplicates. All three growth curves obtained appeared to be very similar displaying clear lag, log and stationary phases as expected. The cultures were monitored for up to 90 hours, and the OD₆₀₀ remained constant at around 8.0 for the stationary phase.

2.4.2 Preparation and storage of AH22 competent cells

100 µL of an O/N AH22 culture (Single colony inoculated in 10 mL of Yeast Extract–Peptone–Dextrose (YPD) medium in a 50 mL Falcon tube, shaken at 200 rpm at 30°C) was added to 200 mL of fresh YPD medium in 1 L flask and grown O/N shaken at 200 rpm at 30°C. The culture reached near mid-log phase after ~15 hours (OD₆₀₀ = 3.2). Cells were harvested by centrifugation at 4000 rpm for 15 minutes at 4°C in 4x 50 mL Falcon tubes. The cell pellets were resuspended in 0.01 volume of the original culture volume in filter-sterilised freezing competent cells solution (5% sterile glycerol, 10% DMSO). 100 µL of cells were then transferred to a new 1.5 mL eppendorf tube. To assist slow freezing, tubes were placed in a Styrofoam box at –80°C.

2.4.3 Transformation of AH22 yeast strain

Transformation of yeast was performed using two methods. Firstly, by the method of electroporation (as per instruction manual for Gene Pulser Xcell™ Electroporation System, BioRad UK). Nevertheless, this was only effective after cells were permitted to recover for a prolonged period following the electroporation phase. Subsequently, a different method using Lithium acetate (LiAc), polyethylene glycol 3350 (PEG) and single-stranded (SS) carrier DNA was employed as described in (Gietz and Schiestl, 2007).

2.4.3.1 Transformation of AH22 yeast strain by Lithium acetate (LiAc), PEG and SS carrier DNA

100 µL of an O/N AH22 culture was added to 200 mL of fresh YPD medium and grown O/N. The culture reached near mid-log phase after ~15 hours ($OD_{600} = 3.2$). Cells were harvested by centrifugation at 4000 rpm for 15 minutes at 4°C. The cell pellet was resuspended in 25 mL of sterile cold dH₂O to wash the cells, and the cells pelleted as before. This wash step was repeated once more and then the cell pellet was resuspended in 1 mL of sterile dH₂O and cells transferred to a 1.5 mL eppendorf. Cells were spun down at 13000 rpm for 0.5 minutes and resuspended in 1 mL of H₂O. 100 µL of cells were then transferred to a new eppendorf tube, spun as before and the supernatant discarded. This cell pellet was now resuspended in 336 µL of transformation mix (this contains 240 µL of 50% PEG, 36 µL of 1.0 M Lithium acetate, 50 µL of 2 mg/mL denatured salmon sperm carrier SS DNA). 34 µL of plasmid solution containing the required amount of DNA was then added to the cells and tubes incubated at 42°C for the desired time. Following this, cells were spun at 13000 rpm for 0.5 minutes and resuspended in 1.0 mL of H₂O. 10 µL and 100 µL of transformed cells were plated on selective YNB+His medium (Appendix I) and plates incubated at 30°C. Colonies became visible after two days and were counted to determine transformation efficiency (Section 2.11.2). Two concentrations of plasmid DNA were tested (200 ng and 680 ng) and incubated at 42°C for 40 minutes and 60 minutes since the optimal plasmid DNA concentration and incubation time for AH22 were unknown at the time. The transformation efficiencies obtained for the first transformation experiment showed that all transformations performed yielded colonies on selective media, with the exception of the minus DNA negative control. Even though the variation in efficiency between different plasmids ranged between 0.18×10^5 to 10.3×10^5 (over 50 times), there appeared to be no clear dependence on the specific plasmid, the amount of DNA used or the incubation temperature. Two further experiments confirmed this hypothesis.

2.5 Expression of F13A cDNA

2.5.1 Growth pattern of AH22 recombinant cells

Optimal expression is obtained when cells are grown to early log phase and then the *GALI* promoter is induced with Galactose (Bergman, 2001). A growth curve was carried out on one recombinant clone to assess if growth pattern differed from that of AH22, and to appropriately plan the induction experiment. AH22 carrying the pYF13AH_PCS_650I plasmid was chosen for this purpose, and cells were cultured (and their growth monitored) as described for AH22 in (Section 2.4.1). Furthermore, recombinant AH22 cells continued to grow after the log phase, although at a slower rate, and did not appear to reach a true stationary phase even after over three days of culturing. As cells entered log phase at OD₆₀₀ of 1.0, it was decided to start the induction with Galactose at this point of the growth phase.

2.5.2 Expression of recombinant FXIIIa protein

A protocol was developed based on the understanding of the features of AH22 yeast strain growth pattern. A week before the experiment, some fresh cells were grown on minimal selective medium YNB+His plates to ensure cell viability. A large quantity of cells were scraped off the selective medium plate and grown O/N at 30°C, 200 rpm, in 10 mL of Yeast Extract – Peptone (YP) medium containing 2% Raffinose. The absorbance of the O/N culture was read at 600 nm using YP medium + Raffinose as a blank. The culture was diluted appropriately to give an OD₆₀₀ of 0.25 in 25 mL YP with 2% Raffinose medium (two 50 mL Falcon tubes were made). The culture required growth at 30°C, at 200 rpm for about four hours to reach the required OD₆₀₀ of ~ 1.0. FXIIIa protein expression was induced by switching on the *GALI* promoter using 1.25 mL of 0.22 µm filter-sterilised 40% Galactose (for a final concentration of 2%). The cultures were optimised to grow for approximately 48 hours.

2.5.3 Production of yeast cell lysates

Before beginning the cell lysis process, all reagents were cooled to 4°C, including lysis buffer (50 mM HEPES pH 7.5, 150 mM NaCl, 1 % Triton X-100, 1 mM Phenylmethylsulphonylfluoride [PMSF]), glass beads (0.5 mm diameter, Bio Spec products, UK) and 50% sterile glycerol. Eppendorf 5810 R centrifuge rotor was cooled to 4°C prior to use. All tubes were weighed prior to use in order to facilitate calculation of the weight of wet cell pellets. The culture was transferred to 50 mL Falcon tubes on ice and allowed to cool before harvesting cells by centrifugation at 4000 rpm for 15 minutes, at 4°C. The supernatant was poured off without disturbing the cell pellets. The tubes were then re-weighed to determine the cell pellets weight. The cell pellets were resuspended in lysis buffer (0.5 mL Lysis buffer per 1.0 g of wet cell weight). 2 mL eppendorf tubes were half-filled with cold beads and the tube was then filled right to the top with cell suspension to avoid frothing. Whirl-mixing/vortex operated for a total of 3–6 minutes (30 seconds on, 30 seconds off) up to a maximum of 12 minutes. Cell lysis was checked under a light microscope. Cell lysates were removed into fresh 1.5 mL eppendorf tubes. An appropriate amount of sterile 50% glycerol was added to give a final concentration of 20%. The lysates were stored at – 20°C in 50 µL aliquots until analyses. Upon thawing, the lysates were centrifuged again to ensure only the clear lysate phase was used in any further experiments.

2.6 Generation of heterozygous model of FXIII A V34L variant

AH22 yeast strain was also used to generate heterozygous (Ht) model of V34L at residue 34 (34L + 34V) to study the role of this genotype in EOC. Equal amounts of 34V plasmid (FXIII A WT) and 34L plasmid (Table 2-3) were mixed and used to transform AH22 as detailed in (Section 2.4.3.1). Recombinant cells were cultured and lysates of soluble proteins prepared as before (Section 2.5.3).

2.7 Protein techniques

2.7.1 Purification of recombinant FXIIIa protein variants

FXIIIa protein variants were purified by gravity-flow chromatography under native conditions using Nickel-Nitrilotriacetic acid (Ni-NTA) Agarose (Cat No. 30210, Qiagen). Ni-NTA resin was chosen as a purification method for its high affinity, increased binding capacity (up to 50 mg His-tagged protein/mL resin), and minimal nonspecific binding to the His-tagged proteins. The process consisted of four stages: equilibration, binding, washing, and elution. 400 μ L of the Ni-NTA resin was pipetted into 2 mL eppendorf tube, centrifuged briefly at 12,000 g for 1 minute at 4°C, and the supernatant was discarded. The resin were equilibrated by adding 850 μ L of equilibration buffer (20 mM Hepes, 0.3 M NaCl, 20 mM imidazole), mixed gently using a rotatory shaker at 50 rpm for 5 minutes at RT, then centrifuged briefly at 12000 g for 1 minute at 4°C, and the buffer was discarded using a pipette. The equilibration step was done twice. The equilibrated agarose was then loaded onto 2 mL Pierce™ Disposable Columns (Cat No. 29920, ThermoFisher Scientific) following the packing of the columns as per the manufacturer's instructions and was allowed to settle for 30 minutes on ice. FXIIIa yeast cell lysates were prepared as detailed in section 2.5.3. 400 μ L of yeast cell lysate was gently mixed with 1200 μ L of equilibration buffer by pipetting up and down. The mixture (lysate + equilibration buffer) was then slowly added to the equilibrated resin in the column without disturbing the resin with the bottom outlet capped, and allowed to bind for 60 minutes on ice. The bottom cap of the column was removed, and the column flow-through (FT) was collected into a sterile 1.5 mL eppendorf tube. The FT was gently re-loaded into the column, allowed to settle, and re-collected. This step was repeated five times. The last FT was saved for analysis by sodium dodecyl sulphate polyacrylamide gel electrophoresis (SDS-PAGE). Following the binding step, the resin was washed with 7 mL washing buffer (20 mM Hepes, 0.3 M NaCl, 20 mM imidazole), and wash fractions were collected for analysis. Another washing step, using 5 mL of (20 mM Hepes, 0.3 M NaCl, 50 mM imidazole), was performed to minimise nonspecific binding and reduce the quantity of contaminating proteins. 1 mL wash fractions were collected for analysis. The amount of protein in the wash fractions was quantified directly by measuring OD₂₈₀ and found to be negligible. FXIIIa protein variants were eluted using 1 mL of elution buffer (20 mM Hepes, 0.3 M NaCl, 250 mM imidazole). The elution buffer was added to the washed resin, incubated for 10 minutes at RT. The eluate fractions were collected into 4–6 sterile 1.5 mL eppendorf tubes and analysed by SDS-PAGE.

2.7.2 De-salting of FXIIIa purified protein

Buffer-exchange using Pierce™ protein Concentrator PES, 30K MWCO, 0.5 mL columns (Cat. No 88502, Thermo Scientific™, USA) was performed to remove imidazole and de-salt FXIIIa purified variants. The columns were sterilised by submerging them into 70% ethanol solution for 10 minutes at RT; they were then prepared by immersion onto 0.22 µm filter-sterilised elution buffer without imidazole (20 mM Hepes, 0.3 M NaCl). The tubes, and the polyethersulfone (PES) membranes of the columns were tested by adding buffer only and centrifugation at 12,000 g for 1 minute at RT before the addition of the purified protein. FXIIIa pure fractions were pooled, and a maximum of 500 µL was added to the columns at any time and centrifuged at 10,000 g at 4°C for 30 seconds, 60 seconds, 90 seconds and 120 seconds until most of the protein sample has gone through membrane (the stop volume was ~ 100 µL above the membrane level). Elution buffer without imidazole was added to a maximum of 500 µL, centrifuged at 10,000 g at 4°C for 1–2 minutes. Buffer-exchange step was repeated four times.

2.7.3 SDS-PAGE

The Sodium dodecyl sulphate polyacrylamide gel electrophoresis (SDS-PAGE) was carried out to separate proteins by their molecular weight prior to protein staining by Coomassie brilliant blue R-250 or western blotting (WB) techniques. Samples preparation was carried out using 4x Bolt™ lithium dodecyl sulphate (LDS) sample buffer (Cat. No: B0007, Invitrogen™, ThermoFisher Scientific) and 10x Bolt™ sample reducing agent (Cat. No: B0009, Invitrogen™, ThermoFisher Scientific) to the required concentration in a final volume of 30 µL. Samples were heated at 70°C for 10 minutes to denature proteins and break the disulphide bonds. Mini Gel Tank (Cat. No: A25977, ThermoFisher Scientific) was assembled as per the manufacturer's instructions, and the chambers were filled with 1x Bolt™ MES SDS running buffer prepared from 20x stock (Cat. No: B0002, Invitrogen™, ThermoFisher Scientific) using sterile dH₂O. Reduced samples (30 µL) were loaded onto pre-cast Bolt™ 4-12%, Bis-Tris, 1.0 mm, Mini protein gel, 10-well or 15-well (Cat. No: NW04120BOX, or Cat. No: NW04125BOX, Invitrogen™, ThermoFisher Scientific) with 7 µL of SeeBlue™ Plus2 Pre-stained Protein Standard (Cat. No: LC5925, Invitrogen™, ThermoFisher Scientific) molecular weight marker which contains 10 recombinant proteins of known sizes from 4-250 kDa. Electrophoresis was performed at 80 V for four hours at RT.

2.7.4 Western Blot

Samples were separated by SDS-PAGE as described above in section 2.7.3. Following electrophoresis, gel cassettes were removed and rinsed briefly with dH₂O. Polyvinylidene-difluoride (PVDF) membrane of 0.45 µm pore size (Cat. No: 88518, Invitrogen™, ThermoFisher Scientific) was cut to 9x9 cm and pre-wetted in methanol for 30 seconds, rinsed briefly with dH₂O and equilibrated in 1x Bolt™ transfer buffer made from 20x stock (Cat. No: BT0006, Invitrogen™, ThermoFisher Scientific) using sterile dH₂O and supplemented with Bolt™ antioxidant (Cat. No: BT0005, Invitrogen™, ThermoFisher Scientific) for 5 minutes. Sponge pads and filter papers were pre-soaked in 1x transfer buffer before assembling the blotting sandwich using the Mini Blot Module (Cat. No: B1000, Invitrogen™, ThermoFisher Scientific) in the following order: Cathode core (-) – sponge pad – filter paper – SDS-PAGE gel – PVDF membrane – filter paper – sponge pad – Anode core (+). The two module halves were pressed together and inserted into the tank. The transfer was performed at 20 V for 2 hours, followed by blocking step with 5% non-fat dried milk (NFDM) in PBS for 2 hour at RT to prevent nonspecific binding of antibodies during incubation periods. Membrane was incubated O/N at 4°C with primary antibody: Atlas antibodies (Cat. No HPA001804) at 1:500 dilution in 5% NFDM in PBS. The following morning, the membrane was washed 3 x 10 minutes with PBS, and then incubated for two hours at RT in a roller with the secondary antibody: HRP conjugated antibody against the primary species (goat anti-rabbit HRP) at 1 in 2000 dilution in 10 mL blocking solution. Following 3 x 10 minutes washings, the membrane was incubated with chemiluminescent substrates: SuperSignal West Femto Maximum Sensitivity Substrates (Cat. No: 34095, ThermoFisher Scientific) at a ratio 1:1 for 5 minutes at RT to detect Horseradish peroxidase (HRP) conjugated in the secondary antibody. Blots were imaged by chemiluminescent using BioRad ChemiDoc MP imager.

2.7.5 Coomassie brilliant blue R-250 staining

One of the triphenylmethane dyes, Coomassie brilliant blue R-250, was used to visualise stained protein samples. It binds to proteins through ionic interactions between the dye sulfonic acid group and positive protein amine groups in acidified solutions. Coomassie blue R-250 can detect as little as 0.1 µg of protein. Following SDS-PAGE, the gel was removed from the cassette and incubated in a fixing solution (50% Methanol, 10% acetic acid) for one hour at RT in a shaking platform. The gel was stained by immersion in a staining solution containing 0.025% Coomassie dye in 10% acetic acid O/N at RT in a shaking platform. The gel was de-stained in 10%

acetic acid solution using gently shaking platform until the background was clear. The bands began to appear in around one to two hours. Images of the gel were obtained using Bio-Rad ChemiDoc™ MP Imager. The gel was stored in 10% acetic acid solution at 4°C.

2.7.6 Factor XIIIa activity assay

The FXIII activity assay depends on its TG activity, which catalyses the cross-linking reaction between the 5-(Biotinamido)pentylamine [BAPA], providing the Lysine to the reactive Glutamine residue(s) available in the fibrinogen or other FXIIIa substrate. This assay was developed and established within Dr Anwar's laboratory, and is very sensitive, requiring only 1 µL of standard human plasma (Anwar et al., 1999). An adapted version of this in-house FXIIIa activity assay was used. The modifications performed include optimisation of the 5-biotinamino pentylamine and thrombin final concentrations to 60 µM and 10 units/mL respectively.

2.7.6.1 Protocol

96-well microtiter plates (Immulon® 1B Part No. 3355, Thermo Scientific, USA) were coated with 100 µL/well of fibrinogen [Cat No. F8630, Sigma- Aldrich] at 40 µg/mL in 1x TBS buffer (40 mM TBS pH 8.3, 140 mM NaCl, and 0.01% Sodium azide) for 1 hour at RT or O/N at 4°C. The fibrinogen solution was removed and the plates were blocked with 200 µL/well of 0.5% non-fat dried milk (NFDM) in 1x TBS for 60 minutes at room temperature and then washed three times with 1x TBS. 10 µL standard human plasma (diluted 1 in 10), FXIIIa yeast lysates (diluted 1 in 200), mammalian cell lysates (neat), or purified FXIIIa protein variants (diluted 1 in 10) were added to designated wells. All samples were diluted in 1x TBS buffer. 90 µL of the master mix containing 1 mM CaCl₂, 0.5 mM DTT, 60 µM 5-(Biotinamido)pentylamine, 10 U/mL thrombin were added to each well using multichannel pipette for 0–35 minutes, at 5 minutes intervals. The reaction was performed at RT in duplicate wells for each time point, and stopped at various time points by the addition of 200 µL of 200 mM EDTA to chelate calcium ions. For time = 0, EDTA was added to the wells prior to the addition of the master mix reagents. The plates were then rinsed three times with 1x TBS. 100 µL of streptavidin-alkaline phosphatase conjugate (1 mg/mL solution in 0.5% NFDM in TBS) was added to each well, and the plates incubated for 1 hour at RT. The plates were washed three times with TBS containing 0.01% Triton™ X-100, followed by two rinses with TBS. To each well, 100 µL of alkaline phosphatase substrate, p-nitrophenol phosphate at 1 mg/mL in 1M diethanolamine, pH 9.8,

containing 0.5 mM MgCl₂, was added and the colour development performed at RT. The colour development reaction was stopped by the addition of 100 µL of 4 M NaOH. The absorbance was then read at 405 nm using BertholdTech Mithras, Driver version:1.05, (1.0.5.0), S/N: 42-6037, Embedded Version:1.1 Multimode Microplate Reader.

2.7.6.2 Quantification

For each sample, the initial rate of generation of product is determined and the activity is calculated as a ratio of the rate observed with standard normal plasma (Lot No./Ch.-B./Lot: 502576, Dade Behring Marburg GmbH, Marburg, Germany) or the 1st International Human Factor XIII Plasma Standard, NIBSC.

2.7.6.3 Validation

Validation of the new Human FXIII Plasma Standard was achieved by performing activity assays using fresh frozen human plasma samples and calculating the intra/inter-assay variation.

2.7.7 ELISA for recombinant FXIIIA

2.7.7.1 Protocol

Sandwich ELISA was used to determine FXIIIA antigen level in yeast lysates samples and purified FXIIIA protein variants. 96-well microtiter plates (Immulon[®] 1B Part No. 3355, Thermo Scientific, USA) were coated with 100 µL/well of monoclonal anti-6X-His Tag (HIS.H8/EH158, Thermo Scientific, Cat No. MA1-21315) diluted 1 in 1000 in 50 mM Sodium carbonate (Na₂CO₃) pH 9.6 and incubated O/N at 4°C. The antibody solution was removed and the plates were blocked for two hours at RT using 150 µL blocking buffer (50 mM Tris-HCl pH 7.5, 150 mM NaCl, 1.0% Bovine Serum Albumin [BSA]). The plates were then washed four times with 200 µL washing buffer (50 mM Tris-HCl pH 7.5, 150 mM NaCl, 0.1% Tween-20). For each test yeast lysate sample, purified protein sample, and FXIIIA WT standard, a range of different dilutions were made in blocking buffer covering the maximum and minimum possible response. 100 µL/well of diluted WT standard and unknown samples were added to the plate in duplicates and incubated for 2 hours at RT. The plate was washed four times with 200 µL washing buffer prior to the addition of 100 µL/well of polyclonal Rabbit anti-FXIII A-subunit Human Placenta antibody (Cat No. 233502, Calbiochem) diluted 1 in 1000 in dilution buffer (50 mM Tris-HCl pH 7.5, 150 mM NaCl, 0.1% BSA) and incubated for two hours at RT. Following a washing step four times with 200 µL washing buffer, 100 µL/well of polyclonal Goat anti-Rabbit IgG conjugated to alkaline

phosphatase diluted 1 in 5000 in dilution buffer was added to each well and the plate incubated for two hours at RT. After a final washing step, 100 μ L/well of alkaline phosphatase substrate, p-nitrophenol phosphate (pNPP; 1 mg/mL in 1M Diethanolamine, pH 9.8 containing 0.5 mM $MgCl_2$) was added and the colour development (yellow) reaction was performed at RT. The reaction was stopped by the addition of 100 μ L of 4M NaOH. The absorbance was then read at 405 nm using Mithras LB 940 Multimode Microplate Reader.

2.7.7.2 Quantification

FXIII A WT yeast lysate was used as a standard to quantify the antigen in all pooled yeast lysate and purified protein samples. For making WT standard, recombinant WT FXIII A was expressed in *S. Cerevisiae* and lysate was prepared as per protocol (Sections 2.5.2 and 2.5.3 respectively). The functional activity of this standard was then verified using FXIII A activity assay using the 1st International Human Factor XIII Plasma Standard, NIBSC (Raut et al., 2007) and was found to be 38.59 IU/mL. The potency of FXIII A₂B₂ antigen of the international standard has been assigned as 0.93 IU/mL (Raut et al., 2007). 20 μ L aliquots were prepared and frozen at $-80^{\circ}C$. As the yeast lysate loses TG activity during storage over time, another activity assay was performed on aliquots removed from the freezer and used to determine the antigen level in the standard. Recent activity data was used for determining the antigen level in the WT standard when plotting the ELISA graphs to ensure the reliability of the results.

The amount of FXIII A antigen in each sample was quantified using a Four Parameter Logistic (4PL) curve fit appropriate for calculating concentrations from the symmetrical sigmoidal standard. The four parameters estimated to fit the curve were: the minimum value (designated as 0% response), the maximum value (designated as 100% response), the point of inflection (i.e. the point on the middle of the curve between the maximum and minimum values), and the Hill's slope of the curve. For this analysis, the standard data points (concentration versus measurement) were plotted on log-log axes and a 4PL was made through the points. Relative FXIII A antigen levels in each test sample were determined from the dilutions within the linear part of the curve as a relative quantification comparing 50% maximum binding (IC_{50}) using dilutions for each sample. The coefficient of variation percent (%CV), Standard deviation, and Standard Error were calculated for each duplicate sample. Samples outside the range of the standards or the curve were repeated using different dilutions. This analysis was achieved using MyAssays.com software (MyAssays.Com, 2021).

2.7.8 ELISA for plasma FXIII

FXIIIa antigen levels in the ICON7 translational cohort plasma samples were measured using an in-house sandwich ELISA suitable for plasma FXIII (n=90; one sample was not measured due to a lack of volume). The initial three ELISA experiments were done to identify suitable antibodies to quantify the FXIIIa level on ICON7 plasma samples.

2.7.8.1 Protocol

Ninety-six-well microtiter plates (Immulon® 1B Part No. 3355, Thermo Scientific, USA) were coated with 100 µL/well of polyclonal anti-FXIIIa antibody (Atlas antibodies, Cat. No: HPA001804) as a capture antibody diluted 1 in 1000 in 50 mM Sodium carbonate (Na₂CO₃) pH 9.6 and incubated O/N at 4°C. The antibody solution was removed and the plates were blocked for two hours at RT using 150 µL blocking buffer (50 mM Tris-HCl pH 7.5, 150 mM NaCl, 1.0% BSA). The plates were then washed four times with 200 µL washing buffer (50 mM Tris-HCl pH 7.5, 150 mM NaCl, 0.1% Tween-20). WHO 1st International Standard Factor XIII, Human (NIBSC code: 02/206, Version 6.0) was used to generate a standard curve. The standard contains 0.91 units/mL of FXIIIa, it was diluted to eight known concentrations ranging from 0.091 to 0.00056875 units/mL. Four dilutions were performed for the ICON7 plasma samples in dilution buffer (50 mM Tris-HCl pH 7.5, 150 mM NaCl, 0.1% BSA) as follows: 1 in 10, 1 in 25, 1 in 50, and 1 in 100. 100 µL/well of diluted standard and plasma samples were added to the plate in duplicate wells and incubated for two hours at RT. The plate was washed four times with 200 µL washing buffer prior to the addition of 100 µL/well of polyclonal Sheep anti-Human Factor XIII antibody (Cat. No: PAHFXIII-S, Haematologic Technologies) diluted 1 in 1000 in the dilution buffer and incubated for 2 hours at RT. Following a washing step four times with 200 µL washing buffer, 100 µL/well of polyclonal Donkey anti-Sheep IgG conjugated to alkaline phosphatase diluted 1 in 5000 in the dilution buffer was added to each well and the plate incubated for two hours at RT. After a final washing step, 100 µL/well of alkaline phosphatase substrate (pNPP; 1 mg/mL in 1M Diethanolamine, pH 9.8 containing 0.5 mM MgCl₂) was added and the colour development (yellow) reaction was performed at RT. The reaction was stopped by the addition of 100 µL of 4 M NaOH. The absorbance was then read at 405 nm using Mithras LB 940 Multimode Microplate Reader. The relative amount of FXIII on plasma samples were calculated as detailed in Section 2.7.7 above.

Table 2-7: Antibodies used in ELISA

Antibody	Company	Clonality	Isotype	Species	Dilution
Anti 6X-His Tag (HIS.H8/EH158)	Thermo Scientific [Cat No. MA1-21315]	Monoclonal	IgG2b	Mouse	1 in 1000
Anti FXIIIa subunit Human Placenta (Cat. No. 233502)	Calbiochem	Polyclonal	-	Rabbit	1 in 1000
Anti F13A1 antibody (HPA0011804)	Atlas Antibodies	Polyclonal	IgG-1	Rabbit	1 in 500
Anti-Human Factor XIII antibody (Cat. No: PAHFXIII-S)	Haematologic Technologies	Polyclonal	-	Sheep	1 in 1000
Anti-Rabbit alkaline phosphatase conjugate (Cat. No: A3687-25ML)	Sigma-Aldrich	Polyclonal	IgG	Goat	1 in 5000
Anti-Sheep alkaline phosphatase conjugate (Cat. No: A5187)	Sigma-Aldrich	Polyclonal	IgG	Donkey	1 in 5000

The table lists capture and detection antibodies used for ELISA to determine the relative amount of FXIII both in yeast lysates and plasma samples, as well as their host species, clonality and working dilutions.

2.7.9 ELISA for plasma D-Dimer

D-Dimer antigen levels in ICON7 translational cohort plasma samples (n=91) were measured using a human D-Dimer sandwich ELISA Kit (Thermo Scientific, Cat No: EHDDIMER) as per the manufacturer's protocol to quantify FXIIIa-mediated cross-linking of two D fragments of the fibrin protein. In the wells of the supplied plate, a D-Dimer specific antibody has been pre-coated. These wells are subsequently filled with samples, standards or controls, which bind to the capture antibody. The second (detector) antibody is added to the wells, followed by a substrate solution that reacts with the enzyme-antibody-D-Dimer complex to produce a quantifiable signal. The signal's intensity is related to the amount of D-Dimer contained in the sample.

D-Dimer levels were quantified using MyAssays online analysis software (MyAssays.Com, 2021). A Four Parameter Logistic (4PL) curve fit was used to calculate concentrations from symmetrical sigmoidal standards to determine the amount of unknown antigen in each sample. The standard data points (concentration vs. measurement) were plotted on log-log axes for this analysis, and a 4PL curve was fitted through them. The relative antigen level in each test sample was calculated using dilutions within the linear region of the curve as a relative quantification by comparing 50 percent maximal binding (IC_{50}) using dilutions for each sample. For each duplicate sample, the CV%, standard deviation, and the standard error were calculated.

2.8 Tissue culture techniques

2.8.1 Mammalian cell lines

Two adherent human ovarian cancer cell lines (OC cell lines) were used in this study (Table 2-8). At the beginning of the cell culture work, several stock vials of each cell line (1 mL each) were frozen down in liquid nitrogen vapour phase. When cells reached 20 passages, they were discarded and replaced with fresh vial from cryostores. Authentication of cell lines by Short Tandem Repeats (STR) profiling was performed by Dr Claire Taylor (CRUK Cancer Centre, Genomics Facility, Leeds Institute of Cancer and Pathology) with reference to cell lines from Cancer Research UK (CRUK) and American Type Culture Collection (ATCC).

2.8.2 Cell culture chemicals and reagents

All cell culture plasticware: flasks, plates and stripettes were purchased from Corning® Coaster (USA). All buffers were made up in sterile dH₂O unless otherwise stated. The pH of all buffered solutions was adjusted to its required pH at room temperature (19–25°C).

2.8.3 Sub-culture of cell lines

OC cell lines were maintained in T75 and T150 flasks according to the standard cell culture protocols under aseptic sterile conditions in a NuAire Labgard Class II Biosafety cabinet. Cells were grown at 37°C in 5% CO₂ in complete culture medium as detailed in Table 2-9. Cells were sub-cultured at approximately 70–80% confluent. Conditioned medium was removed by aspiration, cells were washed with 5 mL of 1x Dulbecco's Phosphate Buffered Saline (DPBS), pH 7.0–7.2 [Gibco™, Cat. No: 14190-094, Life Technologies] and detached from the flask by incubation with 1-5 mL of 1x Trypsin solution made from 10x stock (Life Technologies, Carlsbad, USA Cat. No: 15400-054), 1:10 Trypsin – EDTA (0.5 g/L Trypsin and 0.2 g/L EDTA) in DPBS at 37°C for 5–15 minutes. 5 mL of complete medium was added to the cells to de-activate Trypsin. The cell suspension was then centrifuged at 400 g for five minutes at RT and supernatant was discarded. The cell pellet was resuspended in complete medium and seeded into fresh flasks in 15 mL medium. Cells were split 1 in 10, 1 in 15 every 5–7 days, to sustain exponential growth curve.

Table 2-8: Mammalian cell lines

Cell Line	Source	Type of Cancer	Clinical Information
OVCA433	Dr Sandra Bell (University of Leeds)	Ovarian serous papillary cystadenocarcinoma	Female age & ethnicity unknown. High-grade serous ovarian carcinoma cell line.
SKOV3	Dr Sandra Bell (University of Leeds)	Ovarian Adenocarcinoma	Ovarian adenocarcinoma; ascites from a 64 years Caucasian female. In nude mice; forms moderately well differentiated adenocarcinoma consistent with ovarian primary. SK-OV-3 cells are resistant to tumor necrosis factor and to several cytotoxic drugs including diphtheria toxin, cis-platinum and Adriamycin.

Table 2-9: Mammalian cell lines medium

Cell Line	Complete Culture Medium
OVCA433	Roswell Park Memorial Institute (RPMI1640 (1X) plus GlutaMAX™, Ref: 61870-010, Gibco® by Life Technologies™, Paisley, UK) supplemented with 10% (v/v) heat inactivated Foetal Bovine Serum (FBS, Sigma Aldrich, Cat no. F7524-500 ML).
SKOV3	McCoy's 5A with L- Glutamine, sodium bicarbonate; without Phenol red. (GE Healthcare Life Science, HyClone™ SH30270.01, Product Code: 10358633, by Fisher Scientific) supplemented with 10% (v/v) heat inactivated Foetal Bovine Serum.

2.8.4 Storage and resuscitation of cell lines

Cells were grown to ~70% confluency in T75 flask. Cells were harvested as described for sub-culture (Section 2.8.3), centrifuged at 400 g for five minutes at RT and supernatant was discarded. The pellet was resuspended in 3 mL freezing medium (90% Fetal calf serum (FCS) [Sigma-Aldrich, St. Louis, USA, Cat. No: F7524-500 ML] and 10% dimethyl sulphoxide [DMSO] (Cat. No. 276855-100 ML, Sigma-Aldrich)) drop-wise while mixing the cells. 1 mL aliquots in cryovials (Cat. No: 366656, ThermoFisher Scientific) were made. Cryovials were transferred to Nalgene® Mr Frosty freezing container (Cat No. BP2618-212, Fisher scientific) in the presence of isopropanol and successful cryopreservation of cells at 1°C/minute cooling rate was achieved O/N at –80°C. After 24 hours, cryovials were stored for long term in vapour phase of liquid nitrogen.

Cells were resuscitated by thawing the cryovials in a 37°C water bath for 1 minute. The contents were moved to 10 mL complete medium in 15 mL Falcon tubes, centrifuged and supernatant was discarded. The cell pellets were resuspended in 5 mL medium and transferred to T75 flasks containing 10 mL complete medium and allowed to recover O/N. The next day, medium change was performed to eliminate any residual DMSO and dead cells.

2.8.5 Cell lysate preparation from cell lines and protein quantification

Cell lysates from OVCA cell lines were prepared using modified radioimmunoprecipitation buffer (2x RIPA buffer compositions: 50 mM Tris-HCl pH 7.4, 150 mM NaCl, 1% Nonyl phenoxypolyethoxyethanol (NP-40). Complete protease inhibitor (Roche, REF: 11697498001, Lot: 17113900) was made as per the manufacturer's instruction and added to make the RIPA Buffer 1x working Solution. Cells were grown in T75 flasks until 75–80% confluent, conditioned medium were removed and cells were washed three times using 13 mL cold DPBS. The cells were incubated with 0.5 – 1 mL of the 1x RIPA buffer for 10 minutes on ice before removing the cells using a cell scraper and transferring the solution into a 1.5 mL eppendorf tube. Afterwards, the solution was centrifuged at 4°C, 12,000 g for 10 minutes. The supernatant lysate was transferred into sterile 1.5 mL eppendorf tubes and stored at –80°C. Protein concentration was quantified using Pierce™ BCA Protein Assay Kit (ThermoFisher Scientific, Cat No: 23225) according to the manufacturer's protocol for microtiter plate procedure.

2.8.6 MTT assay

MTT assays were used to evaluate cell proliferation (Mosmann, 1983). The assay was carried out in 96-well plates by mixing 10 μ L of yellow, water soluble Thiazolyl blue Tetrazolium Bromide MTT [3-(4,5- dimethylthiazol-2-yl)-2,5-diphenyltetrazolium bromide]; (SIGMA-Aldrich Cat. No: M2128-1G, Lot: MKBX8173V) stock solution (5 mg/mL) with 100 μ L complete medium in each well, then incubated at 37°C, 5% CO₂ for three hours wrapped in foil until the purple formazan precipitate, which is insoluble in water, was formed. After the incubation, the medium was removed, the formazan crystals were dissolved in 100 μ L of Isopropanol (Fisher Scientific, USA, cat. No: BP2618-212, Lot: 165306) gently using an orbital shaker for 20 minutes at RT. The absorbance was read at 620 nm using a plate reader (Berthold Mithras LB 940). The optical density readings from medium-only wells were used as a blank background.

2.8.6.1 MTT standard response curves for OVCA cell lines

As the measurement of cell viability was chosen to assess the OVCA cell line growth in the presence of FXIIIA protein, the response of OVCA cell line population to MTT solution was evaluated as only metabolically active viable cells can convert the yellow MTT solution into purple formazan crystals. Cells were plated at 1.0×10^4 to 4.0×10^5 cells/well and incubated at 37°C, 5% CO₂, 95% relative humidity for 12 hours. MTT assay was then performed. The plots of the data obtained for OVCA433 and SKOV3 cell lines are presented in Figure 2-5. The optimal number of cells to perform the assays fell within the linear portion of the curve and gave absorbance values between 0.5 and 1.5 for OVCA433 and SKOV3 cell lines.

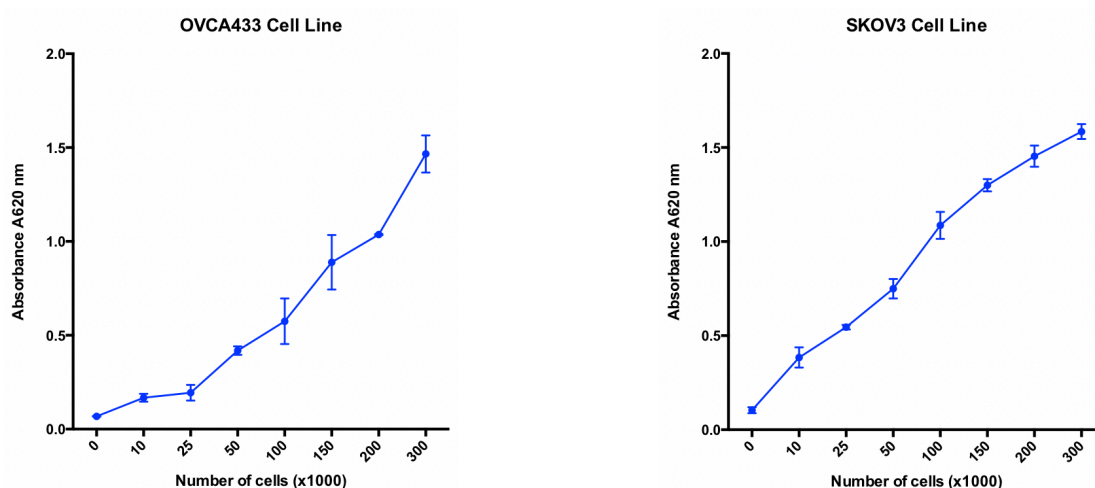


Figure 2-6: MTT standard response curves

Mammalian cell lines were seeded at a range of different concentrations from 10,000–300,000 cells/100 μ L /well and incubated O/N at at 37°C, 5% CO₂. The response of mammalian cell lines at various seeding densities to MTT solution following a 12 hours incubation period was assessed using MTT assay (Section 2.8.6). Data points represent the mean of the absorbance readings from three technical replicates, whereas error bars represent the standard deviation.

2.8.6.2 Determination of seeding density for growth experiments

To determine the optimal number of EOC cells to use in proliferation experiments, the growth characteristics of OVCA cell lines used in this study were evaluated by generating growth curve for each cell line using MTT assays. Once the cells reached around 80% confluency, the adherent cells were trypsinised (Section 2.8.3), then cells suspensions were harvested by centrifugation followed by resuspension in complete medium. The cells were plated at different seeding densities: 1.0×10^3 , 3.0×10^3 , 5.0×10^3 , 1.0×10^4 , 1.5×10^4 , 2.0×10^4 and 2.5×10^4 cells/200 μ L /well in a 96 well microtiter plates and incubated at 37°C, 5% CO₂. The experiment was carried out in triplicate wells in a single plate and followed up for seven days. MTT assays (Section 2.8.6) were performed daily over seven days to assess viability and proliferation. Absorbance readings for each day were normalised to the readings taken on the first day for each seeding density, and growth curves for cells lines tested were produced (Figure 2-6). After seven days of growth, none of the cell lines tested had reached the stationary phase. These graphs demonstrate that cells seeded at 1.0×10^3 have a low density and a long lag phase. Up until days 4–5, there was little variation between the other cell densities. After the fifth day, the higher cell concentrations start to level off. Therefore, a seeding density of 1.0×10^4 cells/well was chosen for growth experiments.

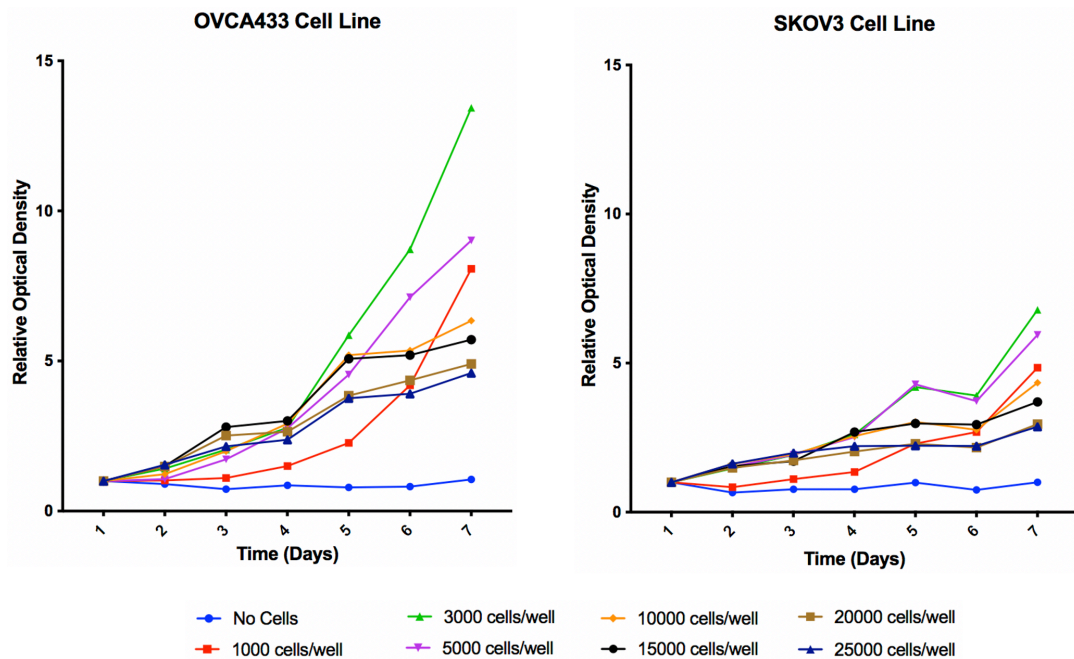


Figure 2-7: Mammalian cell lines growth curves

SKOV3 and OVCA433 cell lines were seeded at a range of various concentrations from 1,000–25,000 cells/200 μ L/well in triplicate wells in 96-well plates, and incubated at 37°C, 5% CO₂ for seven days (overall seven plates). Every 24 hours, MTT assay was performed on one plate. Optical density readings at A620 nm were normalised by dividing by the readings taken on the first day for each seeding density. The curves plotted in GraphPad Prism from a single experiment (n=1) with each data point representative of a triplicate wells.

2.8.7 EOC cell proliferation assay

OVCA433 and SKOV3 cells were counted using Countess II Automated Cell Counter (Cat. No: AMQAX1000, ThermoFisher Scientific) and seeded at a density of 1.0×10^4 cells/100 μ L/well in 96-well plates in triplicates and incubated at 37°C, 5% CO₂ for six days in the presence of active and inactive FXIIIA purified protein variants in the medium. MTT assays were used to evaluate EOC cell proliferation in the presence of FXIIIA variants. The absorbance readings were normalised to the readings taken for EOC cells on day one. Student's *t*-tests were performed to compare the mean for three independent wells within each experiment, and from combined means from three different biological repeat experiments. Recombinant FXIIIA variants were purified, and their TG activity was determined within one week prior to the experiment. A variety of FXIIIA purified protein concentrations ranging from 0.01–0.001 IU/mL were tested (represent 1%–0.1% of *in vivo* concentration) to establish an appropriate concentration to assess the influence of this enzyme on OC cell proliferation. FXIIIA variants were activated by adding the following components: 0.1 U of bovine thrombin (Prod. No. T4648-1KU, Sigma-Aldrich, Gillingham, UK) for each 0.02 IU of FXIIIA (Dardik et al., 2003), 10 mM calcium chloride (CaCl₂), and

incubation for 30 minutes at 37°C, 5% CO₂. Following FXIIIa variants activation, inhibition of thrombin was achieved by the addition of PPACK (1mg/mL stock solution of D-phenylalanyl-N-[(1S)-4-[(aminoiminomethyl)amino]-1-(2-chloroacetyl)butyl]-L-prolinamide, trifluoroacetate salt (PPACK, Cat. No: 15160, Cayman Chemical, Ann Arbor, USA) was made by dissolving the lyophilised powder in DMSO) at 140 µg per 0.5 U of thrombin for 10 minutes at 37°C, 5% CO₂ (Schroeder et al., 2007). For inactive FXIIIa state, the protein was added to the cells in a similar manner to the active protein, with the exception that additional required volume was made up with DPBS.

2.8.8 Scratch wound assay

Scratch wound assays were used to assess the influence of the presence of FXIIIa protein variants at active and inactive states on EOC cell migration. This assay was carried out using OVCA433 cell line. Cells were stained with 1x CytoPainter-488 nm (500x stock solution of Cell Proliferation Staining Reagent – Green Fluorescence [Cat. No: ab176735, Abcam, Cambridge, UK] was made by resuspending the lyophilised powder in 500 µL DMSO. 20 µL aliquots were stored at –20°C) for 10 minutes at RT wrapped in foil. Cells were seeded at 5.0×10^4 cells/200 µL/well in 96-well ImageLock™ microplate in triplicates and incubated at 37°C, 5% CO₂ for 2 days, to reach confluency at the time required to make the scratch. A scratch wound was created in the wells simultaneously using the Essen® 96-well WoundMaker™. The WoundMaker™ is a mechanical device designed with 96 pins placed at equal distance corresponding to the 96-wells. 700–800 micron wide scratch wounds were created by sliding the WoundMaker™ on freshly confluent cell monolayers. The plate was washed twice with complete medium to remove cell debris. Matrigel® (Cat No. 354248, Corning®) Basement Membrane Matrix was made up to a final concentration of 5 mg/mL in cold 5x RPMI medium (Media and Balanced Salt Solutions Preparation from powder and concentrates, Cat No. MAN0006845, gibco®, Life Technologies). A layer of 50 µL of Matrigel-depleted growth factors was overlaid on top of the wounded cells monolayers in designated wells and incubated at 37°C, 5% CO₂ for 30 minutes to form the matrix. 200 µL total volume of complete medium containing FXIIIa protein variants native and activated was loaded in each well and the plate was incubated at 37°C, 5% CO₂ in LIPSI (Nikon, Amsterdam, Netherland) for 24 hours. Activation of FXIIIa variants was performed as described in section 2.12.1 above. The LIPSI Motorised inverted microscope ECLIPSE Ti2 was programmed to live image each well at 10x magnification, every hour for 24 hours. NIS-Elements AR (Advanced

Research) 5.20.01 64-bit system on Nikon A1 plus Confocal imaging software was used to analyse the data.

2.8.9 Cell adhesion assay

OVCA433 and SKOV3 cells were counted using Countess II Automated Cell Counter and seeded at a density of 5.0×10^4 cells/100 μ L/well in 96-well plates in triplicates. 30 μ g of FXIIIA variants as pooled yeast lysates were added to the medium and the plates were incubated at 37°C, 5% CO₂ O/N. Next day, the medium and non-adherent cells were removed. Plates were washed 2x with DPBS. Adherent cells were fixed with 200 μ L/well of freezer cold neat methanol (Cat. No. M/4956/17, Fisher Scientific) for 10 minutes at RT. After that, Methanol was replaced by 100 μ L/well of 0.1% Crystal Violet (Cat. No. C3886, Sigma-Aldrich) solution in 10% Ethanol (Cat. No. 32221-2.5L-M, Sigma-Aldrich) for 30 minutes at RT. Crystal Violet (CV) was removed, and cells were washed three times with dH₂O to take out excess dye. CV was dissolved in 100 μ L/well of neat Methanol on a gently shaking platform for 20 minutes at RT. The absorbance was measured at 570 nm using Mithras LB 940 Multimode Microplate Reader.

2.9 Genetic analysis techniques

2.9.1 Extraction of genomic deoxyribonucleic acid (gDNA)

Genomic DNA (gDNA) was successfully extracted from all cell lines using QIAamp[®] DNA Mini Kit (50), (Invitrogen[™] by ThermoFisher Scientific, Ref: 51304) as per the manufacturer's protocol. The ODs measurements (260/280 ratio) for all samples obtained by NanoDrop[®] 1000 Spectrophotometer [(ND-1000), Labtech International, UK] and analysis on 0.8% agarose gel electrophoresis has confirmed that the gDNA was of high quality.

2.9.2 Isolation of ribonucleic acid (RNA)

Total RNA was isolated from all OVCA cell lines under study using TRIzol[®] Reagent (Life Technologies, Cat No. 15596) as per the manufacturer's protocol. The amount of RNA extracted was quantified by NanoDrop[®] 1000 Spectrophotometer. RNA samples were treated with TURBO DNA-free[™] Kit (Invitrogen[™], USA, Cat No: AM1907) as per manufacturer's protocol to remove any contaminating DNA from RNA preps. Genomic DNA absence was confirmed in all RNA samples prior to use by amplification using genomic primers.

2.9.3 Synthesis of complementary deoxyribonucleic acid (cDNA)

First strand cDNA was synthesised using 5 µg RNA templates from each cell line via the GoScript[™] Reverse Transcription System (Promega, USA), according to the manufacturer's protocol.

2.9.4 Genotyping ovarian cancer cell lines for F13A1 SNPs

For genotyping FXIIIA, OVCA cell lines genomic DNAs were extracted (Section 2.9.1) and amplified with *F13A1* exon 2, 5, 12 and 14 primers, kindly provided by Dr Kathryn Hutchinson, University of Leeds (Table 2-10). PCR reactions were performed using the Hot Shot Dimond Mastermix (Clent Life Science, Stourbridge, UK) as detailed in Section 2.3.2 and analysed on 1.5% agarose gel in TAE buffer. PCR products were then cleaned up using Exo-SAP IT (Affymetrix, High Wycombe, UK) as per protocol and Sanger sequencing services of (SourceBioscience, 2021) was employed to generate DNA sequence. Purified PCR products and primers were supplied to SourceBioscience at the required concentrations. SourceBioscience returned the data as electropherograms (Figure 2-8).

Table 2-10: Primers used to amplify *F13A1* exons

<i>F13A1</i> Exon	Primer Orientation	Primer Sequence 5'- 3'	Primer length (bp)	TM°	PCR Product size (bp)
Exon 2	F	TAT GCA AAC GGC AAA ATG TG	20	65	384
	R	ACC CCA GTG GAG ACA GAG G	19		
Exon 5	F	GGG AAA TGA GCT ATG CTT GG	20	59	385
	R	AAG CAG GAA ATT GTG CTT GTC	21		
Exon 12	F	CCC AAC AAG TGC AGT ACA CG	20	63	454
	R	ACG GGC ATT AAC ACC TAG CA	20		
Exon 14	F	TGT ATC ATA AAA CTC TAG TAA AAG TG	26	58	328
	R	TGG GGA GCA GAT CTA TG	17		

All primers were purchased from Sigma-Aldrich (Gillingham, UK) Custom Oligos, unless otherwise stated.

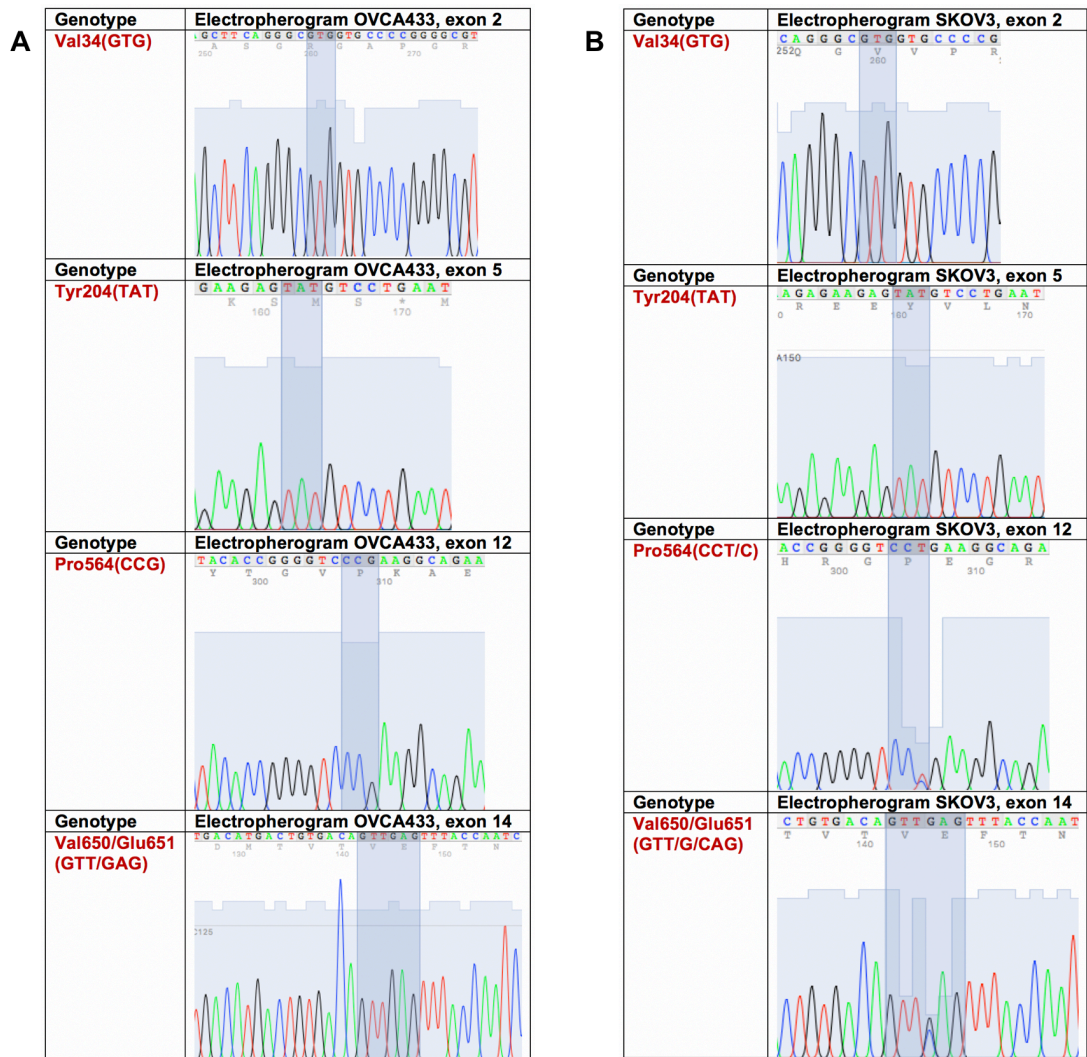


Figure 2-8: Genotypes of OVCA cell lines

4Peaks software was used to analyse sequencing traces for the *F13A1* SNPs in amplified exons from OVCA cell lines genomic DNAs. Five coding *FXIII*A gene polymorphisms were examined. **A)** electropherograms present the genotype for OVCA433 cell line. **B)** electropherograms present the genotype for SKOV3 cell line. The codon of interest is highlighted in light blue. A single peak signify a homozygous carrier, whereas, overlapped peaks denote heterozygous carriage of both alleles. Both cell lines were *FXIII*A wildtype at codon 204 (²⁰⁴TAT) and codon 650 (⁶⁵⁰GTT). While the SKOV3 cell line was heterozygous at codon 564 (⁵⁶⁴CCT/C) and codon 651 (⁶⁵¹G/CAG), OVCA433 cell line was *FXIII*A wildtype at these specific codons.

2.10 Immunofluorescence on cultured OVCA cells

OC cell lines SKOV3 and OVCA433 were seeded onto sterile glass coverslips in a six well plate, and cultured until ~70% confluent. Conditioned medium was removed, and cells were washed with 1x DPBS followed by, fixation and permeabilisation in 2 mL neat Methanol at RT for 10 minutes. Methanol was removed and cells were left to air-dry for 15 minutes. Cells were then blocked using blocking buffer (0.5% NFDM in 1x DPBS) for 1 hour at RT. Primary antibody anti-Isopeptide antibody [81D1C2] (Cat No: ab422) Mouse Monoclonal to isopeptide IgG1 Kapa dilution was optimised to 1 in 100 in freshly made buffer (0.5% NFDM in 1x DPBS, centrifuged at 13.000g for 5 minutes prior to use). Several concentrations were tested ranging from 1 in 25 to 1 in 500. 100 μ L primary antibody supernatant was added to cells, covered with parafilm coverslip and incubated O/N at 4°C. For no primary control, 100 μ L of blocking buffer was added to the designated well and incubated as per the primary antibody. The next morning, parafilms were removed carefully and cells were washed three times with 2 mL 1x DPBS for five minutes each. Alexa Fluor fluorescent secondary antibody Goat anti mouse AF488 was prepared in the same way as the primary antibody using the 0.5% NFDM as diluent and centrifuged as above. 100 μ L secondary fluorescent antibody supernatant at 1:300 dilution was added to all cells including no primary control, and incubated at RT for 30 minutes covered with parafilm as well. For all the remaining steps, the glass coverslips were protected from light. Cells were washed as above, followed by coverslips mounting using ProLong Gold with DAPI (Cat. No. P36935, Invitrogen, ThermoFisher Scientific) onto SuperFrost Plus glass slides and allowed to cure O/N at RT covered in tin foil. Once cured, glass coverslips were sealed onto the glass slides with nail varnish. Slides were stored at 4°C. Zeiss Microscope (Zeiss Imager.Z1 Ax10) was used to visualised the immunofluorescent staining. A FITC Emission filter (wavelength 530 nm) was used to detect the AF488-conjugated secondary antibody. While DAPI-stained nuclei were detected using DAPI emission filter (wavelength 440 nm). A 63x oil objective lens was used to capture the images.

2.11 Data analysis

2.11.1 Transformation efficiency

Colonies on each plate were counted. Transformation efficiency is defined as colonies obtained per μg of DNA in each transformation and calculated as follows:

Transformation Efficiency = Number of colonies on one plate \times (1 / μg of DNA used) \times (μl of final transformation mix / μl of transformation mix plated).

2.11.2 ICON7 clinical cohort and survival analysis

IBM SPSS statistics version 26 was used to analyse the ICON7 clinical cohort plasma FXIII activity, plasma FXIIIa levels and plasma D-Dimer levels as well as the survival data. The ICON7 cohort had three survival intervals measured: PFS, which is the period from enrolment to progression of the disease or death, OS, which is the period from enrolment to death or censorship from the study, and survival post-progression (SPP), which is the time after the progression until death. The Kolmogorov-Smirnov test was applied to determine whether the data had a normal distribution. One Way ANOVA analysis of variance was used to examine the associations between categorical variable of *F13A1* polymorphisms and plasma FXIII activity, FXIIIa levels and D-Dimer levels. Chi-square tests were used to assess the associations between categorical variables of EOC prognostic factors and *F13A1* polymorphisms. The non-parametric test, Spearman's rank-order correlation was performed to assess the correlation between numerical variables with non-normally distributed data such as plasma FXIIIa levels and D-Dimer levels. For all analysis performed, the alpha value was set at 0.05, and p-values were deemed significant if they were less than 0.05.

2.11.3 Cell biology work

GraphPad Prism 9 Version 9.1.1 (233) for MacOS was used to analyse the results of the adhesion and growth experiments using OVCA cell lines. Student *t*-tests were used to compare two sets of normally distributed data, when the data was not normally distributed, non-parametric tests were used to compare the differences between average group ranks, such as the Kruskal-Wallis test with Dunn's multiple comparison test. Nikon A1 plus with NIS-Elements AR, 5.20.01 64-bit system for the confocal (A1R LSM) imaging software was used to analyse LIPSI migration experiment at the Flow Cytometry and Imaging Facility, University of Leeds. A protocol was created using the Homogenous Area detection within General Analysis 3, Analysis Explorer which is opened in NIS-Elements. Measurements were

customised to include the TotalObjectArea and AreaFraction. The results were displayed as bar charts, line graphs, results tables, and were exported to Microsoft Excel from the results tables.

2.11.4 Calculations of Linkage Disequilibrium (LD)

LD is the non-random association of alleles at various loci, leading to statistical relationships between alleles at distinct loci that differ from what would be expected if alleles were independent, based on their individual allele frequencies. It was calculated as detailed in (Lewontin, 1988) and summarised below:

- ❖ Step 1: Calculations of allele frequencies using the sum of the Punnett square entries: $P^2 + 2pq + q^2 = 1$.
- ❖ Step 2: Calculations of the haplotype frequencies from genotypic data and their corresponding allelic frequencies expected under equilibrium.
- ❖ Step 3: Calculations of the LD as the deviation of observed haplotype frequency from its corresponding allelic frequencies expected under equilibrium: $D = (p_{11} p_{22}) - (p_{12} p_{21})$.
- ❖ Step 4: Standardisation of D as the value of D could be negative. The typical normalisation method adopted was a relative measure of disequilibrium (D) compared to its maximum: $D' = D / D_{max}$.

To estimate D_{max} , allelic frequencies and value for D were used in the following equation: $D_{max} = \min [(p_1q_2) \text{ or } (p_2q_1)]$.

Chapter 3 Coagulation Factor XIIIa in Epithelial Ovarian Cancer

3.1 Introduction

Several studies have investigated *F13A1* genotypes, FXIIIa levels and enzymatic activity in plasma in different cancers (Section 1.3.4.1 to 1.3.4.3). Previous research has linked *F13A1* gene polymorphisms with diseases, for instance V34L and thromboembolic disease (Wells et al., 2006). FXIIIa is expressed in connective tissue stroma and in the vicinity of many different carcinomas (Wojtukiewicz et al., 2001), suggesting that FXIIIa may be important in tumour development and metastasis. Lower plasma FXIII levels in metastatic gynaecological tumours relative to benign disease, indicate that FXIII may play a role in the progression of OC (van Wersch et al., 1994). A previous study of FXIIIa in EOC from the Anwar laboratory demonstrated that FXIIIa V650I variant to be significantly associated with shorter OS in women with EOC ($p=0.008$), whereas, homozygous carriers of 34L variant presented longer OS in women with advanced-stage EOC ($p=0.0219$). This study has assessed the effect of *F13A1* genotypes in 260 patients with EOC, and identified V34L and V650I variants as valuable indicators of EOC prognosis (Anwar et al., 2004). However, the molecular basis of this relationship remains unclear.

In many cancers, including EOC ascites, high amounts of cross-linked FDPs have been identified (Wang X. et al., 2005). Advanced-stage OC is often associated with hypercoagulation and increased fibrinolysis. Numerous haemostatic factors and procoagulant are released as a result of activation of the coagulation-fibrinolytic system by the cancer cells. Extensive activation of clotting and fibrinolysis stimulates tumour growth, angiogenesis, invasion and spread (Kołodziejczyk and Ponczek, 2013).

The plasma D-Dimer level is an important biomarker for the activation of coagulation and fibrinolytic systems. The D-Dimer antigen is a specific fibrin degradation product. It is formed by the combined action of three enzymes: thrombin, activated FXIIIa (FXIIIa) and plasmin. Initially, thrombin plays an important role by converting plasma fibrinogen into fibrin monomers and activates FXIIIa, which circulates in plasma bound to fibrinogen. Activated FXIIIa polymerises fibrin and catalyses the formation of covalent bonds between the D-domains within the fibrin polymers. Upon the activation of the fibrinolytic system, the proteolytic activity of plasmin degrades cross-linked fibrin and releases FDPs. The degradation of the fibrin cross-linked by

activated FXIIIa produces fragment E (central domain), and D-D-dimers (two terminal D fragments), and other numerous intermediate polypeptides.

This study set out to explore the influence of FXIIIa on EOC for several reasons. Firstly, the lethality of this cancer presents a clinical need to understand this disease and the factors and processes which may impact it. Secondly, the work performed to date on EOC is limited, presenting an open opportunity to explore further, and finally, of the limited work available, it is suggestive that FXIIIa may influence OC, but that the precise mechanisms are yet to be fully understood. Therefore, a cohort of patients newly diagnosed with EOC was obtained to investigate the role of factor XIIIa on this cancer (n=91 of plasma samples), which is part of the ICON7 trial translational cohort. ICON7 clinical trial (n=1528) evaluated the benefit of adding bevacizumab to standard chemotherapy. The trial translational cohort included patients who consented for their samples and clinical data to be used in translational research.

FXIII activity, FXIIIa subunit levels, and D-Dimer levels in plasma samples were undertaken blind, to eliminate bias. Following data acquisition, a database was created, including the anonymised clinicopathological data, plasma FXIII activity, plasma FXIIIa subunit levels, selected *F13A1* genotypes and FXIIIa expression in EOC tumour tissue, to explore the associations between these variables. Relationships were also investigated between FXIII plasma activity and plasma FXIIIa subunit levels with FXIIIa expression in EOC tumour tissues. Statistical analyses were also undertaken to investigate the relationship between plasma FXIIIa levels, activity, D-Dimer levels and EOC prognostic factors such as age at diagnosis, grade, stage, histology, risk of disease progression, extent of residual disease, therapeutic effect of regimen received and survival intervals (PFS, SPP and OS). Although *F13A1* genotypes, levels and activity and D-Dimer levels have been previously explored in various cancers, these investigations were not performed on the same cohort of patients. In this regard, the experimental work presented herein provides a unique and original contribution.

The objectives of this chapter were therefore to:

1. Assess the relationship between FXIII activity and its A-subunit levels in the plasma.
2. Evaluate the association between FXIII A and D-Dimer levels in the plasma.
3. Examine relationship between plasma FXIII A activity, plasma FXIII A levels, D-Dimer levels and any of the disease prognostic factors and/or survival intervals.
4. Examine relationship between plasma FXIII A levels and FXIII A levels in the EOC tumour tissue.

3.2 ICON7 prospective cohort

3.2.1 Characteristics of the ICON7 plasma cohort

Plasma samples analysed in this chapter (n=91) account for 20.1% of the samples from the full ICON7 translational cohort (n=448). The median age at diagnosis was 56 years, with a range of 31 to 75 years. The cohort is predominantly serous histology, advanced-stage and high grade, as expected. EOC prognostic factors distribution within the chosen sample for this study were comparable to those of the full translational ICON7 cohort (Table 3-1).

Patients at high risk of disease progression, is a prognostic factor described by the ICON7 trial investigators to compare the ICON7 study populations with the GOG-218 trial participants. This classification was developed at the time of the initial PFS analysis and upgraded just before the final analysis of the whole trial. This category comprised of women with inoperable FIGO stage III disease, women with stage III who had > 1 cm macroscopically residual tumour after cytoreduction surgery, and women with stage IV (Oza et al., 2015). In their final analysis of the ICON7 results on OS, Oza and colleagues reported two different high-risk classifications to allow comparison with the first trial analysis: omission of inoperable stage III and IV patients, to match the prior ICON7 high-risk group; and addition of patients with 0–1 cm residual disease, to match the GOG-218 participants. During the period from the first PFS analysis by Perren et al. (2011) and the final OS analysis by Oza et al. (2015), patients with up to 1 cm of residual disease were re-classified to include those with no macroscopic tumour bulk or those with macroscopic tumour bulk measuring 1 cm or less. Women who did not fit the conditions for high-risk disease were classified as non-high-risk (Oza et al., 2015).

It is now well established that one of the most important prognostic factors for patients with OC is the extent of residual disease following primary debulking surgery. By definition, ICON7 patients at high-risk of disease progression had > 1 cm of residual disease, and not high-risk patients had < 1 cm of residual disease following debulking surgery. If a patient is stage III and high-risk, then they have > 1 cm of residual disease, and if they are stage III and not high-risk then they have < 1 cm of residual disease. Another clinical variable examined in this study was serous histology with high-grade disease, representing type II HGSC.

Patients were enrolled into the study between December 2006 and February 2009. Patients had to be fully recovered from primary surgery in order to participate in the study. If treatment begins within four weeks following surgery, bevacizumab can be omitted in the first treatment cycle, while standard chemotherapy must begin within eight weeks.

Samples were collected only after the patients gave their consent and were confirmed to be qualified for the study. There were four levels of participation on the ICON7 translational research programme:

- ❖ Level 1: Tumour tissue blocks were collected during the primary surgery for tissue microarrays.
- ❖ Level 2: A single baseline peripheral blood sample for DNA pharmacogenomics was taken before treatment cycle 1, although it can be taken at any point during management if required.

At levels 1 and 2, all centres were anticipated to participate in the translational research programme because no extra research facilities were required.

- ❖ Level 3: Blood samples were collected for proteomics and immunoassays at time intervals: pre-cycle 1, pre-cycle 2, pre-cycle 6 and at protocol defined disease progression, or at five years from the commencement of therapy if the disease progression did not occur.
- ❖ Level 4: Additional 6 blood samples were collected (an extra pre-cycle 1 to assess intra-patient variability, one following administration of all medications post-cycle 1, one after administration of all medications post-cycle 6, and a follow up from the end of chemotherapy at three, six and nine months). Immunoassay and proteomic analyses were also performed on these blood samples.

Levels 3 and 4 were suitable for clinical laboratories with access to a centrifuge and a -80°C .

Plasma samples analysed in this chapter have been collected at level 3 participation during the time interval following primary debulking surgery and before administration of treatment cycle 1 into an EDTA collection tube. Within 28 days of enrolment in the trial, a coagulation screen was performed, and repeated during the course of the study treatment, if required. Patients had recovered from the effects of surgery on coagulation by the time samples were collected, hence, surgery had no influence on these samples. Prophylactic anticoagulation using the Low Molecular Weight Heparin (LMWH) was not included in ICON7 trial treatment regimens. This treatment would

not have an effect on FXIIIa levels and/or activity, if it had been used, as it works primarily by inactivating thrombin and activated factor X via an antithrombin-dependent mechanism. Consequently, Heparin suppresses fibrin generation as well as thrombin-induced stimulation of platelets, factors V and factor VIII (Hirsh et al., 2001).

Normally, samples for coagulation testing would be collected into citrate-based anticoagulant tubes (generally, 105–109 mM or 129 mM sodium citrate, also referred to as 3.2% or 3.8%, respectively). However, it was appropriate to use the ICON7 samples as EDTA tubes have been used for FXIIIa studies by different research groups as a standardised procedure without significant impact on analytical outcomes (Nikolajsen et al., 2014, Tuck et al., 2009).

Table 3-1: Characteristics of study subjects of the full ICON7 translational cohort and the study-cohort

Prognostic factor	ICON7 Full Cohort (n=1528)		ICON7 Translational Cohort (n=448)		ICON7 Study-cohort (n=91)	
	Number of Cases	Percentage	Number of Cases	Percentage	Number of Cases	Percentage
Age at diagnosis (Years)						
Median	57		57		56	
Range	18-82		24-79		31-75	
Grade of Tumour						
I	97	6.3	22	4.9	3	3.3
II	317	20.7	73	16.3	16	17.6
III	1094	71.7	347	77.5	72	79.1
Unknown	20	1.3	0	0.0	0	0.0
Missing	0	0.0	6	1.3	0	0.0
FIGO stage						
I	142	9.3	35	7.8	7	7.7
II	80	5.2	55	12.3	9	9.9
III	1105	72.3	306	68.3	66	72.5
IV	201	13.2	52	11.6	9	9.9
Histological subtype						
Serous	1054	69.0	306	68.3	61	67.0
Non-Serous	474	31.0	142	31.7	30	33.0
Risk of Disease Progression						
High Risk	1063	70.0	150	33.5	36	39.6
Not High Risk	465	30.0	298	66.5	55	60.4

Ninety-one plasma samples only were available for analysis from the full ICON7 translational cohort (ICON7 study-cohort). These samples were collected after the primary surgery, and before treatment cycle 1. In ICON7 study-cohort, age at diagnosis was unknown for two cases. Tumour grade: I=well differentiated, II=moderately differentiated, III=poorly differentiated. In the full ICON7 translational cohort, Grade was determined for all cases, but data was missing for six women. The category 'non-serous' under histological subtype includes: mucinous, endometrioid, clear cell, mixed, and others. High-risk of disease progression is defined as inoperable FIGO stage III, stage III disease with an inadequate debulking (> 1 cm residual disease following surgery), and FIGO stage IV (Supplementary Appendix) (Oza et al., 2015).

3.3 Plasma FXIII

Plasma FXIII is a tetramer made up of 2 A and 2 B-subunits. The activity of this molecule is expressed by the A subunit only (Section 1.3.2). This section describes the activity and the A-subunit levels data obtained for the ICON7 plasma samples available (n=91).

3.3.1 Plasma FXIII activity

The plasma FXIII activity varied between 0.16 and 1.99 IU/mL (16% and 199% of the activity observed for normal standard plasma) with a mean of 0.95 IU/mL (95%) \pm 0.37 (37%) standard deviation for n=91 as shown in Figure 3-1. There is no agreed range data on FXIII activity normal range in plasma between researchers. Normally, there is five-folds variations 0.5 to 2.5 IU/mL approximately.

In an international collaborative study including 23 laboratories from 10 countries, the biological activity of the 1st international standard for Blood Coagulation FXIII was calibrated in international Units (IU), and has been assigned to 0.91 IU/mL (Raut et al., 2007). This standard has been developed from pooled human plasma by the Expert Committee on Biological Standardisation (ECBS) of the WHO in November 2004.

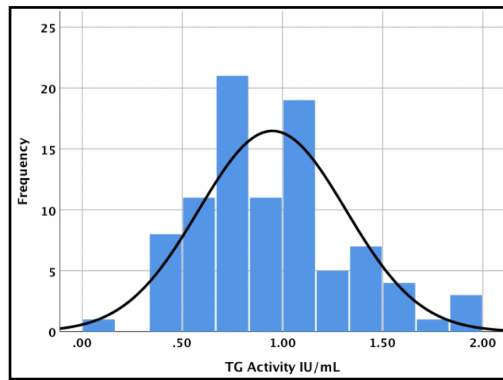


Figure 3-1: FXIII activity in ICON7 plasma samples

FXIII activity was measured in plasma isolated from women newly diagnosed with EOC (n=91), using a biotin incorporation assay (Section 2.5.6). The Kolmogorov-Smirnov test confirmed that the data was normally distributed (p=0.163).

3.3.2 Plasma FXIIIA levels

FXIIIA subunit antigen levels were quantified in ICON7 plasma samples (n= 90 of the 91 plasma samples, level was not measured for one sample because there was not enough of it). The A-subunit levels in plasma samples ranged between 0.11 and 5.74 IU/mL (11% and 574% of that of the 1st International Human Factor XIII Plasma Standard, NIBSC) with a mean of 1.04 IU/mL (104%) \pm 0.87 (87%) SD for n=90.

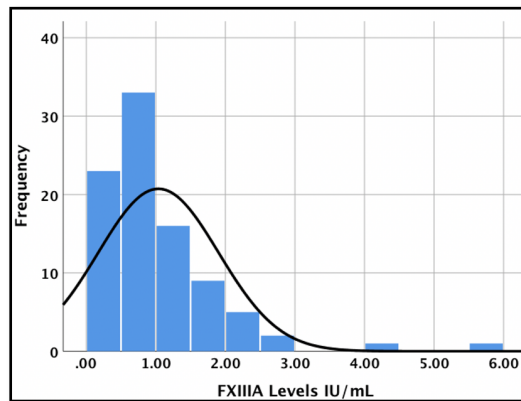


Figure 3-2: FXIIIA subunit level in ICON7 plasma samples

This figure displays the results obtained from the quantification of FXIIIA subunit antigen level in plasma from women newly diagnosed with EOC, using an in-house sandwich ELISA (Section 2.5.8). The Kolmogorov-Smirnov test confirmed that the data was not normally distributed ($p < 0.001$), and was skewed towards lower values (left side of the histogram).

3.3.3 Correlation between plasma FXIII activity and plasma FXIIIA levels

A Spearman's rank-order correlation was performed to assess the relationship between plasma FXIII activity and FXIIIA subunit levels. There was no correlation between these two variables (Spearman's rho Correlation Coefficient = 0.053, n=90, $p = 0.620$).

3.3.4 Summary

In summary, plasma FXIII activity and FXIIIA levels in this EOC ICON7 cohort were similar to those found in the normal population. No direct relationship was seen between FXIII activity and its A-subunit level.

3.4 Plasma D-Dimer levels

The plasma D-Dimer levels varied between 1.87 and 9.19 $\mu\text{g/mL}$ with a mean of 5.07 $\mu\text{g/mL} \pm 1.79$ SD for $n=91$, (Figure 3-3). The normal reference range of plasma D-Dimer for adults (Male/Female) used by the laboratory services within the UK National Health Service is 0.22–0.46 $\mu\text{g/mL}$. The current cut-off used by the Leeds Teaching Hospitals NHS Trust (LTHT) as a negative predictive indicator of a VTE is 0.230 $\mu\text{g/mL}$ (LTHT, 2021). D-Dimer levels in this EOC ICON7 study-cohort were found to be higher than the values for normal healthy individuals.

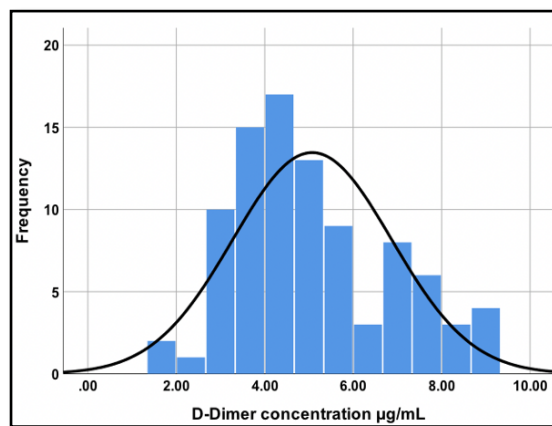


Figure 3-3: D-Dimer levels in ICON7 plasma samples

This histogram shows the variations of plasma D-Dimer concentrations observed in plasma samples from patients newly diagnosed with EOC ($n=91$), using Human D-Dimer ELISA (Section 2.5.9). The Kolmogorov-Smirnov test confirmed that the data was not normally distributed ($p=0.021$).

3.4.1 Correlation between plasma D-Dimer levels and plasma FXIII

A Spearman's rank-order correlation was performed to assess the relationship between plasma D-Dimer levels, plasma FXIII activity and plasma FXIIIa levels. There was no correlation observed between these variables (Table 3-2).

Table 3-2: Test of correlation between plasma D-Dimer levels and plasma FXIII

Plasma FXIII	D-Dimer Levels		
	Spearman's rho Correlation Coefficient	P-value	Sig.
FXIII activity	0.042	0.695	ns
FXIIIa levels	0.128	0.229	ns

The Spearman's rho Correlation Coefficient range from -1 to +1. Strong relationship between covariates tested are represented by values near -1 or +1 than by values near zero. Alpha was set at 0.05. Since the significance test results were > 0.05, therefore, the null hypothesis that there is no monotonic correlation could not be rejected.

3.4.2 Summary

In summary, plasma D-Dimer levels were higher in this EOC ICON7 cohort than in the general population. No direct relationship was seen between plasma D-Dimer levels, FXIII activity and FXIIIa subunit levels.

3.5 *F13A1* genotypes

Peripheral blood DNAs for ICON7 samples included in this study were obtained from the MRC Clinical Trial Unit at the University College London. Genotyping for the FXIII A gene polymorphisms (103G>T, 1951G>A and 1954G>C) was performed within the Anwar Research Group by Dr Kathryn Hutchinson, University of Leeds. Summary of normal *F13A1* genotypes under study can be found in Table 3-3.

3.5.1 *Hardy Weinberg Equilibrium for ICON7 F13A1 genotypes*

All SNPs examined were in Hardy Weinberg Equilibrium (HWE) (Table 3-4). There was insignificantly less 103G>T heterozygous individual observed than expected for this genotype and more homozygous for the G and T alleles ($p=0.771$). In contrast, more 1954G>C heterozygous individual were observed than expected for this genotype, and less homozygous for the G and C alleles, but this variation was not significant ($p=0.918$).

3.5.2 *Comparison between allele frequencies in ICON7 patients and normal population*

Calculated allele frequencies for *F13A1* polymorphisms in ICON7 study cohort were compared to the expected frequencies for a normal European population from the genome aggregation database (gnomAD), as the majority of ICON7 trial patients were Caucasian (98%). There were no significant differences between allele frequency data for this cohort and that expected for a normal population (Table 3-5).

3.5.3 *Linkage Disequilibrium*

Calculations of Lewontin's D' estimates showed that 1951G>A and 1954G>C were in LD (Table 3-6A). There were no individuals carrying the alternative allele A (at 1951 locus) and the wildtype allele G (at 1954 locus); the haplotype AG does not exist because A is always found with C. Hence, 1951A variant is only seen on haplotypes that also carry the 1954C polymorphism. Chi-squared test of independence confirmed this association ($p<0.001$), (Table 3-6B). This relationship has also been observed by other researches in normal population studies (de Lange et al., 2006).

3.5.4 Summary

In conclusion, *F13A1* genotypes: 103G>T, 1951G>A and 1954G>C in ICON7 study-cohort were all in HWE. There was no significant differences between allele frequencies of *F13A1* SNPs in ICON7 patients and the normal population. *F13A1* 1951G>A and 1954G>C were found to be in LD in this cohort.

Table 3-3: Normal *F13A1* polymorphisms at codons 34, 650 and 651

Numerical code	<i>F13A1</i> Normal Polymorphisms							
	103G>T (V34L)		1951G>A (V650I)		1954G>C (E651Q)		1951G>A_1954G>C 650_651 alleles	
	Genotype	Amino acids	Genotype	Amino acids	Genotype	Amino acids	Genotype	Amino acids
1= wildtype homozygous	GTG/GTG (GG)	Val/Val (VV)	GTT/GTT (GG)	Val/Val (VV)	GAG/GAG (GG)	Glu/Glu (EE)	GTT_GAG (GG)	Val/Glu (V/E)
2= heterozygous	GTG/TTG (G/T)	Val/Leu (V/L)	GTT/ATT (G/A)	Val/Ile (V/I)	GAG/CAG (G/C)	Glu/Gln (E/Q)	GTT_G/CAG (GC)	Val/Glu (V/E)
3= alternative homozygous	TTG/TTG (TT)	Leu/Leu (LL)	ATT/ATT (AA)	Ile/Ile (II)	CAG/CAG (CC)	Gln/Gln (QQ)	ATT_CAG (AC)	Ile/Gln (I/Q)

Abbreviations: (V) Valine, (L): Leucine, (I): Isoleucine, (E): Glutamic acid, (Q): Glutamine.

Table 3-4: Distribution of *F13A1* genotypes in ICON7 study-cohort

<i>F13A1</i> Polymorphism	Number of Genotype Observed	(%) of Genotype Observed	Allele Frequencies	Number of Genotype Expected	HWE p-value
103G>T (V34L)					
GG	52	58.4	0.75/0.25	50	0.771
G/T	30	33.7			
TT	7	7.9			
1951G>A (V650I)					
GG or G/A	77	86.5	0.93/0.07	77	1.000
AA	12	13.5			
1954G>C (E651Q)					
GG	46	51.7	0.72/0.28	46	0.918
G/C	37	41.6			
CC	6	6.7			
650_651 alleles					
GG + GG	46	51.7			
GG + G/C or C/C	31	34.8			
G/A or AA + G/C or CC	12	13.5			

Table 3-2 provides the summary statistics for *F13A1* genotypes, allele frequencies, and HWE data in ICON7 study-cohort (n=89, 2 patients were not genotyped). The wildtype genotype is on the first line for each polymorphism, followed by the heterozygous genotype, and then the homozygous alternative genotype. For 1951G>A (V650I) polymorphism, the data for heterozygous and homozygous alternative was combined due to small numbers (n<5). For the allele frequencies, the wildtype allele was displayed on the left side of the '/', while the alternative allele was shown on the right-side. Gene counting was used to determine allele frequencies of *F13A1* genotypes in ICON7 patients. Chi-squared goodness-of-fit tests were used to test for independence of alleles (HWE) in SPSS. All *F13A1* SNPs explored in ICON7 study-cohort population were in HWE (p>0.05, the null hypothesis was not rejected).

Table 3-5: Difference in allele frequencies between ICON7 study cohort and a European population

<i>F13A1</i> Polymorphism	Allele Frequencies		p-value
	ICON7 (n=89)	gnomAD	
103G>T (V34L)	0.75/0.25	0.76/0.24	0.869
1951G>A (V650I)	0.93/0.07	0.95/0.05	0.551
1954G>C (E651Q)	0.72/0.28	0.78/0.22	0.327

For the allele frequencies, the wildtype allele is displayed on the left side of the '/', while the alternative allele is shown on the right-side. The allele frequency data from normal European population was retrieved from the genome aggregation database (gnomAD). A Chi-square test of independence was conducted to examine if the ICON7 data matches that from the normal population using an online calculator (Statistics, 2021). There was no significant differences between these two populations for the SNPs tested ($p > 0.05$).

Table 3-6: Pairwise LD for three *F13A1* loci

A	<i>F13A1</i> Polymorphism	103G>T (V34L)	1951G>A (V650I)	1954G>C (E651Q)
		103G>T (V34L)		
	1951G>A (V650I)	(-) 0.64		
	1954G>C (E651Q)	(-) 0.25	1	

B	<i>F13A1</i> Polymorphism	103G>T (V34L)	1951G>A (V650I)	1954G>C (E651Q)
		103G>T (V34L)		
	1951G>A (V650I)	0.153		
	1954G>C (E651Q)	0.246	< 0.001	

A) Lewontin's D' estimate was calculated for *F13A1* polymorphisms as detailed in Chapter 2, Section 2.11.6 (Lewontin, 1988). The results showed that 1951G>A and 1954G>C were in LD. **B)** Chi-square test of independence was used to determine if there is association between *F13A1* polymorphisms. The results showed significant association between 1951G>A and 1954G>C ($p < 0.001$). Significant values highlighted in orange.

3.6 Plasma FXIII, plasma D-Dimer and *F13A1* genotypes

3.6.1 Plasma FXIII activity and *F13A1* genotypes

Plasma FXIII activity (IU/mL) was examined for each of the *F13A1* polymorphisms under study. The mean activity varied among genotypes examined, with the lowest (0.58 IU/mL \pm 0.16 SD) in 651QQ alternative homozygotes, and the highest (1.30 IU/mL \pm 0.47 SD) in 34LL alternative homozygotes (Table 3-7A).

One-way ANOVA analysis of variance was conducted to assess the associations between plasma FXIII activity and *F13A1* genotypes in EOC ICON7 study-cohort. The results are summarised in Table 3-9. Compared to the WT, carriage of 34L is significantly associated with higher mean activity ($p=0.002$), (Figure 3-4). This is an expected result, as it has been observed in multiple studies on normal populations (Kangsadalampai and Board, 1998a, Kohler et al., 1998, van Hylckama Vlieg et al., 2002) since it was first reported by (Mikkola et al., 1994).

In contrast, Strong association between activity and 1951A_1954C (650I_651Q) haplotype carriers was observed demonstrating significantly lower mean activity than the WT ($p=0.004$), (Figure 3-5). This is a novel result, as it has not been reported before. Three haplotypes were examined: carriers of both wildtype alleles: 650V_651E (⁶⁵⁰GTT_⁶⁵¹GAG), carriers of one alternative allele at 651 locus: 650V_651Q (⁶⁵⁰GTT_⁶⁵¹CAG), and carriers of both alternative alleles: 650I_651Q (⁶⁵⁰ATT_⁶⁵¹CAG).

This association is also apparent in carriers of 651Q (⁶⁵¹CAG) ($p=0.002$, Figure 3-6). This sub-group will also contain all of the 650I (⁶⁵⁰ATT) carriers in this cohort since the two polymorphisms are in LD. When 650I carriers were assessed, the strong association with lower activity still present ($p=0.014$, Figure 3-7).

3.6.2 FXIIIa subunit levels and *F13A1* genotypes

Plasma FXIIIa levels (IU/mL) were assessed for each of the *F13A1* polymorphisms under study. The mean FXIIIa levels differed between the genotypes, with the lowest (0.93 IU/mL \pm 0.80 SD) in 651QQ alternative homozygotes, and the highest (1.19 IU/mL \pm 1.24 SD) in 34V/L heterozygotes (Table 3-8A). One-way ANOVA analysis of variance found no relationship between levels and genotypes (Table 3-9).

3.6.3 Plasma D-Dimers levels and F13A1 genotypes

One-way ANOVA analysis of variance was used to test for associations between D-Dimer levels and *F13A1* genotypes. No relationship was found between the two variables (Table 3-9).

3.6.4 Summary

Compared to the WT, carriers of 34L allele presented higher activity. In contrast, carriage of 650I_651Q alleles resulted in significantly lower activity. No relationship was observed between FXIIIa levels and *F13A1* genotypes. As expected, no associations were observed between D-Dimer levels and *F13A1* genotypes.

Table 3-7: Variations in plasma FXIII activity for *F13A1* polymorphisms

A	Statistics	103G>T (V34L)			1954G>C (E651Q)			1951G>A_1954G>C 650_651 alleles		
		GG n=52	G/T n=30	TT n=7	GG n=46	G/C n=37	CC n=6	G_G n=46	G_C n=31	A_C n=12
	Mean	0.85	1.04	1.30	1.06	0.87	0.58	1.06	0.87	0.70
	Median	0.76	1.03	1.23	1.01	0.80	0.64	1.01	0.80	0.58
	SD	0.38	0.25	0.47	0.38	0.32	0.16	0.38	0.26	0.43
	Minimum	0.16	0.63	0.76	0.16	0.40	0.34	0.16	0.44	0.34
	Maximum	1.92	1.62	1.99	1.99	1.92	0.75	1.99	1.43	1.92

B	Statistics	103G>T (V34L)		1951G>A (V650I)		1954G>C (E651Q)	
		GG n=52	G/T or TT n= 37	GG n=77	G/A or AA n=12	GG n=46	GC or CC n=43
	Mean	0.85	1.09	0.99	0.70	1.06	0.83
	Median	0.76	1.05	0.93	0.58	1.01	0.76
	SD	0.38	0.38	0.35	0.43	0.38	0.32
	Minimum	0.16	0.63	0.16	0.34	0.16	0.34
	Maximum	1.92	1.99	1.99	1.92	1.99	1.92

Differences in plasma FXIII activity (IU/mL) mean, median, SD for *F13A1* genotypes are shown in Table A. The same analysis was repeated with genotype carriers in Table B, since n=0 or very low for the alternative alleles. For 1951G>A (V650I) polymorphism, the data for heterozygous and homozygous alternative was combined due to small numbers (n < 5) and presented in Table B. Frequency of homozygous, heterozygous and homozygous alternative for each of the *F13A1* polymorphisms is presented (total frequency : 89, two patients were not genotyped).

Table 3-8: Variations of FXIIIA levels for *F13A1* polymorphisms

A	Statistics	103G>T (V34L)			1954G>C (E651Q)			1951G>A_1954G>C 650_651 alleles		
		GG n=51	G/T n=30	TT n=7	GG n=45	G/C n=37	CC n=6	G_G n=45	G_C n=31	A_C n=12
	Mean	0.98	1.19	1.00	1.06	1.05	0.93	1.06	1.03	1.04
	Median	0.88	0.71	0.66	0.88	0.70	0.64	0.88	0.88	0.52
	SD	0.59	1.24	0.68	0.74	1.04	0.80	0.74	0.70	1.58
	Minimum	0.21	0.11	0.28	0.21	0.11	0.24	0.21	0.11	0.24
	Maximum	2.48	5.85	2.24	4.13	5.85	2.48	4.13	2.64	5.85

B	Statistics	103G>T (V34L)		1951G>A (V650I)		1954G>C (E651Q)	
		GG n=51	G/T or TT n= 37	GG n=76	G/A or AA n=12	GG n=45	G/C or CC n=43
	Mean	0.98	1.15	1.05	1.04	1.06	1.03
	Median	0.88	0.70	0.88	0.52	0.88	0.70
	SD	0.59	1.15	0.72	1.58	0.74	1.00
	Minimum	0.21	0.11	0.11	0.24	0.21	0.11
	Maximum	2.48	5.85	4.13	5.85	4.13	5.85

Differences in plasma FXIIIA levels (IU/mL) mean, median, SD for *F13A1* genotypes are shown in Table A. The same analysis was repeated with genotypes carriers in Table B, since n=0 or very low for the alternative alleles. For 1951G>A (V650I) polymorphism, the data for heterozygous and homozygous alternative was combined due to small numbers (n<5) and presented in table B. Frequency of homozygous, heterozygous and homozygous alternative for each of the *F13A1* polymorphisms is also presented (Total frequency : 88, two patients were not genotyped, and the level was not determined for one patient).

Table 3-9: Results of one-way ANOVA for associations between *F13A1* SNPs, plasma FXIII and D-Dimer levels

A	Variable	<i>F13A1</i> Genotype							
		103G>T (V34L)		1951G>A (V650I)		1954G>C (E651Q)		650_651 alleles	
		p-value	Sig.	p-value	Sig.	p-value	Sig.	p-value	Sig.
	FXIII activity	0.002	**	0.014	*	0.002	**	0.004	**
	FXIIIA levels	0.574	ns	0.944	ns	0.955	ns	0.989	ns
	D-Dimer levels	0.668	ns	0.258	ns	0.326	ns	0.389	ns

B	Variable	<i>F13A1</i> Genotype Carriers							
		103G>T (V34L)		1951G>A (Val650I)		1954G>C (E651Q)		650_651 alleles	
		p-value	Sig.	p-value	Sig.	p-value	Sig.	p-value	Sig.
	FXIII activity	0.002	**	0.014	*	0.003	**	0.004	**
	FXIIIA levels	0.352	ns	0.944	ns	0.882	ns	0.989	ns
	D-Dimer levels	0.516	ns	0.258	ns	0.801	ns	0.389	ns

Alpha was set at 0.05. Level of Significance (Sig.): *=p<0.05, **=p<0.001, ns=not significant. Significant values highlighted in orange.

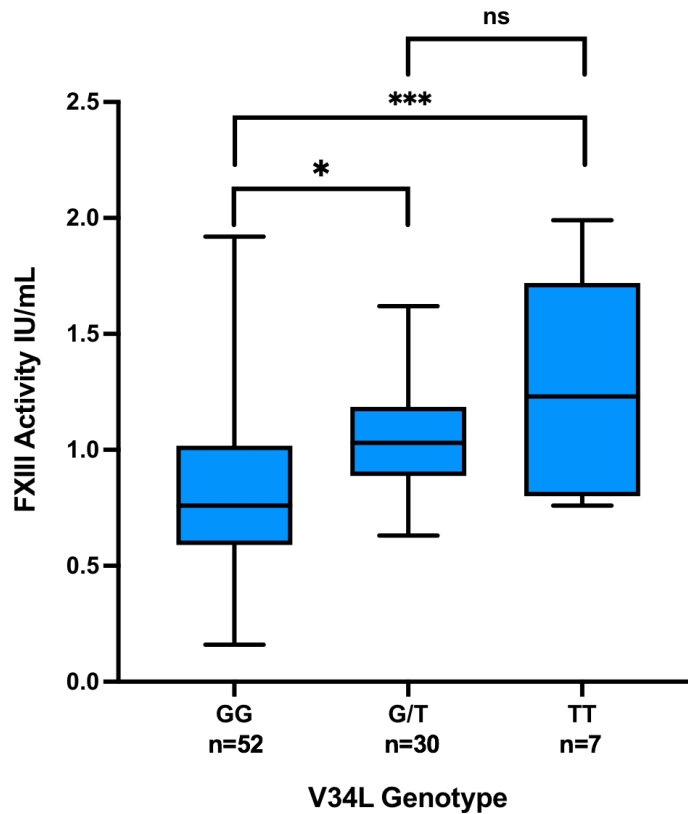


Figure 3-4: 34L carriers demonstrate higher activity than the WT

This boxplot illustrates the median values (middle bold line within the box) of FXIII activity for V34L genotype in EOC ICON7 patients (n=89). The ends of the boxes show the upper and lower quartiles, the length of the boxes show the inter-quartile range. The ends of the whiskers represent the minimum and maximum values. Tukey's Post Hoc test was performed to identify which groups differed from each other. The results showed the statistically significant difference is the difference between V34L wildtype homozygous (GG) and both heterozygous (G/T) (p=0.041) and alternative homozygous (TT) (p=0.005) groups. However, the difference between the heterozygous (G/T) and alternative homozygous (TT) was not significant (p=0.184). Levene's test was performed to evaluate the homogeneity of variances needed for the one-way ANOVA. The result showed that, the homogeneity requirement was not met and the null hypothesis that there is no difference in the variances between the groups was rejected and the alternative hypothesis that there is a statistically significant difference in the variances between groups was accepted (p=0.041).

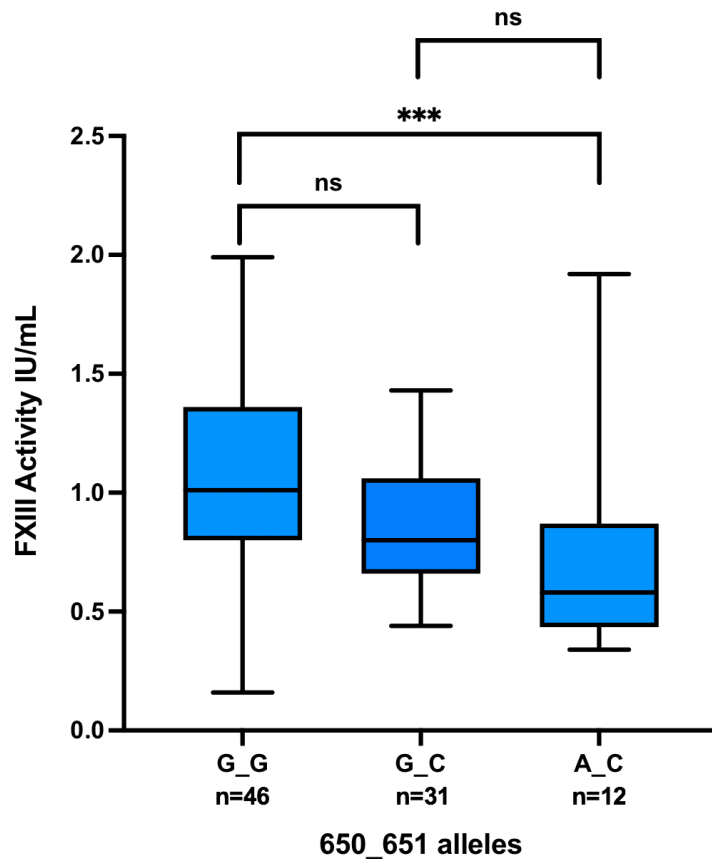


Figure 3-5: 650I_651Q (⁶⁵⁰A⁶⁵¹CAG) alleles demonstrate significantly lower activity

The box and whisker plot displays the distribution of the FXIII activity by 650_651 alleles. The line splitting the box into two represent the median. The middle 50% of the values lie between the upper and lower edges of the box. Endpoints of the whiskers represent the minimum and maximum values. Compared to the WT, FXIII activity was significantly lower in individuals carrying the haplotype 650I_651Q (⁶⁵⁰A⁶⁵¹CAG), (p=0.004). Tukey's Post Hoc test showed statistically significant difference between wildtype homozygous GG (⁶⁵⁰GTT₆₅₁GAG) and carriers of both alternative alleles AC (⁶⁵⁰ATT₆₅₁CAG), (p=0.007). However, the difference between wildtype homozygous GG and carriers of one alternative allele GC (⁶⁵⁰GTT₆₅₁CAG) was not significant (p=0.065), nor the difference between carriers of one alternative allele GC and homozygous for the alternative alleles AC (p=0.337). Levene's test of Homogeneity of Variances between groups was not significant (p=0.289). The null hypothesis could not be rejected, the variances were homogeneous, and the results are considered reliable. The level of significance: ***=p<0.001 and ns=not significant.

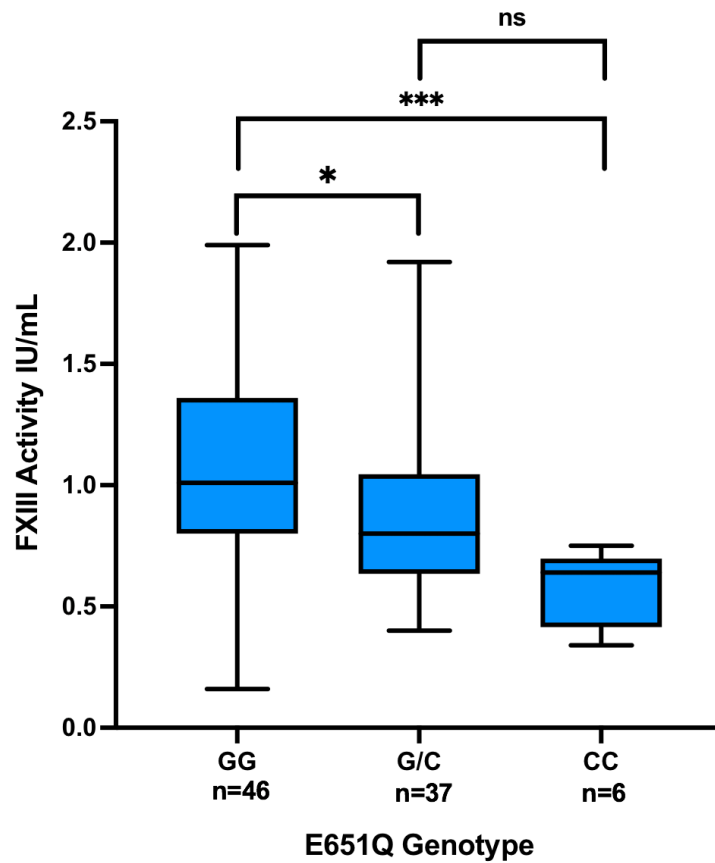


Figure 3-6: 651Q carriers show significantly lower activity

This boxplot illustrates the median values (middle bold line within the box) of FXIII activity for E651Q genotype in EOC ICON7 patients (n=89). The ends of the boxes show the upper and lower quartiles, the length of the boxes show the inter-quartile range. The ends of the whiskers represent the minimum and maximum values. Tukey's Post Hoc test showed statistically significant difference between E651Q wildtype homozygous (EE) and both heterozygous (E/Q) ($p=0.037$) and alternative homozygous (QQ) ($p=0.006$) groups. However, the difference between the heterozygous (E/Q) and alternative homozygous (QQ) was not significant ($p=0.154$). Levene's test of Homogeneity of Variances between groups was not significant ($p=0.164$). The null hypothesis could not be rejected, the variances were homogeneous, and the results are considered reliable.

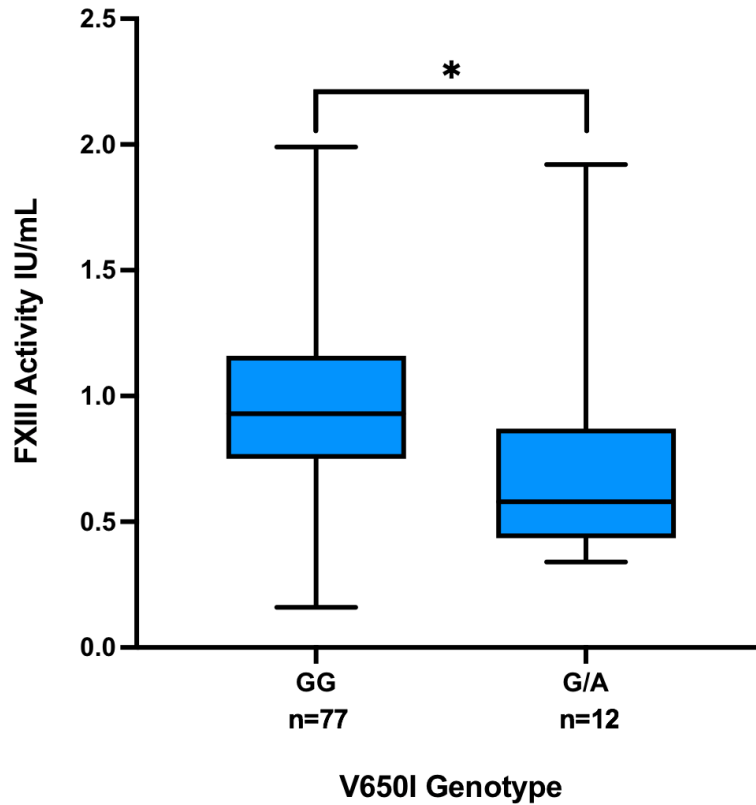


Figure 3-7: 650I carriers show significantly lower activity

This boxplot illustrates the median values (middle bold line within the box) of FXIII activity for V650I genotype in EOC ICON7 patients (n=89). The ends of the boxes show the upper and lower quartiles, the length of the boxes show the inter-quartile range. The ends of the whiskers represent the minimum and maximum values. One-way ANOVA indicated statistically significant lower mean plasma FXIII activity in heterozygotes 650G/A compared to the WT (p=0.014). Levene's test of Homogeneity of Variances between groups was not significant (p=0.837). The null hypothesis could not be rejected, the variances were homogeneous, and the results are considered reliable.

3.7 Plasma FXIII, plasma D-Dimer levels, *F13A1* genotypes and EOC prognostic factors

A prognostic factor is a feature of a disease or clinical presentation that independently influences the outcome. Tests of association were used to evaluate the relationship between FXIII activity, FXIII A levels, *F13A1* genotypes, plasma D-Dimer levels and disease prognostic factors such as grade of disease, stage, histology, risk of disease progression and extent of the residual disease. A larger percentage of high-grade tumours were of serous histology (Table 3-10B). Stage was significantly associated with the extent of residual disease and high risk of disease progression status ($p < 0.001$), (Tables 3-10A, 3-10C and D). Patients at high risk of disease progression were diagnosed at advanced stage, accounting for 40% of those in stage III and 100% in stage IV (Table 3-10E).

3.7.1 FXIII activity

The one-way ANOVA analyses of variance was used to assess the relationship between plasma FXIII activity and EOC clinical variables. Plasma FXIII activity was significantly associated with advanced stage ($p = 0.029$). Activity was significantly lower in stage IV than in stage III (means: $0.65 \text{ IU/mL} \pm 0.28 \text{ SD}$, $n = 9$, and $1.01 \text{ IU/mL} \pm 0.38 \text{ SD}$, $n = 66$, respectively) (Figure 3-8). No associations were observed between FXIII activity and age, grade, histology, SerousHighGrade, high risk of disease progression, residual disease or treatment received (Table 3-11).

3.7.2 FXIII A levels

The relationship between plasma FXIII A subunit levels and EOC prognostic factors was assessed using the one-way ANOVA. Plasma FXIII A subunit levels were significantly lower in patients with poorly differentiated serous tumours compared to other histologies ($p = 0.015$) (means: $0.82 \text{ IU/mL} \pm 0.57 \text{ SD}$, $n = 46$ and $1.26 \text{ IU/mL} \pm 1.05 \text{ SD}$, $n = 44$, respectively), (Figure 3-9). No correlation was found between FXIII A levels and age, stage, histology, high risk of disease progression, residual disease and treatment received (Table 3-11).

3.7.3 D-Dimer levels

The relationship between plasma D-Dimer levels and EOC prognostic factors was evaluated using one-way ANOVA analyses of variance. Plasma D-Dimer levels were higher in patients at high risk of disease progression compared with those who were not at high risk; however, this relationship was not statistically significant ($p=0.103$), (Table 3-11). Higher D-Dimer levels are seen with increasing EOC stage (means: stage I: $4.17 \mu\text{g/mL} \pm 1.22 \text{ SD}$, $n=7$; Stage II: $4.45 \pm 0.94 \text{ SD}$, $n=9$; stage III: 5.10 ± 1.89 , $n=66$; stage IV: $6.17 \pm 1.62 \text{ SD}$, $n=9$) respectively; however, this association was not significant (ANOVA $p=0.102$), (Figure 3-10). Nevertheless, a strong positive correlation between plasma D-Dimer levels and increasing EOC stage would suggest that D-Dimer levels could be used as a predictive indicator of disease progression. Correlation analysis showed a strong positive monotonic relationship between these two variables (Spearman's rho Correlation Coefficient = 1.000, $n=91$, $p=0.018$). No significant associations were found with either grade of tumour, histology or treatment received (Table 3-11).

3.7.4 F13A1 genotypes

Chi-squared test for association was performed to examine the association between *F13A1* genotypes and EOC prognostic factors. V34L and E651Q were tested in genotype and carrier status. V650I SNP was only present as carriers, and 650_651 alleles were tested as carrier of the relevant allele. No associations were observed between *F13A1* polymorphisms and prognostic factors in this EOC cohort (Table 3-12).

3.7.5 Summary

Plasma FXIII activity is significantly lower in EOC stage IV than in stage III. Plasma FXIIIa levels are significantly lower in SerousHighGrade ovarian tumours compared to other histologies. Plasma D-Dimer levels are significantly correlated with EOC stage. No correlation found between FXIII activity and grade, histology, high-grade serous, high risk for disease progression or treatment received. No correlation was found between FXIIIa levels and stage, histology, high risk for disease progression or treatment received.

Table 3-10: Results of Chi-squared test for association between the clinical variables in ICON7 study-cohort

A

EOC Prognostic Factor	EOC Prognostic Factor							
	Age	Grade	Stage	Histology	Treatment	SerousHigh Grade	Risk of progression	Residual disease
Age		0.337	0.670	0.876	0.176	0.083	0.193	0.267
Grade			0.550	0.450	0.462	< 0.001	0.636	0.658
Stage				0.358	0.728	0.846	< 0.001	< 0.001
Histology					0.087	0.118	0.394	0.760
Treatment						0.075	0.608	0.549
SerousHigh Grade							0.266	0.124
Risk of progression								< 0.001
Residual disease								

B

SerousHighGrade	Grade		
	I	II	III
SerousHighGrade	0	0	47 (65%)
Others	3 (100%)	16 (100%)	25 (35%)

C

Risk of disease progression	Stage			
	I	II	III	IV
High risk	0	0	27 (41%)	9 (100%)
Not high risk	7 (100%)	9 (100%)	39 (59%)	0

D

Extent of residual disease	Stage			
	I	II	III	IV
Residual disease ≤ 1 cm	7 (100%)	9 (100%)	0	0
FIGO Stage III + Residual disease ≤ 1 cm	0	0	39 (59%)	0
Residual disease > 1 cm	0	0	27 (41%)	9 (100%)

E

Risk of disease progression	Extent of residual disease		
	Residual disease ≤ 1 cm	FIGO Stage III + Residual disease ≤ 1 cm	Residual disease > 1 cm
High risk	0	0	36 (100%)
Not high risk	16 (29%)	39 (71%)	0

A) Results of Chi-squared test for association between the EOC prognostic factors in ICON7 study-cohort (n=91). **B)** Distribution of SerousHighGrade histology and tumour grade, with percentage calculated form the total of each grade. **C)** Distribution of high risk for disease progression and stage of disease, with percentage calculated form the total of each stage. **D)** Distribution of stage and extent of residual disease status, with percentage calculated form the total of each stage. **E)** Distribution of patients at high-risk of disease progression and extent of residual disease status, with percentage calculated form the total of high-risk. Alpha was set at 0.05. If the p-value was <0.05, the findings were deemed significant. The significant values highlighted in orange.

Table 3-11: Results of one-way ANOVA for association between EOC prognostic factors, plasma FXIII and D-Dimer levels

Prognostic factor	FXIII activity		FXIII A Levels		D-Dimer levels	
	p-value	Sig.	p-value	Sig.	p-value	Sig.
Age at diagnosis	0.381	ns	0.451	ns	0.523	ns
Grade of disease	0.677	ns	< 0.001	***	0.464	ns
FIGO stage	0.029	*	0.822	ns	0.102	ns
Histology	0.768	ns	0.684	ns	0.846	ns
Risk of disease progression	0.945	ns	0.914	ns	0.103	ns
SerousHighGrade	0.747	ns	0.015	*	0.947	ns
Extent of residual disease	0.433	ns	0.989	ns	0.105	ns
Treatment received	0.609	ns	0.386	ns	0.331	ns

Alpha was set at 0.05. Level of Significance (Sig.): *= $p < 0.05$, ***= $p < 0.001$, ns=not significant. Significant values highlighted in orange.

Table 3-12: Results of Chi-squared test for association between *F13A1* genotypes and EOC prognostic factors

A

EOC Prognostic Factor	<i>F13A1</i> Genotype			
	103G>T (Val34Leu)		1954G>C (Glu651Gln)	
	p-value	Sig.	p-value	Sig.
Age at diagnosis	0.125	ns	0.348	ns
Grade	0.471	ns	0.718	ns
FIGO Stage	0.509	ns	0.897	ns
Histology	0.949	ns	0.971	ns
SerousHighGrade	0.495	ns	0.950	ns
Risk of disease progression	0.194	ns	0.804	ns
Extent of residual disease	0.310	ns	0.949	ns
Treatment received	0.843	ns	0.603	ns

B

EOC Prognostic Factor	<i>F13A1</i> Genotype Carriers							
	103G>T (Val34Leu)		1951G>A (Val650Ile)		1954G>C (Glu651Gln)		1951G>A_1954G>C 650_651 alleles	
	p-value	Sig.	p-value	Sig.	p-value	Sig.	p-value	Sig.
Age at diagnosis	0.117	ns	0.316	ns	0.572	ns	0.342	ns
Grade	0.466	ns	0.592	ns	0.417	ns	0.415	ns
FIGO Stage	0.547	ns	0.876	ns	0.916	ns	0.978	ns
Histology	0.810	ns	0.199	ns	0.824	ns	0.314	ns
SerousHighGrade	0.900	ns	0.508	ns	0.753	ns	0.802	ns
Treatment received	0.761	ns	0.967	ns	0.338	ns	0.565	ns
Risk of disease progression	0.523	ns	0.275	ns	0.636	ns	0.332	ns
Extent of residual disease	0.769	ns	0.553	ns	0.785	ns	0.604	ns

A) Results of Chi-squared test for association between the EOC prognostic factors and *F13A1* genotypes in ICON7 study-cohort (n=91). **B)** The same analysis was repeated with genotype carriers. Age at diagnosis is a numerical variable, for this analysis it was categorised into below and above the median (56 years). Alpha was set at 0.05. Level of Significance (Sig.): ns=not significant.

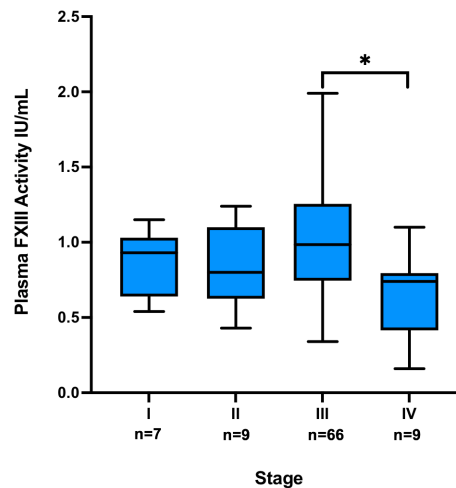


Figure 3-8: Plasma FXIII activity is significantly lower in EOC stage IV than in stage III

The boxplots (Box-Whisker Diagram) above illustrate the median values (middle bold line within the box) for FXIII activity by stage at diagnosis for ICON7 patients (n=91). The ends of the boxes show the upper and lower quartiles, the length of the boxes show the inter-quartile range. The ends of the whiskers represent the minimum and maximum values. Tukey's Post Hoc test showed significant difference in FXIII mean activity between stage III and stage IV (p=0.027). However, no statistically significant difference between the means of other stages was found. Levene's test of Homogeneity of Variances between groups was not significant (p=0.332). The null hypothesis could not be rejected, the variances were homogeneous, and the results are considered reliable.

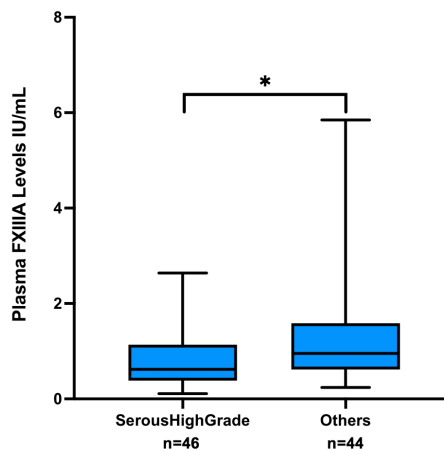


Figure 3-9: Plasma FXIIIA levels is significantly lower in SerousHighGrade (Type II) EOC

The boxplots (Box-Whisker Diagram) above illustrate the median values (middle bold line within the box) for FXIIIA levels by high-grade serous for ICON7 patients (n=90). The ends of the boxes show the upper and lower quartiles, the length of the boxes show the inter-quartile range. The ends of the whiskers represent the minimum and maximum values. One-way ANOVA showed significant decrease in FXIIIA mean levels in patients with serous high-grade disease compared to others (p=0.015). Levene's test of Homogeneity of Variances between groups was significant (p=0.036), hence, the null hypothesis was rejected.

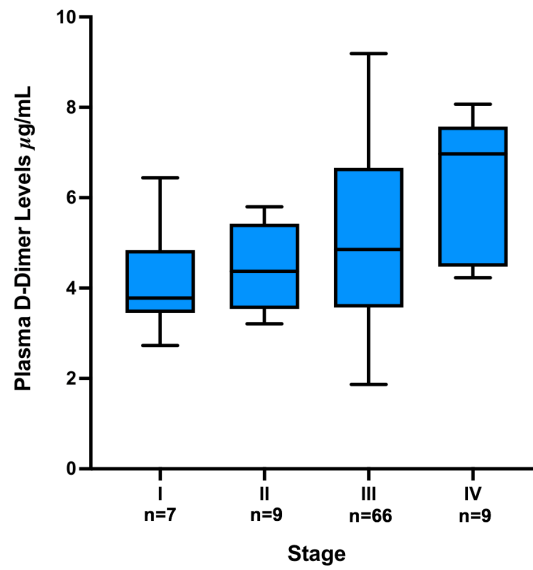


Figure 3-10: Higher D-Dimer levels observed with increasing EOC stage

The boxplot above illustrates the median values (lined); interquartile range (boxed); and the minimum to maximum values (whiskers) for plasma D-Dimer levels versus EOC stage at diagnosis for ICON7 patients (n=91). Higher level of plasma D-Dimer levels is significantly correlated with stage of disease (Spearman's rho Correlation Coefficient = 1.000, n=91, p=0.018).

3.8 FXIII A tissue expression

Expression of FXIII A protein was explored in EOC for the first time within the Dr Anwar Research Laboratory. The expression level and localisation was evaluated in the ICON7 translational cohort using constructed formalin-fixed paraffin-embedded tissue microarrays (TMAs). Immunohistochemistry staining of the slides and TMAs scoring and quantification of signal presented in these sections was performed by Dr Kathryn Hutchison, University of Leeds (Hutchinson, 2019).

3.8.1 Expression site

For this dataset (91 ICON7 plasma cases), only 29 cases had stroma cores, 40 cases had tumour/stroma cores and 44 cases had tumour cores available. To determine the distribution of percent positive cores among different tissue types, staining data and patients data were compiled. Table 3-13 presents descriptive statistics for FXIII A IHC positive stained ICON7 TMAs. The results showed evidence of positive staining and presence of FXIII A protein in the EOC ICON7 tissues examined. The highest average percentage of positive staining was observed in OC stroma cores, followed by tumour/stroma, and finally tumour cores (Figure 3-11). Examples of the IHC staining for the different core types, staining intensity and positive and negative controls are presented in Appendix III.

3.8.2 Plasma FXIII A subunit

The aim of this section was to answer an important research question: is there an association between plasma FXIII A subunit levels and expression of FXIII A subunit in OC tissues? A Spearman's rank-order correlation was performed to test for this association. No direct relationship was observed between plasma FXIII A subunit levels and expression of FXIII A in EOC tissue types. Results are shown in Table 3-14.

3.8.3 F13A1 genotypes

Chi-squared tests were performed to evaluate whether associations were present between positive FXIII A staining in EOC tissue types and *F13A1* polymorphisms. No association with *F13A1* genotypes was observed (Table 3-15).

3.8.4 FXIII A tissue expression and EOC prognostic factors

The relationship between FXIII A protein expression in EOC tumour tissue and the disease clinical variables was evaluated by assessing associations between FXIII A expression in the three different locations (tumour, tumour stroma and stroma) and disease prognostic factors such as age at diagnosis, grade, stage, histology, risk for progression and treatment received. The associations were examined using the Chi-squared test. FXIII A expression in tumour tissue was significantly lower in poorly differentiated ovarian carcinoma ($p=0.015$), (Figure 3-12). No significant relationship was observed with age, stage, histology, high risk of disease progression, residual disease or treatment received (Table 3-16).

3.8.5 Summary

No direct relationship between FXIII A expression in tumour tissue and its levels in plasma or *F13A1* genotypes was found. However, FXIII A expression levels in EOC tumour tissue are significantly linked with high-grade disease (poorly differentiated carcinoma).

Table 3-13: Descriptive statistics for FXIIIA stained ICON7 TMAs

Statistics	ICON7 Tissue Microarrays (n=91)		
	Tumour (T) % positive	Tumour stroma (TS) % positive	Stroma (S) % positive
Number	44	40	29
Median	1.205	1.194	1.842
Mean	1.440	1.822	2.747
SD	1.392	1.877	2.819
Minimum	0.052	0.117	0.044
Maximum	5.766	9.472	14.81

This table presents the positive percentage of the sections stained for each of the ICON7 TMAs tissue type. All cores examined had some level of FXIIIA staining, and all positively stained cores were included because of the small numbers available.

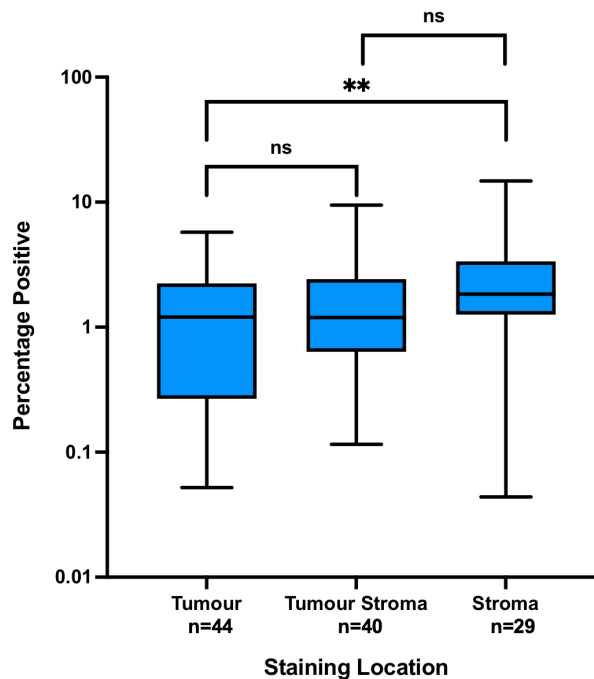


Figure 3-11: Level of staining of FXIIIA in ICON7 TMAs

The box and whisker diagram illustrates the distribution of percentage positive staining of FXIIIA in ICON7 TMAs. The line splitting the box into two represent the median. The middle 50% of the values lie between the upper and lower edges of the box. Endpoints of the whiskers represent the minimum and maximum values. Y-axis is logarithmic. The data does not match a normal distribution, therefore, the Kruskal-Wallis non-parametric test with Dunn's test for multiple pairwise comparisons were carried out to compare the groups. Alpha was set at 0.05. Level of Significance (Sig.): **= $p < 0.01$, ns=not significant. The stroma cores showed the higher percentage positive staining, followed by tumour/stroma and finally tumour cores. A statistically significant difference was observed only between stroma and tumour staining (adjusted p-value: 0.009).

Table 3-14: Tests of correlation between FXIIIA tissue expression and plasma FXIIIA subunit levels in EOC ICON7 tissue microarrays

Tissue type	FXIIIA Levels		
	Spearman's rho Correlation Coefficient	P-value	Sig.
Tumour	(-) 0.030	0.847	ns
Tumour/Stroma	0.082	0.621	ns
Stroma	0.054	0.784	ns

The closer the rho correlation coefficient value to ± 1 , the stronger the relationship between the covariates tested. Alpha was set at 0.05. Results of the significance tests were > 0.05 , therefore, the null hypothesis that there is no monotonic correlation was accepted.

Table 3-15: Results of Chi-squared tests for association between FXIIIA positive stained ICON7 tissue microarrays and *F13A1* genotypes

A	SNP		Tumour		Tumour/Stroma		Stroma	
			n	%	n	%	n	%
103G>T (V34L)	GG		18	34.6	16	30.8	13	25.0
	GT		22	73.3	19	63.3	13	43.3
	TT		4	57.1	5	71.4	3	42.9
1951G>A (V650I)	GG		40	51.9	37	48.1	26	33.8
	G/A or AA		4	33.3	3	25.0	3	25.0
1954G>C (E651Q)	GG		24	52.2	22	47.8	17	37.0
	G/C		18	48.6	15	40.5	10	27.0
	CC		2	33.3	3	50.0	2	33.3
1951G>A_1954G>C 650_651 alleles	GG_GG		24	52.2	22	47.8	17	37.0
	GG_GC or CC		16	51.6	15	48.4	9	29.0
	G/A or AA_G/C or CC		4	33.3	3	25.0	3	25.0

B	Staining location	<i>F13A1</i> genotype			
		103G>T (V34L)		1954G>C (E651Q)	
		p-value	Sig.	p-value	Sig.
	Tumour	0.420	ns	0.420	Ns
	Tumour/Stroma	0.416	ns	0.416	ns
	Stroma	0.401	ns	0.401	ns

C	Staining location	<i>F13A1</i> genotype carriers							
		103G>T (V34L)		1951G>A (V650I)		1954G>C (E651Q)		1951G>A_1954G>C 650_651 alleles	
		p-value	Sig.	p-value	Sig.	p-value	Sig.	p-value	Sig.
	Tumour	0.429	ns	0.429	ns	0.429	ns	0.420	ns
	Tumour/Stroma	0.426	ns	0.426	ns	0.426	ns	0.416	ns
	Stroma	0.413	ns	0.413	ns	0.413	ns	0.401	ns

A) Distribution of *F13A1* polymorphisms in ICON7 TMAs. **B)** Results of Chi-squared tests for association between *F13A1* genotypes and FXIIIA positive stained ICON7 tissue microarrays. **C)** Same analysis was performed for genotype carriers. Alpha was set at 0.05. Level of Significance (Sig.): ns=not significant.

Table 3-16: Results of one-way ANOVA tests for association between FXIIIa protein expression in EOC tumour types and EOC prognostic factors

A	Prognostic factor	Tissue Microarrays (TMAs) % positive					
		Tumour Cores (T)		Tumour stroma Cores (TS)		Stroma Cores (S)	
		P-value	Sig.	P-value	Sig.	P-value	Sig.
	Age at diagnosis	0.440	ns	0.847	ns	0.832	ns
	Grade	0.015	**	0.169	ns	0.445	ns
	FIGO stage	0.927	ns	0.559	ns	0.785	ns
	Histology	0.824	ns	0.789	ns	0.801	ns
	At risk of progression	0.966	ns	0.432	ns	0.827	ns
	SerousHighGrade	0.105	ns	0.500	ns	0.148	ns
	Extent of residual disease	0.970	ns	0.274	ns	0.559	ns
	Treatment received	0.324	ns	0.726	ns	0.229	ns

B	Tumour cores	Grade	
		I + II	III
		11 (57.9%)	33 (45.8%)

A) Alpha was set at 0.05. Level of Significance (Sig.): *=p<0.05, **=p<0.01, ns=not significant. Significant values highlighted in orange. **B)** Distribution of tumour grade for significant one-way ANOVA association with tumour expression, with percentage calculated from the total of each grade. Age at diagnosis is a numerical variable that was dichotomised for this study into below and above the median (56 years).

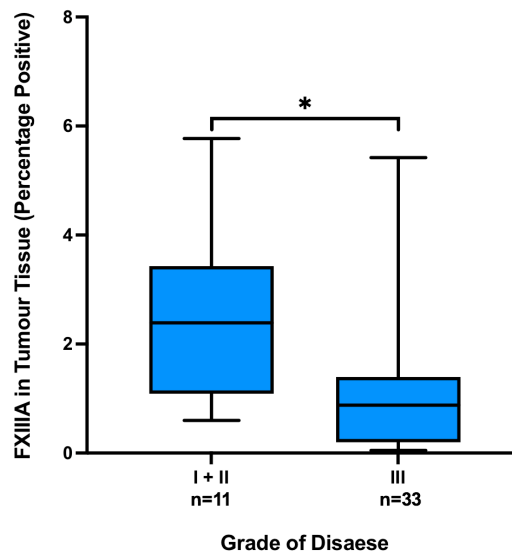


Figure 3-12: FXIIIa expression in tumour tissue is significantly lower in poorly differentiated disease

The boxplot (Box-Whiskers Diagram) above illustrates the median values (lined); interquartile range (boxed); outliers (open unfilled circles and asterisk); and the minimum to maximum values (whiskers) for FXIIIa expression in EOC tumour tissue versus grade for ICON7 patients (n=44). FXIIIa expression in EOC tumour tissue was significantly lower in poorly differentiated ovarian carcinoma (p=0.015). Levene's test of Homogeneity of Variances between groups was not significant (p=0.269), hence the null hypothesis was not rejected, and the variances are homogeneous across groups, therefore, these results are reliable.

3.9 Survival analysis

3.9.1 Univariate analysis

Kaplan-Meier (KM) survival curves were plotted to visualise the influence of each variable on survival over the study time intervals. Each downward step in the lines represents an event (Outcome of interest: Death in OS and SPP, progression of disease in PFS) experienced by a patient in the corresponding group. The small vertical ticks represents a censored observation (e.g. a patient who did not experience the event of interest by the last follow-up; study period ends without having an event or died from an unrelated cause). Log rank tests were employed to compare the differences in survival and estimate the statistical significance using $p < 0.05$ as a significance indicator.

3.9.1.1 Overall Survival

OS is the interval of time from enrolment on a study to either patient death or censorship from the study (date of last follow up). Survival rate is the percentage of patients who are still alive after a certain period of time (e.g: five years) after diagnosis with or starting treatment for a disease. The median OS for this study-cohort was 57.6 months (Table 3-17). KM graphs clearly show that, patients with the advanced FIGO stage, those at high risk of disease progression, and those with SerousHighGrade histology were significantly associated with reduced OS (Figure 3-13A, B and F). The extent of macroscopic residual disease following debulking surgery was also significantly associated with poor prognosis, with those who had inoperable disease or FIGO stage VI with > 1 cm of a residual disease have the lowest median (37.027 months), (Figure 3-13C). Plasma FXIII activity and its A subunit levels were not associated with OS (Figure 3-16C). Univariate analysis did not find any benefit in OS associated with the addition of the bevacizumab to the standard chemotherapy (Figure 3-17C). Low plasma D-Dimer levels showed close to significant benefit to OS, with the KM curve showing a clear increased gap between high and low plasma D-Dimer levels ($p=0.109$), (Figure 3-17C). *F13A1* polymorphisms were not associated with OS (Table 3-17).

3.9.1.2 Progression-Free Survival

PFS is the interval of time from the date of the enrolment on the study to the date of disease progression or death. During the whole study period, of the 91 patients chosen for this study, disease progression occurred in 62 patients (68.1%). FIGO stage, risk of disease progression and extent of residual disease were significantly associated with PFS (Figure 3-14). Patients at the advanced stage of the disease showed shorter PFS ($p < 0.001$). Women at high-risk of disease progression presented shorter PFS compared to those in the not at high-risk group ($p < 0.001$). Plasma D-Dimer levels were significantly associated with PFS, with high levels in plasma displaying greater risk of disease progression ($p = 0.030$, Figure 3-17A). Plasma FXIII activity and its A-subunit levels were not associated with PFS (Figure 3-16A). *F13A1* genotypes were not linked to PFS. Interestingly, 651EE wildtype homozygotes (1954GG) showed improved PFS (estimated median PFS was 19.2 months for 651GG homozygotes compared to 17.3 months for 651E/Q heterozygotes [1954G/C]), although not significantly ($p = 0.100$), potentially due to the small sample size (Table 3-18).

3.9.1.3 Survival Post-Progression

SPP is the length of time between disease progression and death or censorship. Recently, there has been growing interest in this outcome as an endpoint. Factors that have been shown to improve survival following disease progression confer clinical benefit and are considered protective. On the other hand, factors inversely impact survival and are associated with high mortality. FIGO stage, risk of disease progression, and SerousHighGrade histology were significantly associated with SPP (Figure 3-15). Plasma FXIII activity and its A-subunit levels were not associated with SPP (Figure 3-16B). Plasma D-Dimer levels were not associated with SPP (Figure 3-17B). *F13A1* SNPs were not associated with SPP (Table 3-19). Nevertheless, 34V/L heterozygotes (103G/T) had close to significant increased SPP ($p = 0.088$, median SPP is 43.2 months) compared to the wildtype (median SPP is 24.1 months) (Table 3-19).

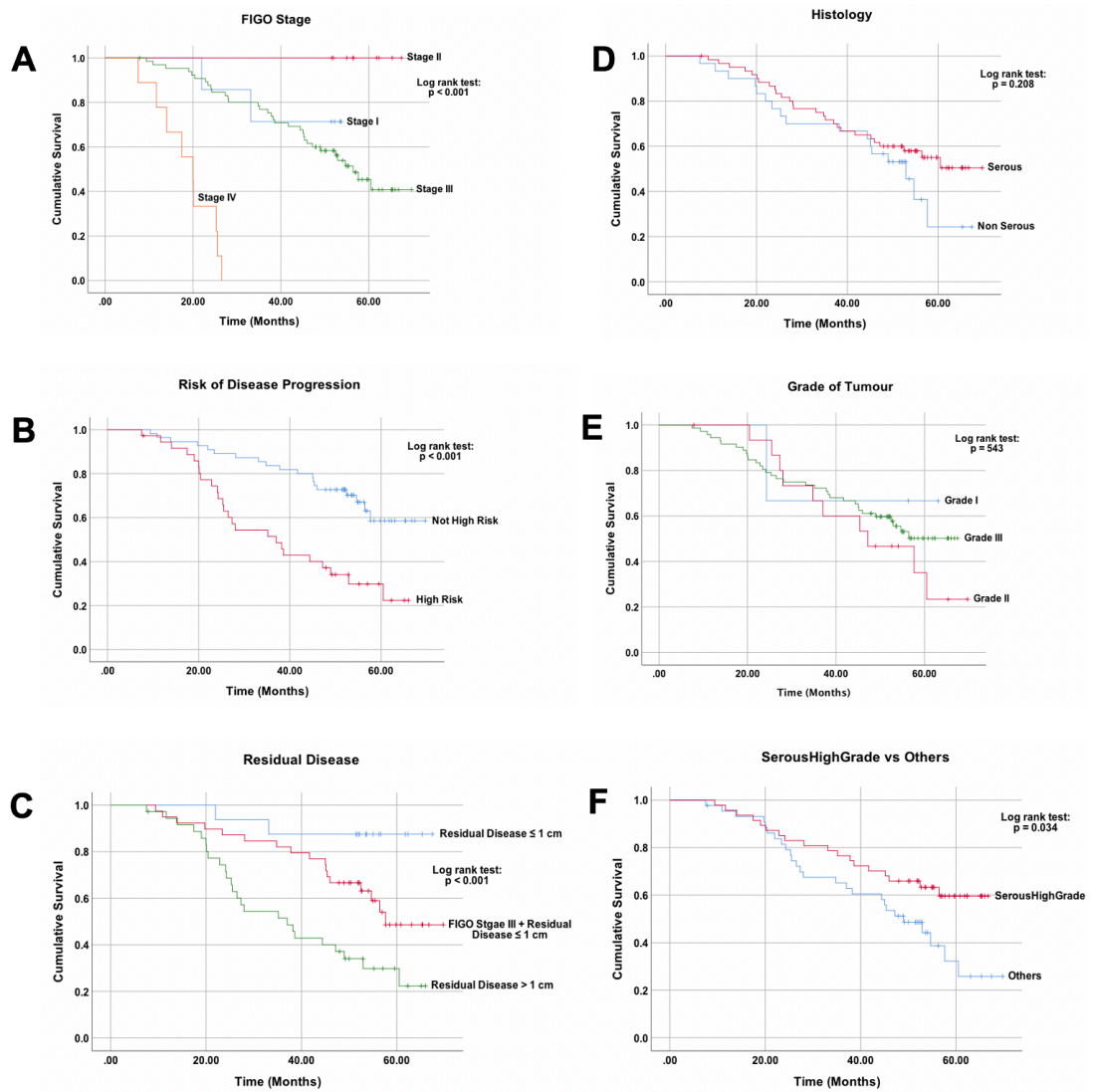


Figure 3-13: Kaplan-Meier Curves for EOC Prognostic Factors For OS

Results of the Log rank tests are displayed on the top right corner of each curve. A) FIGO stage, B) Risk of disease progression, C) Residual disease, D) Histology, E) Grade of tumour, F) SerousHighGrade. Level of Significance: $p < 0.001 = ***$. The small vertical lines represent the point at which an individual was censored.

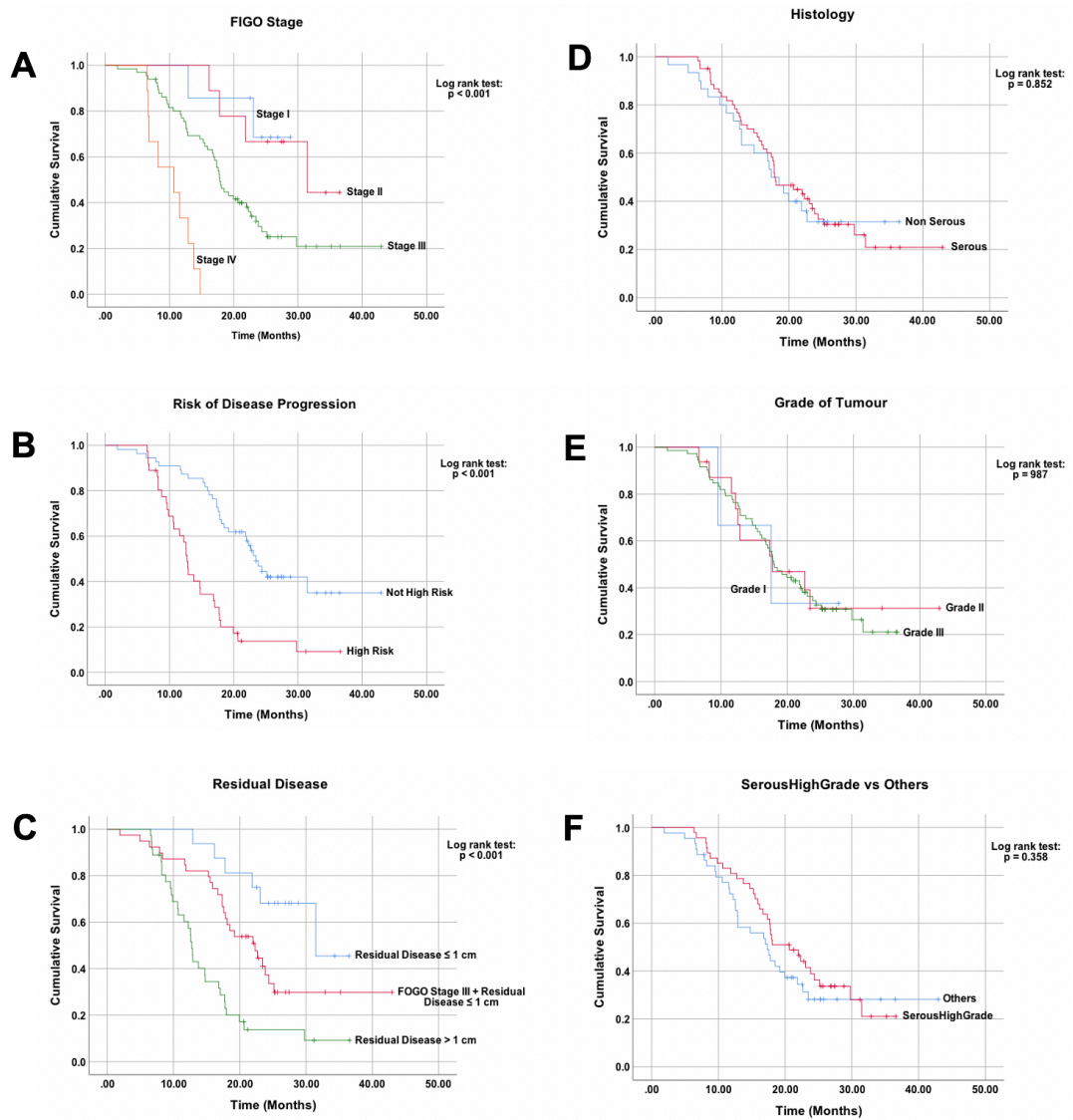


Figure 3-14: Kaplan-Meier Curves for EOC Prognostic Factors and PFS

Results of the Log rank tests are displayed on the top right corner of each curve. A) FIGO stage, B) Risk of disease progression, C) Residual disease, D) Histology, E) Grade of tumour, F) SerousHighGrade. Level of Significance: $p < 0.001 = ***$. The small vertical lines represent the point at which an individual was censored.

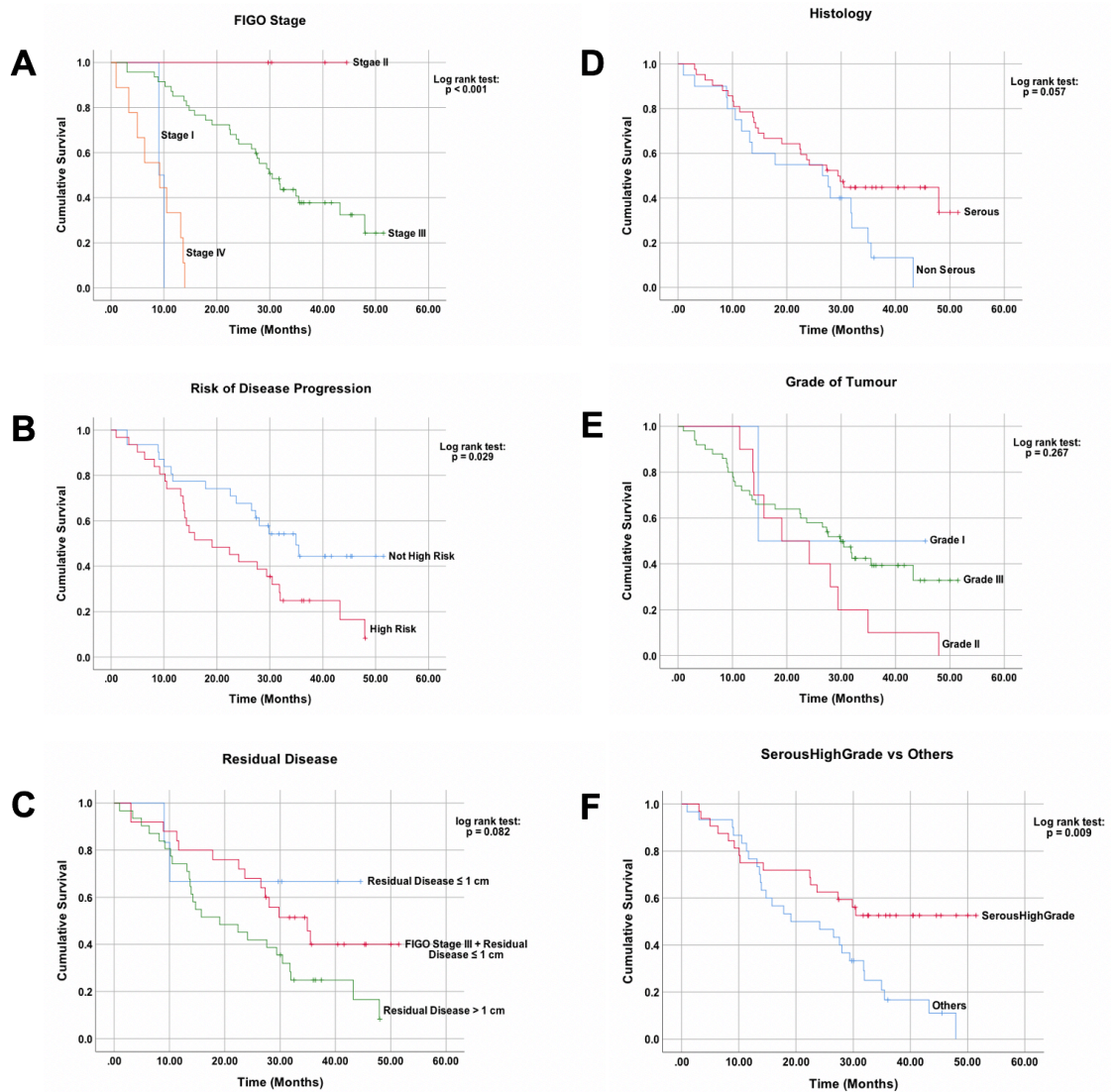


Figure 3-15: Kaplan-Meier Curves for EOC Prognostic Factors and SPP

Results of the Log rank tests are displayed on the top right corner of each curve. A) FIGO stage, B) Risk of disease progression, C) Residual disease, D) Histology, E) Grade of tumour, F) SerousHighGrade. The small vertical lines represent the point at which an individual was censored.

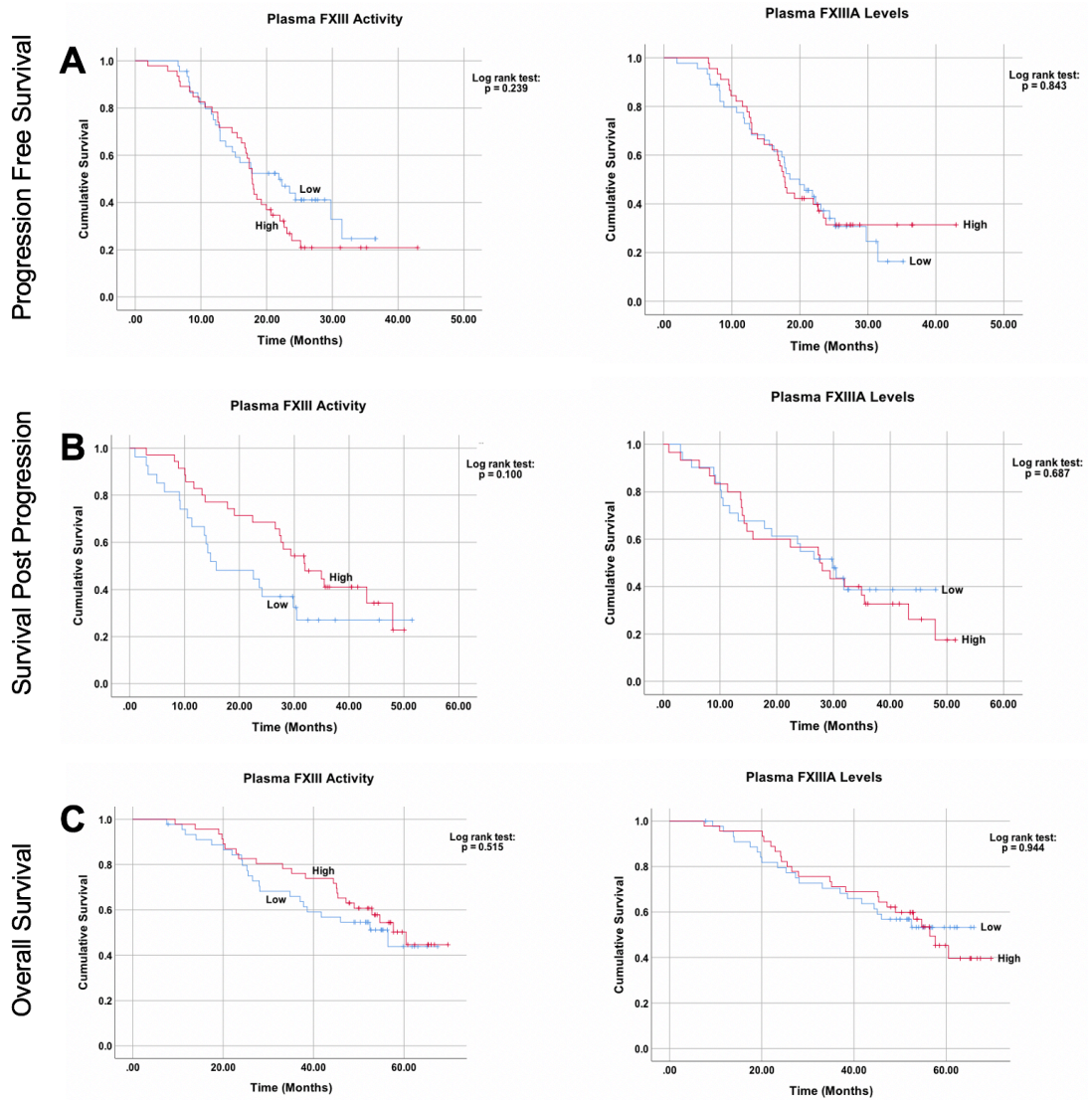


Figure 3-16: Kaplan-Meier Curves for Survival Intervals for Plasma XIII Activity and Plasma FXIII A Levels

Plots for plasma FXIII activity are displayed on the left-side of the page and plots for FXIII A levels are presented on the right-side, with the survival interval determined shown on the left of each row. For this analysis, study subjects were splitted into two categories: above the median (High) and below the median (Low). Median plasma FXIII activity was 0.92 IU/mL, whereas, median plasma FXIII A level was 0.77 IU/mL. Results of the Log rank tests are displayed on the top right corner of each graph. The small vertical lines represent the point at which an individual was censored.

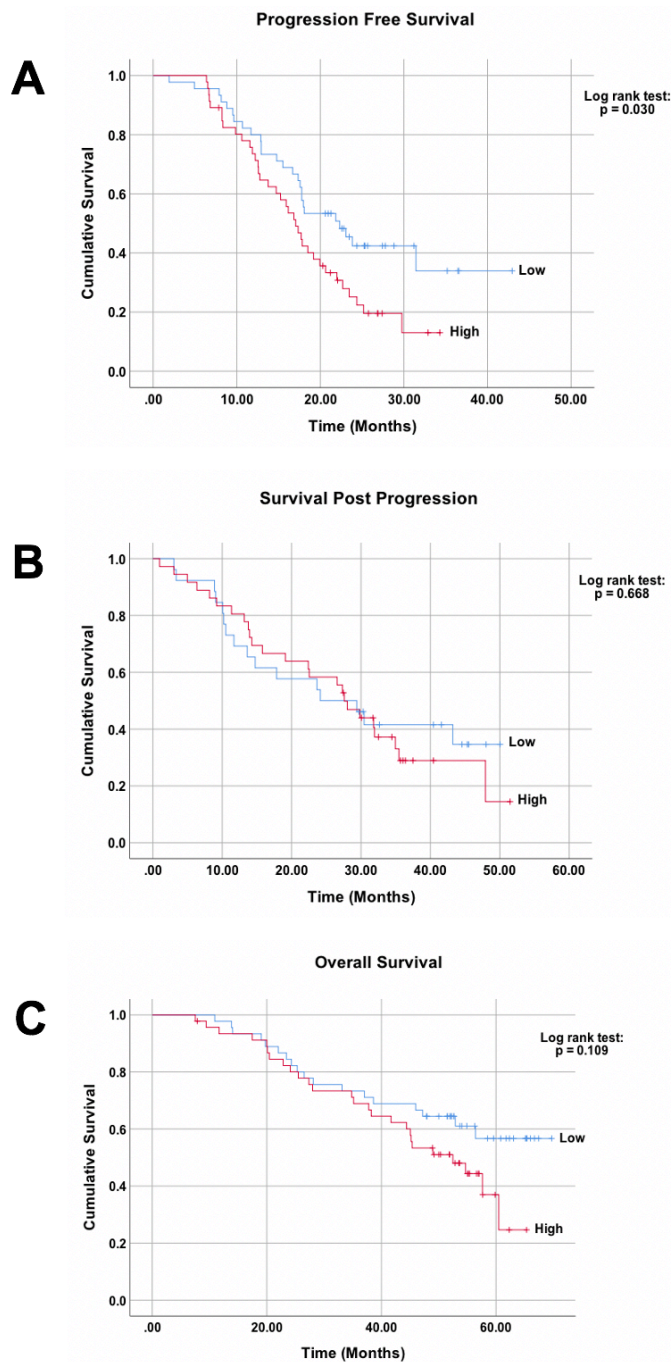


Figure 3-17: Kaplan-Meier Curves for Survival Intervals for Plasma D-Dimer Levels

For this analysis, study subjects were split into two categories: above the median (High) and below the median (Low). Median plasma D-Dimer was 4.71 $\mu\text{g}/\text{mL}$. Results of the Log rank tests are displayed on the top right corner of each curve. The small vertical lines represent the point at which an individual was censored.

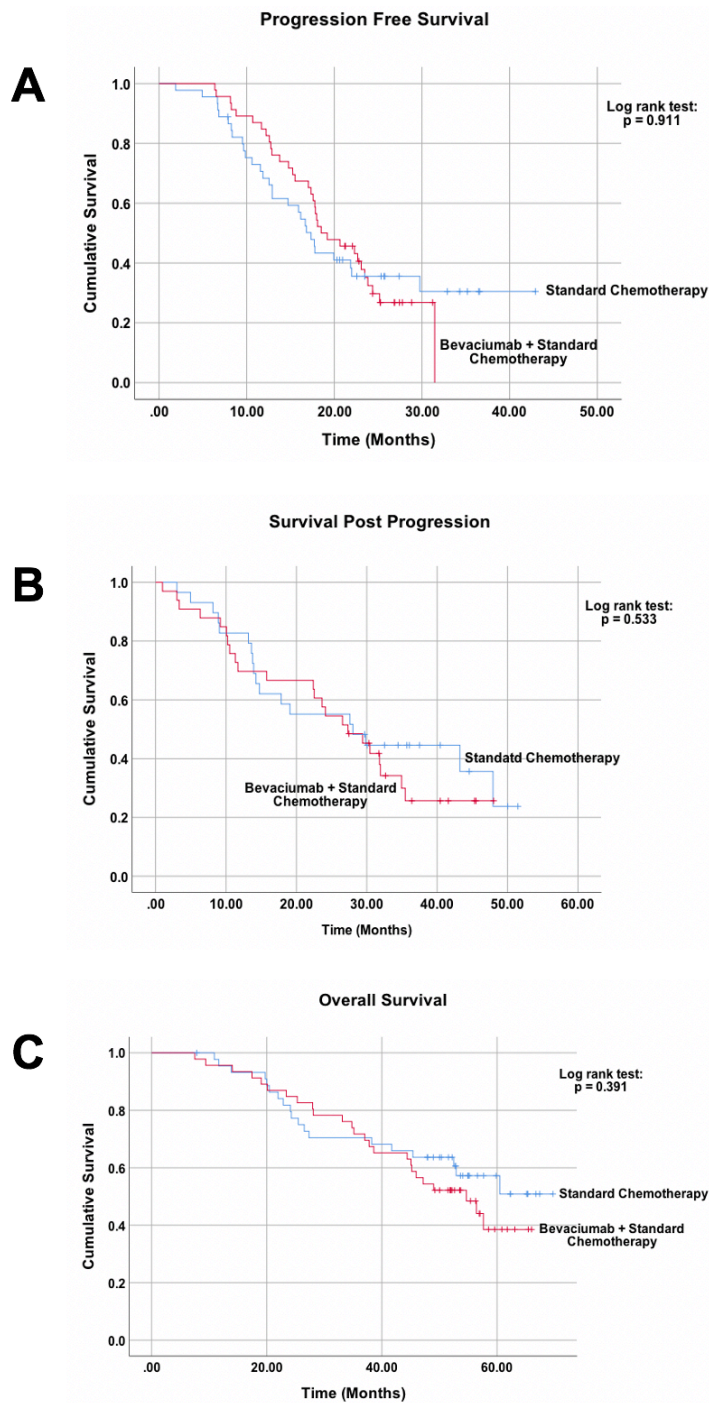


Figure 3-18: Kaplan-Meier Curves for Survival Intervals for Treatment Received

Results of the Log rank tests are displayed on the top right corner of each curve. Standard chemotherapy group includes carboplatin and paclitaxel, $n=45$. Bevacizumab + Standard chemotherapy group includes bevacizumab in addition to carboplatin and paclitaxel, $n=46$. The small vertical lines represent the point at which an individual was censored.

Table 3-17: Univariate analysis of *F13A1* SNPs for OS

<i>F13A1</i> Polymorphism	Total number	Number of Dead (%)	Number of Censored (%)	Median OS (Months)	<i>p</i>	Sig
103G>T (V34L)	89	43 (48.3)	46 (51.7)	57.626	0.138	ns
Val/Val (GG)	52	29 (55.8)	23 (44.2)	52.468		
Val/Leu (G/T)	30	10 (33.3)	20 (66.7)	-		
Leu/Leu (TT)	7	4 (57.1)	3 (42.9)	48.986		
103G>T (V34L) Carriers	89	43 (48.3)	46 (51.7)	57.626	0.133	ns
Val/Val (GG)	52	29 (55.8)	23 (44.2)	52.468		
Val/Leu (G/T) or Leu/Leu (TT)	37	14 (37.8)	23 (62.2)	-		
1951G>A (V650I)	89	43 (48.3)	46 (51.7)	57.626	0.260	ns
Val/Val (GG)	77	39 (50.6)	38 (49.4)	56.411		
Val/Ile (G/A)	12	4 (33.3)	8 (66.7)	-		
1954G>C (E651Q)	89	43 (48.3)	46 (51.7)	57.626	0.459	ns
Glu/Glu (GG)	46	20 (43.5)	26 (56.5)	-		
Glu/Gln (G/C)	37	21 (56.8)	16 (43.2)	52.895		
Gln/Gln (CC)	6	2 (33.3)	4 (66.7)	-		
1954G>C (E651Q) Carriers	89	43 (48.3)	46 (51.7)	57.626	0.450	ns
Glu/Glu (GG)	46	20 (43.5)	26 (56.5)	-		
Glu/Gln (G/C) or Gln/Gln (CC)	43	23 (53.5)	20 (46.5)	52.895		
1951G>A_1954G>C 650_651 alleles	89	43 (48.3)	46 (51.7)	57.626	0.196	ns
G_G	46	20 (43.5)	26 (56.5)	-		
G_C	31	19 (61.3)	12 (38.7)	47.179		
A_C	12	4 (33.3)	8 (66.7)	-		

The wildtype genotype is on the first line for each polymorphism, followed by the heterozygous genotype, and then the homozygous alternative genotype. Level of Significance (Sig.): ns=not significant.

Table 3-18: Univariate analysis of *F13A1* SNPs for PFS

<i>F13A1</i> Polymorphism	Total number	Number of Progressed/ Dead (%)	Number of Censored (%)	Median PFS (Months)	<i>p</i>	Sig.
103G>T (V34L)	88	61 (69.3)	27 (30.7)	17.841	0.870	ns
Val/Val (GG)	52	35 (67.3)	17 (32.7)	17.841		
Val/Leu (G/T)	29	21 (72.4)	8 (27.6)	17.972		
Leu/Leu (TT)	7	5 (71.4)	2 (28.6)	17.052		
103G>T (V34L) Carriers	88	61 (69.3)	27 (30.7)	17.841	0.882	ns
Val/Val (GG)	52	35 (67.3)	17 (32.7)	17.841		
Val/Leu (G/T) or Leu/Leu (TT)	36	26 (72.2)	10 (27.8)	17.775		
1951G>A (V650I)	88	61 (69.3)	27 (30.7)	17.841	0.294	ns
Val/Val (GG)	76	54 (71.1)	22 (28.9)	17.775		
Val/Ile (G/A)	12	7 (58.3)	5 (41.7)	21.849		
1954G>C (E651Q)	88	61 (69.3)	27 (30.7)	17.841	0.100	ns
Glu/Glu (GG)	45	30 (66.7)	15 (33.3)	19.188		
Glu/Gln (G/C)	37	29 (78.4)	8 (21.6)	17.348		
Gln/Gln (CC)	6	2 (33.3)	4 (66.7)	-		
1954G>C (E651Q) Carriers	88	61 (69.3)	27 (30.7)	17.841	0.538	ns
Glu/Glu (GG)	45	30 (66.7)	15 (33.3)	19.188		
Glu/Gln (G/C) or Gln/Gln (CC)	43	31 (72.1)	12 (27.9)	17.709		
1951G>A_1954G>C 650_651 alleles	88	61 (69.3)	27 (30.7)	17.841	0.260	ns
G_G	45	30 (66.7)	15 (33.3)	19.188		
G_C	31	24 (77.4)	7 (22.6)	16.165		
A_C	12	7 (58.3)	5 (41.7)	21.849		

The wildtype genotype is on the first line for each polymorphism, followed by the heterozygous genotype, and then the homozygous alternative genotype. Disease progression occurred in 62 patients of the whole cohort (n=91), but in 61 patients for those have been genotyped. Level of Significance (Sig.): ns=not significant.

Table 3-19: Univariate analysis of F13A1 SNPs for SPP

F13A1 Polymorphism	Total number	Number of Dead (%)	Number of Censored (%)	Median SPP (Months)	p	Sig.
103G>T (V34L)	61	40 (65.6)	21 (34.4)	28.025	0.088	ns
Val/Val (GG)	35	26 (74.3)	9 (25.7)	24.148		
Val/Leu (G/T)	21	10 (47.6)	11 (52.4)	43.236		
Leu/Leu (TT)	5	4 (80.0)	1(20.0)	8.903		
103G>T (V34L) Carriers	61	40 (65.6)	21 (34.4)	28.025	0.153	ns
Val/Val (GG)	35	26 (74.3)	9 (25.7)	24.148		
Val/Leu (G/T) or Leu/Leu (TT)	26	14 (53.8)	12 (46.2)	34.957		
1951G>A (V650I)	61	40 (65.6)	21 (34.4)	28.025	0.226	ns
Val/Val (GG)	54	37 (68.5)	17 (31.5)	26.546		
Val/Ile(G/A)	7	3 (42.9)	4 (57.1)	-		
1954G>C (E651Q)	61	40 (65.6)	21 (34.4)	28.025	0.492	ns
Glu/Glu (GG)	30	18 (60.0)	12 (40.0)	27.335		
Glu/Gln (G/C)	29	20 (69.0)	9 (31.0)	29.832		
Gln/Gln (CC)	2	2 (100.0)	0 (0.0)	14.259		
1954G>C (E651Q) Carriers	61	40 (65.6)	21 (34.4)	28.025	0.631	ns
Glu/Glu (GG)	30	18 (60.0)	12 (40.0)	27.335		
Glu/Gln (G/C) or Gln/Gln (CC)	31	22 (71.0)	9 (29.0)	29.405		
1951G>A_1954G>C 650_651 alleles	61	43 (48.3)	46 (51.7)	28.025	0.278	ns
G_G	30	18 (60.0)	12 (40.0)	27.335		
G_C	24	19 (79.2)	5 (20.8)	22.407		
A_C	7	3 (42.9)	4 (57.1)	-		

The wildtype genotype is on the first line for each polymorphism, followed by the heterozygous genotype, and then the homozygous alternative genotype. Level of Significance (Sig.): ns=not significant.

3.9.2 Sub-group analysis

A further exploration was carried out. This time with greater focus on the relevance of plasma FXIII activity to EOC outcomes, achieved by assessing the impact of activity on survival intervals and taking into account the disease prognostic factors. Activity was dichotomised into low and high using a cut-off value determined by the median (0.92 IU/mL). The analysis was performed using KM and log rank tests. No association was found with OS and PFS; however, there were some interesting findings with SPP, which are summarised below.

3.9.2.1 Treatment received

No previous study has investigated the role of plasma FXIII activity with respect to response to chemotherapy in EOC. The ICON7 trial evaluated whether adding bevacizumab to the standard chemotherapy improved outcomes. Standard chemotherapy group includes carboplatin and paclitaxel, n=45. Bevacizumab + Standard chemotherapy group includes bevacizumab in addition to carboplatin and paclitaxel, n=46. Patients with high plasma FXIII activity in receipt of bevacizumab, were found to have better prognosis and longer SPP (Log rank test: $p=0.041$, median SPP is 31.9 months) compared to those with low activity (Median SPP is 15.8 months), (Figure 3-19A).

3.9.2.2 FIGO stage

High plasma FXIII activity in patients with advanced-stage EOC had a near-significant improvement to SPP (Log rank test: $p=0.082$, median SPP is 31.8 months) compared to those with low activity (Median SPP is 14.8 months) (Figure 3-19B).

3.9.2.3 Histology

Increased plasma FXIII activity in patients with SerousHighGrade histology appears to improve SPP, although not statistically significant (Log rank test: $p=0.188$, mean SPP is 37.2 months) compared to patients with other histologies (Mean SPP is 29.5 months), (Figure 3-19C).

3.9.2.4 Grade of disease

Patients with poorly differentiated EOC appear to see improved SPP if they have high plasma FXIII activity, although not significant (Log rank test: $p=0.115$, median SPP is 35.5 months) compared to those with low activity (median SPP is 22.5 months), (Figure 3-19D).

3.9.2.5 Risk of disease progression

Patients at high risk of disease progression as defined by the ICON7 trial, include: all women with FIGO stage III inoperable disease, and women with FIGO stage III who had > 1 cm of residual disease after primary surgery and women with stage IV disease. The outcome of the whole ICON7 trial showed that the addition of the bevacizumab to the platinum-based chemotherapy has significantly improved PFS for these women (Perren et al., 2011). Sub-cohort analysis in this section showed that patients with high plasma FXIII activity who are at high risk of disease progression with > 1 cm macroscopic residual disease post primary surgery had significantly longer SPP (Log rank test: $p=0.030$, median SPP is 29.4 months) compared to patients with low activity (median SPP is 13.9 months), (Figure 3-19E).

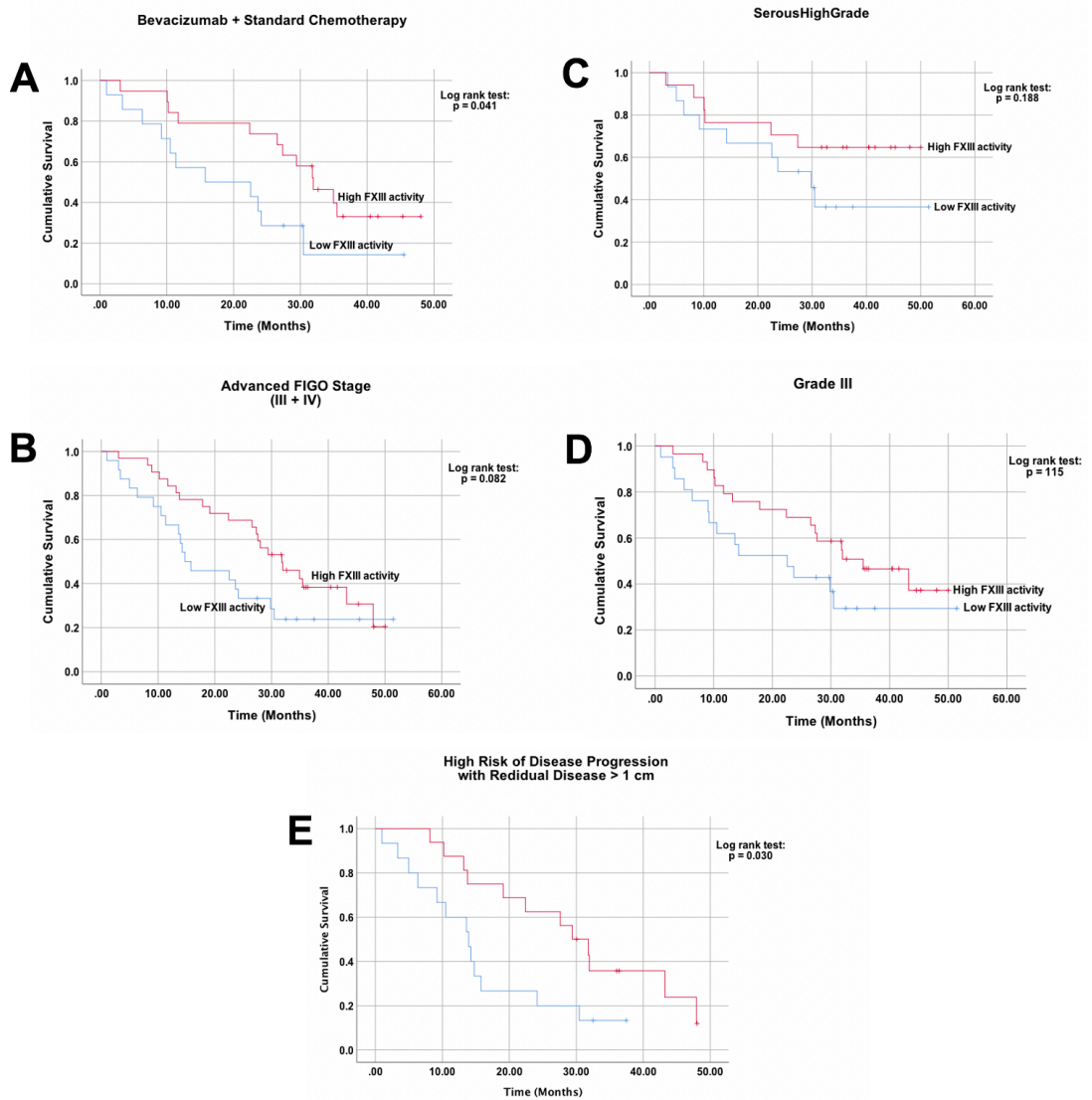


Figure 3-19: Kaplan-Meier Curves for Plasma FXIII Activity and EOC Prognostic Factors for SPP

Results of the Log rank tests are displayed on the top right corner of each curve. A) Bevacizumab in addition to standard platinum-based chemotherapy, B) Advanced FIGO stage (III + IV), C) SerousHighGrade histology, D) Grade III of disease, E) High risk of disease progression plus residual disease > 1 cm following cytoreduction surgery. The small vertical lines represent the point at which an individual was censored.

3.9.3 Multivariate analysis

The previous section has shown that no significant relationship was found between plasma FXIII A subunit levels and survival intervals. In addition, none of *F13A1* polymorphisms has significantly influenced survival intervals. However, although not statistically significant, FXIII A Val34Leu (103G/T) heterozygous carriers showed benefit in SPP, and E651Q WT homozygotes (1954GG) showed benefit in PFS. Potential prognostic factors found using univariate analysis were FIGO stage and risk of disease progression status. One limitation to using Log rank tests to investigate variations in survival in KM analysis is that it can only investigate a single binary factor without accounting for the effect of other multiple predictors.

OC is a heterogeneous disease with several factors involved that can affect response to treatment and influence survival outcome. Therefore, the aim of this section was to perform multivariate Cox proportional hazards regression model analysis to assess relationships between several variables and survival intervals simultaneously, and to identify independent prognostic factors. For Cox modelling to most accurately describe the outcome in a complex disease such as OC, a variables selection approach was used instead of a stepwise regression covariates method.

3.9.3.1 Overall Survival

Results of Cox regression analyses for OS identified advanced FIGO stage as a significant predictor of patients' deaths (HR=5.199, p=0.003), (Figure 3-20F). Women with clear cell, mucinous, endometrioid and mixed tumours had significantly reduced OS compared to those with SerousHighGrade histology (HR=2.433, p=0.044), (Figure 3-20C). Other covariates tested in the Cox model were not significantly associated with OS.

3.9.3.2 Progression-Free survival

Patients with high plasma FXIII activity had a significantly greater risk of disease progression compared to those with low plasma activity (HR=2.341, p=0.025), (Figure 3-20A). This is an interesting novel result. Women with advanced-stage EOC were significantly at greater risk of death and/or disease progression (HR=5.405, p<0.001), (Figure 3-20D). Other variables tested did not significantly associate with PFS.

3.9.3.3 Survival Post-Progression

FIGO stage was significantly associated with SPP (HR=3.700, p=0.021), (Figure 3-20E). Patients with clear cell, mucinous, endometrioid, and mixed tumours had significantly reduced survival following EOC progression compared to SerousHighGrade histology (HR=4.017, p=0.004), with a more than three-folds increased risk of death (Figure 3-20B). Other variables were not found to have a significant relationship with SPP.

Table 3-20: Multivariate Cox Proportional Hazard Regression Model for OS

Variables/ Indicators	Total number	HR	95% CI		p	Sig.
			Lower	Upper		
	88					
Age at Diagnosis		1.000	0.961	1.040	0.998	ns
Grade of Disease		1.258	0.509	3.106	0.619	ns
FIGO Stage		5.199	1.762	15.345	0.003	**
Histological Subtype		0.671	0.329	1.369	0.273	ns
Risk of Disease Progression		1.349	0.400	4.552	0.629	ns
SerousHighGrade		2.433	0.173	0.977	0.044	*
Extent of Residual Disease		0.732	0.281	1.906	0.523	ns
Treatment Received		1.296	0.639	2.627	0.472	ns
103G>T (V34L) Carriers		0.609	0.275	1.350	0.222	ns
650_651 alleles Carriers		0.798	0.470	1.357	0.406	ns
Plasma FXIII Activity		0.833	0.350	1.985	0.680	ns
Plasma FXIIIA Levels		0.901	0.447	1.813	0.770	ns
Plasma D-Dimer Levels		1.373	0.709	2.660	0.347	ns

A Cox model involves examining the relationship between covariates and survival rate. Three cases were excluded. For one case, plasma FXIIIA level was not measured and for the other two, age at diagnosis was unknown, n=88. The model included all the variables listed above. Age at diagnosis was used as a linear variable. V34L included in this model as carriers (wildtype homozygous, heterozygous + alternative homozygous). 650I_651Q allele were tested as a haplotype (wildtype, and carriers of the alternative allele). Hazard Ratios (HR) of 1 indicates that there is no correlation, HR > 1 suggest a higher probability of experiencing the event assessed (Death in OS). Whereas, HR < 1 indicates a lower risk. Abbreviations: 95% CI: 95% Confidence Intervals, Sig. : Significance, FIGO: International Federation of Gynaecology and Obstetrics. Level of Significance (Sig.): *=p<0.05, **=p<0.01, ns=not significant. Significant values highlighted in orange.

Table 3-21: Multivariate Cox Proportional Hazard Regression Model for PFS

Variables/ Indicators	Total number	HR	95% CI		p	Sig.
			Lower	Upper		
	88					
Age at Diagnosis		0.977	0.944	1.011	0.184	ns
Grade of Disease		1.046	0.428	2.557	0.922	ns
FIGO Stage		5.405	2.174	13.439	< 0.001	**
Histological Subtype		1.355	0.745	2.465	0.319	ns
Risk of Disease Progression		1.045	0.412	2.651	0.927	ns
SerousHighGrade		0.993	0.478	2.064	0.985	ns
Extent of Residual Disease		0.562	0.281	1.123	0.103	ns
Treatment Received		0.852	0.484	1.499	0.578	ns
103G>T (V34L) Carriers		0.850	0.439	1.647	0.630	ns
650_651 alleles Carriers		1.041	0.663	1.634	0.861	ns
Plasma FXIII Activity		2.341	0.224	0.954	0.025	*
Plasma FXIIIA Levels		0.918	0.501	1.680	0.780	ns
Plasma D-Dimer Levels		1.409	0.817	2.430	0.217	ns

A Cox model involves examining the relationship between covariates and survival rate. Three cases were excluded. For this model n=88, as patients with missing data points for specified variables are excluded. The model included all of the variables listed above. Age at diagnosis was used as a linear variable. V34L included as carriers (wildtype homozygous, heterozygous + alternative homozygous). 650I_651Q allele were tested as a haplotype (wildtype, and carriers of the alternative allele). HR of 1 indicates that there is no correlation, HR > 1 suggest a higher probability of experiencing the event assessed (Progression of disease in PFS). Whereas, HR < 1 indicates a lower risk. Abbreviations: 95% CI: 95% Confidence Intervals, Sig. : Significance, FIGO: International Federation of Gynaecology and Obstetrics. Level of Significance (Sig.): *=p<0.05, **=p<0.01, ns=not significant. Significant values highlighted in orange.

Table 3-22: Multivariate Cox Proportional Hazard Regression Model for SPP

Variables/ Indicators	Total number	HR	95% CI		p	Sig.
			Lower	Upper		
	88					
Age at Diagnosis		1.027	0.982	1.075	0.246	ns
Grade of Disease		1.333	0.490	3.622	0.573	ns
FIGO Stage		3.700	1.221	11.209	0.021	*
Histological Subtype		0.604	0.266	1.371	0.228	ns
Risk of Disease Progression		0.596	0.170	2.089	0.418	ns
SerousHighGrade		4.017	1.556	10.372	0.004	**
Extent of Residual Disease		0.513	0.180	1.461	0.211	ns
Treatment Received		1.512	0.691	3.308	0.300	ns
103G>T (V34L) Carriers		0.672	0.304	1.487	0.327	ns
650_651 alleles Carriers		0.942	0.545	1.626	0.829	ns
Plasma FXIII Activity		1.797	0.688	4.695	0.231	ns
Plasma FXIIIA Levels		0.892	0.398	1.998	0.780	ns
Plasma D-Dimer Levels		1.088	0.523	2.261	0.822	ns

A Cox model involves examining the relationship between covariates and survival rate. Three cases were removed. The plasma FXIIIA level was not measured in one case, and the age at diagnosis was unknown in the other two (n=88). The model included all of the variables listed above. Age at diagnosis was used as a linear variable. V34L included in this model as carriers (wildtype homozygous, heterozygous + alternative homozygous). 650I_651Q allele were tested as a haplotype (wildtype, and carriers of the alternative allele). HRs of 1 indicates that there is no correlation, HR > 1 suggest a higher probability of experiencing the event assessed (Death in SPP). Whereas HR < 1 indicates a lower risk. Abbreviations: 95% CI: 95% Confidence Intervals, Sig.: Significance, FIGO: International Federation of Gynaecology and Obstetrics. Level of Significance (Sig.): *=p<0.05, **=p<0.01, ns=not significant. Significant values highlighted in orange.

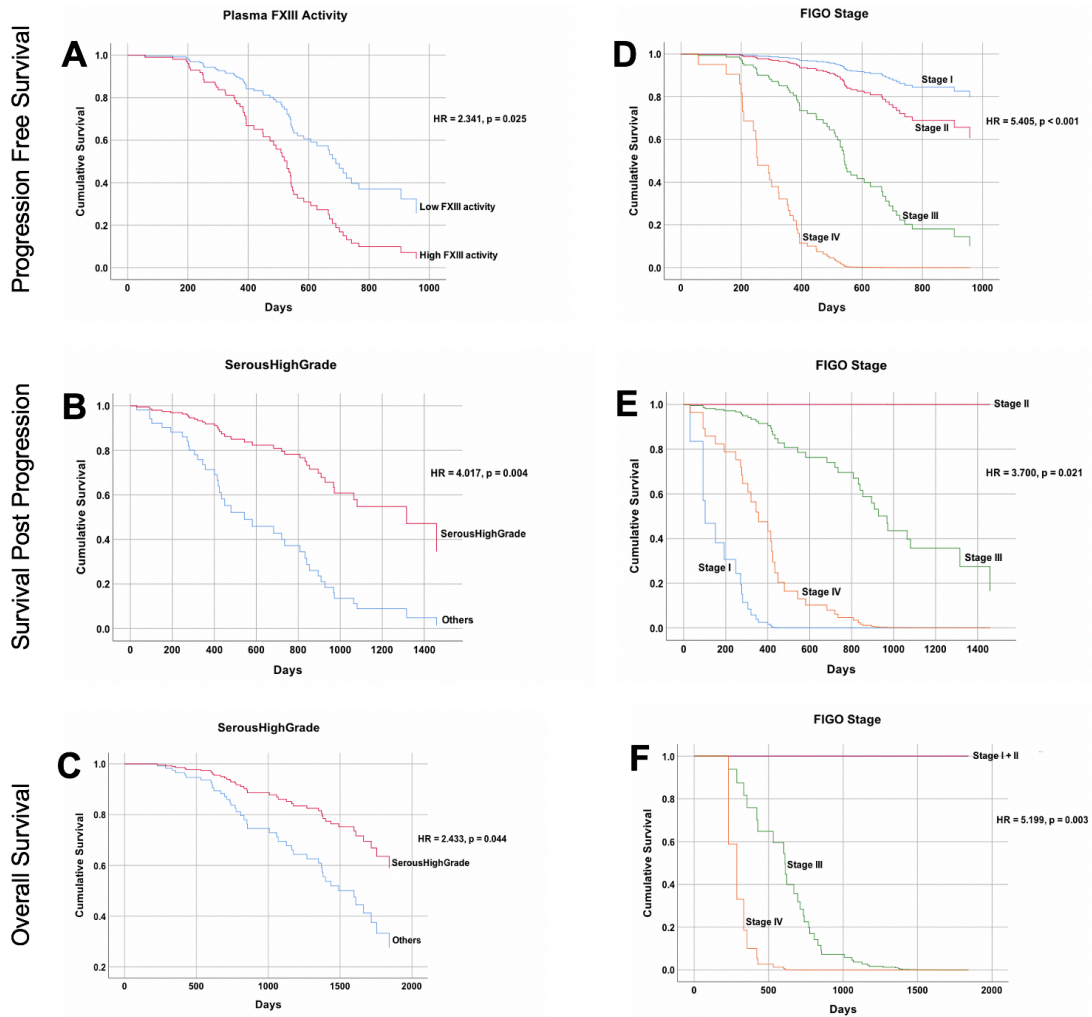


Figure 3-20: Independent Prognostic Indicators for Survival Identified by Cox Proportional Hazard Models

This figure shows time to event curves analysed by Cox proportional hazards regression models and represents the significant predictors for survivals detected by these models. Covariates included in each model were: Age at diagnosis, grade of tumour, FIGO stage, histology, risk of disease progression, extent of residual disease, V34L carriers, 650_651 alleles carriers, treatment received, plasma FXIII activity, plasma FXIII levels, D-Dimer levels. Due to the omission of patients for whom data for a covariate is unavailable, n=88. HRs of 1 indicates that there is no correlation, HR > 1 suggest a higher probability of experiencing the event assessed (Death in SPP and OS, and progression of disease in PFS). Whereas HR < 1 indicates a lower risk of experiencing the event. The survival interval measured is shown on the left of each row.

3.9.4 Summary

❖ In univariate analysis:

Stage of disease and risk of disease progression were significantly associated with all survival intervals. Extent of the residual disease was significantly associated with OS and PFS intervals, but not with SPP. In contrast, SerousHighGrade histology was significantly associated with OS and SPP intervals, but not with PFS. Treatment received, grade of tumour and histology were not associated with survival, however, serous histology presented a near-significant benefit on SPP ($p=0.057$). High plasma D-Dimer levels are significantly associated with increased risk of EOC progression. Low plasma D-Dimer levels displayed a close to significant benefit to OS. *F13A1* SNPs, FXIII activity and its A-subunit levels were not associated with survival intervals.

❖ In sub-group analysis:

Patients who had elevated plasma FXIII activity and received bevacizumab had a better prognosis and a benefit to SPP than those who had low plasma FXIII activity. SPP was significantly increased in patients with elevated plasma FXIII activity who were at high risk of disease progression and had residual disease of > 1 cm after primary debulking surgery.

❖ In multivariate analysis:

Stage of disease was significantly associated with all survival intervals: OS, PFS and SPP, while, SerousHighGrade histology was significantly associated with OS and SPP intervals, but not with PFS. Grade of disease data was combined grade I vs others, histology data was also combined serous vs other to keep numbers high in sub-groups, however, both factors were not associated with survival. Age at diagnosis, risk of disease progression, extent of residual disease, plasma FXIII levels, plasma D-Dimer levels, *F13A1* SNPs assessed and the treatment received did not associate with survival. The most striking result to emerge from this dataset is that, high plasma FXIII activity is significantly associated with EOC progression.

3.10 Key findings:

- ❖ Compared to the wildtype, carriers of 650I_651Q allele had significantly lower plasma FXIII activity ($p=0.007$).
- ❖ Plasma FXIII activity was significantly associated with advanced-stage EOC ($p=0.029$). Activity was significantly lower in FIGO stage IV than in stage III.
- ❖ Plasma FXIII levels are significantly lower in SerousHighGrade EOC compared to other histologies ($p=0.015$).
- ❖ FXIII protein expression in tumour tissues ($n=44$) was significantly lower in higher grade disease ($p = 0.015$). There was no association seen between FXIII levels in plasma and in tumour, perhaps due to the small sample size.
- ❖ 34V/L heterozygotes had close to significant increased SPP in univariate survival analysis, ($p=0.088$, median SPP is 43.2 months) compared to the wildtype (median SPP is 24.1 months), (Table 3-19).
- ❖ As expected, in univariate analysis for survival, patients with advanced-stage EOC, those at high risk of disease progression, and those with macroscopic residual disease > 1.0 cm after primary surgery demonstrate significantly reduced OS and PFS.
- ❖ Patients with high plasma FXIII activity in receipt of bevacizumab showed significantly improved SPP (Log rank test: $p=0.041$).
- ❖ SPP was significantly improved in patients with high plasma FXIII activity who were at high risk of disease progression and had more than 1.0 cm residual disease after primary cytoreduction surgery (Log rank test: $p=0.030$).
- ❖ Patients with high plasma FXIII activity and high risk of disease progression survived for longer after their disease progression (Log rank test: $p=0.030$).
- ❖ Elevated plasma FXIII activity resulted in a significantly greater risk of disease progression ($HR=2.341$, $p=0.025$), in multivariate analysis for survival.

3.11 Discussion

3.11.1 Plasma FXIII activity and subunit A levels

No previous study has evaluated plasma FXIII levels and activity combined in EOC or any other cancer cohort. This study found that plasma FXIII levels and activity in EOC patients were comparable to those observed in the general population (Section 3.3). This outcome is contrary to that observed in NSCLC and another cohort of patients with different cancers. FXIII activity was found to be higher in advanced-stage NSCLC patients than in healthy controls and early-stage NSCLC patients (Lee et al., 2013). Recently, a significant increase in plasma FXIII activity was observed in cancer patients compared to healthy individuals. In addition, patients with high FXIII activity showed a significant decrease in survival by KM analysis (Sawai et al., 2020).

Consistent with the literature, this research found that V34L polymorphism is significantly associated with higher mean activity compared to the WT. Both heterozygotes at 103G>T and homozygotes for the alternative 'T' allele showed high activity, with the homozygotes presenting even higher activity than the carriers of one copy of the 'T' allele ($p=0.002$; Figure 3-4). These results are in line with those of previous studies, which found that 34L polymorphism leads to higher plasma FXIII activity and SA (activity per unit amount) compared to 34V variant (Anwar et al., 1999), and is linked to rapid activation of the enzyme (Wartiovaara et al., 2000, Balogh et al., 2000).

V34L polymorphism is located just three amino acids upstream from the thrombin cleavage site. It was shown that the release of the AP by thrombin from the plasma FXIII 34L variant, as well as the subsequent activation of FXIII, occurs at 2.5 times faster rate than the WT leading to closer fibrinogen cross-links with slimmer fibres (Ariëns et al., 2000). Lim et al. (2003) demonstrated that fibrinogen concentration mediates the effect of V34L on fibrin clot structure. Individuals who were homozygous for the 'T' allele, produced smaller, tightly packed fibrin cross-links at decreased fibrinogen concentrations, and larger loosely packed cross-links at increased fibrinogen concentrations, compared to 'V' allele homozygous (Lim et al., 2003). It has also been revealed that fibrin formation influences the initiation of FXIII activation in whole plasma, while the rate of activation is augmented by the V34L polymorphism (Shemirani et al., 2006). Although it has been demonstrated that 34L significantly elevates plasma FXIII activity, it has very little impact on plasma FXIII levels.

Previous studies have shown that V34L polymorphism is linked to thromboembolic diseases (Bagoly et al., 2012). The effect of V34L on cancer is unknown. While homozygotes for the SNP (103T/T) had a reduced risk of colorectal cancer development (Vossen et al., 2011), the heterozygotes (103G/T) of the variant showed a high risk of oral cancer (Vairaktaris et al., 2007). This inconsistency could be due to the differences in cancer types and the fact that V34L imposes a tissue-specific effect. Carriage of the mutant allele 'T' at 103 locus leads to amino acid changes at codon 34 in the FXIII A polypeptide: Val/Leu or Leu/Leu. As explained above, they are associated with increased activity and causes matrix proteins to cross-link more swiftly and narrowly compared to Val/Val carriers. Thus, it is possible that these changes in cross-linking composition and rate could affect the TME, or these protein variants could be affecting the cancer tissues in a way that is still unknown and needs to be explored further. In this ICON7 EOC study cohort (n=89), V34L heterozygous carriers (103G/T) had close to significant benefit to SPP in univariate survival analysis (p=0.088, Table 3-19). This suggest that significant improvements in survival may be seen in a larger cohort of patients.

One of the important results in this study was that significant association between plasma FXIII activity and 650_651 haplotype with carriers of 650I and 651Q demonstrating lower levels of activity was observed for the first time (p=0.004, Figure 3-5). This finding is a novel contribution to the current knowledge and provides important insights into the function of this haplotype.

The associations between plasma FXIII activity and genotypes showed that 651Q/Q homozygotes had significantly lower activity compared to WT homozygotes 651E/E individuals (p=0.002, Figure 3-6). This result accords with previous research conducted by Dr Anwar, which showed that E651Q polymorphism influenced plasma FXIII A protein levels, with reduced levels having been observed for the 651Q variant compared to WT homozygous (651E/E), (Gallivan et al., 1999a). The relationship between genotype and phenotype for several FXIII A gene variants has been described, with several variants appearing to influence levels of FXIII A SA, leading to clear effects on their functional role. However, the polymorphisms at codons 650 and 651 seem to have a negligible impact on FXIII SA (Anwar et al., 1999). This implies that, if levels are low, activity will be low as well.

The most important factors influencing FXIII A enzyme activity in plasma are the cross-linking reaction itself, the effectiveness of the activation process, the specificity and efficiency of substrate binding, and FXIII B subunit levels in plasma. 651Q variant is located on the surface of barrel 2 domain of FXIII A polypeptide (Chapter 1, Figure

1-3), approximately 1,800 to 1,850 base pairs upstream of the AP and thrombin cleavage site. Therefore, it may not have direct role in the enzyme conformational change during activation, resulting in low activity. Another possible explanation for this is that the nucleotide change leading to a replacement of Glutamic acid with Glutamine at residue 651 may have contributed to a structural change in the A-subunit affecting the stability of this protein through altering the interactions with the B-subunits. It is likely that these single amino acid variations in the protein sequence cause small structural changes in the protein, which would explain the differences in FXIII SA.

Some evidence has emerged that 650I and 651Q variants influence the enzyme biochemical characteristics e.g. the isoelectric mobility, but not FXIII A protein levels or activity in the Japanese population (Taniguchi et al., 2002). However, this differs from the findings presented here and they are not directly comparable, therefore, the result from this cohort is likely to be true.

There is no previous report in the literature identifying the 1951G>A and 1954G>C polymorphisms as genetic factors underlying any clinical condition. More investigation are required to elucidate their specific effect.

In a study evaluating FXIII activation mechanism in relation to plasma FXIII heterotetramer assembly, interaction, and dissociation, the presence of FXIIIB subunits have been shown to speed up the activation of FXIIIA subunits *in vitro* (Gupta et al., 2016). Recent evidence suggests that, compared to the zymogen type, the activated FXIIIA homodimer undergoes major conformational rearrangement during activation, it splits into monomers (Anokhin et al., 2017).

Regulation of FXIIIA levels in plasma is a complex multifactorial process. It has been demonstrated that mutations within the FXIIIB subunit have a key role in the regulation of plasma factor XIII levels in healthy individuals. The FXIIIB intron K G allele was found to result in a significant reduction of FXIII levels, and it appeared to work in conjunction with the FXIIIA 34L allele. This work has also identified age and fibrinogen level as important factors (Mezei et al., 2016).

The median plasma FXIIIA level in this cohort under investigation was 0.77 IU/mL, which is within the normal range for healthy individuals, despite the fact that it was not normally distributed. These ICON7 plasma samples were taken around 3–4 weeks following the primary cytoreduction surgery. While this period of time may have been sufficient for those patients to completely recover from the surgical effect on the coagulation factors, the possibility of an influence on some of these samples skewing the data towards the low levels cannot be ruled out.

In healthy individuals, a positive significant correlation was found between FXIII A levels and age, female sex and smoking. In this same study, FXIII activity did not significantly correlate with these variables (Ariëns et al., 1999). It has been suggested that the wide variation of FXIII activity levels in the normal population is due to the sensitivity of the FXIII activity assay to the V34L polymorphism (Kohler et al., 1998). This variability in activity could explain why there was such a poor association between FXIII activity levels and FXIII A-subunit levels in their study, and why, unlike FXIII A subunit, FXIII activity levels were not correlated with age, female sex and smoking (Ariëns et al., 1999).

Anwar et al. (1999) demonstrated that FXIII A SA of different individuals varies significantly, despite the population having a normal distribution. FXIII levels are not directly related to FXIII activity, according to the study data. As a result, some people have high levels of FXIII A protein but low levels of FXIII activity, and vice versa (Anwar et al., 1999). These results are consistent with those observed in other studies, which showed in the general population that FXIII A antigen and plasma activity levels are normally distributed, and the enzyme protein levels are unrelated to activity levels (Muszbek et al., 2011).

Factor XIII circulates in human plasma predominantly combined to fibrinogen at 14–28 µg/mL (Kattula et al., 2018). It has been acknowledged that low plasma FXIII amount, as < 5% of the normal range; 0.01–0.05 IU/mL is adequate to achieve satisfactory haemostasis (Anwar and Miloszewski, 1999).

Several studies have shown that plasma FXIII A levels were increasingly being recognised as a useful indicator of disease activity in a variety of inflammatory disorders such as Crohn's Disease (Wisén and Gardlund, 1988) and Ulcerative Colitis (Suzuki et al., 1989).

In 1994, Van Wersch and co-workers compared plasma FXIII A levels in patients with benign and malignant gynaecological tumours to healthy controls. Those with benign tumours, had significantly higher plasma FXIII A levels than healthy individuals. However, relative to non-metastatic tumours, malignant tumours that had metastasised had slightly lower levels (van Wersch et al., 1994). While research on EOC and FXIII A has been limited, it has shown that this protein and its gene can play a role in EOC.

3.11.2 Plasma D-Dimer

Elevated post-operative D-Dimer levels were observed in this study cohort compared to the normal range in healthy individuals (Figure 3-3). In accordance with the present result, previous studies have demonstrated that plasma D-Dimer levels were significantly higher in patients with different malignancies, including breast, gastric, pancreatic, colon and rectal cancers compared to healthy individuals. These levels were also associated with cancer metastasis and stage of disease (Dai et al., 2018). High preoperative plasma D-Dimer levels were found to be significantly associated with poor prognostic outcome and increased chemoresistance in patients with serous EOC. compared to patients with plasma D-Dimer levels in the normal range (Liu et al., 2015). However, preoperative D-Dimer levels were not measured in this study.

There was no direct relationship between plasma D-Dimer levels and plasma FXIII activity and its A-subunit levels (Table 3-2). If a relationship was present, which indicates activation of coagulation and fibrinolysis, then a combination measurement of plasma FXIII A and D-Dimer levels could be used as a diagnostic marker in EOC. This result is different from previous studies which have found D-Dimer and CA-125 to be directly and positively associated (Tas et al., 2013, Wu et al., 2013). The combination of CA-125 and D-Dimer was found to be more effective than either CA-125 or D-Dimer alone in distinguishing benign from malignant ovarian tumours (Gadducci et al., 1996). In addition, when compared to other OC markers as TPA, SLX, and CEA, D-Dimer levels had a higher sensitivity (Kanayama, 1991).

There is a recognised role for the plasma D-Dimer levels as a prognostic biomarker in cancer. D-Dimer levels were also presented as valuable predictor of poor clinical outcome in patients with EOC independent of VTE disease (Yamada et al., 2020). This differs from the findings presented here, which showed no significant associations were identified with survival intervals in univariate or multivariate analysis (Figure 3-18 and Tables 3-23–3-25). Several studies have evaluated the role of D-Dimer levels in prognosis of OC. A meta-analysis of 1,437 patients found that there was no benefit to OS in patients with high D-Dimer levels when the sample sizes were <100 (Wu et al., 2017). Therefore, a possible explanation of the result in this current study might be that the sample size is small.

3.11.3 Prognostic factors

Contrary to expectations, some factors were not found to be significant prognostic predictors in this cohort. For instance, age at diagnosis, grade of tumour, residual disease and histological subtype. At the time of diagnosis, the median age of the study participants was in the menopausal range. In addition to their cancer, older patients with EOC may have other medical conditions, hence, co-morbidities are important factors to consider. Data of pre-existing medical conditions was not available for this study cohort; however, it has been shown that age at diagnosis influence pre-existing medical conditions, and hence co-morbidity has no independent prognostic effect on survival (Chan et al., 2003). There are rather contradictory findings in the literature with regards to the impact of the tumour histology and grade of disease on survival. Several factors could explain this observation, for example: inadequate sample size across studies; FIGO stage at diagnosis may affect histology and grade as serous histology and high-grade tumours present in advanced stages; and variability in histological sub-typing and tumour grading between various centres.

The relationship between plasma FXIII and prognostic factors may contribute to the understanding of the mechanisms by which FXIII exert its role in EOC. Plasma FXIII activity was significantly lower in patients with stage IV than in patients with stage III ($p=0.027$, Figure 3-8). However, there were no significant differences in FXIII activity between the patients with stage IV and patients with stage I, or II. The decrease in FXIII activity in advanced stage of the disease suggests that it may have been depleted while promoting metastatic progression or inducing tumour angiogenesis. However, this result differs from Lee's (2013) which showed that the activity of FXIII was higher in patients with advanced stage NSCLC (Lee et al., 2013).

Type II tumours, which include SerousHighGrade, endometrioid, and undifferentiated carcinomas, are the most common types, aggressive, genetically unstable, and are typically diagnosed at an advanced stage. Plasma FXIII levels were significantly lower in SerousHighGrade disease ($p=0.015$, Figure 3-9). A possible explanation for this result may be the consumption of FXIII during cross-linking of extracellular matrix proteins within the TME, which can lead to increase tumour growth and metastatic spread, or that FXIII was playing a different role in SerousHighGrade tumours. This result supports findings from previous research, which showed that plasma FXIII levels in metastatic OC are lower than in benign ovarian tumours and, if compared to non-metastatic tumours, malignant tumours that had metastasised demonstrated much lower levels (van Wersch et al., 1994).

Many cancers have been found to have activated coagulation and fibrinolysis (Lyman and Khorana, 2009). High plasma D-Dimer levels is well established as a biomarker of fibrinolysis activation. It is generated when plasmin-induced fibrinolytic activity degrades cross-linked fibrin. The measurement of D-Dimer is widely utilised in conjunction with clinical parameters in the first assessment of suspected acute VTE, since D-Dimer plasma levels are elevated following clot formation. VTE is a common cancer complication, particularly in ovarian, brain and pancreatic malignancies, and is one of the leading causes of death in cancer patients (Levitan et al., 1999). It has been shown that elevated D-Dimer levels are significantly associated with decreased OS in patients with EOC (Sakurai et al., 2015). In this study, higher levels of plasma D-Dimer levels were significantly and positively correlated with advanced stage of disease (Spearman's rho Correlation Coefficient = 1.000, $p=0.018$, Figure 3-10). These D-Dimer levels are far higher than the existing 230 ng/mL cut-off employed by the Leeds Teaching Hospitals NHS Trust (LTHT) as a negative predictive sign of a VTE (LTHT, 2021). This suggested that D-Dimer could influence EOC prognosis via a VTE-dependent route.

In this EOC study-cohort, there was no relationship between *F13A1* polymorphisms and prognostic factors. The *F13A1* polymorphisms 1951G>A and 1954G>C have never been linked to cancer, or any other medical condition. They have been proven to have no effect on the levels of FXIIIa protein or its SA (Anwar et al., 1999). Thus, the exact influence of these SNPs is still unknown and is yet to be determined. In contrast, 103G>T polymorphism has been linked to several malignancies including oral (Vairaktaris et al., 2007), colorectal (Vossen et al., 2011), ovarian (Hutchinson, 2019) and benign tumours such as uterine fibroids (Ahmadi, 2016), as well as coronary artery diseases and VTE (Bagoly et al., 2012). As the effect of 103G>T in these various conditions is inconsistent, it is possible that this variant influence patients' prognosis through pathways connected to these medical conditions.

This study-cohort (part of the ICON7 translational cohort) does not have data for the European Cooperative Oncology Group's (ECOG) patient performance status prognostic factor, which reflects a patient's degree of functioning in terms of their ability to care for themselves, daily activity and physical ability. The status level varies from 0 to 5, with 0 indicating that the patient is active and capable of performing everyday duties without restriction, and 4 indicating that the patient is severely incapacitated, typically bound to their bed (Perren et al., 2011). A lack of a covariate in a disease model hinders comprehensive multivariate analysis and introduces potential limitation. Nonetheless, the Cox multivariate modelling conducted herein

this thesis is unaffected, because the remaining prognostic factors were sufficient to model the disease of these patients and allow for adequate analysis.

3.11.4 Tissue expression

The average percentage positivity of FXIII A staining was highest in stroma cores, lowest in tumour cores, and average percentage positivity for tumour/stroma cores in the middle (Figure 3-11). This result corroborates the findings from the online mRNA expression database, The Ovarian Cancer Database of the Cancer Science Institute Singapore (CSIOVDB), which show that the highest expression of mRNA are seen in the EOC stroma, while the lowest are seen in tumour tissue compared to normal epithelium (Tan et al., 2015). This difference in the gene transcription level provided by the CSIOVDB, and the variations of FXIII A expression levels within the EOC tissues found by this research, could provide more insight into FXIII A's role in EOC. It has been reported that increased *F13A1* gene expression was significantly linked with mesenchymal molecular subtype of serous EOC (Tan et al., 2013, Tan et al., 2015). The stroma forms a significant part of the mesenchymal tumours, and collagen expression is linked with metastatic mesenchymal disease (Zhang et al., 2019). Collagen is one of FXIII A substrates. In the light of the findings obtained from the CSIOVDB data, which revealed that *F13A1* gene expression is higher in EOC stroma, it can therefore be assumed that the presence of FXIII A in EOC stroma may play a role in the disease metastasis.

The presence of this protein may influence EOC prognosis or response to therapy. The role of FXIII A in the stroma is unknown, and this study does not address it entirely. FXIII A may play a role in the TME by cross-linking the extracellular matrix and changing its structure. It is also possible that FXIII A of the tumour-associated macrophages plays a role in modulating the immune response by influencing their activation, differentiation and migration.

There was no significant correlation between plasma FXIII A levels and FXIII A expression in EOC tumour tissues (Table 3-14). If a strong association is established between the amount of FXIII A antigen in plasma and in tumour tissues, then it can be used as a biomarker for EOC.

FXIII A protein expression within the tumour tissues was significantly lower in high tumour grade (Figure 3-12). Low FXIII A expression in the tumour tissues of poorly differentiated carcinoma could be explained by its potential role in cross-linking important substrates within the TME, leading to the remodelling of the tumour matrix.

Other potential roles include crosstalk and dynamic interactions between immune and stromal cells, creating metastatic niche or angiogenic signalling. Given the small sample size of tissue microarrays available for this study-cohort, further work is needed to evaluate if the result of the relationship between grade of tumour and FXIIIa expression in tumour tissue can be repeated.

3.11.5 Survival

This study has identified FIGO stage at presentation, SerousHighGrade histology and plasma FXIII activity as independent prognostic factors for survival in multivariate analysis (Figure 3-21). In most studies that have used multivariate analysis, the FIGO stage at diagnosis has been found as the most significant indicator (Linasmith et al., 2004, Arkan et al., 2014). This was also found in this study.

It has been established that the extent of the residual disease following debulking surgery is an important prognostic factor for survival intervals (Winter et al., 2008, Chang et al., 2013). Consistent with the previous research, this study found that patients with macroscopic residual disease of > 1.0 cm after primary surgery have significantly shorter OS and PFS (Figures 3-13 and 3-14).

Patients who had high plasma FXIII activity and received bevacizumab in addition to standard chemotherapy had significantly improved SPP compared to those with low activity ($p=0.041$, Section 3.9.2.1). This is a novel result that has not been reported before. On the other hand, patients with low FXIIIa activity in receipt of bevacizumab had shorter SPP. The influence of plasma FXIII activity on SPP reported here was not observed in patients in receipt of platinum-based chemotherapy alone. It can thus be suggested that FXIIIa may play a role in bevacizumab's beneficial therapeutic response via its pro-angiogenic effect. Activated FXIIIa cross-links $\alpha_v\beta_3$ to the VEGFR-2, the tyrosine kinase receptor, leading to the activation of the receptor by autophosphorylation. The activated VEGFR-2 receptor then starts a signalling cascade that leads to downstream effects and stimulation of angiogenesis (Dardik et al., 2006). Bevacizumab works by binding to the circulating VEGF and preventing it from binding to its cell surface receptor VEGFR-2, the same receptor which is activated by FXIIIa. It seems possible that high FXIIIa activity may have an effect on the angiogenic receptor cross-linking, making bevacizumab treatment more effective, and that plasma FXIII activity may play a role in anti-angiogenic treatment responsiveness. Based on these results, it would have been noteworthy to explore how FXIII activity might influence those receiving bevacizumab in the high-risk group. However, the sample size of this group ($n=17$) was insufficient to achieve any reliable

results. These results are in agreement with those presented in Section 3.11.3, which links low plasma FXIII activity with the advanced stage of the disease. This association between advanced OC stage and the drop in plasma FXIII activity that makes those patients die far sooner could be explained by a possible change in the structure of the VEGFR-2 receptor cross-linking caused by the difference in FXIII activity that makes those patients less receptive to the bevacizumab anti-angiogenic effect.

In univariate survival analysis, V34L heterozygotes carriers had nearly a significant increase in OS and SPP compared to the wildtype ($p=0.056$, Table 3-17) and ($p=0.062$, Table 3-19) respectively. These findings are consistent with that of Hutchinson (2019) who found that this SNP is significantly linked to beneficial effect on these survival intervals given the larger cohort of their study (Hutchinson, 2019). To better understand the role that V34L heterozygous variant may play in EOC survival benefits, more research is required to evaluate whether heterozygotes differ in their activation or function. It is unclear how much of the FXIII molecules in V34L heterozygotes are heterodimers vs homodimers, and how the heterodimer differs from the homodimer in terms of molecular stability, activation and connection with FXIIIB subunit as a heterotetramer in the circulation.

Risk of disease progression is a novel prognostic variable defined by the ICON7 trial investigators, which includes women with extensive disease where resective surgery cannot be undertaken and women with > 1 cm of residual disease post-surgery and/or women with FIGO Stage IIIC/IV disease (Perren et al., 2011, Oza et al., 2015). Patients with high plasma FXIII activity and a high risk of disease progression have seen a significant improvement in SPP ($p=0.030$, Figure 3-19D). Similarly, SPP was significantly higher in patients with elevated plasma FXIII activity and residual disease of more than 1 cm ($p=0.030$, Figure 3-19F). The novel findings reported here suggest a direct link between disease severity and a beneficial effect of increased plasma FXIII activity. It may be that high FXIII activity influences the ovarian TME by cross-linking extracellular matrix proteins in some way, resulting in an SPP benefit. These findings also broadly support the ICON7 trial follow-up results which showed that, for patients at high risk of disease progression with poorer prognosis, there was a benefit to OS (Log rank test $p=0.03$, restricted mean survival time was 39.3 months for the bevacizumab treatment arm vs 34.5 months for standard chemotherapy alone treatment arm) (Oza et al., 2015).

This study identified plasma FXIII activity as independent prognostic factor for survival (HR=2.341, $p=0.025$, Figure 3-20A). Elevated plasma FXIII activity resulted

in a significantly greater risk of disease progression. The foundation of this association between plasma FXIII activity and PFS has not been directly elucidated in this chapter. Previous studies have shown that advanced EOC is complicated by hypercoagulation (increased thrombin production) and increased fibrinolysis (increased D-Dimer, a cross-linked fibrin degradation product) (Koh et al., 2001, Wang X. et al., 2005, Xu et al., 2017). It is well known that increased coagulation can lead to thrombotic disorders. The FXIII A 103G>T polymorphism has now been linked to VTE in numerous studies, with the 34L allele showing a protective benefit (Bereczky and Muszbek, 2011). The influence of plasma FXIII activity on survival seen in this cohort of newly diagnosed EOC patients is not necessarily attributable to co-existing VTE illness in those patients. Another important finding in this regards was that V34L heterozygotes showed a nearly significant increase in SPP (p=0.062, Table 3-19). As a result, a larger study is needed to see if this polymorphism plays a role in OC prognosis.

The exploration of this newly diagnosed ovarian cancer cohort showed some interesting novel findings, including the association between plasma FXIII A levels and SerousHighGrade histology, between plasma FXIII activity and advanced stage of the disease, and identification of plasma FXIII activity as an independent predictive factor for survival. Based on these findings, further *in vitro* studies were crucial to explore the ability of FXIII A to cross-link different substrates important in ovarian cancer microenvironment, and to assess the influence of FXIII A on cancer cell behaviour such as adhesion, proliferation and migration.

Chapter 4 Influence of Recombinant FXIII A Variants on Epithelial Ovarian Cancer Cell Behaviour

4.1 Introduction

The data obtained from the previous chapter by analysing a cohort of patients newly diagnosed with EOC, ICON7 clinical trial translational cohort plasma samples, revealed that carriers of the 650_651 haplotype with 650I and 651Q showed a significant reduction in FXIII activity compared to the WT (Section 3.6.1). The FXIII A V650I (1951A) variant presented significantly lower FXIII activity; this association was also observed in E651Q (1954C) polymorphism. The 1951A SNP is always found in haplotypes carrying the 1954C polymorphism, since 650I and 651Q SNPs are in LD in this cohort (Section 3.5.3), and in the general population (de Lange et al., 2006). Interestingly, there were also significant associations between low FXIII activity and advanced-stage EOC (Section 3.7.1), low plasma FXIII A levels and high-grade serous (SerousHighGrade) disease (Section 3.7.2).

Further sub-group analysis of ICON7 plasma cohort showed that patients with high FXIII activity, in receipt of bevacizumab and at high risk of disease progression showed significantly improved SPP (Section 3.9.2). Another remarkable result that emerged from the previous chapter was that, in multivariate analysis for survival, increased plasma FXIII activity was associated with a significantly higher risk of EOC progression (Section 3.9.3.2).

Despite these findings, the impact of FXIII A on EOC remains unknown, and the relevance of these findings to the behaviour of this cancer is still to be fully elucidated. Further *in vitro* investigations are needed to better understand FXIII A's role in EOC growth, response to therapy, and survival.

Therefore, in this chapter, the planned *in vitro* work is set to further explore these findings, and to evaluate the role of FXIII A protein variants in EOC with respect to cancer-related behaviours of adhesion, proliferation and migration.

Objectives of this chapter were, therefore:

1. Construction of plasmids containing desired FXIII A SNPs and cloning the mutant plasmids in a yeast host (*Saccharomyces cerevisiae* AH22 yeast strain).
2. Production of recombinant FXIII A protein variants using yeast expression system, and purification of FXIII A protein.
3. Assessment of the functional properties of FXIII A protein variants including their cross-linking abilities on substrates important in EOC (Fibrinogen, fibronectin, vitronectin, and collagen-1).
4. Evaluation of the influence of FXIII A variants on the behaviour of EOC cells in terms of adhesion, proliferation and migration.

4.2 Construction of plasmids encoding the human FXIII A variants

Yeast-expression plasmids containing FXIII A cDNA for wildtype *F13A1* (pYF13A), 103G>T (V34L), 1951G>T (V650I) and 1954G>C (E651Q) were available within Dr Anwar's laboratory and site-directed mutagenesis was used to construct the DM 1951G>T_1954G>C (650I_651Q), (Section 2.3.9). FXIII A negative control plasmid was constructed as detailed in Section 2.3.10. Transformation using a two-constructs strategy was used to create *F13A1* 103G>T heterozygous variant (V34L Ht), as described in Section 2.6.

4.2.1 Expression of recombinant FXIII A protein variants

FXIII A variants required for the study were expressed using an established in-house yeast-expression system. Protein preparation from FXIII A yeast clones was performed as described in Section 2.5.3. The total protein concentration produced in yeast lysate was estimated using Pierce™ BCA protein assay kit (ThermoFisher Scientific, Cat No. 23225) as per the manufacturer's instructions for microtiter plate procedure, and was found to be in the range 10.77 mg to 27.05 mg per one gram of cell mass in three different experiments. Since 1 gram of cells was used for each lysis, this 2.5-fold difference could be explained most likely due to the variations in the efficiency of the process of making the lysate i.e. the effectiveness with which the glass beads break open the yeast cell wall, and the differences of the percentages of cells that have broken. The presence of the recombinant FXIII A protein variants expressed in yeast was evaluated by SDS-PAGE (Section 2.7.3). Bands corresponding to the FXIII A molecular weight (83 kDa) were observed for all yeast clones. With the exception of the AH22 yeast clone (–vector), no band was present as expected (Figure 4-1). An interesting unexpected phenomenon was observed for the V650I variant on the SDS-PAGE gel shown in Figure 4-3. Its migration did not appear to correspond with the levels of the other FXIII A variants. Although all yeast lysates were made consistently, there is an indication of some culture to culture variations witnessed in the amount of soluble proteins produced and levels of FXIII A expression.

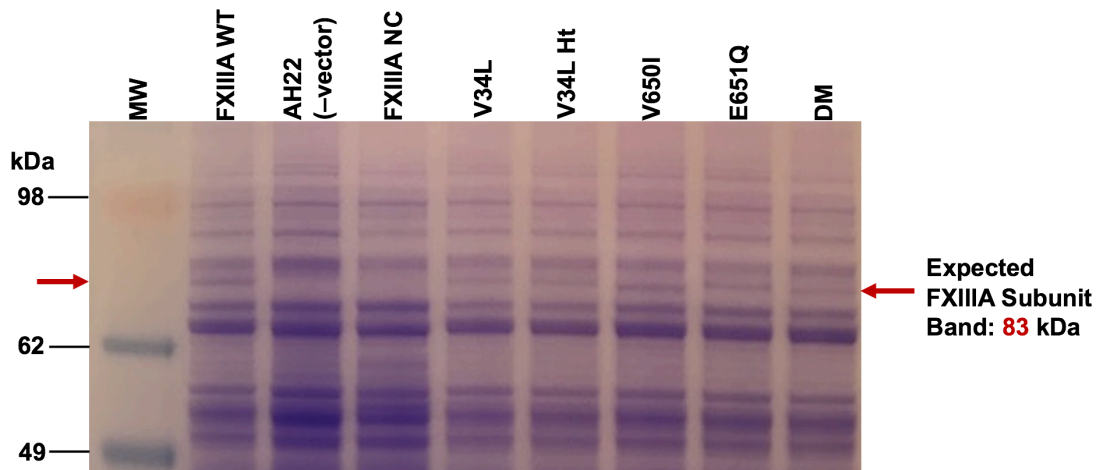


Figure 4-1: Presence of recombinant FXIII A variants in yeast lysates

Representative Coomassie-Blue R-250 stained SDS-PAGE gel for FXIII A yeast lysates. 30 μ g of total protein of yeast lysate was loaded per lane and separated on a 4–12 % Bis-Tris polyacrylamide Novex gel in MES SDS running buffer (Section 2.7.3). The expected size of the FXIII A subunit band is 83 kDa, which is indicated by the red arrows. Abbreviations: MW=Molecular weight marker: SeeBlue™ Plus2 Pre-stained Protein standard, ThermoFisher Scientific, Cat No. LC5925). DM=Double mutant.

4.2.2 Pooled yeast lysates

To minimise the influence of the culture-to-culture variations observed on the results data, an equal volume (200 μ L) from each of the three lysates prepared for each clone from three different experiments was pooled to make one homogenous sample for each variant (pooled FXIII A yeast lysates sample), as these yeast lysates will be used later on experiments to examine FXIII A activity on different substrates. WB confirmed the presence of strong rFXIII A protein bands at 83 kDa in all pooled yeast samples except AH22 and FXIII A NC lysates, and no other bands were observed (Figure 4-2). This result demonstrated that the yeast expression system was effective in producing rFXIII A protein variants, and no protein was produced when FXIII A NC was analysed. These lysates were used for experiments in Section 4.3.

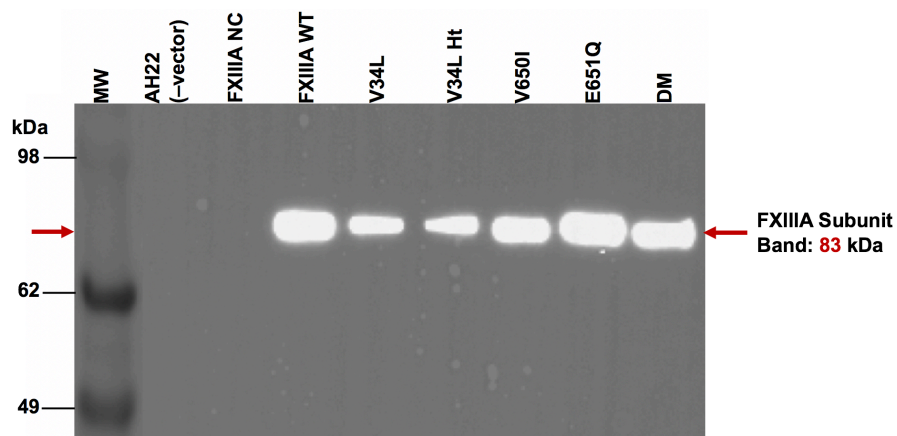


Figure 4-2: WB to confirm detection of FXIII A protein on pooled yeast lysates

WB of pooled FXIII A yeast lysates (20 μ g) with a rabbit polyclonal anti-*F13A1* antibody (HPA001804) at 1:500 (Section 2.7.4). The expected size of FXIII A bands are indicated with red arrows (83 kDa). Expected FXIII A protein band was observed in all lanes, except AH22 (-vector) and FXIII A negative control (FXIII A NC) lysates. MW=molecular weight marker; DM=double mutant.

4.2.3 Purification of recombinant FXIIIa variants

FXIIIa protein variants were purified using the high affinity and selectivity of Ni-NTA Agarose for recombinant proteins tagged with six tandem histidine residues (His-tag). FXIIIa protein variants bound to the resin were eluted by competition with 250 mM imidazole (Section 2.5.1). The presence of purified recombinant FXIIIa protein in elution fractions for each variant was evaluated by SDS-PAGE. Bands with the expected size of the FXIIIa subunit (83 kDa) were observed (Figure 4-3). Fractions containing only clean eluates (where no other bands were observed) with the best yield were selected and pooled. An equal amount (50 μ g) from each of the pooled eluates from each variant was then analysed by WB to ensure that 250 mM imidazole had only isolated FXIIIa and not any other protein, i.e. to detect the FXIIIa protein. A single band corresponding to 83 kDa was present confirming the detection of FXIIIa pure protein in each pooled, pure protein sample (Figure 4-4). Interestingly, the difference in SDS-PAGE migration found for FXIIIa V650I yeast cell lysate in comparison to other FXIIIa variants disappeared once this protein was purified, as shown in Figure 4-4.

The result demonstrated that 250 mM imidazole concentration has isolated FXIIIa and not any other His-tagged protein from the yeast lysates. On average, 1 gram of yeast cell mass produced 62.5–250 μ g of pure FXIIIa protein, which was sufficient for planned experiments. A buffer-exchange technique was employed to remove the excess imidazole salt before using the purified protein in downstream applications (Section 2.7.2).

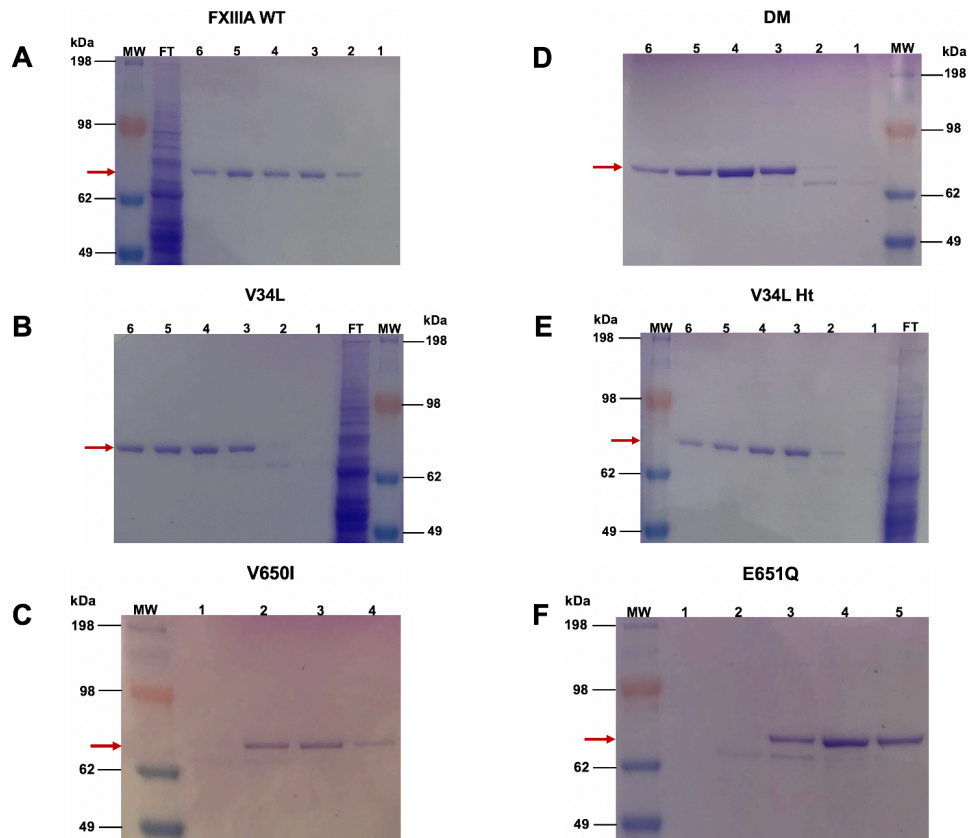


Figure 4-3: SDS-PAGE of purified recombinant FXIIIa variants

Purified FXIIIa fractions for each variant were separated by reducing SDS-PAGE (50 μ g). Gels were then stained with Coomassie Blue R-250. Lane 1: elution fraction 1; lane 2: elution fraction 2; lane 3: elution fraction 3; lane 4: elution fraction 4; lane 5: elution fraction 5; lane 6: elution fraction 6. Expected FXIIIa bands at 83 kDa are indicated with red arrows. Fractions containing only clean eluates were pooled: for **FXIIIa WT** fractions 3, 4, and 5 were pooled; for **V34L** fractions 3, 4, 5 and 6 were pooled; for **V560I** fractions 3, and 4 were kept; for **DM** fractions 3, 4, 5 and 6 were kept; for **V34L Ht** fractions 3, 4, 5 and 6 were kept; for **E651Q** fractions 4 and 5 were kept. Abbreviations: MW=molecular weight marker; DM=double mutants; FT=flow-through.

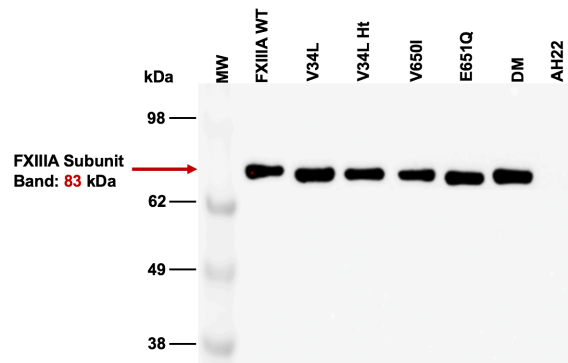


Figure 4-4: WB of purified FXIII A variants

50 μ g of clean pooled elution fractions from each variant was loaded per lane and WB was performed as detailed in Section 2.5.4 to detect FXIII A with a rabbit polyclonal anti-*F13A1* antibody (HPA001804) at 1:500. FXIII A protein band at the expected molecular weight of 83 kDa (red arrow) was present in all samples, except AH22. No other bands were observed. MW=molecular weight marker.

4.2.4 Stability of purified FXIIIa variants on storage

Purified FXIIIa protein variants were stored at 4°C following purification and their stability at 4°C was assessed by performing serial activity assays as detailed in Section 2.7.6 at different time intervals (Table 4-1). Both purified FXIIIa WT and DM protein variants appeared to be stable for six weeks at 4°C. However, at 14 weeks, the DM remains more active compared to the WT. In contrast, V34L had lost ~13%, V34L Ht had lost ~11%, and E651Q had lost ~27% of their activity at 6 weeks. Despite losing 13% of its activity in six weeks, V34L variant was still the most active protein at 14 weeks, with just under 50% of its original activity still present. The FXIIIa V34L Ht and DM variants appeared to have a similar course of stability at 4°C. Although E651Q emerged as the least stable of all of the variants tested at six weeks, it was still more active than the WT at 14 weeks. Therefore, FXIIIa pure protein variants were used within the first week after purification to ensure the state of most functionality and activity.

Table 4-1: Activity of purified FXIIIa variants stored at 4°C at different time intervals

FXIIIa pure protein Sample	Activity observed IU/mL			
	Start	2 weeks	6 weeks	14 weeks
FXIIIa WT	1	0.99	0.99	0.13
V34L	1	0.96	0.87	0.47
V34L Ht	1	0.94	0.89	0.36
E651Q	1	0.69	0.73	0.24
DM	1	0.91	0.91	0.36

This table displays the results of serial activity assays on purified FXIIIa protein samples stored at 4°C (Section 2.7.6). The starting value of activity was given as a whole, and the remaining time points were presented as a fraction of the initial activity observed.

4.2.5 Summary

The yeast expression plasmid containing human *F13A1* cDNA was obtained and checked. Mutant FXIIIa constructs were created and expressed in yeast. Recombinant FXIIIa protein variants required for this study were produced and purified. The yeast expression system was used efficiently to produce functional rFXIIIa protein variants, and that FXIIIa NC did not result in any protein being produced. FXIIIa was the only His-tagged protein to be isolated using an elution buffer containing 250 mM imidazole. The V34L is the most stable protein of the FXIIIa variants stored at 4°C.

4.3 Functional studies on recombinant FXIII A variants

FXIII A substrates were reported to play a key role in EOC. Therefore, the aims of this section were to explore how these substrates are cross-linked by different FXIII A variants, and to examine the functional capability of FXIII A variants on these substrates which mediate cancer cell adhesion and dissemination. The function of recombinant FXIII A produced in yeast was verified by means of biotin-pentylamine incorporation activity assay (Section 2.7.6).

4.3.1 Optimising yeast lysate dilution for FXIII A activity assays

In vitro recombinant FXIII A protein expression levels were expected to be present at a higher concentration in the yeast cell lysate compared to levels *in vivo* (human plasma). The immediate experiments performed were to determine yeast lysate dilution factor to be used in the activity assays. In order to ensure recombinant protein samples analysis remained within the sensitivity range of the activity assay, a wildtype yeast lysate was analysed by using serial dilutions. Results showed that all dilutions tested (1:100 to 1:500) were effective in assessing FXIII A activity in yeast lysates. Mean activity was over 6 times that of human plasma, with SD of 0.49 (Table 4-2). Dilution 1:200 was selected for all the following experiments. This would allow measurement of FXIII A activity in samples containing higher and lower activity to be compared to the sample tested in this experiment.

Table 4-2: Yeast lysate dilution factor for FXIII A activity assays

Sample	Ratio of activity observed	Equivalent Activity in original sample IU/mL
Standard Human Plasma (1:10)	1.00	1.06
WT Lysate 1:100	0.57	5.73
WT Lysate 1:200	0.33	6.58
WT Lysate 1:300	0.21	6.38
WT Lysate 1:400	0.16	6.24
WT Lysate 1:500	0.14	7.08
Mean activity in WT lysate		6.40
SD		0.49
CoV (%)		7.69

This table shows the results obtained for the activity assay on FXIII A WT yeast lysate at different concentrations (Section 2.7.6). Abbreviations: WT=Wildtype, SD=Standard deviation, CoV% = the coefficient of variation percent.

4.3.2 Levels of FXIII A expression in pooled yeast lysates

Levels of FXIII A protein variants expressed in pooled yeast lysates were quantified using an established in-house FXIII A sandwich ELISA. FXIII A WT was expressed at around twice the concentration compared to V34L, V650I and E651Q variants. FXIII A V34L Ht variant presented the highest expression level at 1.23 IU/mg of total protein. The DM variant displayed the lowest level at 0.08 IU/mg of total protein. The ELISA results confirmed that the host (AH22) and FXIII A NC do not express FXIII A (Figure 4-5).

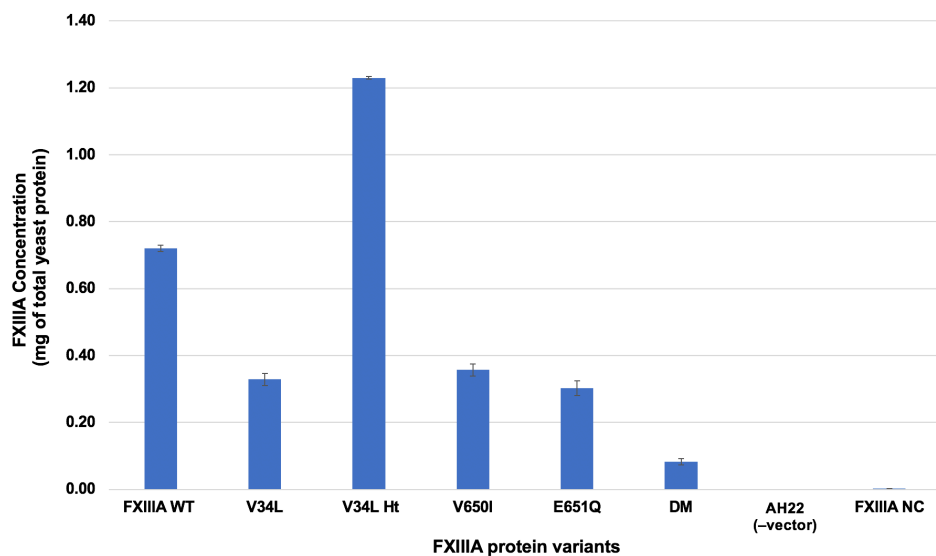


Figure 4-5: FXIII A antigen concentration

FXIII A antigen was measured using an in-house sandwich ELISA as detailed in Section 2.7.7. The chart shows the relative amount of FXIII A variant expressed in each pooled lysate sample per mg of total yeast protein with error bars representing standard deviation (Wells et al.). Abbreviations: DM=Double mutant.

4.3.3 Differences in cross-linking between FXIIIa substrates

Fibrinogen, fibronectin, vitronectin and collagen-1 were found to be heavily involved in EOC. Several studies have investigated these multifunctional proteins in regulatory mechanisms, construction and repair processes. Activation of FXIIIa produces isopeptide bonds cross-linking a number of different proteins linked to biological processes involved in cell adhesion and ECM organisation. It has been demonstrated that cross-linking of FN to fibrin by activated FXIIIa increases fibroblast adhesion and migration (Grinnell et al., 1980), and was required to maximise cell attachment, spreading, and migration in a fibrin matrix (Corbett et al., 1997).

It has been established that, ascites from patients with OC contain high levels of FDPs, the majority of which are cross-linked by FXIIIa (Hafter et al., 1984). High levels of fibrin-fibronectin compounds, as well as cross-linked FDPs such as D-Dimer were found in ascitic fluid of patients with advanced EOC (Wilhelm et al., 1988). Animal studies have demonstrated that cross-linked fibrin gel supports formation of mature tumour stroma in solid tumours as well as in the tissue lining the peritoneal surface (Nagy et al., 1995).

Fibrinogen as an ECM protein plays a recognised role in the development of breast cancer (Simpson-Haidaris and Rybarczyk, 2001). Several studies have shown that, elevated plasma fibrinogen levels are associated with poor prognosis in endometrial (Ghezzi et al., 2010, Seebacher et al., 2010), advanced gastric (Lee et al., 2012), advanced rectal (Lu et al., 2011), colorectal (Tang et al., 2010), as well as epithelial ovarian (Polterauer et al., 2009, Qiu et al., 2012, Luo et al., 2017) cancers.

Fibronectin is found in ascitic fluid in women with EOC (Hafter et al., 1984) and OC stroma (Wilhelm et al., 1988). Fibronectin promotes attachment, migration and metastasis of OC cells (Rieppi et al., 1999, Kenny et al., 2008, Kenny et al., 2014a). Moreover, it has been reported that, fibronectin enhances OC cell invasion and metastasis via signalling pathway mediated by $\alpha_v\beta_1$ integrin (Mitra et al., 2011), and also via up-regulation of FAK-PI3K/Akt pathway (Yousif, 2014). It has also been suggested that the interaction of $\alpha_v\beta_3$ with fibronectin plays a role in tumour cell invasion (Knowles et al., 2013). It has been proposed as a therapeutic target due to its interactions with cell receptor proteins, which affects downstream signalling events linked to tumour progression (Wang and Hielscher, 2017), reduction of vascular thickness using pUR4B, a fibronectin polymerisation inhibitor (Chiang et al., 2009), and restrict vasculogenesis by inhibiting the cellular deposition of fibronectin matrix, and diminishing deposition of other ECM proteins (Hielscher et al., 2016).

The interaction of vitronectin with $\alpha_v\beta_3$ integrin has been shown to increase OC cell growth and migration (Hapke et al., 2003). Further studies have also demonstrated that vitronectin enhances OC cell adhesion, migration and metastasis (Kenny et al., 2008, Heyman et al., 2010). Compared to ascites fluid from non-oncologic patients, ovarian cancer ascites fluid was shown to be higher in vitronectin (Bery et al., 2014). The presence of vitronectin in ascites has been found to aid in the migration and invasion of ovarian cancer cells, as well as a potential migration-enhancing factor of OC cells and metastasis of cancer stem cells to the peritoneum and other organs (Schneider et al., 2016).

Collagens are the major proteins in ovarian ECM (Cho et al., 2015). Collagen is found to be implicated in remodelling the ECM (Shen Y. et al., 2012), and augmenting matrix rigidity leading to increased migration and spread of EOC cells (Oudin and Weaver, 2016, Rice et al., 2017, McKenzie et al., 2018). There is evidence that collagen is involved in regulation of the expression of tau protein isoforms in the nucleolus, contributing to paclitaxel resistance (Smoter et al., 2013, Gurler et al., 2015). Collagen supports proliferation, invasion and migration (Li et al., 2020).

Given the findings reported here from previous studies, it can thus be suggested that these substrates may play an important role in EOC, because they alter the structure of the tumour matrix, promote metastatic progression, angiogenic signalling and treatment response.

The differences in cross-linking substrates important in EOC adhesion and spread may help to understand the role that FXIIIa might have within the tumour microenvironment. The objective of this section was to evaluate how these different FXIIIa substrates are cross-linked by FXIIIa protein variants. This objective was achieved by cross-linking each substrate with FXIIIa variants using the FXIII activity assay, focusing on the substrates and observing the variations in the cross-linking between these substrates.

For the four substrates tested, the highest level of cross-linking was found in fibronectin, followed by fibrinogen, vitronectin and finally collagen-1, except for DM, which showed slightly lower activity on vitronectin compared to collagen-1. The range in activity variations between substrates was the highest for the V34L variant (~9-fold difference between fibronectin and collagen-1), but lowest for the DM variant (2.5-fold difference between fibronectin and vitronectin) (Table 4-3). These results demonstrate substantial differences between the substrates.

In Figure 4-6, the bar chart compares the substrates' variations in the cross-linking ability of FXIIIa variants. Fibronectin showed the highest level of cross-linking by V34L variant, followed by the WT, V650I, E651Q, and finally, the lowest cross-links on this substrate were formed by the DM variant.

Table 4-3: Variations in cross-linking among FXIIIa substrates

FXIIIa variant	Actual TG activity (IU/mg of total yeast protein)			
	Fibrinogen	Fibronectin	Vitronectin	Collagen 1
WT	0.80	1.66	0.52	0.29
V34L	1.37	3.53	0.81	0.39
V650I	1.07	1.55	0.60	0.43
E651Q	0.59	0.77	0.23	0.18
DM	0.29	0.31	0.12	0.15

Results of actual FXIIIa substrates cross-linking by FXIIIa pooled yeast lysates using FXIIIa functional assay (Section 2.7.6). Details of the substrates examined: Fibrinogen: from bovine plasma, Cat. No. F8630, Sigma-Aldrich; Fibronectin: Solution from bovine plasma, Cat. No. F1141, Sigma-Aldrich; Vitronectin: Lyophilised from PBS, human, recombinant expressed in HEK 293 cells, Cat. No. SRP3186, Sigma Aldrich; Collagen-1: Solution from rat-tail, Cat. No. C3867, Sigma Aldrich. Abbreviations: Cat. No.=catalogue number. PBS=Phosphate buffered saline.

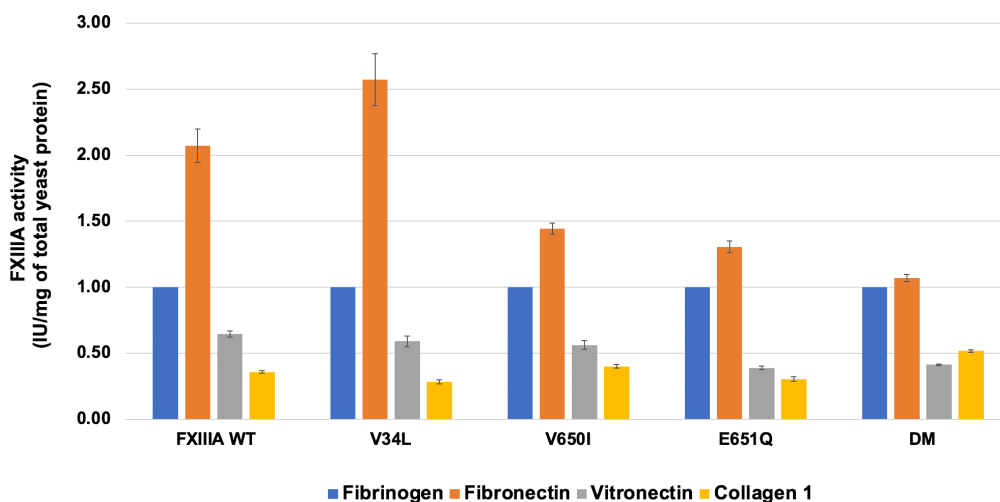


Figure 4-6: FXIIIa substrates are being cross-linked differently by FXIIIa protein variants

The bar chart shows the variations between FXIIIa substrates cross-linking by FXIIIa variants presented in Table 4-3 above relative to the fibrinogen. The level of cross-linking reaction for each substrate was measured by determining the initial rate of incorporation of the 5-(Biotinamido) pentylamine (BAPA), which provides the Lysine into the Glutamine residue (s) available in the chosen substrate, with error bars representing SD. Abbreviations: SD=standard deviation; DM= FXIIIa double mutant variant.

4.3.4 Relative comparative assessment of FXIIIa protein variants

The previous chapter showed that the *F13A1* genotypes V34L, E651Q, and 650_651 haplotype are linked to plasma FXIII activity in the ICON7 study-cohort (Section 3.6.1). In accordance with published studies, V34L demonstrated higher plasma FXIII activity in this study cohort. In contrast, this research has demonstrated, for the first time, that carriers of the E651Q variant and the 650_651 haplotype had lower activity compared to the WT patients.

These noteworthy findings need to be investigated further *in vitro* in order to better understand the role FXIIIa might have in EOC development, progression, and survival. The objective of this section was therefore to evaluate how FXIIIa variants differ in the cross-linking of the different FXIIIa substrates discussed earlier. To achieve this objective, information on FXIIIa expression levels has become necessary. Therefore, FXIIIa sandwich ELISAs suitable for recombinant FXIIIa protein were performed to quantify FXIIIa levels in pooled yeast lysates. The results of these ELISA experiments were presented in Section 4.3.2. The activity of FXIIIa variants on these substrates was measured using activity assays.

Since the activity is related to the concentration, the SA (defined as the FXIIIa activity per unit of the FXIIIa concentration) was then determined by calculating the relative activity of each variant to its subunit A amount (by dividing the activity of FXIIIa for each variant by its amount of FXIIIa protein) and presented in IU per mg of FXIIIa protein for the four substrates tested (Table 4-4). What is interesting about the data in Table 4-4 is that it shows important details about the actual levels of activity and amounts observed, which are vastly different for each variant.

The variant V34L presented the highest level of SA on fibronectin (4.8 times higher than WT), fibrinogen (3.9 times higher than the WT), and vitronectin (3.6 times higher than WT) except on collagen-1 (Table 4-4). This is an interesting result, as V34L genotype has been reported to be associated with improved OS in EOC patients (Anwar et al., 2004).

V650I variant displayed a higher TG activity than E651Q and DM variants on all substrates tested, followed by the DM variant, and in the end the E651Q variant presented the lowest TG activity on all proteins examined (Table 4-4).

On all four substrates tested, V34L, and V650I variants created higher level of cross-links compared to the WT protein, while the lowest cross-links were made by the E651Q and DM variants on vitronectin (Figure 4-7).

The range in SA differences between variants was the highest on fibronectin (~4.8-fold difference between V34L and the WT), but the lowest on the fibrinogen substrate (2.3-fold difference between V34L and E651Q), (Table 4-4).

Table 4-4: FXIII SA

FXIII substrate	FXIII variant	FXIII activity IU/mg of total protein	FXIII amount U/mg of total protein	FXIII activity per unit amount (SA)
Fibrinogen	FXIII WT	0.72	0.72	1.00
	V34L	1.29	0.33	3.94
	V650I	0.99	0.36	2.78
	E651Q	0.51	0.30	1.68
	DM	0.21	0.08	2.58
Fibronectin	FXIII WT	1.57	0.72	2.19
	V34L	3.45	0.33	10.50
	V650I	1.47	0.36	4.10
	E651Q	0.68	0.30	2.26
	DM	0.23	0.08	2.77
Vitronectin	FXIII WT	0.44	0.72	0.62
	V34L	0.74	0.33	2.25
	V650I	0.53	0.36	1.48
	E651Q	0.16	0.30	0.52
	DM	0.05	0.08	0.54
Collagen-1	FXIII WT	0.21	0.72	0.29
	V34L	0.31	0.33	0.96
	V650I	0.35	0.36	0.99
	E651Q	0.11	0.30	0.35
	DM	0.07	0.08	0.88

This table shows FXIII activity, levels, and SA for FXIII variants under study on four different substrates present in the EOC microenvironment. FXIII activity was determined using FXIII functional assay (Section 2.7.6), and presented as IU per mg of total yeast protein. The amount of FXIII in each sample was determined using ELISA for recombinant FXIII protein (Section 2.7.7), and presented as U per mg of total yeast protein. FXIII SA was calculated as relative activity per unit amount and presented for each variant for the four proteins tested. Abbreviations: SA=specific activity.

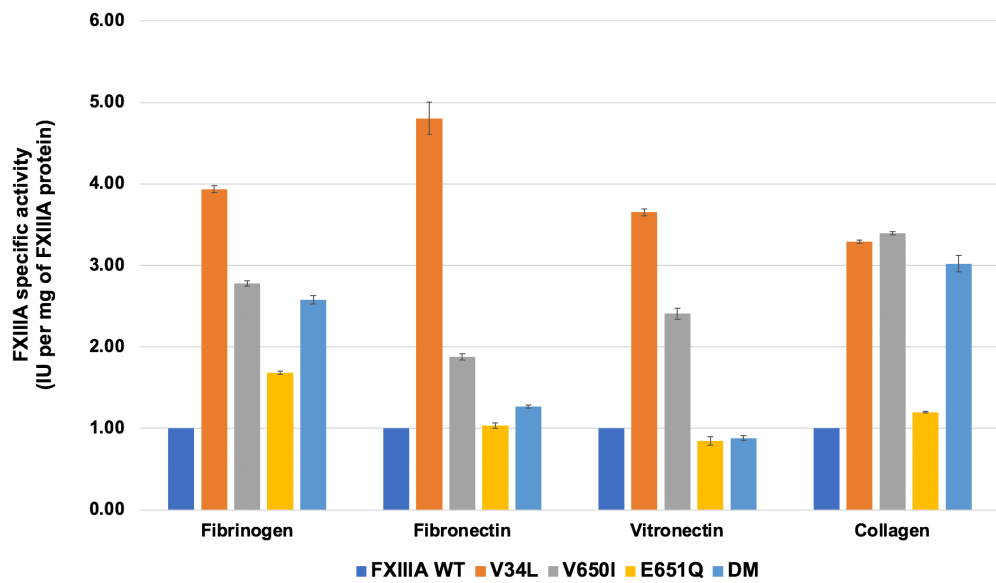


Figure 4-7: Comparison of FXIII variants SA for FXIII substrates

This bar chart shows the relative differences on FXIII activity per unit of FXIII amount between the variants on four FXIII substrates.

4.3.5 Summary

FXIII^A WT was expressed at twice the concentration compared to the V34L, V650I and E651Q variants. FXIII^A V34L heterozygous variant had the highest expression level, while the DM variant had the lowest. Neither the host (AH22 yeast strain) nor the FXIII^A negative control express FXIII^A protein (confirmed by ELISA). The highest level of FXIII^A substrates cross-linking was seen in fibronectin, followed by fibrinogen, vitronectin and then collagen-1. Four FXIII^A substrates examined showed clear variations when cross-linked by FXIII^A protein variants.

Relative to the WT, FXIII^A variants clearly demonstrate functional differences for the four FXIII^A substrates important in EOC:

- **Fibrinogen:** Compared to the WT, the highest activity was seen for V34L, V650I and DM variants had similar activity on fibrinogen; around 2.5 times higher than the WT on this substrate.
- **Vitronectin:** V34L showed the highest activity followed by V650I, while E651Q and DM variants have rather similar activity to WT on this protein.
- **All proteins tested except collagen-1:** V34L showed higher activity than the WT, V650I, E651Q, and DM variants.
- **Collagen-1:** V34L, V650I and DM variants have similar activity; around three fold higher than the WT, while E651Q variants presented similar activity to the WT on this substrate.

4.4 Characterisation of ovarian cancer cell lines

EOC is highly heterogenous disease and remains the most lethal gynaecological malignancy in developed countries. Immortalised EOC cell lines were chosen to represent the wide range of this heterogeneity, as they are important and invaluable *in vitro* tools because they allowed reproducibility of experimental results over the duration of time required to conduct the study. Interestingly, these cells have also been successfully used in proliferation and migration experiments by other researchers in published work (Nowicka et al., 2013, Chen et al., 2009). Therefore, the objectives of this section were: Firstly, to identify and characterise OC cell lines suitable for the project and should be dispersed by an official cell bank adopting firm rules on minimum available data. Secondly, to examine if OC cell lines identified express and secrete FXIIIa.

OVCA433, an established cell line derived from a patient with advanced stage serous ovarian cystadenocarcinoma (aggressive form), and the human ovarian carcinoma cell line, SKOV3 were chosen to perform all the cell biology experiments in this thesis representing EOC. Detailed characterisation of these cell lines models with respect to their cell origin was performed by Short Tandem Repeat (STR) profiling. This analysis was kindly carried out by Dr Claire Taylor (Leeds Cancer Research UK Centre, Genomics Facility). Full reports are presented in Appendix II.

4.4.1 Genotyping OVCA cell lines for F13A1 SNPs

Since these cell lines will be used in experiments involving specific FXIIIa variants, *F13A1* genotyping analysis was performed on cell lines chosen for this study as detailed in Section 2.9.4. Five coding *F13A1* gene polymorphisms were examined. Table 4-5 provides a summary of the results. OVCA433 cell line was FXIIIa wildtype at all amino acids examined. However, SKOV3 cell line was FXIIIa Wildtype at 204 (²⁰⁴TAT) and 650 (⁶⁵⁰GTT) amino acid residues, and heterozygous at 564 (CCT⁵⁶⁴C) and 651(G⁶⁵¹CAG) amino acid residues (Section 2.9.4, Figure 2-8).

Table 4-5: Summary of OVCA cells *F13A1* genotypes

A	Cell Line	Exon 2		Exon 5	
		Codon	Amino acid	Codon	Amino acid
	OVCA433	(GTG)	Val34	(TAT)	Tyr204
	SKOV3	(GTG)	Val34	(TAT)	Tyr204

B	Cell Line	Exon 12		Exon 14	
		Codon	Amino acid	Codon	Amino acid
	OVCA433	(CCG)	Pro564	(GTT_GAG)	Val650/Glu651
	SKOV3	(CCT/C)	Pro564	(GTT_G/CAG)	Val650/Glu651

This table presents the results of genotyping OVCA cell lines for five common *F13A1* SNPs. For each cell line, the SNPs examined and the exons in which they were found were displayed.

4.4.2 *FXIII*A protein expression

Before employing these lines in research involving the addition of *FXIII*A, it was necessary to determine whether they express and secrete *FXIII*A. Thus, evaluation of *FXIII*A expression and secretion was accomplished before using these cell lines in further experiments.

*FXIII*A exists in plasma as a heterotetramer (p*FXIII*), and found intracellularly as homodimer of two A-subunits (c*FXIII*) in cells of bone marrow origin; monocytes and macrophages (Adany and Bardos, 2003), platelets (Mitchell et al., 2014), osteoblasts (Al-Jallad et al., 2011). The aim of this section was to assess whether *FXIII*A is expressed in EOC cell lines used herein and secreted in the medium before using these cell lines as a tool to evaluate the role of *FXIII*A in EOC.

*FXIII*A activity assay was used to assess the expression and secretion of *FXIII*A protein by OVCA cell lines used in this thesis. A 60-70% confluent T75 flask for each cell line was trypsinised, resuspended in 10 mL complete fresh medium, and sub-cultured into three different T75 flasks. The first flask was grown for 24 hours, the second flask was grown until the cells were 50% confluent, the third flask was grown until the cells were 100% confluent. Cells were harvested and lysates were made after each time point: 24 hours of seeding the cells, mid-way through at 50% confluent, and at the end of the culture at full confluent. Cell lysates were prepared from all cell lines as described in Section 2.10.2.4. The suitability of our homemade RIPA lysis buffer [50mM Tris-HCl of pH 8, 150 mM NaCl, 1% nonidet p-40 (NP-40)] for activity assay was checked (Ngoka, 2008). *FXIII*A activity assays were performed on EOC cell line lysates made at different cell densities to assess *FXIII*A expression. 300 µL of the conditioned medium was collected at the same time points, spun down

to remove any floating cells, and examined to assess FXIIIa secretion. Aliquots of complete fresh medium from the bottle, that had not seen cells were incubated with the cells at 37°C for the same length of time to assess whether the temperature has any effect on the TG over the period. Data from these experiments revealed that, the highest TG activity was observed for OVCA433 cell line after 24 hours of incubation compared to the other cell lines, followed by the same cell line when the cells were 100% confluent, followed by the same cell line when the cells were 50% confluent . For the fresh complete medium which was incubated alongside the cell, the activity was decreasing over the time, whereas the conditioned medium for all cell lines at different cell densities showed differential TG activity (Table 4-6).

Given the data obtained from these experiments, which revealed that TG activity was present at certain cell densities in OVCA cell line lysates and conditioned medium, it has become necessary to examine local FXIIIa activity *in vivo* before using these cells.

Table 4-6: Summary of TG in OVCA cell line lysates and conditioned medium

Cell Line	Transglutaminase activity		
	Medium only no cells (IU/mL)	Conditioned medium (IU/mL)	Cell line lysate (IU/mg of total protein)
OVCA433 24 Hours	0.058	0.015	1.37
OVCA433 50% Confluent	0.011	0.026	0.49
OVCA433 100% Confluent	0.008	0.010	0.96
SKOV3 24 Hours	0.039	0.018	0.08
SKOV3 50% Confluent	0.013	0.033	0.11
SKOV3 100% Confluent	0.012	0.008	0.04

Results of TG assays on OVCA cell lines lysates and medium. Cell line lysates were spun down to remove any floating cells prior to performing the activity assays. An aliquots of blank complete medium were incubated with the cells for the same length of time and examined simultaneously for TG activity to assess the temperature effect on the activity. The total protein concentration was quantified using BCA protein assay for all cell line lysates as per the manufacturer's instruction. The observed TG activity was calculated as a percentage of the rate noted with standard human plasma as IU/mL. The actual cross-linking level in each cell line lysate examined was calculated as IU/mg of total protein.

4.4.3 Localisation of N-(γ -glutamyl)- ϵ -lysine isopeptide bond in OC cell lines *in situ*

The previous section has shown that some TG was present on OC cell lysates and conditioned medium. Therefore, it was important to assess if FXIIIa enzyme was active *in vivo* before using these cells in experiments involving FXIIIa protein. Immunofluorescence staining of OC cells was used to determine the location of the N-(γ -glutamyl)- ϵ -lysine cross-links (isopeptide bonds) *in situ* to address this research question. The results demonstrated less than 5% of cells contain the isopeptide bonds inside the OC cells (peri-nuclear), indicating minimal local activity (Figure 4-7).

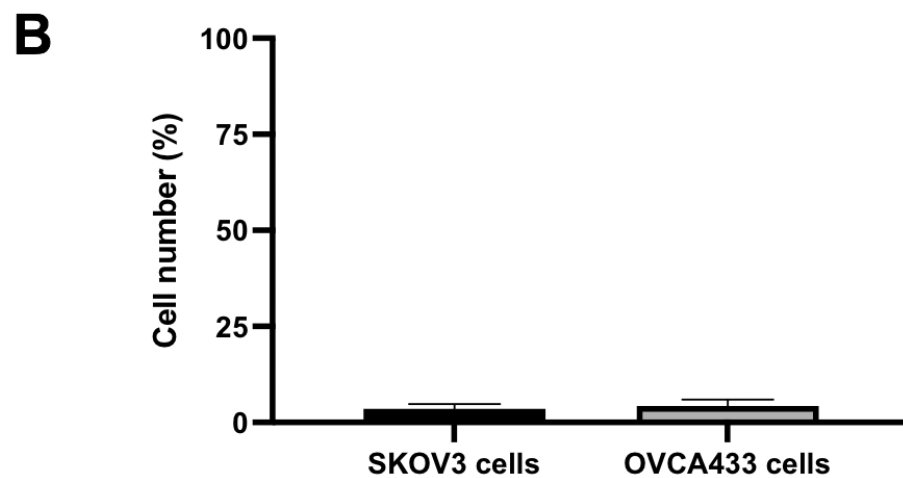
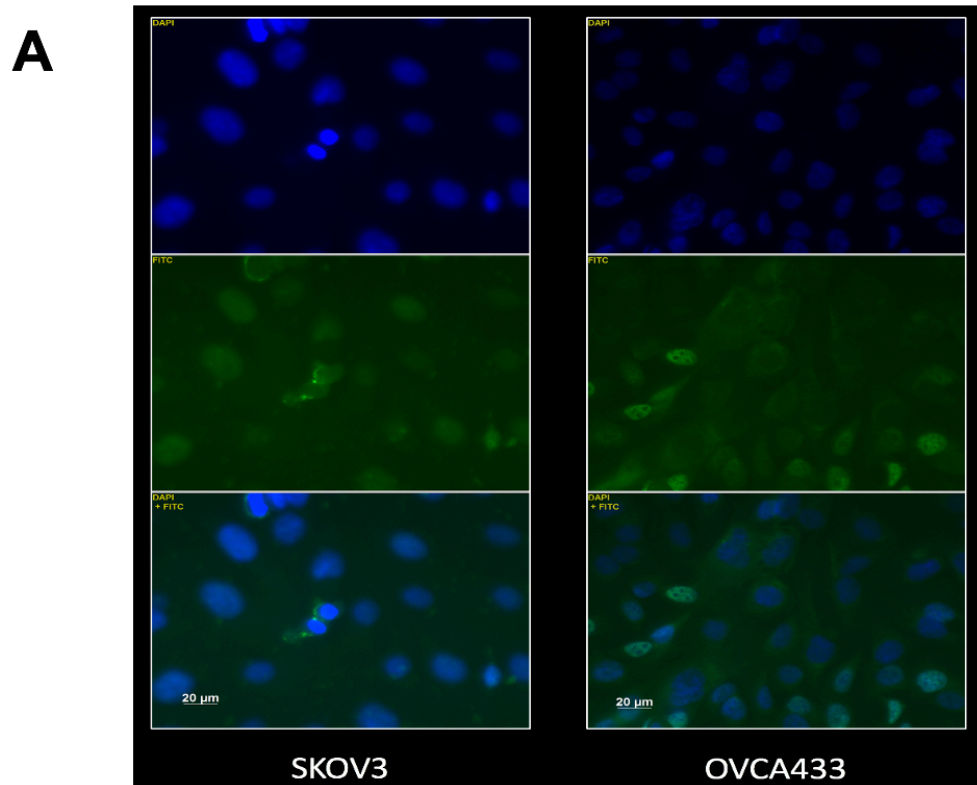


Figure 4-8: *In-situ* localisation of isopeptide bonds in OC cell lines

A) Representative Immunofluorescence (IF) staining images for localisation of N-(γ -glutamyl)- ϵ -lysine cross-links (isopeptide bonds) in SKOV3 and OVCA433 cell lines (passage 2). Staining for anti-isopeptide antibody [81D1C2] (ab422) mouse monoclonal to isopeptide IgG Kapa at 1:100 was detected with a goat anti mouse Alexa Fluor® AF488 fluorescent secondary antibody at 1:300 and a FITC emission filter (bright green, peri-nuclear). Nuclei were stained with DAPI, and detection performed with DAPI emission filter (blue), (Section 2.10). Scale bar represents 20 μ m. Images were acquired using Zeiss Microscope with 63x oil magnification lens. **B)** Quantitation of isopeptide bonds in OVCA433 and SKOV3 cells in GraphPad Prism 9. The histogram shows mean \pm SD (4 representative areas, 100 cells per area).

4.4.4 Reverse Transcription- Polymerase Chain Reaction (RT-PCR)

In order to determine the origin of the TG observed in the EOC cell lines above, the expression of FXIII A and human tissue transglutaminase 2 (*TG2*) was assessed in OC cell lines by reverse-transcriptase Polymerase Chain Reaction (RT-PCR). Total RNA was isolated from OC cell lines under study using TRIzol[®] Reagent (Section 2.9.2), followed by first strand cDNA synthesis (Section 2.9.3). Genomic DNA absence was confirmed in all RNA samples prior to use. PCR products were obtained only using *TG2* cDNA primers. No PCR products were observed with any FXIII A cDNA primers used, except with the THP-1 cell line, which produces the expected size product of 402 bp (Figure 4-9A). This result also confirms primers' functionality. Hence, FXIII A mRNA is lacking in OC cell lines tested, but is present in THP-1 cells. The THP-1 cell line was selected to serve as a positive control for the FXIII A expression. In the absence of FXIII A mRNA, the production of FXIII A protein is highly unlikely in OC cell lines tested, this was confirmed by WB (Figure 4-9B). This finding suggests that TG observed is most likely arises from *TG2* and that FXIII A protein is not expressed in OC cell lines (Figure 4-9C). As a result, these cell lines were deemed suitable for experiments involving the addition of FXIII A protein in order to study the objectives outlined at the start of this chapter.

4.4.5 Summary

OC cell lines used for this study do not express FXIII A. The TG activity observed on OC cell lines lysates and conditioned medium is most likely produced by *TG2*. IF localisation of *in situ* isopeptide bonds showed minimal signal, suggesting that the results of the planned experiments using FXIII A will not be compromised.

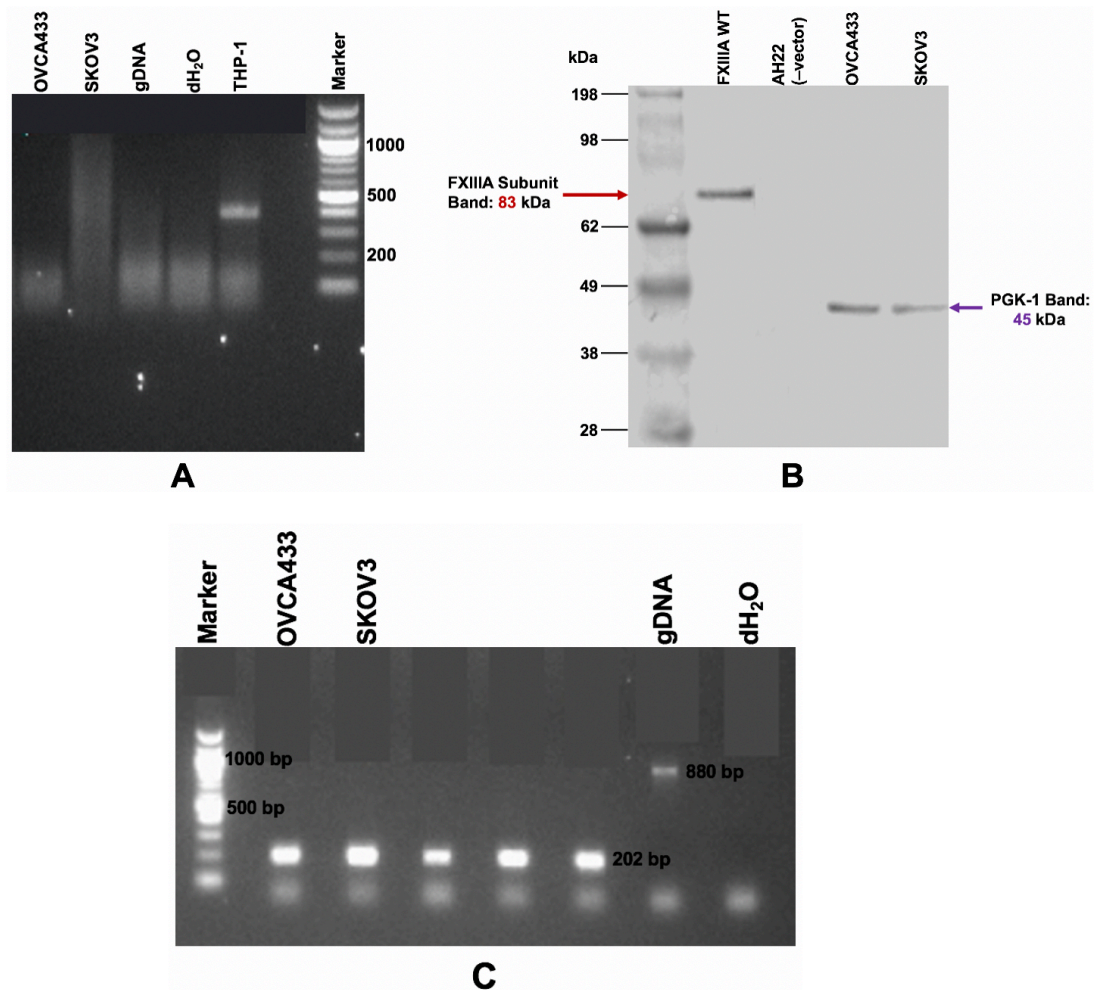


Figure 4-9: OVCA433 and SKOV3 do not express *F13A1* mRNA, nor FXIIIa protein

A) 30 ng of first strand cDNAs of OVCA433, SKOV3, and THP-1 cell line were amplified by PCR using *F13A1* exon 13 forward and exon 15 reverse primers to assess FXIIIa expression (Section 2.3.2). PCR products were analysed on 1.5% agarose gel against MW: 100 bp DNA ladder (GeneRuler™). THP-1 cDNA amplified with *F13A1* primers produced the expected size PCR product: 402 bp. Genomic DNA (gDNA) amplified with *F13A1* primers - positive control (expected PCR product size: > 20 kb). Nuclease-free water (dH₂O) amplified with *F13A1* primers (negative control); **B)** WB to confirm that FXIIIa protein is not expressed in OVCA433 and SKOV3 cell lines using anti-FXIIIa antibody HPA001804 diluted 1 in 500. 20 ng of protein was loaded per lane. WB was performed as detailed in Section 2.7.4. Anti-PGK-1 antibody was used as loading control for OVCA cell lines lysates, however, it was not suitable for yeast lysates which were used as controls for this experiment. **C)** 30 ng of first strand cDNA of OVCA433 and SKOV3 cell lines were amplified by PCR using *TG2* exon 8 forward and *TG2* exon 9 reverse primers (Section 2.3.2) to assess expression. Genomic DNA (gDNA) amplified with *TG2* primers - positive control (expected PCR product size: 880 bp). Nuclease-free water (dH₂O) amplified with *TG2* primers (negative control).

4.5 Assessment of FXIIIa variants on EOC cell behaviour

EOC cells are thought to spread through shedding from the ovarian surface epithelium (OSE) and re-adhering in the intraperitoneal cavity, as well as by invasion across the basal lamina into the stroma and then into the lymphatic or vascular systems. Consequently, gaining a thorough understanding of adhesion and migratory mechanisms, as well as how these may be related to the tumour's metastatic potential, is critical, as it provides insights into the underlying cell-matrix inter-relationships.

The work presented in Section 4.3 has clearly shown functional differences between FXIIIa protein variants on four proteins found in the OC microenvironment which are also FXIIIa substrates. The results observed could be important in tumour development and progression. Since FXIIIa variants have demonstrated differential ability to cross-link these substrates, the relevance of these findings to the behaviour of EOC cells was uncertain and remains to be identified. Activation of FXIIIa produces isopeptide bonds cross-linking a number of different proteins linked to biological processes involved in cell adhesion and ECM organisation. The role of FXIIIa in endothelial cell adhesion via cross-linking $\alpha_v\beta_3$ integrin is well-characterised (Dallabrida et al., 2000). Therefore, the objectives of this section are to explore the role of FXIIIa in the ovarian TME with respect to cancer-related behaviour of adhesion, proliferation and migration using OC cell lines.

4.5.1 FXIII A-mediated cross-linked substrates significantly increase EOC cell adhesion

The ability of EOC cell attachment on proteins important in cancer growth, and metastasis, which are also substrates for FXIII A, was evaluated. Generally, researchers tend to use these proteins at low concentrations ranging from 1–5 $\mu\text{g/mL}$, as in the study, where vitronectin was used at 5 $\mu\text{g/mL}$ for examining integrins (Yang et al., 2014). Ninety-six microtiter plates were pre-coated with 5 $\mu\text{g/mL}$ final concentration of FXIII A substrates in native and cross-linked forms. OC cells were added, and the adherent cells were visualised using Crystal Violet staining (Section 2.8.9) (Hwang et al., 2008). For OVCA433 cells, the experiments were performed as three independent biological replicates, and are analysed both in combination and separately (Figure 4-10). However, on SKOV3 cells, the experiments were done as two independent biological replicates, and are analysed both in combination and individually (Figure 4-12). On all cross-linked FXIII A substrates examined, OVCA433 and SKOV3 cell adhesion was significantly increased, while on all native versions of each substrate, EOC cell adhesion was unaffected.

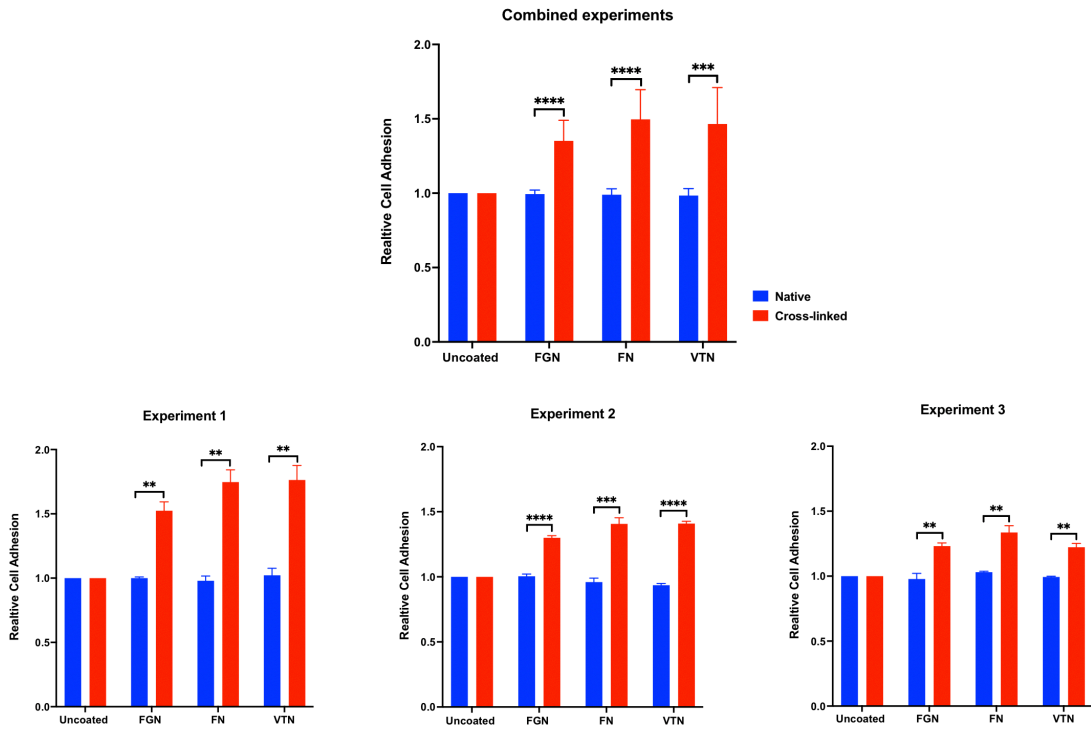


Figure 4-10: Cross-linked FXIIIa substrates significantly increase OVCA433 cell adhesion

Fibrinogen, fibronectin and vitronectin were formed as substrates for OVCA433 cell adhesion. Wells of a 96-microtiter plate were pre-coated with 5 $\mu\text{g}/\text{mL}$ final concentration of FXIIIa substrates at RT for 2 hours. Activation mix was prepared and added to designated wells to produce cross-linked version of each substrate (0.01 IU of Thrombin, 0.1M CaCl_2 , 0.002 IU of FXIII concentrate [Fibrogammin-P]) and incubated at 37°C for 30 minutes. Activation mix was removed and plate was washed 2x with DPBS. 5.0×10^4 cells/well/200 μL were added. Cells were allowed to attach, and plates were incubated O/N at 37°C, 5% CO_2 . Plates were washed three times to remove the non-adherent cells. The percentage of cells adhered to each substrate was quantified by Crystal Violet staining (Section 2.8.9). Top graph: The data is presented as the mean (\pm SEM) of three independent experiments and represents the percentage of adherent cells relative to cells grown on uncoated wells. Bottom graphs: Each single experiment performed in triplicates and presented as the mean \pm SD. Level of Significance: **= $p < 0.01$, ***= $p < 0.001$, ****= $p < 0.0001$. The representative image from each substrate tested in this experiment is presented in Figure 4-10.

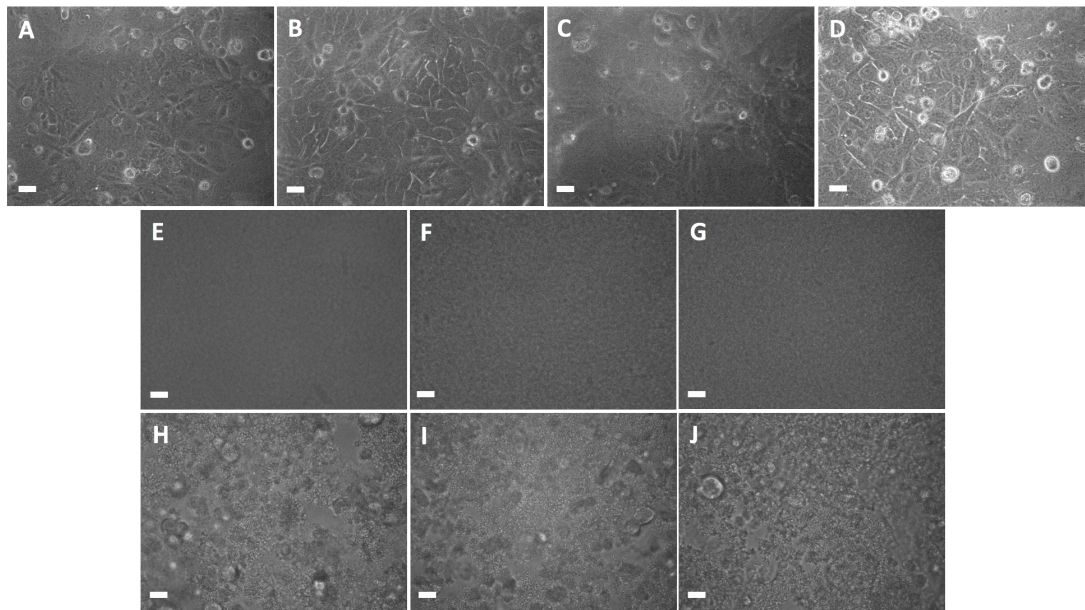


Figure 4-11: Representative images of OVCA433 cells adhered to FXIIIa substrates

96-well plates were coated with FGN, FN and VTN, cross-linked FGN, cross-linked FN, and cross-linked VTN. OVCA 433 cells were added at 5×10^4 cells/well/200 μ L. Representative 40x images are shown for each FXIIIa substrate tested. **A)** OVCA433 cells adherent to the plate without protein coated. **B)** OVCA433 cells adherent to FGN. **C)** OVCA433 cells adherent to FN. **D)** OVCA433 cells adherent to VTN. **E)** Cross-linked FGN before adding the cells. **F)** Cross-linked FN before adding the cells. **G)** Crosslinked VTN before adding the cells. **H)** OVCA433 cells adherent to cross-linked FGN. **I)** OVCA433 cells adherent to cross-linked FN. **J)** OVCA433 cells adherent to cross-linked VTN. The white bar in the lower left hand corner equals 100 μ m.

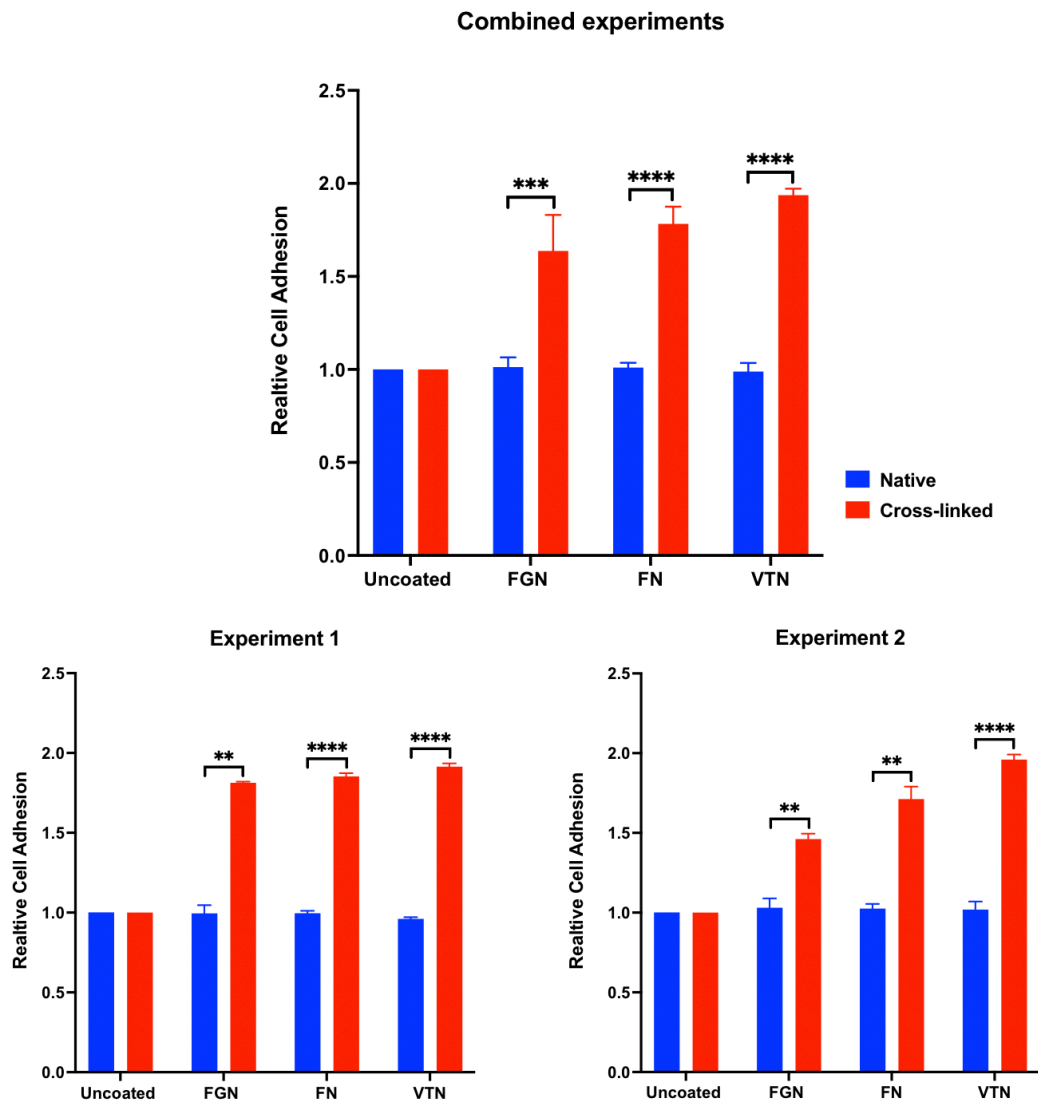


Figure 4-12: Cross-linked FXIIIa substrates significantly increase SKOV3 cell adhesion

Fibrinogen, fibronectin and vitronectin were formed as substrates for OVCA cells adhesion. Wells of a 96-microtiter plate were pre-coated with 5 $\mu\text{g}/\text{mL}$ final concentration of FXIIIa substrates at RT for 2 hours. Activation mix was prepared and added to designated wells to produce cross-linked version of each substrate (0.01 IU of Thrombin, 0.1M CaCl_2 , 0.002 IU of FXIII concentrate [Fibrogammin-P]) and incubated at 37°C for 30 minutes. Activation mix was removed and plate was washed 2x with DPBS. 5.0×10^4 cells/well were added. Plates were incubated O/N at 37°C, 5% CO_2 in standard TC incubator. Cells were allowed to attach and spread. Non-attached cells were removed, and the percentage of cells adhered to each substrate was quantified by Crystal Violet staining (detailed in chapter 2) over the successive 2 days. Top graph: The data is presented as the mean (\pm SEM) of two independent experiments and represents the percentage of adherent cells relative to cells grown on uncoated wells. Bottom graphs: Each single experiment performed in triplicates and presented as the mean \pm SD. Level of Significance: **= $p < 0.01$, ***= $p < 0.001$, ****= $p < 0.0001$. The representative image from each substrate tested in this experiment is presented in Figure 4-112.

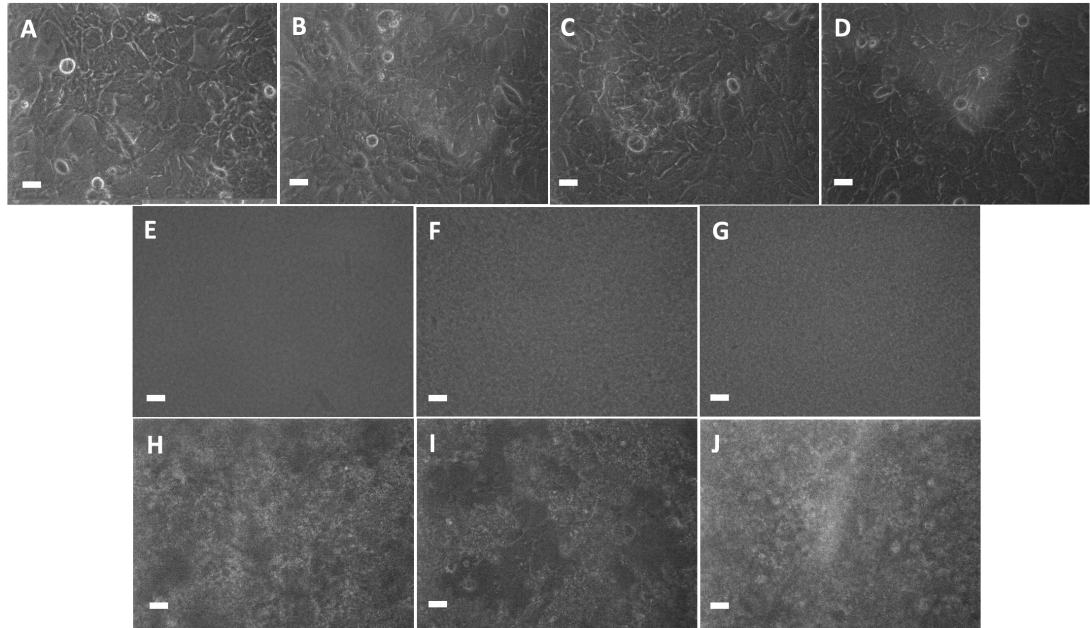


Figure 4-13: Representative images of SKOV3 cells adhered to FXIIIa substrates

96-well plates were coated with FGN, FN, VTN, cross-linked FGN, cross-linked FN, and cross-linked VTN. SKOV3 cells were added at 5.0×10^4 cells/well/200 μ L. Representative 40x images are shown for each FXIIIa substrate tested. **A)** SKOV3 cells adherent to the plate without protein coated. **B)** SKOV3 cells adherent to FGN. **C)** SKOV3 cells adherent to FN. **D)** SKOV3 cells adherent to VTN. **E)** Cross-linked FGN before adding the cells. **F)** Cross-linked FN before adding the cells. **G)** Cross-linked VTN before adding the cells. **H)** SKOV3 cells adherent to cross-linked FGN. **I)** SKOV3 cells adherent to cross-linked FN. **J)** SKOV3 cells adherent to cross-linked VTN. The white bar in the lower left hand corner equals 100 μ m.

4.5.2 FXIIIa purified protein variants affect EOC cell growth differentially

Therefore, further investigations were required to understand the role of FXIIIa protein in EOC cell proliferation. Hence, the next aim was to assess the impact of the FXIIIa protein on EOC cell growth. FXIIIa variants were produced in yeast, purified and added to OVCA433 cells in native and active states (Section 2.8.7). SKOV3 cell line was not examined in this experiment. FXIIIa variants tested were the WT, 34L and heterozygous of the variant, 651Q, and the DM which represent 650I_651Q allele *in vivo*. EOC cell proliferation was monitored every other day for 6 days using MTT assays. The presence of native and activated pure FXIIIa protein variants in the medium did not alter EOC cell growth, except for the native FXIIIa DM variant which showed a significant adverse effect (Figure 4-14).

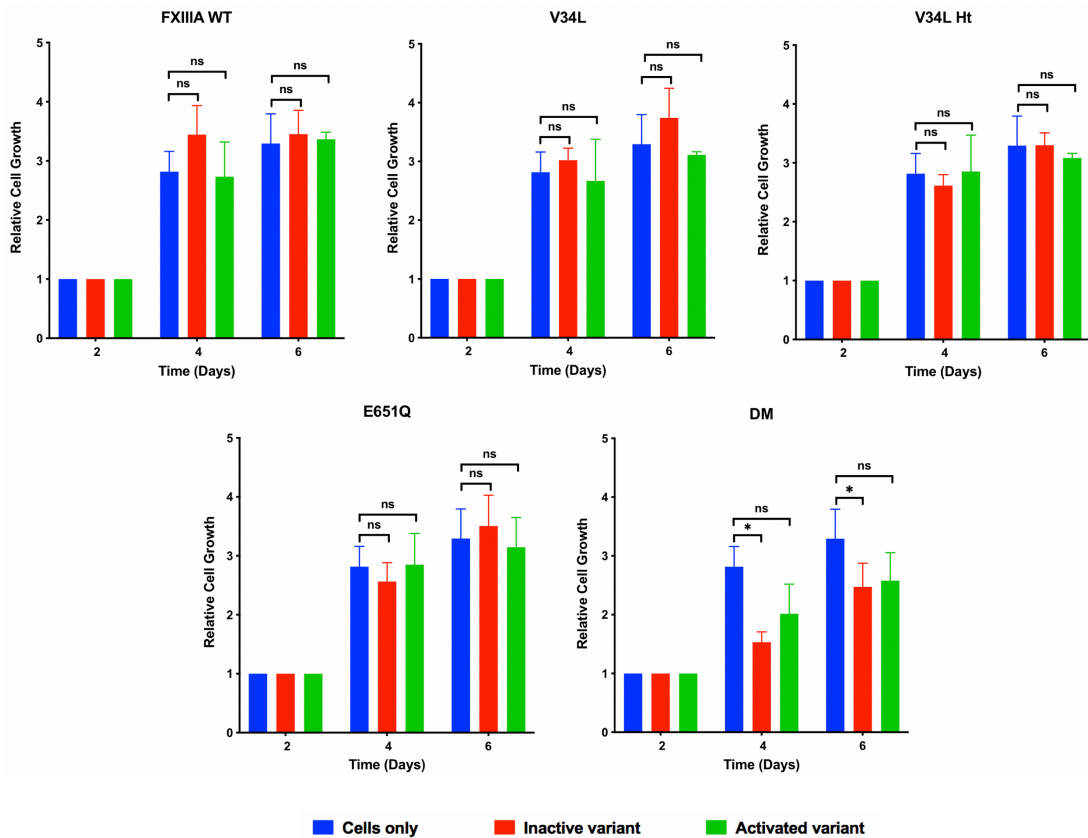


Figure 4-14: The presence of FXIII A purified protein variants in the medium has a differential effect on EOC cell growth

OVCA433 cells were seeded at 5.0×10^4 cells/200 μ L/well in 96-well plates in triplicates and incubated at 37°C, 5% CO₂ for 6 days (6 plates in total) in the presence of active and inactive FXIII A purified protein variants in the medium. 0.001 IU/mL of FXIII A variants were activated by adding 0.02 U of bovine thrombin, 10 mM calcium chloride in a final volume of 300 μ L and incubation for 30 minutes at 37°C, 5% CO₂. 0.001 IU of FXIII A was plated in 200 μ L final volume per well by adding 15 μ L of the reaction mix to 185 μ L cell suspension. Following FXIII A activation, thrombin was inhibited by the addition of PPACK at 140 μ g per 0.5 U of thrombin for 10 minutes at 37°C, 5% CO₂ (Section 2.8.7). For inactive FXIII A variants, the protein was added to the cells in a similar manner to the active protein, with the exception that thrombin volume was exchanged with DPBS. EOC cells proliferation was assessed every other day for 6 days using MTT assays. Data points represent growth relative to day 2 and are displayed as the mean \pm SD (triplicate wells). Student's t-tests were performed to compare the mean for three independent wells for each variant tested with OVCA433 cells only. Level of Significance: *= $p < 0.05$, ns=not significant.

4.5.3 FXIIIa variants have a differential effect on EOC cell migration

Results from the proliferation assays showed that native and activated purified FXIIIa protein variants have no effect on OVCA433 cell line growth. The next aim was to investigate the influence of FXIIIa variants on migration of EOC cells. FXIIIa purified protein variants were produced in yeast, purified and added to OVCA433 cells in native and activated states both in growth medium and Matrigel matrix (Section 2.8.8). Migration was evaluated by means of scratch wound closure assay using live cell imaging, taking images every hour for 24 hours. Migration was quantified using NIS-Elements software. The presence of inactive pure FXIIIa protein variants in the growth medium did not alter EOC cell migration, whereas, activated FXIIIa variants have significantly reduced the EOC cell migration (Figure 4-15). The addition of purified FXIIIa protein variants to the Matrigel showed a differential effect on OC cell migration. The results showed a significant decrease in OC cell migration for the activated variants (Figure 4-16). Given the rate of scratch wound closure for all FXIIIa variants tested, although lower for inactive FXIIIa variants when compared to OC cells without the addition of FXIIIa protein, it is likely that the crosslinking effect of the activated variants on the Matrigel produced the significant reduction in migration. To confirm FXIIIa-induced cross-linking reduces OC cell migration, another experiment would be required.

4.5.4 Summary

OVCA433 and SKOV3 cell adhesion was significantly increased on all cross-linked FXIIIa substrates tested, but adhesion was unaltered on natural forms of each substrate. OVCA433 cell line proliferation was unaffected by the presence of native and activated pure FXIIIa protein variants in the medium. OVCA433 and SKOV3 cell migration was significantly decreased in matrices and growth medium cross-linked by FXIIIa protein.

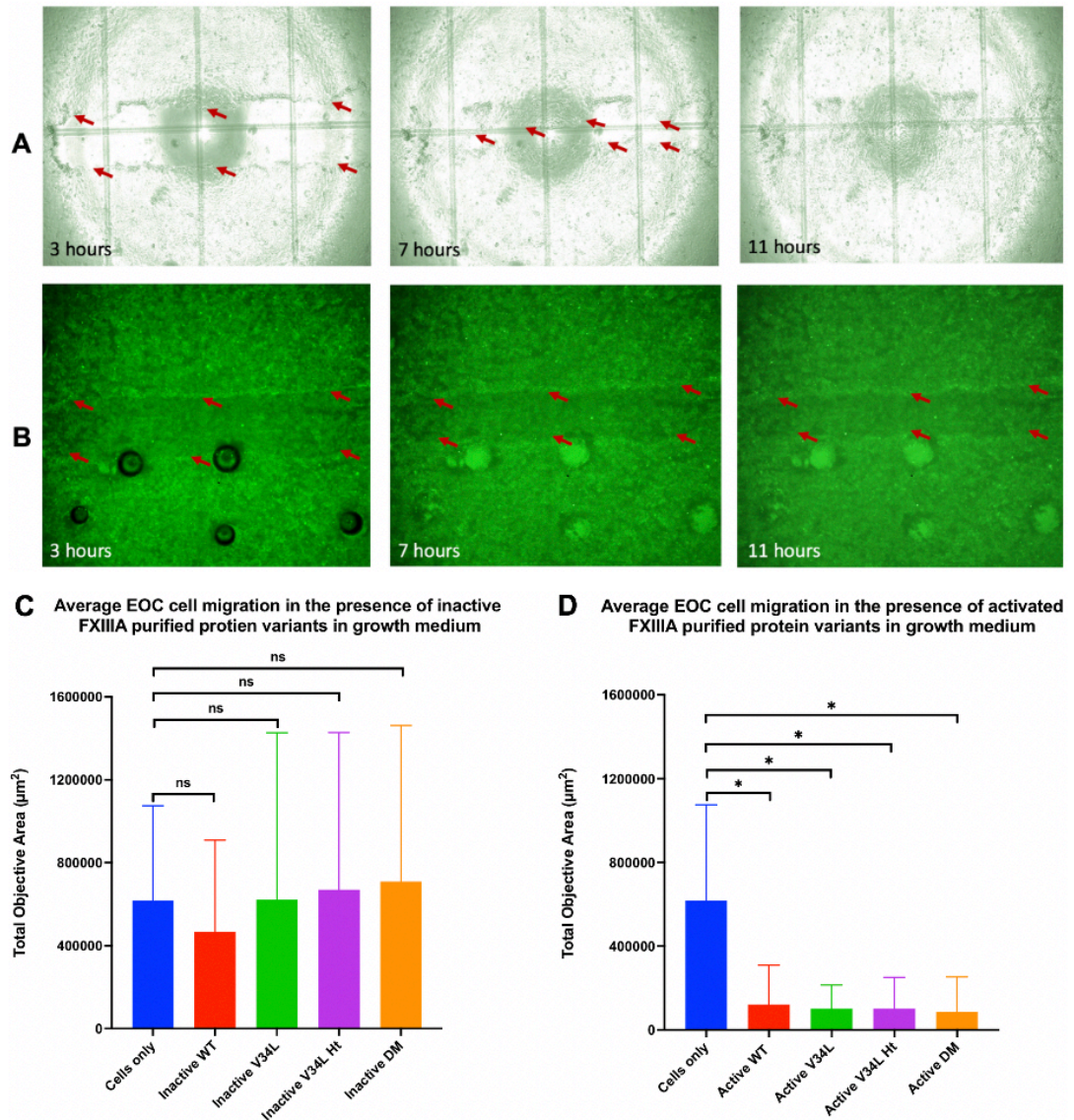


Figure 4-15: Activated FXIIIa variants significantly reduced EOC cell migration in growth medium

OVCA433 cells were stained with 1x CytoPainter-488 nm and seeded at 5.0×10^4 cells/200 μ L/well in 96-well ImageLock™ microplate in triplicates and incubated at 37°C, 5% CO₂ for 2 days, to reach confluency. This was followed by a scratch wound closure assay to assess migration. **A**) OVCA433 cells migration in the presence of inactive FXIIIa DM purified protein variant in the growth medium, the scratch wound has closed completely after 11 hours. **B**) OVCA433 cells migration in the presence of activated FXIIIa DM purified variant in the growth medium (cross-linked). It appears that the wound is closing at a slower rate as it was difficult for EOC cells to migrate through cross-linked matrix. Compared to the inactive state, scratch wound did not close after 11 hours. **C**) Average EOC cell migration in the presence of inactive FXIIIa variants in the growth medium. **D**) Average EOC cell migration in the presence of activated FXIIIa variants in the growth medium. The scratch wound closure in **(A)** and **(B)** is indicated by red arrows. The data represent the average EOC cell migration (means of nine wells) \pm SD. Level of Significance: ns=not significant, *=p<0.05.

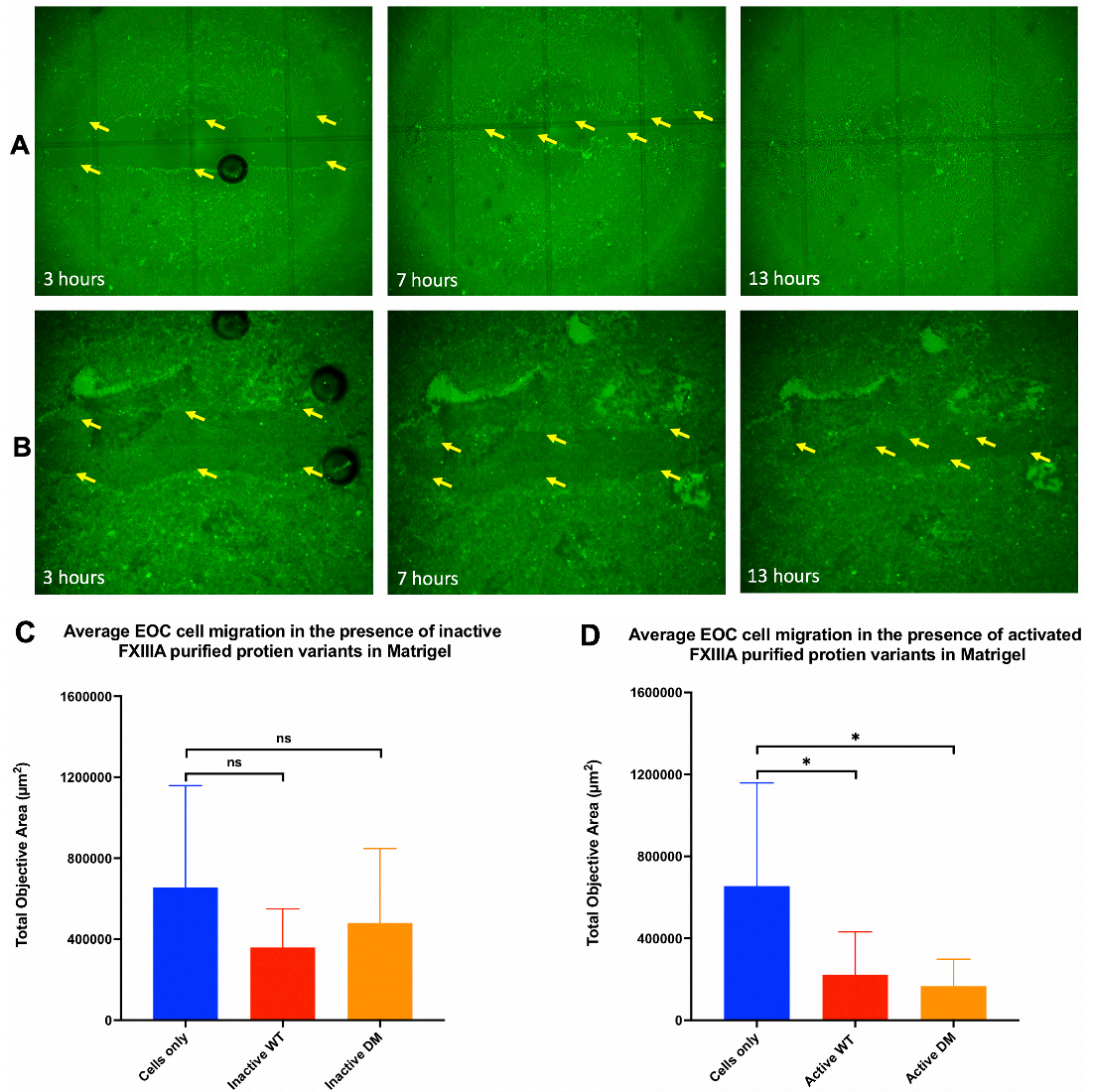


Figure 4-16: Activated FXIIIa variants significantly reduced EOC cell migration in Matrigel

OVCA433 cells were stained with 1x CytoPainter-488 nm and seeded at 5.0×10^4 cells/200 μL /well in 96-well ImageLock™ microplate in triplicates and incubated at 37°C, 5% CO₂ for 2 days, to reach confluency. This was followed by a scratch wound closure assay to assess migration. **A)** OVCA433 cells migration in the presence of inactive FXIIIa DM purified protein variant in Matrigel, the scratch wound has closed completely after 13 hours. **B)** OVCA433 cells migration in the presence of activated FXIIIa DM purified variant in Matrigel (cross-linked). It appears that the wound is closing at a slower rate as it was difficult for EOC cells to migrate through cross-linked matrix. Compared to the inactive state, scratch wound did not close after 13 hours. **C)** Average EOC cell migration in the presence of inactive FXIIIa variants in Matrigel matrix. **D)** Average EOC cell migration in the presence of activated FXIIIa variants in Matrigel matrix. The scratch wound closure in **(A)** and **(B)** is indicated by yellow arrows. The data represent the average EOC cell migration (means of nine wells) \pm SD. Level of Significance: ns=not significant, *= $p < 0.05$.

4.6 Key findings

- ❖ The yeast expression system was used effectively to produce recombinant FXIIIa protein variants, with FXIIIa negative control not producing any detectable FXIIIa protein.
- ❖ FXIIIa substrates were cross-linked differently by FXIIIa variants. The highest level of FXIIIa substrate cross-linking was seen in fibronectin, followed by fibrinogen, vitronectin and then collagen-1.
- ❖ FXIIIa variants demonstrate functional differences for substrates important in EOC.
- ❖ OVCA cell lines used for this study do not express FXIIIa protein.
- ❖ On all FXIIIa cross-linked substrates studied, OVCA433 and SKOV3 cell adhesion was significantly increased, but not on native forms of each substrate.
- ❖ The presence of purified FXIIIa protein variants in the growth medium as native and activated forms does not influence EOC cell proliferation, except when the DM purified variant was added, a significant decrease in OVCA433 cell growth was observed.
- ❖ The presence of FXIIIa purified protein variants in their native inactive state in the growth medium and Matrigel matrix does not influence EOC cell migration.
- ❖ FXIIIa-mediated cross-linked matrices and growth medium significantly decrease EOC cell migration.

4.7 Discussion

4.7.1 Production and purification of recombinant FXIIIa protein

The yeast strain *Saccharomyces cerevisiae* is used extensively to produce recombinant proteins for research and medical purposes because it can be cultured to high density and efficiently to generate proteins; primarily due to its simplicity of genetic manipulation, fast growth as a unicellular organism, low-cost medium, and its ability to perform eukaryotic post-translational modifications.

In the early 1990's the yeast strain *Saccharomyces cerevisiae* was employed to make large quantities of purified FXIIIa protein required for X-ray crystallography studies (Yee et al., 1994). In recent years, the yeast-expression system was chosen to produce abundant quantities of recombinant FXIIIa for use as therapeutics. The data from the clinical trials using this recombinant protein in FXIII deficient patients revealed that the recombinant protein and plasma derived FXIIIa share the same functional properties (Brand-Staufer et al., 2015). Accordingly, yeast was an ideal host for production of the recombinant FXIIIa protein required for *in vitro* studies, and hence this recombinant protein-expression system was chosen for this PhD project. The lithium acetate/carrier DNA/PEG yeast-transformation method was found to be highly efficient, producing up to 10^6 colonies per μg of plasmid DNA. The work presented in this thesis shows that, this method was also faster as no time was required for transformed cells to recover before plating, as was the case for the transformants using the electroporation method (Section 2.4.3). Kawai *et al.* (2010) have evaluated different methods of yeast transformation and present that the lithium/PEG methods can yield up to 10^7 colonies per μg of DNA, while the electroporation methods will produce $2\text{-}5 \times 10^5$ transformants per μg of plasmid DNA (Kawai et al., 2010), although a literature search has found no studies on comparing these transformation methods for *Saccharomyces cerevisiae*. Other scientists have determined that for bacterial cells the electroporation method is less complicated and produces higher transformation efficiencies, even though they may still prefer the chemical method due to its accuracy (Oswald, 2007).

The protein being expressed in this project is a transglutaminase that performs the post-translational modification of cross-linking other proteins. FXIIIa is known to cross-link a large number of substrates, and this cross-linking reaction can modify the function or properties of the substrate molecules.

Production and purification of FXIIIa protein variants was particularly challenging due to the large size of this protein. FXIIIa variants were expressed under the control of a galactose promoter. It was reassuring to find that this expression system produces

recombinant FXIIIa at a much higher concentration than that found in human plasma. The produced and purified protein variants were found to have a molecular weight of around 83 kDa and were identified as FXIIIa based on molecular weight estimates, by WB and by cross-linking function.

FXIIIa yeast lysates analysis on SDS-PAGE showed that the migration of the V650I variant does not appear to correlate with the level of the other variants (Section 4.2.1, Figure 4-1). It has been reported that the protein's tertiary structure influences detergent binding and the rate of migration of proteins on SDS-PAGE, and that disulfide bonds reduce globular protein binding to SDS almost two-fold (Pitt-Rivers and Impiombato, 1968). This interesting phenomenon is known as 'gel shifting' and has been observed to occur often in membrane proteins. Furthermore, it has been attributed to an alteration in detergent binding (Rath et al., 2009). This finding may be related to the substitution of Valine with Isoleucine at 650 amino acid residue, which may have led to some structural changes within FXIIIa protein-altering this variant's migration rate on SDS-PAGE. Interestingly, when 650I pooled yeast lysate sample was purified, the effect observed on SDS-PAGE migration was lost (Figure 4-4). However, further exploration of this phenomenon is beyond the scope of this thesis.

The relative amount of FXIIIa in yeast lysate samples was quantified using the His-tag ELISA, using an anti-histidine monoclonal antibody as a capture antibody before applying the samples has significantly reduced the background and increased the assay accuracy and reproducibility (Goodell et al., 2008). The ELISA assay used in this study to quantify the amount of FXIIIa protein in EOC patients' plasma samples and recombinant yeast lysates was validated in Dr Anwar's laboratory and has been used in published research (Anwar et al., 1999).

4.7.2 Variations in cross-linking of different substrates

In this chapter, the comparative assessment data of FXIIIa substrates cross-links by FXIIIa variants under study found that FN had the highest cross-links followed by FGN, VTN, and finally collagen-1 (Figure 4-6). It has been demonstrated that activated FXIIIa cross-links fibronectin to itself and the alpha-chain of fibrin, as well as mediates fibronectin cross-linking to collagen I and III (Mosher and Schad, 1979). One of the important reasons for these variations may be the source of the substrate proteins used.

The variation in the ability of FXIIIa variants to cross-link the various FXIIIa substrates to each other, e.g. fibrinogen to fibronectin, or fibrinogen to vitronectin and collagen-1, was attempted. SDS-PAGE was used to analyse the cross-linked products. However, problems were encountered and several issues arose during the experimental work. It would have been very exciting and informative to obtain data from these attempted experiments.

4.7.3 Variations in cross-linking by different FXIIIa variants

One of the important findings that has emerged from these experiments was that variants of the FXIIIa protein show functional differences for these substrates (Section 4.3.4). V34L variant presented the highest cross-linking on FN compared to the WT (Table 4-7B).

These are very interesting results, particularly in the context of the key findings presented in Section 3.10. The most important result was that, high plasma FXIII activity is associated with EOC progression (Figure 3-20A). The V34L variant has been linked to increased TG activity and more dense fibrin matrices (Ariëns et al., 2000). Since FXIIIa's TG activity produces isopeptide bond cross-linking these matrix-associated proteins, it is possible that FXIIIa protein plays a role in the development of tumour matrix, which contributes to cancer progression.

Activated FXIIIa cross-links the β_3 part of the $\alpha_v\beta_3$ integrin to vascular endothelial growth factor receptor-2 (VEGFR2), which is essential for the activation of angiogenic signalling cascade (Dardik et al., 2006). Through up-regulation of proteins like Wilm's Tumour-1 (WT-1) and inhibition of thrombospondin-1 (TSP-1) expression, this cross-linking action enhances angiogenic signalling (Dardik et al., 2005). It may be that V34L variant by producing high plasma FXIII activity and cross-linking $\alpha_v\beta_3$ to VEGFR2, initiated these molecular events, leading to increased angiogenesis within the EOC microenvironment promoting cancer growth and progression.

4.7.4 TG activity in OC cell lines

153 OC cell lines were retrieved by Jacob *et al.* (2014). They have reported that, the current EOC cell line available required improved quality of cell banking in terms of documentation of the source of cell derivation, recording the patient's clinical information and demonstration of diverse ethnicity and histological types from the sources available (Jacob et al., 2014). The two human ovarian carcinoma cell lines used in this project (OVCA433 and SKOV3) are well-established lines, used extensively in published literature, and were authenticated prior to use. They do not

express FXIIIa (Section 4.4.4). The expression of the other transglutaminases, which theoretically could be the source of this activity was not examined. The nine members of the TGs family include: TG1 – keratinocyte TG which is mainly expressed in upper gastrointestinal tract, lower female genital tract, and the stratified squamous epithelium of the skin; TG2 – tissue TG is found in a wide variety of tissues and cell types; TG3 – epidermal TG is expressed in brain, hair follicles, and epidermis; TG4 – prostate TG is mainly found in the prostate gland, prostatic fluids, and seminal plasma; TG5 is present in skeletal muscle, epithelial barrier lining, and foreskin keratinocytes; The human testes and lungs, human cancer cells with neural features, as well as the brains of mice express TG6; little is known about TG7, its expression is confined to the testes, lungs, and brain, just like TG6. According to one study, TG7 transcript levels are higher in breast cancer cells from patients who have a bad prognosis; FXIIIa is the TG under study here; and the non-catalytic erythrocyte band 4.2 is inactive (Eckert et al., 2014). Therefore, the minimal TG activity observed in cell lysates and conditioned medium was attributed to TG2 and confirmed by RT-PCR (Section 4.4.4).

4.7.5 FXIIIa-mediated cross-linked substrates and EOC cell adhesion

EOC cell adhesion is significantly increased on FGN, FN, and VTN cross-linked by FXIIIa compared to uncross-linked proteins, while the substrates in their native state did not alter EOC cell adhesion (Section 4.5.1). The interesting results of the adhesion experiments, that EOC cell adhesion is increased in cross-linked matrices, suggest that FXIIIa variants may have a role in the ovarian TME through cross-linking these proteins, producing scaffolds leading to increased attachment of growth factors and facilitating cancer cell adhesion, proliferation, migration, and angiogenesis. Thrombin is expressed by EOC cells (Wang X. et al., 2005), and it can activate FXIIIa, producing TG activity within the TME. It has also been reported that FXIIIa production is up-regulated by thrombin in chondrocytes (Siebenlist et al., 2004).

In a similar study which evaluated the cellular and plasma types of fibronectin (cFN and pFN respectively) on EOC cell attachment and spread, the results of that study presented a differential effect on ovarian cancer cell adhesion, migration and invasion, and these effects vary amongst two cancer cell line populations. SKOV3 adhesion was found to be higher on both types compared to no coating, with cells spreading quicker on cFN than on pFN. In contrast, OVCAR-3 cells took longer to adhere than SKOV3 cells (Zand et al., 2003). The next important step would be to

explore the influence of pure FXIIIa protein variants on EOC cell adhesion in the presence of cross-linked and native substrates.

4.7.6 FXIIIa variants and EOC cell proliferation

This study found that the presence of pure FXIIIa protein variants in growth medium in both native and activated forms did not alter EOC cell proliferation (Figure 4-13). No work to date has been published on the influence of FXIIIa variants on EOC cell growth. However, FXIIIa does have a role in wound healing and tissue regeneration (Soendergaard et al., 2013). It has also been reported that FXIIIa promotes intestinal epithelial proliferation and migration (Cario et al., 1999). Given that this work has established that cross-linked matrices increased EOC cell adhesion (Section 4.5.1), this is a rather strange result because native and activated pure FXIIIa protein variants added to the growth medium had no effect on EOC cell proliferation. The presence of active FXIIIa protein was expected to accelerate EOC cell growth. It is possible that these mutant variants have a different function that is still unknown and needs to be investigated further.

4.7.7 FXIIIa variants and EOC cell migration

EOC cell migration is significantly reduced on matrices and medium cross-linked by FXIIIa, whereas the presence of pure inactive FXIIIa protein variants in the growth medium and Matrigel matrix did not alter EOC cell migration (Section 4.5.3). There has been no detailed investigation that specifically explore the influence of FXIIIa protein on the migration of EOC cells. Matrigel used in this study is mainly comprised of laminin, collagen and proteoglycans, with a small amount of FN. The addition of activated FXIIIa to Matrigel and growth medium produced cross-linked matrices. In the presence of activated FXIIIa, OVCA433 cells motility was significantly reduced through the cross-linked matrices in two-dimensional culture, although, OVCA433 cells are extremely malignant and invasive *in vivo*. A possible explanation of reduced migration might be that, the level of adhesion between tumour cells and the cross-linked matrix affects the cancer cell-matrix interactions on cell migration, which in turn decreased the cell movement (Ruoslahti and Pierschbacher, 1987, Giancotti and Ruoslahti, 1990). Another possible explanation is that, OVCA433 cells were unable to make the proteases needed for cancer migration and invasion into cell culture medium *in vitro*, which have been provided by stromal cells *in vivo* (Westerlund et al., 1997). In addition, inactive FXIIIa does not appear to induce morphological changes on OVCA433 cells when added to the growth medium and the Matrigel matrix

(Figures 4-15 and 4-16). Therefore, the little amount of activated FXIIIa left following the cross-linking of the Matrigel basement membrane matrix and the growth medium is unlikely to promote or influence morphological changes in the cancer cells that enable them to change their shape and squeeze through the cross-linked matrix.

Chapter 5 General Discussion and Future Work

5.1 Summary of thesis results

This project set out to evaluate the clinical and biological roles of FXIIIa in EOC. Clinical data from patients newly diagnosed with the disease, along with their plasma and tissue samples were utilised. In addition, further *in vitro* exploration of the clinical results was performed to gain a better understanding of the importance of FXIIIa in EOC. This is the first time such a study has been conducted in a newly diagnosed EOC patient cohort.

This project provides the first comprehensive assessment of plasma FXIII activity in EOC response to therapy and survival outcome. In the ICON7 study-cohort, patients with high plasma FXIII activity were found to have significantly *increased* risk of EOC progression in multivariate analysis, suggesting a potential role for FXIII in EOC metastasis. This study has also demonstrated that, patients with high plasma FXIII activity who received bevacizumab, had significantly *improved* SPP. Another important finding was that patients with high plasma FXIII activity who were at high risk of disease progression with > 1.0 cm residual disease following primary debulking surgery, survived for longer after their disease had progressed. Nevertheless, as with other research, FXIIIa would need to be validated in several and diverse patient cohorts before it could be classified as a real predictive factor for survival in EOC.

The results of this study showed that, *low* levels of FXIIIa subunit in plasma of patients from ICON7 study-cohort were significantly linked with SerousHighGrade histology. Interestingly, expression of FXIIIa protein in the tumour tissues of patients from this same cohort was significantly *lower* in higher grade disease. These results raise the possibility that FXIIIa is a potential prognostic biomarker in serous poorly differentiated tumours (Type II EOC).

A novel relationship was found in this study-cohort. Compared to the wildtype, carriers of 650I_651Q allele present significantly *reduced* plasma FXIII activity. In contrast, V34L carriers showed *higher* activity, consistent with previous studies. FXIIIa variants demonstrate functional differences for substrates important in EOC, and these substrates were cross-linked differently by FXIIIa variants. Interestingly, FXIIIa-mediated cross-linked substrates have led to a significant *increase* in EOC cell adhesion.

The presence of pure FXIIIa protein in the growth medium in both native and activated forms did not influence EOC cell proliferation, with the exception of the

native FXIII A DM variant, which presented a significant adverse effect on EOC growth. A *decrease* in EOC cell migration was observed when FXIII A purified variants were activated and added to the growth medium and Matrigel matrix, whereas the presence of their native inactive counterparts in the growth medium and Matrigel matrix did not influence EOC cell migration.

5.2 Plasma FXIII activity may aid EOC dissemination

This study has established that FXIII activity in the plasma of newly diagnosed EOC patients is significantly linked with the advanced-stage of the disease. Women with FIGO stage IV showed much *lower* plasma FXIII activity than those with FIGO stage III disease ($p=0.029$, Section 3.7.1). Furthermore, in survival multivariate analysis, patients with high plasma FXIII activity were found to have significantly *increased* risk of EOC progression (Section 3.9.3.2). In addition, the levels of D-Dimer in plasma of this study's cohort were found to be *greater* than those reported in normal, healthy people (Section 3.4). It has been reported that abnormal coagulation indices are present in approximately 90% of cancer patients with metastases and half of all cancer patients, including elevated plasma D-Dimer levels and coagulation factor levels (Gouin-Thibault and Samama, 1999). Multiple mechanisms have been proposed to influence tumour progression through coagulation disorders (Camerer et al., 2004, Palumbo et al., 2000). Despite the fact that some of the published literature has focused on tissue transglutaminase 2 (Hwang et al., 2008), the involvement of the coagulation system in OC was emphasised in a thorough review (Wang X. et al., 2005). FXIII plays a crucial role in tumour angiogenesis by directly stimulating endothelial cell proliferation, migration and survival (Dardik et al., 2006). This could also explain the reason behind the progression of EOC in women with high plasma FXIII activity.

5.3 Plasma FXIII activity may influence the prognosis in advanced-stage EOC and response to therapy

The present study has been one of the first attempts to thoroughly evaluate plasma FXIII activity in EOC prognosis and therapeutic response. The study-cohort, which consists of women newly diagnosed with EOC, was part of the ICON7 translational cohort. The ICON7 trial ($n=1528$) has measured three survival intervals including OS, PFS, and SPP. A unique prognostic variable described as patients at a high risk of

disease progression was defined by the trial investigators as patients with inoperable FIGO stage III, or FIGO stage III with >1 cm of macroscopically residual disease remaining following primary cytoreduction surgery, or with FIGO Stage IV disease to compare the ICON7 study populations to the GOG-218 trial participants (Oza et al., 2015).

Plasma FXIII activity sub-groups from the ICON7 study-cohort were extracted, and analysis was performed to evaluate the effect on EOC prognostic factors, chemotherapeutic response and survival intervals. Plasma FXIII activity does not appear to influence OS or PFS. However, there was a significant benefit for women with high plasma FXIII activity for SPP (Section 3.9.2).

Patients with high FXIII activity in their plasma and at high risk of disease progression with a residual disease of more than 1 cm following surgery, presented significantly *improved* SPP (p=0.030, Section 3.9.2). This results is consistent with that of the whole ICON7 trial, which showed that only those women at high risk of disease progression benefited from the addition of bevacizumab (Oza et al., 2015). Although further explorative endpoint analyses have validated the PFS benefit, improvement in OS was limited to advanced stage patients with > 1 cm of residual disease (González Martín et al., 2019).

This study is the first piece of work to demonstrate a significant benefit for high plasma FXIII activity in patients with EOC in receipt of bevacizumab in addition to standard platinum based chemotherapy of carboplatin and paclitaxel for SPP (p=0.041, Section 3.9.2). Following a progression event, patients with high plasma FXIII activity in receipt of bevacizumab had a *higher* SPP, approximately 31.9 months, compared to patients with low plasma FXIII activity at an approximately 15.8 months (Section 3.9.2.1). It appears to be possible that high FXIII activity could affect the angiogenic receptor cross-linking structure, making bevacizumab treatment more effective, and that increased FXIII activity levels could influence patients' response to anti-angiogenics.

5.4 *F13A1* genotypes are associated with plasma FXIII activity and differentially affect EOC prognosis

The relationship between plasma FXIII activity and *F13A1* genotypes showed a significant *decrease* in activity of FXIII A 650I_651Q haplotype in women newly diagnosed with EOC, representing a novel association emerging from this study. Three alleles were examined. The A allele at 1951G>A, the C allele at 1954G>C, and

650I_651Q haplotype (Section 3.6.1). It was critical to determine how the haplotype was linked to FXIII activity, as this is how these SNPs occur in the normal population (de Lange et al., 2006). 1951A is always found with 1954C as they are in complete LD with each other (Section 3.5.3). These two SNPs within exon 14 of FXIII gene, *F13A1*, are found in the β -barrel 2 (residues 629–731) of FXIII polypeptide (Section 1.3.2). This location means that they are not found around the catalytic core or the regions involved in the protein conformational alterations (Arg310-Tyr311 and Gln425-phe426) to make the active site available for the catalytic reaction during activation of this enzyme (Ariëns et al., 2002). It has previously been shown that V650I and E651Q SNPs have little, if any, impact on FXIII activity and levels in normal population, while the 34L variant has been linked with high SA (Anwar et al., 1999).

This study found that the V34L variant is associated with *increased* plasma FXIII activity (Section 3.6.1, Figure 3-4), in accordance with previous research (Kohler et al., 1998). This is most likely due to a higher thrombin cleavage rate by this variant (Ariëns et al., 2000). This variant was found to be the single most important functional polymorphism that influenced FXIII activity in a linkage analysis (de Lange et al., 2006).

In a previous study (n=260), the V650I variant was significantly linked to a shorter OS ($p=0.008$), whereas, the V34L variant was significantly related to a longer OS in patients with advanced-stage EOC ($p=0.0219$) by Log rank tests (Anwar et al., 2004). However, there were no significant relationship observed between these SNPs and survival intervals in this study (Section 3.9.1 and Section 3.9.3). These results suggest that these SNPs may be important in certain stages of the disease or a particular cohort of patients.

5.5 FXIII levels in plasma and tumour tissues may be used as predictive biomarkers for high grade EOC

Compared to women with benign ovarian tumours, FXIII levels were *lower* in women with metastatic malignant disease. FXIII consumption during the creation of the metastatic niche via cross-linking activity was thought to be the cause of lower levels in metastatic cancer (van Wersch et al., 1994). The results of the CSIOBV database of 3261 patients, which was compiled from international OC gene expression studies such as The Cancer Genome Atlas (TCGA), showed that *F13A1* gene expression was significantly lower in virulent, advanced stage, and poorly differentiated EOC

(Tan et al., 2015). The decreased levels of *F13A1* gene expression found in the stroma of the metastatic EOC are most likely due to cellular FXIIIa rather than plasma FXIIIa, which is most likely produced locally by cells originating from the bone marrow (e.g: macrophages) and/or fibroblasts.

This is the first study to report an association between both *low* plasma FXIIIa levels and EOC SerousHighGrade histology (Section 3.7.2), and between *low* FXIIIa expression in tumour tissue and high-grade disease (Section 3.8.4). These findings back up previous results by van Wersch (1994) and the CSIOBVDV database. Moreover, it contribute additional evidence that in poorly differentiated metastatic EOC, the decrease in FXIIIa levels could be due to increased utilisation of FXIIIa during cross-linking matrix-associated proteins locally within the tumour. Another possible explanation is that FXIIIa may have been used in other cancer-related processes such as angiogenesis, inflammation and immune response (Hanahan and Weinberg, 2011). It appears that women with high-grade disease and *low* plasma FXIIIa levels are more likely to develop metastatic advanced EOC. However, with a small sample size, these results must be interpreted with caution.

5.6 FXIIIa variants demonstrate functional differences for substrates important in EOC microenvironment

The effect of this enzyme on its substrates, which are important in ovarian cancer, may increase our understanding of the complexity of the cross-talk between the cancer cells, these substrates and the FXIIIa enzyme within the ovarian cancer micro-environment. This study has established functional differences between FXIIIa variants for proteins located in the EOC microenvironment, and that these substrates were cross-linked differently by FXIIIa variants. These variations in substrates cross-linking could be important in EOC development and progression by modifying the tumour ECMs. Fibrin cross-linked by FXIIIa was found to be crucial for wound healing and solid tumour growth (Simpson-Haidaris and Rybarczyk, 2001). Through fibrin cross-linking, FXIII has been demonstrated to enhance metastasis by inhibiting natural killer (NK) cell-mediated removal of micro-metastatic tumour cells (Palumbo et al., 2008), which is also thought to act as a stimulator for stable adherence in the early stages of metastasis (Palumbo et al., 2002). This novel data implies that FXIIIa may have an essential role in the growth and dissemination of EOC and should be investigated further. As a result, further research, including FXIIIa genotype, local FXIIIa tumour expression levels, and tumour expression levels of e.g. fibrinogen,

fibronectin, vitronectin, and collagen-1 with larger sample sizes are important requirements to better understand the role of FXIIIa in EOC biology.

5.7 FXIIIa variants may influence EOC cell behaviour

The presence of the pure FXIIIa V34L protein variant in native and activated forms did not significantly affect EOC cell proliferation (Section 4.5.2). However, the DM variant showed a differential effect on EOC. While the DM protein in its native form has significantly inhibited EOC cell growth, the activated form had no effect on EOC proliferation. Interestingly, the activated V34L and DM variants have both significantly *decreased* EOC cell migration in cross-linked Matrigel matrices and in the growth medium (Section 4.5.3). Given the fact that the FXIIIa-mediated cross-linked matrix inhibits cell migration, it can be suggested that FXIIIa has a potential role in EOC progression. Furthermore, the implications of these SNPs, in terms of cell movement, would be useful in understanding how interactions within the TME would influence EOC development, dissemination and prognosis. However, the full impact of these SNPs has yet to be determined.

5.8 Limitations and future work

5.8.1 ICON7 cohort

One of the main limitations of this study is the plasma sample size (n=91), which represent only about 20.3 % of the ICON7 translational cohort (n=448). This limitation means that study findings should be interpreted cautiously. However, in spite of its relatively limited sample, this work offers valuable insight into the importance of the coagulation FXIIIa in EOC. However, more research with a larger cohort is needed to determine whether the novel association discovered in this cohort between *high* plasma FXIII activity and a significant benefit to survival in patients receiving bevacizumab can be replicated.

The ICON7 trial populations consisted primarily of Caucasian patients. Populations of Asian and African heritage were found to have different *F13A1* SNP allele frequencies and FXIII activity than Caucasians (Attíe-Castro et al., 2000, Saha et al., 2000). Further studies evaluating FXIIIa in EOC with diverse ethnic background participants could provide more worldwide impact.

FIGO staging was still widely used to determine EOC when the ICON7 trial was conducted. However, EOC is now considered as a heterogeneous group of disorders

that are distinguished not only by their molecular subtypes but also by the therapeutic response. Currently, high-grade serous ovarian cancer and low-grade serous ovarian cancer are considered the main two types of serous epithelial ovarian cancer. Exploring the significance of FXIII A within these more current classifications would undoubtedly be more clinically relevant, and some of this thesis's key limitations are the age of this cohort and the criteria used. Therefore, a prognostic variable was created by identifying patients from the study-cohort with serous histology and high-grade disease (Grade III) and named (SerousHighGrade), n=47 of the 91 patients.

Patients in the ICON7 study were randomly assigned to one of two therapy groups. It would be important to look at numerous clinical studies for other malignancies with different therapeutic regimens to see if FXIII activity could result in a beneficial response to therapy, as this study has demonstrated.

5.8.2 ICON7 tissue microarrays

This is the first study to report that FXIII A expression level in tumour tissue is significantly *lower* in high-grade EOC (Section 3.8.4). However, the main drawback was the limited number of slides available for staining to match the 91 plasma samples in the study group. This has influenced how the analysis was carried out (Section 3.8.1). Negative staining is generally defined as staining that is less than 1% of the tissue. However, due to small numbers, all cores with a percentage of FXIII A positive staining were included.

In the available formalin-fixed, paraffin-embedded tissue microarrays, staining for FXIII A protein revealed the greatest average percentage of positive results within the stroma cores, and the smallest number in tumour cores (Section 3.8.1). Since only one session of staining was supplied, the precise position of the staining could only be estimated. Considering the method used in tissue preparation to produce the tissue microarrays, the source of FXIII A appeared highly improbable to be blood plasma. FXIII A staining did not appear to be present in tumour cells. Other cells within the tumour stroma were found to have positive staining. There is a possibility that these cells might be tumours-associated macrophages or stromal cells. The absence of FXIII A staining within tumour cells, as well as the presence of staining in the stromal margins adjacent to tumour tissues, may support the findings of Turnock *et al.* (1990), which found that FXIII A was seen in the invasive margins of breast and colorectal carcinomas (Section 1.3.5.4). This indicates that FXIII A is possibly engaged in cross-talk between the tumour niche and the local microenvironment. Therefore, further IHC studies using specific markers (For instance, Immune cells:

Anti-Human CD68 antibody clone PG=M1; Fibroblast: Anti-human Smooth Muscle actin antibody clone 1A4) are required to identify the source of FXIII A within the EOC stroma. In addition, co-localisation tests using IF staining, or markers for FXIII B, which is considered as the carrier protein for the FXIII A dimer in the plasma, should be undertaken to determine the origin of the FXIII A staining in EOC.

5.8.3 EOC expression levels of FXIII A, fibrinogen, fibronectin, and vitronectin

The variations observed in cross-linking between FXIII A substrates (Section 4.3.3), as well as the functional differences between FXIII A variants in cross-linking matrix-associated proteins (Section 4.3.4), were interesting findings and necessitate further exploration. FXIII A may play a role in remodelling the EOC microenvironment by modifying its stiffness and structure. Therefore, as substrates for FXIII A, staining for these proteins in EOC tissues would have been useful to provide valuable insight into its potential role. The University of Leeds Research Tissue Bank (LRTB) cohort (n=129) of unfixed ovarian cancer frozen tissues was chosen to evaluate the expression levels of FXIII A, fibrinogen, fibronectin, and vitronectin. Tissues were cryo-sectioned at 7µm per section, at three sections per slide on SuperFrost Plus glass slides. An IHC staining protocol suitable for frozen sections was modified, with the fixation method optimised for 4% PFA and neat methanol. Workup for anti-FXIII A, anti-FGG, and anti-FN, and anti-VTN antibodies on OC frozen sections and healthy full-term frozen unfixed human placenta (as a control) was undertaken. IHC staining was performed, and all stained sections were scanned. However, due to time constraints, the raw data was not compiled and the final analysis was not performed. It would have been an extremely valuable piece of work, because it would have shed light on the levels and locality of these proteins and their contribution to the formation of the EOC matrix. As high plasma fibrinogen levels have been linked to cancer growth and dissemination (Vilar et al., 2020), examining the relationship between plasma levels and fibrinogen levels in tumour tissues could also lead to some very interesting results.

5.8.4 Growth, migration and invasion experiments

The assessment of OVCA cell proliferation in the presence of FXIIIa revealed exciting results, particularly for the FXIIIa DM variant (Section 4.5.2). This experiment is limited by the fact that it was only performed once. Due to difficulties with the purification of the FXIIIa protein, it was not possible to repeat these proliferation experiments. The migration experiments performed showed significant reduction of OVCA433 cell migration in the presence of activated purified FXIIIa protein (Section 4.5.3). Nevertheless, due to time restraints and limit in available imaging facilities, the number of experiments completed was restricted. These preliminary experiments showed potential new avenues for investigation around the role of FXIIIa in EOC. Production of more FXIIIa pure protein and repetition of the growth and migration studies would have been needed to confirm findings.

As the source of FXIIIa around the TME is unknown, i.e. intracellular or plasma, it will also be important to generate appropriate stable cell lines expressing FXIIIa protein to assess any influence from cellular FXIIIa. OVCA cell lines were genotyped for FXIIIa SNPs as a preliminary preparation step (Section 2.9.4). Attempts were made to generate stable cell lines expressing the GFP/RFP proteins by inserting two reporter plasmids into OVCA cell lines and the THP-1 monocytic cell line to gain distinctive images for these planned experiments:

- ❖ A: pIRES2-EGFP into OVCA cell lines.
- ❖ B: pIRES2-Ds-Red-Express into THP-1 monocytic cell line.

Work was started but was not completed due to time constraints. Plasmids were obtained, checked by restriction mapping, transformed into DH5-alpha cells, and plasmid mini-preps were made. A G418 antibiotic kill curve was performed to determine the minimum concentration required to kill all un-transfected cells in order to select transfected cells. For SKOV3 cells, it was found to be 800 µg/mL, and 200 µg/mL for the OVCA433 cell line. CHO-K1, Chinese hamster normal ovary cell line was identified and characterised (data not shown) to serve as a non-cancer cell control in these experiments.

The THP-1 monocyte cells could be differentiated into M2 macrophages and co-cultured with OVCA cells to see if FXIIIa is produced by the tumour-associated macrophages in the EOC microenvironment. Did this influence the cancer cells in anyway? It has been reported that inflammatory monocytes producing high quantities of FXIIIa create scaffolds by cross-linking fibrin, causing lung squamous carcinoma to spread (Porrello et al., 2018).

New three-dimensional (3D) culture models have been established to study the development, growth and dissemination of EOC (White et al., 2014). These models required optimisation of their physiological conditions as they do not have blood vessels or the cells which facilitate human adaptive immune response. Although they are restricted by the duration of their availability for experiments and dependence on human cells, some of these models will be useful in examining the influence of FXIIIa protein variants on EOC growth. A protocol and design for invasion experiments in a 3D culture model using spheroids were generated. The EOC spheroids will be formed using the hanging drops culture method or the ultra-low attachment 96-well plates (Costar Cat. No. 2007, Corning, USA). Following the formation, the spheroids' growth will be monitored by measuring the diameter every 24 hours to work out the best size to use for these experiments. A 3D ECM will then be created using Matrigel basement membrane matrix (Cat. No. 354248, Corning, USA) and collagen-1, and will be used to embed the formed spheroids. Different conditions could be tested using appropriate controls. It would be interesting to see if EOC spheroids could migrate and invade through native and cross-linked Matrigel and collagen-1 matrices. Furthermore, evaluating migration and invasion through fibrinogen and FXIIIa-mediated cross-linked fibrin could also be done to investigate the influence of the physical structure of the matrix on OVCA cell migration and invasion. As cancer cells produce plasmin (Duffy and O'Grady, 1984), it is possible that it plays a role in degradation of cross-linked fibrin and hence facilitates invasion and dissemination of OVCA cells, which could be assessed by examining the plasmin expression levels in invaders. Experiments were planned, but problems experienced with the FXIIIa protein expression have delayed this work, so it was not possible to complete these invasion and migration experiments.

5.9 Conclusions

This project has examined the role of FXIII in EOC. The findings from this study make several contributions to the current literature. This research has identified the level of FXIII activity in plasma as a predictive factor for EOC progression. This is the first study to report a significant association between *F13A1* 650I_651Q allele and *low* plasma FXIII activity in a clinical patient cohort, and to show that the DM variant (which represents this allele *in vitro*) significantly reduced OVCA433 cell proliferation. Elevated plasma FXIII activity has also emerged as a potential factor to influence the response to bevacizumab in addition to standard chemotherapy with a benefit for SPP. Plasma FXIII levels were found to be significantly low in SerousHighGrade tumours, and FXIII tissue expression was significantly lower in high-grade disease. This could explain that patients with low plasma FXIII activity have reduced SPP, as FXIII may have been consumed during modification of the TME or promoting angiogenic signalling leading to EOC progression.

Appendix I Text Map of pYF13_PCS 650I_651Q

The pYF13A_PCS 650I_651Q variant was used to produce this sequence. All pYF13A_PCS variants should be identical in sequence barring the mutations introduced within the F13A cDNA. This Text map was produced using the PlasMapper server (Dong et al., 2004) All unique sites for > 6 bp restriction enzyme cutters are shown. The *EcoRI*, *HindIII*, and *BamHI* sites are also shown since these enzymes were used for restriction analysis. The F13A Open reading frame, the thrombin cleavage site and the His tag are all indicated on this text map of the plasmid.

```
1      AAAAATCCGTAAGAAGTCAATTGTACGCCAACTTAAGACCATGTAACCTTGCATCCGA 60
      TTTTTAGGCATTTCTTGAAGTTAACATGCGGTTGAATCTGGTACATTGAAACGTAGGCT

61     CTCTCTTTTAGACTTATCTCCAATCAAGCCACAATTTGCTAAAGGTACTGACTTCGTTGT 120
      GAGAGAAAATCTGAATAGAGGTTAGTTCGGTGTTAAACGATTTCCATGACTGAAGCAACA

121    TGTCAGAGAATTAGTGGGAGGTATTTACTTTGGTAAGAGAAAAGGAAGACGATGGTGATGG 180
      ACAGTCTCTTAATCACCTCCATAAATGAAACCATTCTCTTCTTCTGCTACCACTACC

181    TGTCGCTTGGGATAGTGAACAATACACCGTTCAGAAAGTCAAAGAATCACAAGAATGGC 240
      ACAGCGAACCTATCACTTGTTATGTGGCAAGGTCTTCACGTTTCTTAGTGTCTTACCG

241    CGCTTTCATGGCCCTACAACATGAGCCACCATTGCCTATTTGGTCCTTGGATAAAGCTAA 300
      GCGAAAGTACCGGGATGTTGTACTCGGTGGTAACGGATAAACAGGAACCTATTTTCGATT

301    TGTTTTGGCCTCTTCAAGATTATGGAGAAAACTGTGGAGGAAACCATCAAGAACGAATT 360
      ACAAACCGGAGAAGTCTAATACCTCTTTTGGACACCTCCTTTGGTAGTTCTTGCTTAA

361    TCCTACATTGAAGGTTCAACATCAATTGATTGATTCGCGCCATGATCCTAGTTAAGAA 420
      AGGATGTAACCTCCAAGTTGTAGTTAACTAATAAGACGGCGGTACTAGGATCAATTTCT

421    CCCAACCCACCTAAATGGTATTATAATCACCAGCAACATGTTTGGTGATATCATCTCCGA 480
      GGGTTGGGTGGATTTACCATAATATTAGTGGTCGTTGTACAAACCCTATAGTAGAGGCT

481    TGAAGCCTCCGTTATCCCAGGTTCTTGGGTTTGTGGCCATCTGCGTCCTTGGCCTCTTT 540
      ACTTCGGAGGCAATAGGTTCCAAGGAACCCAAACAACGGTAGACGCAGGAACCGGAGAAA

541    GCCAGACAAGAACACCGCATTTGGTTTGTACGAACCATGCCACGGTCTGCTCCAGATTT 600
      CGGTCTGTCTTGTGGCGTAAACCAAACATGCTTGGTACGGTGCCAAGACGAGGTCTAAA

601    GCCAAAGAATAAGGTCAACCCTATCGCCACTATCTTGTCTGCTGCAATGATGTTGAAATT 660
      CGGTTTCTTATTCCAGTTGGGATAGCGGTGATAGAACAGACGACGTTACTACAACCTTAA

661    GTCATTGAACTTGCCCTGAAGAAGGTAAGGCCATTGAAGATGCAGTTAAAAAGGTTTTGGA 720
      CAGTAACCTGAACGGACTTCTTCCATTCCGGTAACTTCTACGTCAATTTTCCAAAACCT

721    TGCAGGTATCAGAAGTGGTGATTTAGGTGGTTCCAACAGTACCACCGAAGTCGGTGATGC 780
      ACGTCCATAGTCTTGACCACTAAATCCACCAAGGTTGTCATGGTGGCTTCAGCCACTACG

781    TGTCGCCGAAGAAGTTAAGAAAATCCTTGCTTAAAAAGATTCTCTTTTTTTATGATATTT 840
      ACAGCGGCTTCTTCAATTCTTTTAGGAACGAATTTTCTAAGAGAAAAAATACTATAAA

841    GTACATAAACTTTATAAATGAAATTCATAATAGAAACGACACGAAATTACAAAATGGAAT 900
      CATGTATTTGAAATATTTACTTTAAGTATTTATCTTTGCTGTGCTTTAATGTTTTACCTTA

901    ATGTTTCATAGGTTAGAATTAATTTCTCATGTTTACAGCTTATCATCGGATCGATCCAATA 960
      TACAAGTATCCCATCTTAATTAAGAGTACAAACTGTGCAATAGTAGCCTAGCTAGGTTAT
```

EcoRV

↓

961 TCAAAGGAAATGATAGCATTGAAGGATGAGACTAATCCAATTGAGGAGTGGCAGCATATA 1020
AGTTTCCTTTACTATCGTAACTTCCTACTCTGATTAGGTTAACTCCTCACCGTCGTATAT

1021 GAACAGCTAAAGGGTAGTGCTGAAGGAAGCATAACCGCATGGAATGGGATAATA 1080
CTTGTCGATTTCCCATCACGACTTCCTTCGTATGCTATGGGGCGTACCTTACCCTATTAT

|
RA7 Primer

2micron2 origin (1134,2298) >>>

1081 TCACAGGAGGTACTAGACTACCTTTTCATCCTACATAAAATAGACGCATATAAGTACGCATT 1140
AGTGTCCCTCCATGATCTGATGGAAAGTAGGATGATTTATCTGCGTATATTCATGCGTAA

1141 TAAGCATAAACACGCACTATGCCGTTCTTCTCATGTATATATATACAGGCAACACGCA 1200
ATTTCGTATTTGTGCGTGATACGGCAAGAAGAGTACATATATATATATGTCCGTTGTGCGT

1201 GATATAGGTGCGACGTGAACAGTGAGCTGTATGTGCGCAGCTCGCGTTGCATTTTCGGAA 1260
CTATATCCACGCTGCACCTGTCTACTCGACATACACGCGTCGAGCGCAACGTAAAAGCCTT

1261 GCGCTCGTTTTTCGGAAACGCTTTGAAGTTCCTATTCCGAAGTTCCTATTCTCTAGCTAGA 1320
CGCGAGCAAAAAGCCTTTGCGAAACTTCAAGGATAAGGCTTCAAGGATAAGAGATCGATCT

1321 AAGTATAGGAACTTCAGAGCGCTTTTGAAAACAAAAGCGCTCTGAAGACGCACCTTCAA 1380
TTCATATCCTTGAAGTCTCGCGAAAACCTTTGGTTTTTCGCGAGACTTCTGCGTGAAAGTT

1381 AAAACAAAAACGCACCGACTGTAACGAGCTACTAAAATATTGCGAATACCGCTTCCAC 1440
TTTTGGTTTTTTCGCTGGCCTGACATTGCTCGATGATTTTATAACGCTTATGGCGAAGGTG

1441 AAACATTGCTCAAAAGTATCTCTTTGCTATATATCTCTGTGCTATATCCCTATATAACCT 1500
TTTTGTAACGAGTTTTTCATAGAGAAACGATATATAGAGACACGATATAGGGATATATTGGA

1501 ACCCATCCACCTTTTCGCTCCTTGAACCTGCATCTAAACTCGACCTCTACATTTTTTATGT 1560
TGGGTAGGTGGAAAGCGAGGAACCTGAACGTAGATTTGAGCTGGAGATGTAATAAATACA

1561 TTATCTCTAGTATTACTCTTTAGACAAAAAATTGTAGTAAGAACTATTCATAGAGTGAA 1620
AATAGAGATCATAATGAGAAATCTGTTTTTTAACATCATCTTTGATAAGTATCTCACTT

1621 TCGAAAAAATACGAAAAATGTAACATTTCTTATACGTAGTATATAGAGACAAAAATAGAA 1680
AGCTTTTGTATGCTTTTACATTTGTAAAGGATATGCATCATATATCTCTGTTTTATCTT

1681 GAAACCGTTTATAATTTTCTGACCAATGAAGAATCATCAACGCTATCACTTTCTGTTTAC 1740
CTTTGGCAAGTATTTAAAAGACTGGTTACTTCTTAGTAGTTGCGATAGTAAAAGACAAGTG

|
RA5 Primer

1741 AAAGTATGCGCAATCCACATCGGTATAGAATATAATCGGGGATGCCTTTATCTTGAAAAA 1800
TTTCATACGCGTTAGGTGTAGCCATATCTTATATTAGCCCTACGAAAATAGAACTTTTT

1801 ATGCACCCGAGCTTCGCTAGTAATCAGTAAACGCGGGAAGTGGAGTCAGGCTTTTTTTTA 1860
TACGTGGGCGTCGAAGCGATCATTAGTCAATTTGCGCCCTTCACCTCAGTCCGAAAAAAT

1861 TGGAAGAGAAAATAGACACCAAAGTAGCCTTCTTCTAACCTTAACGGACCTACAGTGCAA 1920
ACCTTCTCTTTTATCTGTGGTTTCATCGGAAGAAGATTGGAATTGCCTGGATGTCACGTT

1921 AAAGTTATCAAGAGACTGCATTATAGAGCGCACAAAGGAGAAAAAAGTAATCTAAGATG 1980
TTTCAATAGTTCTCTGACGTAATATCTCGCGTGTTCCTCTTTTTTTTTCATTAGATTCTAC

1981 CTTTGTAGAAAAATAGCGCTCTCGGGATGCATTTTTGTAGAACAAAAAGAAGTATAGA 2040
GAAACAATCTTTTTATCGCGAGAGCCCTACGTAAAACATCTGTTTTTTCTTCATATCT

2041 TTCTTTGTTGGTAAAAATAGCGCTCTCGCGTTGCATTTCTGTTCTGTAAAAATGCAGCTCA 2100
AAGAAACAACCATTTTTATCGCGAGAGCGCAACGTAAAGACAAGACATTTTTACGTCGAGT

2101 GATTCTTTGTTTGA AAAATAGCGCTCTCGCGTTGCATTTTTGTTTTTACAAAAATGAAGC 2160
CTAAGAAAACAACTTTTTAATCGCGAGAGCGCAACGTAAAACAAAATGTTTTTACTTCG

2161 ACAGATTCTTCGTTGGTAAAAATAGCGCTTTTCGCGTTGCATTTCTGTTCTGTAAAAATGCA 2220
TGTCTAAGAAGCAACCATTTTTATCGCGAAAAGCGCAACGTAAAGACAAGACATTTTTACGT

2221 GCTCAGATTCTTTGTTTGAAAAATTAGCGCTCTCGCGTTGCATTTTTGTTCTACAAAATG 2280
CGAGTCTAAGAAACAACTTTTTAATCGCGAGAGCGCAACGTAAAAACAAGATGTTTTAC

HpaI
|

2281 AAGCACAGATGCTTCGTTAACAAAGATATGCTATTGAAGTGCAAGATGGAAACGCAGAAA 2340
TTCGTGTCTACGAAGCAATTGTTTCTATACGATAACTTCAGTTCTACCTTTGCGTCTTT

2341 ATGAACCGGGGATGCGACGTGCAAGATTACCTATGCAATAGATGCAATAGTTTCTCCAGG 2400
TACTTGGCCCCACGCTGCACGTTCTAATGGATACGTTATCTACGTTATCAAAGAGGTCC

2401 AACCGAAATACATACATTGTCTTCCGTAAAGCGCTAGACTATATATTATTATACAGGTTT 2460
TTGGCTTTATGTATGTAAACAGAAGGCATTTCGCGATCTGATATATAATAATATGTCCAAG

2461 AAATATACTATCTGTTTCAGGGAAAACCTCCAGGTTCCGGATGTTCAAAAATCAATGATGG 2520
TTTATATGATAGACAAAGTCCCTTTTGAGGGTCCAAGCCTACAAGTTTTAAGTTACTACC

2521 GTAACAAGTACGATCCGATAAATGCGGTGTGAAATACCGCACAGATGCGTAAGGAGAAAA 2580
CATTGTTTATGCTAGGCTATTTACGCCACACTTTATGGCGTGTCTACGCATTCCTCTTTT

lacZ_a reporter (2595, 2754) <<<
|
NarI
| |

2581 TACCGCATCAGGCGCCATTCGCCATTTCAGGCTGCGCAACTGTTGGGAAGGGCGATCGGTG 2640
ATGGCGTAGTCCGCGGTAAGCGGTAAGTCCGACGCGTTGACAACCCTTCCCGCTAGCCAC

2641 CGGGCCTCTTCGCTATTACGCCAGCTGGCGAAAGGGGGATGTGCTGCAAGGCGATTAAGT 2700
GCCCCGAGAAGCGATAAATGCGGTCG**ACCGCTTCCCCCTACACGA**CGTTCGCTAATTCA

|
RA3 Primer

2701 TGGGTAAACGCCAGGGTTTTCCAGTCACGACGTTGTAAAACGACGGCCAGTGAATTCCTT 2760
ACCCATTGCGGTCCCAAAAGGGTCAGTGTGCAACATTTTGCTGCCGCTCACTTAAGGAA

2761 GAATTTTCAAAAATTCCTTACTTTTTTTTTGGATGGACGCAAAGAAAGTTTAAATAATCATAT 2820
CTTAAAAGTTTTTAAGAATGAAAAAAAACCTACCTGCGTTTCTTCAAATATTAGTATA

2821 TACATGGCATTACCACATATACATATCCATATACATATCCATATCTAATCTTACTTATA 2880
ATGTACCATAATGGTGGTATATGTATAGGTATATGTATAGGTATAGATTAGAATGAATAT

2881 TGTTGTGAAAATGTAAAGAGCCCCATTATCTTAGCCTAAAAAACCTTCTCTTTGGAAC 2940
ACAACACCTTTACATTTCTCGGGTAATAGAATCGGATTTTTTTGGAAGAGAAACCTTGA

GAL1 prom (2980, 3430) >>>
|

2941 TTCAGTAATACGCTTAACTGCTCATTGCTATATTGAAGT**A**CGGATTAGAAGCCGCCGAGC 3000
AAGTCATTATGCGAATTGACGAGTAACGATATAACTTCATGCCTAATCTTCGGCGGCTCG

3001 GGGTGACAGCCCTCCGAAGGAAGACTCTCCTCCGTGCGTCTCTCGTCTTACCAGGTCGCGT 3060
CCCCTGTCGGGAGGCTTCTTCTGAGAGGAGGCACGCAGGAGCAGAAGTGCCAGCGCA

3061 TCCTGAAACGCAGATGTGCCTCGCGCCGCACTGCTCCGAACAATAAAGATTCTACAATAC 3120
AGGACTTTGCGTCTACACGGAGCGGGCTGACGAGGCTTGTATTCTAAGATGTTATG

3121 TAGCTTTTATGGTTATGAAGAGGAAAAATTGGCAGTAACCTGGCCCCACAAACCTTCAA 3180
ATCGAAAATACCAATACTTCTCCTTTTTAACCGTCATTGGACCGGGGTGTTTGAAGTTT

3181 TGAACGAATCAAATTAACAACCATAGGATGATAATGCGATTAGTTTTTTAGCCTTATTTT 3240
ACTTGGCTTAGTTTAATTGTTGGTATCCTACTATTACGCTAATCAAAAAATCGGAATAAAG

3241 TGGGGTAATTAATCAGCGAAGCGATGATTTTTGATCTATTAACAGATATATAAATGCAAA 3300
ACCCCATTAATTAGTCGCTTCGCTACTAAAACCTAGATAATTGTCTATATATTTACGTTT

3301 AACTGCATAACCACTTTAACTAATACTTTCAACATTTTCGGTTTGTATTACTTCTTATTC 3360

TTGACGTATTGGTGAAATGATTATGAAAGTTGTAAGCCAAACATAATGAAGAATAAG

3361 AAATGTAATAAAAGTATCAACAAAAAATTGTTAATATACCTCTATACTTTAACGTCAAGG 3420
 TTTACATTATTTTCATAGTTGTTTTTAAACAATTATATGGAGATATGAAATGCAGTTC

ORF 1 rf(1) (3475,5703)>>>

BamH1 | XbaI | AccI | PstI | **Alii primer** |
 | | | | |

3421 AGAAAAACCCC**GGATCC**TCTAGAGTCGACCTGCAGGACCTTGTAA**AAGTCAAAAATGTCA** 3480
 TCTTTTTTGGGGCCTAGGAGATCTCAGCTGGACGTCTTGGAAACATTTTCAGTTTTTACAGT

3481 **GAAACTTC**AGGACCGCCTTTGGAGGCAGAAGAGCAGTTCACCCAATAACTCTAATGCA 3540
 CTTTGAAGGTCTTGGCGGA**AACCTCCGCTTCTCGTCAAG**GTGGGTTATTGAGATTACGT

|
RA2 Primer

SmaI
 |
AA 34 XmaI
 | |

3541 GCGGAAGATGACCTGCCACAGTGGAGCTTCAGGGC**GTG**GTGCCCCGGGGCGTCAACCTG 3600
 CGCCTTCTACTGGACGGGTGTCACCTCGAAGTCCCG**CAC**CACGGGGCCCGCAGTTGGAC

3601 CAAGAGTTTCTTAATGTACAGGCGTTACCTGTTCAAGGAGAGATGGGACACTAACAAG 3660
 GTTCTCAAAGAATTACAGTGCTCGCAAGTGGACAAGTTCTCTTACCCTGTGATTGTTCT

3661 GTGGACCACCACACTGACAAGTATGAAAACAACAAGCTGATTGTCCGCAGAGGGCAGTCT 3720
 CACCTGGTGGTGTGACTGTTTACACTTTTGTGTTTCGACTAACAGGCGTCTCCCGTCAGA

NdeI
 |

3721 TTCTATGTGCAGATTGACTTCAGTCGTCCATATGACCCCAAGGGATCTTTCAGGGTG 3780
 AAGATACAGTCTAACTGAAGTCAGCAGGTATACTGGGGTCTTCCCTAGAGAAGTCCCAC

3781 GAATACGTCATTGGTTCGTACCCACAGGAGAACAAGGGAACTACATCCCAGTGCCTATA 3840
 CTTATGCAGTAACCAGCGATGGGTGTCCTTGTTCCTTGGATGTAGGGTACCGGATAT

3841 GTCTCAGAGTTACAAAGTGGAAAGTGGGGGGCAAGATTGTCATGAGAGAGGACAGGTCT 3900
 CAGAGTCTCAATGTTTACCTTTACCCCGGTTCTAACAGTACTCTCTCCTGTCCAGA

3901 GTGCGGTGTCCATCCAGTCTTCCCCAAATGTATTGTGGGGAAATTCCGCATGTATGTT 3960
 CACGCCGACAGGTAGGTGAGAAGGGGGTTACATAACACCCCTTTAAGGCGTACATACAA

B1 Primer
 |

3961 GCTGTCTGGACTCCCTATGGCGTACTTCC**AACCAGTCGAAACCCAGAAACAGA**CACGTAC 4020
 CGACAGACCTGAGGGATACCGCATGAAGCTTGGTCAGCTTTGGGTCTTTGTCTGTGCATG

AA 204
 |

4021 ATTCTCTCAATCCTTGGTGTGAAGATGATGCTGTG**TAT**CTGGACAATGAGAAAGAAAGA 4080
 TAAGAGAAGTTAGGAACCACTTCTACTACGACAC**ATA**GACCTGTTACTCTTTCTTTCT

4081 GAAGAGTATGTCCTGAATGACATCGGGGTAATTTTTTATGGAGAGGTCAATGACATCAAG 4140
 CTTCTCATAAGGACTTACTGTAGCCCATTAATAAATACTCTCCAGTTACT**TGTAGTTC**

4141 ACCAGAAGCTGGAGCTATGGTCAGTTTGAAGATGGCATCCTGGACACTTGCCTGTATGTG 4200
TGGTCTTCGACCTCGATACCAGTCAAACCTTCTACCGTAGGACCTGTGAACGGACATACAC

|
A2 Primer

4201 ATGGACAGAGCACAAATGGACCTCTCTGGAAGAGGGAAATCCCATCAAAGTCAGCCGTGTG 4260
 TACCTGTCTCGTGTTTACCTGGAGAGACCTTCTCCCTTAGGGTAGTTTCAGTCGGCACAC

4261 GGGTCTGCAATGGTGAATGCCAAAGATGACGAAGGTGTCCTCGTTGGATCCTGGGACAAT 4320
CCCAGACGTTACCACTTACGGTTTTCTACTGCTTCCACAGGAGCAACCTAGGACCCTGTTA

4321 ATCTATGCCTATGGCGTCCCCCATCGGCCTGGACTGGAAGCGTTGACATTCTATTGGAA 4380
TAGATACGGATACCGCAGGGGGTAGCCGACCTGACCTTCGCAACTGTAAGATAACCTT

SacI
|

4381 TACCGGAGCTCTGAGAATCCAGTCCGGTATGGCCAATGCTGGGTTTTTGTGGTGTCTTT 4440
ATGGCCTCGAGACTCTTAGGTCAGGCCATACCGTTACGACCCAAAAACGACCACAGAAA

4441 AACACATTTTTACGATGCCTTGAATACCCGCAAGAATGTTACCAATTATTTCTCTGCC 4500
TTGTGTAATAATGCTACGGAACCTTATGGCGTCTTAACAATGGTTAATAAAGAGACGG

C1 Primer
|

4501 CATGATAATGATGCCAATTTGCAAATGGACATCTTCTGGAAGAAGATGGGAACGTGAAT 4560
GTACTATTACTACGGTTAAACGTTTACCCTGTAGAAAGGACCTTCTTCTACCTTGCACCTTA

4561 TCCAAACTCACCAAGGATTCAGTGTGGAATACCACCTGCTGGAATGAAGCATGGATGACA 4620
AGGTTTGAGTGGTTCCTAAGTCACACCTTGATGGTGACGACCTTACTTCGTACCTACTGT

StuI
|

4621 AGGCCTGACCTTCTGTGGATTTGGAGGCTGGCAAGCTGTGGACAGCACCCCCCAGGAA 4680
TCCGGACTGGAAGGACAACCTAAACCTCCGACCGTTCGACACCTGTCGTGGGGGGTCTTT

B2 Primer
|

4681 AATAGCGATGGCATGTATCGGTGTGGCCCCGCTCGGTTCAAGCCATCAAGCACGGCCAT 4740
TTATCGCTACCGTACATAGCCACACCGGGGGGAGCCAAGTTCGGTAGTTCGTGCCGGTA

4741 GTCTGCTTCCAATTTGATGCACCTTTTGTTTTTGCAGAGGTCAACAGCGACCTCATTTAC 4800
CAGACGAAGGTTAAACTACGTGGAAAACAAAAACGTCTCCAGTTGTCTCGTGGAGTAAATG

4801 ATTACAGCTAAGAAAGATGGCACTCATGTGGTGGAAAATGTGGATGCCACCCACATTGGG 4860
TAATGTCGATTCTTTCTACCGTGAGTACACCACCTTTTACACCTACGGTGGGTGTAACCC

4861 AAATTAATTGTGACCAAACAAATTGGAGGAGATGGCATGATGGATATTACTGATACTTAC 4920
TTTTAATTAACACTGGTTTGTTTAACCTCCTCTACCGTACTACCTATAATGACTATGAATG

4921 AAATTCAGAAGGTCAAGAAGAAGAGATTGGCCCTAGAAACTGCCCTGATGTACGGA 4980
TTTTAAGTTCTTCCAGTCTTCTTCTCTAACC GGATCTTTGACGGGACTACATGCCT

D1 Primer
|

4981 GCTAAAAAGCCCCTCAACACAGAAGGTGTCATGAAATCAAGGTCCAACGTTGACATGGAC 5040
CGATTTTTCGGGGAGTTGTGTCTTCCACAGTACTTTAGTTCAGGTTGCAACTGTACCTG

5041 TTTGAAGTGGAAAATGCTGTGCTGGGAAAAGACTTCAAGCTCTCCATCACCTTCCGGAAC 5100
AAACTTACCTTTTACGACACGACCCTTTCTGAAGTTCGAGAGGTAGTGAAGGCCTTG

5101 AACAGCCACAACCGTTACACCATCACAGCTTATCTCTCAGCCAACATCACCTTCTACACC 5160
TTGTCGGTGTGGCAATGTGGTAGTGTGCAATAGAGAGTCGGTTGTAGTGAAGATGTGG

AA 564
|

5161 GGGGTCCCGAAGGCAGAATTCAGAAGGAGACGTTTCGACGTGACGCTGGAGCCCTTGTCC 5220
CCCCAGGGCTTCCGCTTAAGTTCTTCCTCTGCAAGCTGCACTGCGACCTCGGGAACAGG

C2 Primer
|

5221 TTCAAGAAAGAGGGCGGTGCTGATCCAAGCCGGCGAGTACATGGGTGACGTGCTGGAACAA 5280
AAGTTCTTTCTCCGCCACGACTAGGTTCCGGCCGCTCATGTACCCAGTCGACGACCTTGT

5281 GCGTCCCTGCACTTCTTTGTGCACAGCTCGCATCAATGAGACCAGGGATGTTCTGGCCAAG 5340
CGCAGGGACGTGAAGAAACAGTGTGCGAGCGTAGTTACTCTGGTCCCTACAAGACCGGTTTC

5341 CAAAAGTCCACCGTGCCTAACCATCCCTGAGATCATCATCAAGGTCCGTGGCACTCAGGTA 5400
GTTTTCAGGTGGCAGGATTTGGTAGGGACTCTAGTAGTAGTTCCAGGCACCGTGAGTCCAT

Codon 650/651

5401 GTTGGTTCGACATGACTGTGACAA**ATTCAG**TTTACCAATCCTTTAAAAGAAACCTGCGA 5460
CAACCAAGACTGTACTGACACTGT**TAAGTC**AAATGGTTAGGAAATTTCTTTGGGACGCT

5461 AATGTCTGGGTACACCTGGATGGTCCCTGGAGTAACAAGACCAATGAAGAAGATGTTCCGT 5520
TTACAGACCCATGTGGACCTACCAGGACCTCATTGTTCTGGTTACTTCTCTACAAGGCA

5521 GAAATCCGGCCCAACTCCACCGTGCAGTGGGAAGAAGTGTCCGGCCCTGGGTCTCTGGG 5580
CTTTAGCCGGGTTGAGGTGGCAGGTCACCCCTCTTCACACGGCCGGGACCCAGAGACCC

5581 CATCGGAAGCTGATAGCCAGCATGAGCAGTGACTCCCTGAGACATGTGTATGGCGAGCTG 5640
GTAGCCTTCGACTATCGGTCGTACTCGTCACTGAGGGACTCTGTACACATACCGCTCGAC

Thrombin Cleavage site

His Tag

5641 GACGTGCAGATTCAAAGACGACCTTCCATG**ATCGAGGGCCGG****CATCACCATCACCATCAC** 5700
CTGCACGTCTAAGTTTCTGCTGGAAGGTACTAGCTCCCGGCCGTAGTGGTAGTGGTAGTG

HindIII

5701 **TAA**GCCTGGCGTAATCATGGTCATAGCTGTTTCTGTGTGAAATTGTTATCCGCTCACAA 5760
ATTGCAACCGCATTAGTACCAGTATCGACAAAGGACACACTTTAACAATAGCGAGTGT

lac prom(5769,5798)<<<

5761 TTCCACACAACATAACGAGCCGGAAGCATAAAGTGTAAAGCCTGGGGTGCCTAATGAGTGA 5820
AAGGTGTGTTGTATGCTCGGCCTTCGTATTTACATTTTCGGACCCACGGATTACTCACT

RA1 Primer

5821 GCTAACTCACATTAATTGCGTTGCGCTCACTGCCCGCTTTCCAG**TCGGGAAACCTGTCGT** 5880
CGATTGAGTGTAATTAACGCAACGCGAGTGACGGGCGAAAGGTGAGCCCTTTGGACAGCA

5881 **GCCA**GCTGCATTAATGAATCGGCCAACGCGCGGGGAGAGCGGTTTGCCTATTGGGCGCT 5940
CGGTCGACGTAATTACTTAGCCGGTTGCGCGCCCTCTCCGCCAAACGCATAAACC CGA

5941 CTTCCGCTTCTCGCTCACTGACTCGCTGCGCTCGGTCGTTTCGGCTGCGGCGAGCGGTAT 6000
GAAGGCGAAGGAGCGAGTGACTGAGCGACGCGAGCCAGCAAGCCGACGCGCTCGCCATA

6001 CAGCTCACTCAAAGGCGTAATACGGTTATCCACAGAATCAGGGGATAACGCAGGAAAGA 6060
GTCGAGTGAGTTTCCGCCATTATGCCAATAGGTGTCTTAGTCCCCTATTGCGTCCTTTCT

pBR322 origin(6107,6726)<<<

6061 ACATGTGAGCAAAAGGCCAGCAAAAGGCCAGGAACCGTAAAAAGGC**CGC**GTTGCTGGCGT 6120
TGTACACTCGTTTTCCGGTCGTTTTCCGGTCCTTGGCATTTCCTCCGGCGCAACGACCGCA

6121 TTTTCCATAGGCTCCGCCCCCTGACGAGCATCACAAAAATCGACGCTCAAGTCAGAGGT 6180
AAAAGGTATCCGAGGCGGGGGACTGCTCGTAGTGTTTTTAGCTGCGAGTTCAGTCTCCA

6181 GGCGAAACCCGACAGGACTATAAAGATAACCAGGCGTTTCCCCTGGAAGCTCCCTCGTGC 6240

CCGCTTTGGGCTGTCCTGATATTTCTATGGTCCGCAAAGGGGGACCTTCGAGGGAGCACG

6241 GCTCTCCTGTTCCGACCCTGCCGCTTACCGGATACCTGTCCGCTTTTCTCCCTTCGGGAA 6300
CGAGAGGACAAGGCTGGGACGGCGAATGGCTATGGACAGGCGGAAAGAGGGAAGCCCTT

6301 GCGTGGCGCTTTCTCATAGCTCACGCTGTAGGTATCTCAGTTCGGTGTAGGTTCGTTTCGCT 6360
CGCACCGCGAAAGAGTATCGAGTGCACATCCATAGAGTCAAGCCACATCCAGCAAGCGA

6361 CCAAGCTGGGCTGTGTGCACGAACCCCCGTTTCAGCCCGACCGCTGCGCCTTATCCGGTA 6420
GGTTCGACCCGACACAGTGTGGGGGGCAAGTCCGGCTGGCGACGCGGAATAGGCCAT

6421 ACTATCGTCTTGAGTCCAACCCGGTAAGACAGACTTATCGCCACTGGCAGCAGCCACTG 6480
TGATAGCAGAACTCAGGTGGGCCATTCTGTGCTGAATAGCGGTGACCGTCGTCCGGTAC

6481 GTAACAGGATTAGCAGAGCGAGGTATGTAGGCGGTGCTACAGAGTCTTGAAGTGGTGGC 6540
CATTTGCTTAATCGTCTCGCTCCATACATCCGCCACGATGTCTCAAGAACTTACCACCG

6541 CTAACTACGGCTACACTAGAAGAACAGTATTTGGTATCTGCGCTCTGCTGAAGCCAGTTA 6600
GATTGATGCCGATGTGATCTTCTTGTCAAAACCATAGACGCGAGACGACTTCGGTCAAT

6601 CCTTCGAAAAAGAGTTGGTAGCTCTTGATCCGGCAAACAAACCACCGCTGGTAGCGGTG 6660
GGAAGCCTTTTTCTCAACCATCGAGAACTAGGCCGTTTGTGGTGGCGACCATCGCCAC

6661 GTTTTTTTGTTTGCAAGCAGCAGATTACGCGCAGAAAAAAGGATCTCAAGAAGATCCTT 6720
CAAAAAACAAACGTTTCGTCTAATGCGCGTCTTTTTTCTTAGAGTCTTCTAGGAA

6721 TGATCTTTTCTACGGGTCTGACGCTCAGTGGAAACGAAACTCACGT**TAAGGGATTTTGG** 6780
ACTAGAAAAGATGCCCCAGACTGCGAGTACCTTGCTTTTGAGTGAATTCCTTAAACC

6781 **TCATGAGA**TTATCAAAAAGGATCTTACCTAGATCCTTTTAAATTAATAAATGAAGTTTA 6840
AGTACTCTAATAGTTTTTCTAGAAAGTGGATCTAGGAAAATTTAATTTTACTTCAAAT

ORF_2 rf(4) (6881,7741) <<<
|
amp marker (6881,7741) <<<
|

6841 AATCAATCTAAAGTATATATAGATAAACTTGGTCTGACAGT**T**TACCAATGCTTAATCAGTG 6900
TTAGTTAGATTTTATATATACTCATTTGAACCAGACTGTCAATGGTTACGAATTAGTCAC

6901 AGGCACCTATCTCAGCATCTGTCTATTTTCGTTTCATCCATAGTTGCCAGCTCCCGTCG 6960
TCCGTGGATAGAGTCGCTAGACAGATAAAGCAAGTAGGTATCAACGGACTGAGGGGCAGC

6961 TGTAGATAACTACGATACGGGAGGGCTTACCATCTGGCCCAAGTGTGCAATGATACCGC 7020
ACATCTATTGATGCTATGCCCTCCCGAATGGTAGACCGGGGTACGACGTTACTATGGCG

7021 GAGACCCACGCTCACCAGCTCCAGATTTATCAGCAATAAACCAGCCAGCCGGAAGGGCCG 7080
CTCTGGGTGCGAGTGGCCGAGGTCTAAATAGTCTGTTATTTGGTTCGGTTCGGCCTTCCCGGC

7081 AGCGCAGAAGTGGTCTGCAACTTTATCCGCTCCATCCAGTCTATTAATTTGTTGCCGGG 7140
TCGCGTCTTACCAGGACGTTGAAATAGCGGAGGTAGGTGAGATAATTAACAACGGCCC

7141 AAGCTAGAGTAAGTAGTTCCGCCAGTTAATAGTTTTCGCAACGTTGTTGCCATTGCTACAG 7200
TTCGATCTCATTTCATCAAGCGGTCAATTATCAAACGCGTTGCAACAACGGTAACGATGTC

7201 GCATCGTGGTGTACGCTCGTCTGTTTGGTATGGCTTCATTCAGCTCCGGTTCCCAACGAT 7260
CGTAGCACCACAGTGCAGCAGCAAACCATAACGAAGTAAAGTCGAGGCCAAGGGTTGCTA

7261 CAAGGCGAGTTACATGATCCCCATGTTGTGCAAAAAAGCGGTTAGCTCCTTCGGTCTC 7320
GTTCCGCTCAATGTACTAGGGGGTACAACAGTTTTTTTCGCCAATCGAGGAAGCCAGGAG

7321 CGATCGTTGTGAGAAGTAAGTTGGCCGAGTGTATCACTCATGGTTATGGCAGCACTGC 7380
GCTAGCAACAGTCTTCAATCAACCGGCGTACAATAGTGAAGTACCAATACCGTCTGTGACG

7381 ATAATTCTTACTGTATGCCATCCGTAAGATGCTTTTCTGTGACTGGTGAAGTACTCAA 7440
TATTAAGAGAATGACAGTACGGTAGGCATTTACGAAAAGACACTGACCACTCATGAGTT

7441 CCAAGTCATTCTGAGAATAGTGTATGCGGCGACCGAGTTGCTCTTGCCCGCGTCAATAC 7500
GGTTCAGTAAGACTCTTATCACATACGCCGCTGGCTCAACGAGAACGGGCCGAGTTATG

7501 GGGATAATACCGGCCACATAGCAGAACTTTAAAAGTGCTCATCATTGGAAAACGTTCTT 7560
CCCTATTATGGCGCGGTGTATCGTCTTGAATTTTTCACGAGTAGTAACCTTTTGAAGAA

RA6 Primer

7561 CGGGGCGAAAACCTCTCAAGGATCTTACCCTGTTGAGAT**TCCAGTTCGATGTAACCCACTC** 7620
GCCCCGCTTTTGGAGTTCTTAGAATGGCGACAACCTCTAGGTCAAGCTACATTGGGTGAG

7621 GTGCACCCAACCTGATCTTCAGCATCTTTTACTTTACCAGCGTTTCTGGGTGAGCAAAAA 7680
CACGTGGGTGACTAGAAAGTCGTAGAAAAATGAAAGTGGTCGCAAAGACCCACTCGTTTTT

7681 CAGGAAGGCAAAATGCCGCAAAAAAGGAATAAGGGCGACACGGAAATGTTGAATACTCA 7740
GTCCTTCCGTTTTACGGCGTTTTTCCCTTATTCCCGCTGTGCCTTTACAACCTTATGAGT

amp prom(7783,7811) <<<

7741 TACTCTTCCTTTTTCAATATTATTGAAGCATTATCAGGGTT**A**TTGTCTCATGAGCGGAT 7800
ATGAGAAGGAAAAAGTTATAATAACTTCGTAAATAGTCCCAATAACAGAGTACTCGCCTA

7801 ACATATTTGAATGTATTTAGAAAAATAAACAAATAGGGGTTCCGCGCACATTTCCCCGAA 7860
TGTATAAACTTACATAAACTTTTTTATTTGTTTATCCCAAGGCGCGTGTAAAGGGGCTT

7861 AAGTGCCACCTGACGTCTAAGAAACCATTATTATCATGACATTAACCTATAAAAAATAGGC 7920
TTCACGGTGGACTGCAGATTCTTTGGTAATAATAGTACTGTAATTGGATATTTTTATCCG

7921 GTATCACGAGGCCCTTTCGTCTTCAAGAATTAAGTGTGGGAATACTCAGGTATCGTAAGA 7980
CATAGTGCTCCGGGAAAGCAGAAGTTCTTAATTGACACCCTTATGAGTCCATAGCATTCT

7981 TGCAAGAGTTCGAATCTCTTAGCAACCATTATTTTTTCTCAACATAACGAGAACACAC 8040
ACGTTCTCAAGCTTAGAGAATCGTTGGTAATAAAAAAAGGAGTTGTATTGCTCTTGTGTG

8041 AGGGGCGCTATCGCACAGAATCAAATTCGATGACTGGAATTTTTTGTAAATTCAGAGG 8100
TCCCCGCGATAGCGTGTCTTAGTTAAGTACTGACCTTAAAAAACAAATTAAGTCTCC

8101 TCGCCTGACGCATATAACCTTTTTCAACTGAAAAATGGGAGAAAAAGGAAAGGTGAGAGC 8160
AGCGGACTGCGTATATGGAAAAAGTTGACTTTTTTAACCTCTTTTTCTTTCCACTCTCG

8161 GCCGGAACCGGCTTTTCATATAGAATAGAGAAGCGTTCATGACTAAATGCTTGCATCACA 8220
CGGCTTGGCCGAAAAGTATATCTTATCTCTTCGCAAGTACTGATTTACGAACGTAGTGT

8221 ATACTGAAGTTGACAATATTATTTAAGGACCTATTGTTTTTCCAATAGGTGGTTAGCA 8280
TATGAACTTCAACTGTTATAATAAATTCCTGGATAACAAAAAAGGTTATCCACCAATCGT

8281 ATCGTCTACTTTCTAACTTTTCTTACCTTTTACATTTACGCAATATATATATATATTTT 8340
TAGCAGAATGAAAGATTGAAAAGAATGAAAATGTAAAGTCGTTATATATATATATAAAG

8341 AAGGATATAACCATTCTAATGTCTGCCCTAAGAAGATCGTCGTTTTGCCAGGTGACCAGC 8400
TTCTTATATGGTAAGATTACAGACGGGATTCTTCTAGCAGCAAAACGGTCCACTGGTGC

8401 TTGGTCAAGAAATCACAGCCGAAGCCATTAAGGTTCTTAAAGCTATTTCTGATGTTTCGTT 8460
AACCAGTTCTTTAGTGTGGGCTTCGGTAATTCCAAGAATTCGATAAAGACTACAAGCAA

RA8 Primer

8461 CCAATGTCAAGTTCGATTTTCGAAAATCATTTAATTGGT**GGTGCTGCTATCGATGCTAC**AG 8520
GGTTACAGTTCAAGCTAAAGCTTTTAGTAAATTAACCACCACGACGATAGCTACGATGTC

8521 GTGTTCCACTTCCAGATGAGGCGCTGGAAGCCTCCAAGAAGGCTGATGCCGTTTTGTTAG 8580
CACAAGGTGAAGGTCTACTCCGCGACCTTCGGAGGTTCTTCCGACTACGGCAAAACAATC

8581 GTGCTGTGGGTGGTCCCTAAATGGGGTACAGGTAGTGTAGACCTGAACAAGGTTTACT 8638
CACGACACCCACCAGGATTTACCCCATGCCATCACAATCTGGACTTGTCCAATGA

07/09/2017

Cell line STR profile report

CR-UK Centre Genomics Facility
Leeds Institute of Molecular Medicine

Reference data for OVCA433

Reference profile	Cellosaurus	CVCL_0475	D3 S1358	TH01 (chr11)	DZ1 S11	D18 S51	PentaE (chr15)	D5 S818	D13 S317	D7 S820	D16 S539	CSF1PO (chr5)	PentaD (chr21)	Amel (chr21)	VWA (chr12)	D8 S1179	TPOX (chr2)	FGA (chr4)
			15,16	9	30	14	7,12	11,12	7,12	11,12	12	12,13	13,14	X	16,18	14,15	9,11	24

Sample data

Sample OVCA433_RA_Sep17

Sample	D3 S1358	TH01 (chr11)	DZ1 S11	D18 S51	PentaE (chr15)	D5 S818	D13 S317	D7 S820	D16 S539	CSF1PO (chr5)	PentaD (chr21)	Amel (chr21)	VWA (chr12)	D8 S1179	TPOX (chr2)	FGA (chr4)
GV07293A	15,16	9	30	14	7,12	11,12	7,12	11,12	12	12,13	13,14	X	16,18	14,15	9,11	24
GV07293B	15,16	9	30	14	7,12	11,12	7,12	11,12	12	12,13	13,14	X	16,18	14,15	9,11	24

Samples are labelled using the format:
cell_line_name_initials_of_lab_head_date_of_receipt_or_other_unique_identifier

Analysis

Sample match to reference

Matches Cellosaurus reference profile at 16/16 markers.

DSMZdb

No close matches.

DSMZ STR profile database :
<http://www.dsmz.de/fcgi-bin/str.html>
(registration required).
Searches 2495 cell lines from ATCC, DSMZ, JCRB & RIKEN.

CLIMAdb

Not done.

Cell line integrated molecular authentication (CLIMA) database
<http://bioinformatics.isg.e.iclima/>

CGP

Cell line not included in CGP dataset.

Cancer Genome Project STR data :
<http://www.sanger.ac.uk/research/projects/cancergenome/archive/>
(registration required).
Details of CGP data available only to registered users.

Comment

Experimental data generated using Promega PowerPlex 16 system.

We recommend that a minimum of two profiles are generated for each sample, to control for PCR artefacts such as allele dropout. This is of particular importance when generating reference profiles of new cell lines for publication or for validation of differences to published profiles.

07/09/2017

Cell line STR profile report

Reference data for SKOV3

Reference profile from :	D3 S1258	TH01 (chr11)	D21 S11	D16 S51	PentaE (chr15)	D5 S818	D13 S317	D7 S820	D16 S539	CSF1PO (chr5)	Penta D (chr21)	Amel	VWA (chr12)	D8 S1179	TPDX (chr2)	FGA (chr4)
ATCC		9,9.3			11	8,11	13,14	12	11		X		17,18		8,11	
Cellosaurus	(13),14	9,9.3	30, (31),31.2	16,(17), (18)	5,13	8,11	13,14	12	11		X		(17),(18)	14,15	8,11	(23),24,25, (26)
CVCL_0532																
CLS	14	9,9.3	30,31,31.2	16,17,18	5,13	8,11	13,14	12	11		X		17,18	14,15	8,11	24,25,26
342																

Sample data

Sample SKOV3_RA_Sep17

Sample	D3 S1258	TH01 (chr11)	D21 S11	D16 S51	PentaE (chr15)	D5 S818	D13 S317	D7 S820	D16 S539	CSF1PO (chr5)	Penta D (chr21)	Amel	VWA (chr12)	D8 S1179	TPDX (chr2)	FGA (chr4)
GV07293A	14	9,9.3	30,31.2, 32	16,17,18	5	11	8,11	13,14	12	11	12,13	X	17,18	14,15	8,11	24,25,26
GV07293B	14	9,9.3	30,31.2, 32	16,17,18	5	11	8,11	13,14	12	11	12,13	X	17,18	14,15	8,11	24,25,26

Samples are labelled using the format: cell_line_name__initials_of_lab_head__date_of_receipt_or_other_unique_identifier

Analysis

Sample match to reference

Matches ATCC reference at 9/9 markers. Matches Cellosaurus and CLS references at 14/16 markers, with differences at D21 and PentaE.

DSMZdb

Matches SKOV3 (ATCC HTB-77).

DSMZ STR profile database: <http://www.dsmz.de/fp/cg-hin/str.html> (registration required). Searches 2455 cell lines from ATCC, DSMZ, JCRB & RIKEN.

CLIMadb

Not done.

Cell line integrated molecular authentication (CLIMA) database <http://biominformatics.isge.it/clima/>

CGP

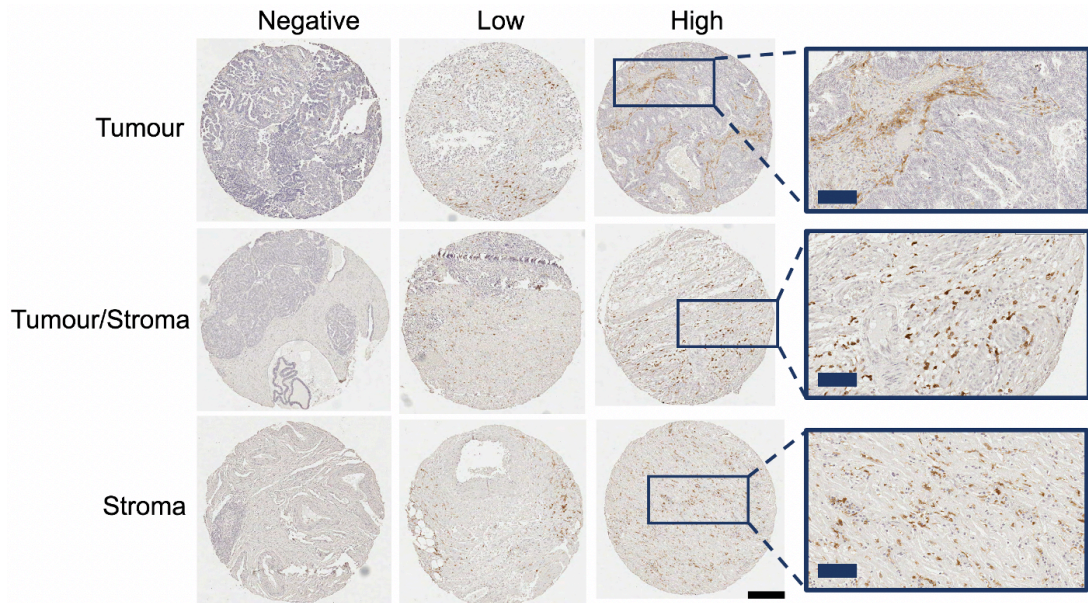
Matches CGP reference at 11/14 markers. There are differences at D3, D21 and FGA, all of which are a loss or gain of a single allele by one sample when compared to the other.

Cancer Genome Project STR data: <http://www.sanger.ac.uk/research/projects/cancergenome/archive/> (registration required). Details of CGP data available only to registered users.

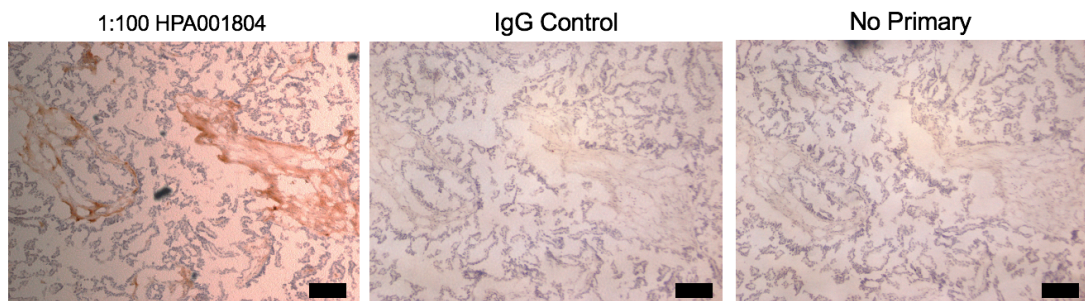
Comment

SKOV3 is deficient in mismatch repair and consequently shows microsatellite instability [Boyer et al., 1995 Cancer Research 55 6063].

Appendix III Examples of the IHC for the different core types, staining intensity and positive and negative controls.



Representative cores from the ICON7 study cohort. The were obtained from the patients' tissue acquired during primary debulking surgery. A qualified histopathologist assembled formalin-fixed paraffin-embedded specimens into tissue microarrays depending on the tissue type of the core. The cores were stained for FXIIIA using HPA001804 at 1:200 dilution. Positive staining is indicated by brown 3,3'-diaminobenzidine (DAB), while the nuclei were counterstained using haematoxylin. Negative staining is defined as a percentage positivity of less than 1%, whereas percentage positivity of greater than 1% is regarded as a positive staining. The positive percentage data was combined and dichotomized, with percentages rounded to the nearest whole integer, to create high and low percentage positive groups. For complete cores, the black bar equals 250 µm. The blue bars in the lower left-hand corner within the zoomed in sections equals 100 µm. This figure was republished with permission of Dr Kathryn Hutchinson from (Hutchinson, 2019).



The presence of FXIIIA staining in non-tumour cells in ovarian cancer tissue indicates a stromal staining pattern. Frozen ovarian cancer tissues were employed as a control for FXIIIA antibody workup. Left: for no primary antibody staining control, only antibody diluent was added to the tissue section during the primary antibody incubation. Middle: to demonstrate that any staining was produced by antigen specificity rather than background created by the antibody's backbone, tissue was stained with a rabbit IgG1 isotype control at the same final concentration as the primary HPA001804 antibody. Right: tissues were stained for FXIIIA using HPA001804 at a 1:100 dilution. For clarity, the image brightness was manually enhanced by 40% for the right and Middle images and 60% for the left image. This figure was republished with permission of Dr Kathryn Hutchinson from (Hutchinson, 2019).

List of References

- Abdel-Samad, N. 2017. Treatment with recombinant factor XIII (Tretten) in a pregnant woman with factor XIII deficiency. *American Journal of Case Reports*. **18**, pp.436-439.
- Adany, R. and Bardos, H. 2003. Factor XIII subunit A as an intracellular transglutaminase. *Cellular and Molecular Life Sciences*. **60**(6), pp.1049-1060.
- Ahmadi, M., Nasiri, M., Ebrahimi, A. 2016. Thrombosis-related factors FV and F13A1 mutations in uterine myomas. *Zahedan Journal of Research in Medical Sciences*. **18**(10), e4836.
- Akiyama, S.K. 1996. Integrins in cell adhesion and signaling. *Human Cell*. **9**(3), pp.181-186.
- Al-Jallad, H.F., Myneni, V.D., Piercy-Kotb, S.A., Chabot, N., Mulani, A., Keillor, J.W. and Kaartinen, M.T. 2011. Plasma membrane factor XIIIa transglutaminase activity regulates osteoblast matrix secretion and deposition by affecting microtubule dynamics. *PLOS ONE*. **6**, e15893.
- Anokhin, B.A., Stribinskis, V., Dean, W.L. and Maurer, M.C. 2017. Activation of factor XIII is accompanied by a change in oligomerization state. *The FEBS Journal*. **284**, pp.3849-3861.
- Anwar, R., Gallivan, L., Edmonds, S.D. and Markham, A.F. 1999. Genotype/phenotype correlations for coagulation factor XIII: specific normal polymorphisms are associated with high or low factor XIII specific activity. *Blood*. **93**, pp.897-905.
- Anwar, R. and Miloszewski, K.J. 1999. Factor XIII deficiency. *British Journal of Haematology*. **107**, pp.468-484.
- Anwar, R., Stewart, A.D., Miloszewski, K.J., Losowsky, M.S. and Markham, A.F. 1995. Molecular basis of inherited factor XIII deficiency: identification of multiple mutations provides insights into protein function. *British Journal of Haematology*. **91**, pp.728-735.
- Anwar, R., Valleley, E., Gallivan, L., Hall, G., Perren, T. and Markham, A. 2004. Influence of coagulation factor 13A (F13A) gene variants on overall survival (OS) of ovarian cancer patients. *Journal of Clinical Oncology*. **22**, p.5002.
- Anwar, R., Valleley, E.J.A., Gallivan, L., Hall, G.D., Barrett, J.H., Perren, T.J., Smyth, J.F., Ganesan, T.S., Balkwill, F.R. and Markham, A.F. [No date]. Coagulation factor XIIIa genetic polymorphisms influence overall survival of cancer patients: a multi-centre study. Unpublished work: University of Leeds.
- Ariëns, R.A., Kohler, H.P., Mansfield, M.W. and Grant, P.J. 1999. Subunit antigen and activity levels of blood coagulation factor XIII in healthy individuals. Relation to sex, age, smoking, and hypertension. *Arteriosclerosis, Thrombosis, and Vascular Biology*. **19**, pp.2012-2016.
- Ariens, R.A., Lai, T.S., Weisel, J.W., Greenberg, C.S. and Grant, P.J. 2002. Role of factor XIII in fibrin clot formation and effects of genetic polymorphisms. *Blood*. **100**, pp.743-754.

- Ariëns, R.A., Philippou, H., Nagaswami, C., Weisel, J.W., Lane, D.A. and Grant, P.J. 2000. The factor XIII V34L polymorphism accelerates thrombin activation of factor XIII and affects cross-linked fibrin structure. *Blood*. 96, pp.988-995.
- Arikan, S.K., Kasap, B., Yetimalar, H., Yildiz, A., Sakarya, D.K. and Tatar, S. 2014. Impact of prognostic factors on survival rates in patients with ovarian carcinoma. *Asian Pacific Journal of Cancer Prevention*. 15, pp.6087-6094.
- Arnout, J., Hoylaerts, M. and Degaetano, G. 2003. Cancer and thrombosis: a two-way interaction. In: Donati, M.B., Falanga, A. and Lorenzet, R. (eds.) *Thrombosis: fundamental and clinical aspects*. Blijde-Inkomststraat 5, B-3000 Leuven (Belgium): Leuven University Press. 23, pp. 417-430.
- Asaduzzaman, M. 2007. *Standardization of yeast growth curves from several curves with different initial sizes*. Master of Science, Chalmers University of Technology and Göteborg University.
- Ashworth, A. 2008. A synthetic lethal therapeutic approach: poly (ADP) ribose polymerase inhibitors for the treatment of cancers deficient in DNA double-strand break repair. *Journal of Clinical Oncology*. 26, pp.3785-3790.
- Attié-Castro, F.A., Zago, M.A., Lavinha, J., Elion, J., Rodriguez-Delfin, L., Guerreiro, J.F. and Franco, R.F. 2000. Ethnic heterogeneity of the factor XIII Val34Leu polymorphism. *Thrombosis and Haemostasis*. 84, pp.601-603.
- Bagoly, Z., Koncz, Z., Hársfalvi, J. and Muszbek, L. 2012. Factor XIII, clot structure, thrombosis. *Thrombosis Research*. 129, pp.382-387.
- Balogh, I.N., Szôke, G., Kárpáti, L., Wartiovaara, U., Katona, E.V., Komáromi, I.N., Haramura, G., Pfliegler, G.R., Mikkola, H. and Muszbek, L.S. 2000. Val34Leu polymorphism of plasma factor XIII: biochemistry and epidemiology in familial thrombophilia. *Blood*. 96, pp.2479-2486.
- Banerjee, S. and Kaye, S.B. 2013. New strategies in the treatment of ovarian cancer: current clinical perspectives and future potential. *Clinical Cancer Research*. 19, pp.961-968.
- Barkan, G. and Gaspar, A. 1923. Zur frage der reversibilität der fibringerinnung II. *Biochem Ztchr*. 139, pp.291-301.
- Becker, D.M. and Guarente, L. 1991. High-efficiency transformation of yeast by electroporation. *Methods in Enzymology*. 194, pp.182-187.
- Beckers, C.M., Simpson, K.R., Griffin, K.J., Brown, J.M., Cheah, L.T., Smith, K.A., Vacher, J., Cordell, P.A., Kearney, M.T. and Grant, P.J. 2017. Cre/lox studies identify resident macrophages as the major source of circulating coagulation factor XIII-A. *Arteriosclerosis, Thrombosis, and Vascular Biology*. 37, pp.1494-1502.
- Bereczky, Z. & Muszbek, L. 2011. Factor XIII and venous thromboembolism. *Seminars in Thrombosis and Haemostasis*. 37, pp.305-314.
- Berek, J.S., Kehoe, S.T., Kumar, L. and Friedlander, M. 2018. Cancer of the ovary, fallopian tube, and peritoneum. *International Journal of Gynecology & Obstetrics*. 143, pp.59-78.

- Bergman, L.W. 2001. Growth and maintenance of yeast. *Methods in Molecular Biology*. 177, pp.9-14.
- Bery, A., Leung, F., Smith, C.R., Diamandis, E.P. and Kulasingam, V. 2014. Deciphering the ovarian cancer ascites fluid peptidome. *Clinical Proteomics*. 11, 13.
- Bishop, P.D., Teller, D., Smith, R., Lasser, G., Gilbert, T. and Seale, R. 1990. Expression, purification, and characterization of human factor XIII in *Saccharomyces cerevisiae*. *Biochemistry*. 29, pp.1861-1869.
- Brand-Staufer, B., Carcao, M., Kerlin, B.A., Will, A., Williams, M., Tornøe, C.W., Sandberg Lundblad, M. and Nugent, D. 2015. Pharmacokinetic characterization of recombinant factor XIII (FXIII)-A2 across age groups in patients with FXIII A-subunit congenital deficiency. *Haemophilia*. 21, pp.380-385.
- Brierley, J.D., Gospodarowicz, M.K. and Wittekind, C. 2017. *TNM classification of malignant tumours*. John Wiley & Sons.
- Burger, R.A., Brady, M.F., Bookman, M.A., Fleming, G.F., Monk, B.J., Huang, H., Mannel, R. S., Homesley, H.D., Fowler, J. and Greer, B.E. 2011. Incorporation of bevacizumab in the primary treatment of ovarian cancer. *New England Journal of Medicine*. 365, pp.2473-2483.
- Burke, MA., Patchefsky, AS. 2003. Pathology, *Atlas of Clinical Oncology Ovarian Cancer*. Ozols RF, ed. American Cancer Society, pp. 1-26.
- Callahan, M.J., Crum, C.P., Medeiros, F., Kindelberger, D.W., Elvin, J.A., Garber, J.E., Feltmate, C.M., Berkowitz, R.S. and Muto, M.G. 2007. Primary fallopian tube malignancies in BRCA-positive women undergoing surgery for ovarian cancer risk reduction. *Journal of Clinical Oncology*. 25, pp.3985-3990.
- Camerer, E., Qazi, A.A., Duong, D.N., Cornelissen, I., Advincula, R. and Coughlin, S.R. 2004. Platelets, protease-activated receptors, and fibrinogen in hematogenous metastasis. *Blood*. 104, pp.397-401.
- Cancer, C. G. O. E. S. O. O. 2008. Ovarian cancer and oral contraceptives: collaborative reanalysis of data from 45 epidemiological studies including 23 257 women with ovarian cancer and 87 303 controls. *The Lancet*. 371, pp.303-314.
- Cardenas, C., Alvero, A.B., Yun, B.S. and Mor, G. 2016. Redefining the origin and evolution of ovarian cancer: a hormonal connection. *Endocrine-Related Cancer*. 23, R411-R422.
- Cario, E., Goebell, H. and Dignass, A. 1999. Factor XIII modulates intestinal epithelial wound healing in vitro. *Scandinavian Journal of Gastroenterology*. 34, pp.485-490.
- Cass, I., Holschneider, C., Datta, N., Barbuto, D., Walts, A.E. and Karlan, B.Y. 2005. BRCA-mutation-associated fallopian tube carcinoma: a distinct clinical phenotype? *Obstetrics & Gynecology*. 106, pp.1327-1334.
- Chan, J.K., Loizzi, V., Lin, Y.G., Osann, K., Brewster, W.R. and Disaia, P.J. 2003. Stages III and IV invasive epithelial ovarian carcinoma in younger versus

- older women: what prognostic factors are important? *Obstetrics & Gynecology*. 102, pp.156-161.
- Chang, S.J., Hodeib, M., Chang, J. and Bristow, R.E. 2013. Survival impact of complete cytoreduction to no gross residual disease for advanced-stage ovarian cancer: a meta-analysis. *Gynecologic Oncology*. 130, pp.493-498.
- Chen, X., Brewer, M.A., Zou, C. and Campagnola, P.J. 2009. Adhesion and migration of ovarian cancer cells on crosslinked laminin fibers nanofabricated by multiphoton excited photochemistry. *Integrative Biology*. 1, pp.469-476.
- Chiang, H.Y., Korshunov, V.A., Serour, A., Shi, F. and Sottile, J. 2009. Fibronectin is an important regulator of flow-induced vascular remodeling. *Arteriosclerosis, Thrombosis, and Vascular Biology*. 29, pp.1074-1079.
- Cho, A., Howell, V.M. and Colvin, E.K. 2015. The extracellular matrix in epithelial ovarian cancer—a piece of a puzzle. *Frontiers in Oncology* 5, 245.
- Cho, K.R. and Shih, I.M. 2009. Ovarian cancer. *Annual Review of Pathology: Mechanisms of Disease*. 4, pp.287-313.
- Clamp, A.R., James, E.C., Mcneish, I.A., Dean, A., Kim, J.W., O'donnell, D.M., Hook, J., Coyle, C., Blagden, S. and Brenton, J.D. 2019. Weekly dose-dense chemotherapy in first-line epithelial ovarian, fallopian tube, or primary peritoneal carcinoma treatment (ICON8): primary progression free survival analysis results from a GCIG phase 3 randomised controlled trial. *The Lancet*. 394, pp.2084-2095.
- Collaborators, I. 1998. ICON2: randomised trial of single-agent carboplatin against three-drug combination of CAP (cyclophosphamide, doxorubicin, and cisplatin) in women with ovarian cancer. *The Lancet*. 352, pp.1571-1576.
- Colombo, N., Guthrie, D., Chiari, S., Parmar, M., Qian, W., Swart, A.M., Torri, V., Williams, C., Lissoni, A. and Bonazzi, C. 2003. International Collaborative Ovarian Neoplasm trial 1: a randomized trial of adjuvant chemotherapy in women with early-stage ovarian cancer. *Journal of the National Cancer Institute*. 95, pp.125-132.
- Corbett, S.A., Lee, L., Wilson, C.L. and Schwarzbauer, J.E. 1997. Covalent cross-linking of fibronectin to fibrin is required for maximal cell adhesion to a fibronectin-fibrin matrix. *Journal of Biological Chemistry*. 272, pp.24999-25005.
- Cramer, D.W. and Welch, W.R. 1983. Determinants of ovarian cancer risk. II. Inferences regarding pathogenesis. *Journal of the National Cancer Institute*. 71, pp.717-721.
- Dai, H., Zhou, H., Sun, Y., Xu, Z., Wang, S., Feng, T. and Zhang, P. 2018. D-dimer as a potential clinical marker for predicting metastasis and progression in cancer. *Biomedical Reports*. 9, pp.453-457.
- Dallabrida, S.M., Falls, L.A. and Farrell, D.H. 2000. Factor xiiiA supports microvascular endothelial cell adhesion and inhibits capillary tube formation in fibrin. *Blood*. 95, pp.2586-2592.

- Dardik, R., Loscalzo, J., Eskaraev, R. and Inbal, A. 2005. Molecular mechanisms underlying the proangiogenic effect of factor XIII. *Arteriosclerosis, Thrombosis, and Vascular Biology*. 25, pp.526-232.
- Dardik, R., Loscalzo, J. and Inbal, A. 2006. Factor XIII (FXIII) and angiogenesis. *Journal of Thrombosis and Haemostasis*. 4, pp.19-25.
- Dardik, R., Solomon, A., Loscalzo, J., Eskaraev, R., Bialik, A., Goldberg, I., Schiby, G. and Inbal, A. 2003. Novel proangiogenic effect of factor XIII associated with suppression of thrombospondin 1 expression. *Arteriosclerosis, Thrombosis, and Vascular Biology*. 23, pp.1472-1477.
- De Lange, M., Andrew, T., Snieder, H., Ge, D., Futers, T.S., Standeven, K., Spector, T.D., Grant, P.J. and Ariëns, R.A. 2006. Joint linkage and association of six single-nucleotide polymorphisms in the factor XIII-A subunit gene point to V34L as the main functional locus. *Arteriosclerosis, Thrombosis, and Vascular Biology*. 26, pp.1914-1919.
- Domchek, S.M., Friebel, T.M., Singer, C.F., Evans, D.G., Lynch, H.T., Isaacs, C., Garber, J. E., Neuhausen, S.L., Matloff, E. and Eeles, R. 2010. Association of risk-reducing surgery in BRCA1 or BRCA2 mutation carriers with cancer risk and mortality. *JAMA*. 304, pp.967-975.
- Dong, X., Stothard, P., Forsythe, I.J. and Wishart, D.S. 2004. Plasmapper: a web server for drawing and auto-annotating plasmid maps. *Nucleic Acids Research*. 32, W660-4.
- Du Bois, A., Reuss, A., Pujade-Lauraine, E., Harter, P., Ray-Coquard, I. and Pfisterer, J. 2009. Role of surgical outcome as prognostic factor in advanced epithelial ovarian cancer: a combined exploratory analysis of 3 prospectively randomized phase 3 multicenter trials: by the Arbeitsgemeinschaft Gynaekologische Onkologie Studiengruppe Ovarialkarzinom (AGO-OVAR) and the Groupe d'Investigateurs Nationaux Pour les Etudes des Cancers de l'Ovaire (GINECO). *Cancer*. 115, pp.1234-1244.
- Duckert, F., Jung, E. and Shmerling, D.H. 1960. A hitherto undescribed congenital haemorrhagic diathesis probably due to fibrin stabilizing factor deficiency. *Thrombosis et Diathesis Haemorrhagica*. 5, pp.179-186.
- Duffy, M.J. and O'grady, P. 1984. Plasminogen activator and cancer. *European Journal of Cancer and Clinical Oncology*. 20, pp.577-582.
- Eckert, R.L., Kaartinen, M.T., Nurminskaya, M., Belkin, A.M., Colak, G., Johnson, G.V.W. and Mehta, K. 2014. Transglutaminase regulation of cell function. *Physiological Reviews*. 94, pp.383-417.
- Edwards, S.J., Barton, S., Thurgar, E. and Trevor, N. 2015. Topotecan, pegylated liposomal doxorubicin hydrochloride, paclitaxel, trabectedin and gemcitabine for advanced recurrent or refractory ovarian cancer: a systematic review and economic evaluation. *Health Technology Assessment (Winchester, England)*. 19(7), pp.1-480.
- Eipe, J., Yakulls, V. and Costea, N. 1977. Factor XIII deficiency in BALB/c mice with plasmacytoma. *Cancer Research*. 37, pp.3551-3555.

- Erickson, B.K., Conner, M.G. and Landen Jr, C.N. 2013. The role of the fallopian tube in the origin of ovarian cancer. *American Journal of Obstetrics and Gynecology*. 209, pp.409-414.
- Facchiano, A. and Facchiano, F. 2009. Transglutaminases and their substrates in biology and human diseases: 50 years of growing. *Amino Acids*. 36, pp.599-614.
- Falanga, A., Marchetti, M. and Vignoli, A. 2013. Coagulation and cancer: biological and clinical aspects. *Journal of Thrombosis and Haemostasis*. 11, pp.223-233.
- Fathalla, M. 1971. Incessant ovulation—a factor in ovarian neoplasia. *The Lancet*. 2, 163.
- Ferlay, J., Colombet, M., Soerjomataram, I., Mathers, C., Parkin, D.M., Pineros, M., Znaor, A. and Bray, F. 2019. Estimating the global cancer incidence and mortality in 2018: GLOBOCAN sources and methods. *International Journal of Cancer*. 144, pp.1941-1953.
- Ferrara, N., Hillan, K.J. and Novotny, W. 2005. Bevacizumab (Avastin), a humanized anti-VEGF monoclonal antibody for cancer therapy. *Biochemical and Biophysical Research Communications*. 333, pp.328-335.
- Fotopoulou, C., Hall, M., Cruickshank, D., Gabra, H., Ganesan, R., Hughes, C., Kehoe, S., Ledermann, J., Morrison, J., Naik, R., Rolland, P. and Sundar, S. 2017. British Gynaecological Cancer Society (BGCS) epithelial ovarian/fallopian tube/primary peritoneal cancer guidelines: recommendations for practice. *European Journal of Obstetrics & Gynecology and Reproductive Biology*. 213, pp.123-139.
- Foulkes, W.D., Gore, M. and McCluggage, W.G. 2016. Rare non-epithelial ovarian neoplasms: pathology, genetics and treatment. *Gynecologic Oncology*. 142, pp.190-198.
- Fox, B.A., Yee, V.C., Pedersen, L.C., Le Trong, I., Bishop, P.D., Stenkamp, R.E. and Teller, D.C. 1999. Identification of the calcium binding site and a novel ytterbium site in blood coagulation factor XIII by x-ray crystallography. *Journal of Biological Chemistry*. 274, pp.4917-4923.
- Fraser, S.R., Booth, N.A. and Mutch, N.J. 2011. The antifibrinolytic function of factor XIII is exclusively expressed through α 2-antiplasmin cross-linking. *Blood*. 117, pp.6371-6374.
- Freedman, R.S., Deavers, M., Liu, J. and Wang, E. 2004. Peritoneal inflammation - A microenvironment for Epithelial Ovarian Cancer (EOC). *Journal of Translational Medicine*. 2, 23.
- Funato, M., Kaneko, H., Kubota, K., Ozeki, M., Kanda, K., Orii, K., Kato, Z., Fukao, T. and Kondo, N. 2011. Pediatric acute lymphoblastic leukemia mimicking Henoch-Schonlein purpura. *Pediatrics International*. 53, pp.766-768.
- Gadducci, A., Baicchi, U., Marrai, R., Ferdeghini, M., Bianchi, R. and Facchini, V. 1996. Preoperative evaluation of D-dimer and CA 125 levels in differentiating

- benign from malignant ovarian masses. *Gynecologic Oncology*. 60, pp.197-202.
- Gallivan, L., Markham, A.F. and Anwar, R. 1999a. The Leu564 factor XIIIa variant results in significantly lower plasma factor XIII levels than the Pro564 variant. *Thrombosis and Haemostasis*. 82, pp.1368-1370.
- Gallivan, L., Markham, A.F. and Anwar, R. 1999b. The Leu564 factor XIIIa variant results in significantly lower plasma factor XIII levels than the Pro564 variant. *Thrombosis and Haemostasis*. 82, pp.1368-70.
- Gemmati, D., Vigliano, M., Burini, F., Mari, R., El Mohsein, H.H., Parmeggiani, F. and Serino, M.L. 2016. Coagulation factor XIIIa (F13A1): novel perspectives in treatment and pharmacogenetics. *Current Pharmaceutical Design*. 22, pp.1449-1459.
- George, A., Kaye, S. and Banerjee, S. 2017. Delivering widespread BRCA testing and PARP inhibition to patients with ovarian cancer. *Nature Reviews Clinical Oncology*. 14, pp.284-296.
- Ghezzi, F., Cromi, A., Siesto, G., Giudici, S., Serati, M., Formenti, G. and Franchi, M. 2010. Prognostic significance of preoperative plasma fibrinogen in endometrial cancer. *Gynecologic Oncology*. 119, pp.309-313.
- Giancotti, F.G. and Ruoslahti, E. 1990. Elevated levels of the $\alpha 5 \beta 1$ fibronectin receptor suppress the transformed phenotype of Chinese hamster ovary cells. *Cell*. 60, pp.849-859.
- Gietz, R.D. and Schiestl, R.H. 2007. High-efficiency yeast transformation using the liac/SS carrier DNA/PEG method. *Nature Protocols*. 2, pp.31-34.
- Goldblum, J.R. and Tuthill, R.J. 1997. CD34 and factor-xiii immunoreactivity in dermatofibrosarcoma protuberans and dermatofibroma. *American Journal of Dermatopathology*. 19, pp.147-153.
- Goncalves, E., Lopes Da Silva, R., Varandas, J. and Diniz, M.J. 2012. Acute promyelocytic leukaemia associated Factor XIII deficiency presenting as retro-bulbar haematoma. *Thrombosis Research*. 129, pp.810-811.
- González Martín, A., Oza, A.M., Embleton, A.C., Pfisterer, J., Ledermann, J.A., Pujade-Lauraine, E., Kristensen, G., Bertrand, M.A., Beale, P., Cervantes, A., Kent, E., Kaplan, R.S., Parmar, M.K.B., Scotto, N. and Perren, T.J. 2019. Exploratory outcome analyses according to stage and/or residual disease in the ICON7 trial of carboplatin and paclitaxel with or without bevacizumab for newly diagnosed ovarian cancer. *Gynecologic Oncology*. 152, pp.53-60.
- González-Martín, A., Pothuri, B., Vergote, I., Depont Christensen, R., Graybill, W., Mirza, M. R., McCormick, C., Lorusso, D., Hoskins, P. and Freyer, G. 2019. Niraparib in patients with newly diagnosed advanced ovarian cancer. *New England Journal of Medicine*. 381, pp.2391-2402.
- Goodell, V., Mcneel, D. and Disis, M.L. 2008. His-tag ELISA for the detection of humoral tumor-specific immunity. *BMC Immunology*. 9, 23.

- Gottschau, M., Kjaer, S.K., Jensen, A., Munk, C. and Mellekjaer, L. 2015. Risk of cancer among women with polycystic ovary syndrome: a Danish cohort study. *Gynecologic Oncology*. 136, pp.99-103.
- Gouin-Thibault, I. and Samama, M.M. 1999. Laboratory diagnosis of the thrombophilic state in cancer patients. *Seminars in Thrombosis and Haemostasis*. 25, pp.167-72.
- Greenberg, C.S. and Shuman, M. 1982. The zymogen forms of blood coagulation factor XIII bind specifically to fibrinogen. *Journal of Biological Chemistry*. 257, pp.6096-6101.
- Grinnell, F., Feld, M. and Minter, D. 1980. Fibroblast adhesion to fibrinogen and fibrin substrata: requirement for cold-insoluble globulin (plasma fibronectin). *Cell*. 19, pp.517-525.
- Group, The International Collaborative Ovarian Neoplasm (ICON) Group. 2002. Paclitaxel plus carboplatin versus standard chemotherapy with either single-agent carboplatin or cyclophosphamide, doxorubicin, and cisplatin in women with ovarian cancer: the ICON3 randomised trial. *The Lancet*. 360, pp.505-515.
- Gupta, S., Biswas, A., Akhter, M.S., Krettler, C., Reinhart, C., Dodt, J., Reuter, A., Philippou, H., Ivaskevicius, V. and Oldenburg, J. 2016. Revisiting the mechanism of coagulation factor XIII activation and regulation from a structure/functional perspective. *Scientific Reports*. 6, pp.1-16.
- Gurler, H., Yu, Y., Choi, J., Kajdacsy-Balla, A.A. and Barbolina, M.V. 2015. Three-dimensional collagen type I matrix up-regulates nuclear isoforms of the microtubule associated protein tau implicated in resistance to paclitaxel therapy in ovarian carcinoma. *International Journal of Molecular Sciences*. 16, pp.3419-3433.
- Hafter, R., Klaubert, W., Gollwitzer, R., Von Hugo, R. and Graeff, H. 1984. Crosslinked fibrin derivatives and fibronectin in ascitic fluid from patients with ovarian cancer compared to ascitic fluid in liver cirrhosis. *Thrombosis Research*. 35, pp.53-64.
- Hah, S.S., Stivers, K.M., De Vere White, R.W. and Henderson, P.T. 2006. Kinetics of carboplatin– DNA binding in genomic DNA and bladder cancer cells as determined by accelerator mass spectrometry. *Chemical Research in Toxicology*. 19, pp.622-626.
- Hanahan, D. & Weinberg, R.A. 2011. Hallmarks of cancer: the next generation. *Cell*. 144, pp.646-674.
- Hapke, S., Kessler, H., Lubert, B., Bengel, A., Hutzler, P., Höfler, H., Schmitt, M. and Reuning, U. 2003. Ovarian cancer cell proliferation and motility is induced by engagement of integrin $\alpha\beta3$ /vitronectin interaction. *Biological Chemistry*. 384, pp.1073-1083.
- Havrilesky, L.J., Moorman, P.G., Lowery, W.J., Gierisch, J.M., Coeytaux, R.R., Urrutia, R.P., Dinan, M., Mcbroom, A.J., Hasselblad, V. and Sanders, G.D. 2013. Oral contraceptive pills as primary prevention for ovarian cancer: a

- systematic review and meta-analysis. *Obstetrics & Gynecology*. 122, pp.139-147.
- Henke, E., Nandigama, R. and Ergün, S. 2020. Extracellular matrix in the tumor microenvironment and its impact on cancer therapy. *Frontiers in Molecular Biosciences*. 6, 160.
- Henschen, A., Lottspeich, F., Kehl, M. and Southan, C. 1983. Covalent structure of fibrinogen. *Annals of the New York Academy of Sciences*. 408, pp.28-43.
- Heyman, L., Leroy-Dudal, J., Fernandes, J., Seyer, D., Dutoit, S. and Carreiras, F. 2010. Mesothelial vitronectin stimulates migration of ovarian cancer cells. *Cell Biology International*. 34, pp.493-502.
- Hielscher, A., Ellis, K., Qiu, C., Porterfield, J. and Gerecht, S. 2016. Fibronectin deposition participates in extracellular matrix assembly and vascular morphogenesis. *PLOS ONE*. 11, e0147600.
- Hirsh, J., Anand, S.S., Halperin, J.L. and Fuster, V. 2001. Mechanism of action and pharmacology of unfractionated heparin. American Heart Association. *Arteriosclerosis, Thrombosis and Vascular Biology*. 21, pp.1094-1096.
- Hornyak, T.J., Bishop, P.D. and Shafer, J.A. 1989.. Alpha.-Thrombin-catalyzed activation of human platelet factor XIII: relationship between proteolysis and factor xiiia activity. *Biochemistry*. 28, pp.7326-7332.
- Horwitz, S.B. 1994. Taxol (paclitaxel): mechanisms of action. *Annals of Oncology: Official Journal of the European Society for Medical Oncology*. 5, S3-6.
- Hutchinson, K.T. 2019. *Factor XIII A genotype to outcome in epithelial ovarian cancer*. Phd Thesis, University of Leeds.
- Hwang, J.Y., Mangala, L.S., Fok, J.Y., Lin, Y.G., Merritt, W.M., Spannuth, W.A., Nick, A.M., Fiterman, D.J., Vivas-Mejia, P.E., Deavers, M.T., Coleman, R.L., Lopez-Berestein, G., Mehta, K. and Sood, A.K. 2008. Clinical and biological significance of tissue transglutaminase in ovarian carcinoma. *Cancer Research*. 68, pp.5849-5858.
- Ichinose, A. and Davie, E.W. 1988. Characterization of the gene for the a subunit of human factor XIII (plasma transglutaminase), a blood coagulation factor. *Proceedings of the National Academy of Sciences of the United States of America*. 85, pp.5829-5833.
- Iismaa, S.E., Mearns, B.M., Lorand, L. and Graham, R.M. 2009. Transglutaminases and disease: lessons from genetically engineered mouse models and inherited disorders. *Physiological Reviews*. 89, pp.991-1023.
- Iyer, V.R. and Lee, S.I. 2010. MRI, CT, and PET/CT for ovarian cancer detection and adnexal lesion characterization. *American Journal of Roentgenology*. 194, pp.311-321.
- Jacob, F., Nixdorf, S., Hacker, N.F. and Heinzelmann-Schwarz, V.A. 2014. Reliable in vitro studies require appropriate ovarian cancer cell lines. *Journal of Ovarian Research*. 7, 60.

- Jacobs, I., Oram, D., Fairbanks, J., Turner, J., Frost, C. and Grudzinskas, J. 1990. A risk of malignancy index incorporating CA 125, ultrasound and menopausal status for the accurate preoperative diagnosis of ovarian cancer. *BJOG: An International Journal of Obstetrics & Gynaecology*. 97, pp.922-929.
- Jiang, W.G., Ablin, R., Douglas-Jones, A. and Mansel, R.E. 2003. Expression of transglutaminases in human breast cancer and their possible clinical significance. *Oncology Reports*. 10, pp.2039-2044.
- Kaku, T., Ogawa, S., Kawano, Y., Ohishi, Y., Kobayashi, H., Hirakawa, T. and Nakano, H. 2003. Histological classification of ovarian cancer. *Medical Electron Microscopy*. 36, pp.9-17.
- Kamazawa, S., Kigawa, J., Kanamori, Y., Itamochi, H., Sato, S., Iba, T. and Terakawa, N. 2002. Multidrug resistance gene-1 is a useful predictor of Paclitaxel-based chemotherapy for patients with ovarian cancer. *Gynecologic Oncology*. 86, pp.171-176.
- Kanayama, N. 1991. [The role of D-dimer in diagnosis of ovarian cancer]. *Nihon Sanka Fujinka Gakkai Zasshi*. 43, pp.485-488.
- Kangsadalampai, S. and Board, P.G. 1998. The Val34Leu polymorphism in the A subunit of coagulation factor XIII contributes to the large normal range in activity and demonstrates that the activation peptide plays a role in catalytic activity. *Blood*. 92, pp.2766-2770.
- Kappelmayer, J., Simon, A., Katona, E., Szanto, A., Nagy, L., Kiss, A., Kiss, C. and Muszbek, L. 2005. Coagulation factor XIII-A. A flow cytometric intracellular marker in the classification of acute myeloid leukemias. *Thrombosis and Haemostasis*. 94, pp.454-459.
- Kárai, B., Hevessy, Z., Szánthó, E., Csáthy, L., Ujfalusi, A., Gyurina, K., Szegedi, I., Kappelmayer, J. and Kiss, C. 2018. Expression of coagulation factor XIII subunit A correlates with outcome in childhood acute lymphoblastic leukemia. *Pathology & Oncology Research*. 24, pp.345-352.
- Karst, A.M. and Drapkin, R. 2011. The new face of ovarian cancer modeling: better prospects for detection and treatment. *F1000 Med Rep*. 3, 22.
- Kasahara, K., Souri, M., Kaneda, M., Miki, T., Yamamoto, N. and Ichinose, A. 2010. Impaired clot retraction in factor XIII A subunit-deficient mice. *Blood*. 115, pp.1277-1279.
- Katsumata, N., Yasuda, M., Isonishi, S., Takahashi, F., Michimae, H., Kimura, E., Aoki, D., Jobo, T., Kodama, S. and Terauchi, F. 2013. Long-term results of dose-dense paclitaxel and carboplatin versus conventional paclitaxel and carboplatin for treatment of advanced epithelial ovarian, fallopian tube, or primary peritoneal cancer (JGOG 3016): a randomised, controlled, open-label trial. *The Lancet Oncology*. 14, pp.1020-1026.
- Kattula, S., Byrnes, J.R., Martin, S.M., Holle, L.A., Cooley, B.C., Flick, M.J. and Wolberg, A.S. 2018. Factor XIII in plasma, but not in platelets, mediates red blood cell retention in clots and venous thrombus size in mice. *Blood Advances*. 2, pp.25-35.

- Kawai, S., Hashimoto, W. and Murata, K. 2010. Transformation of *Saccharomyces cerevisiae* and other fungi: methods and possible underlying mechanism. *Bioeng Bugs*. 1, pp.395-403.
- Kazazi-Hyseni, F., Beijnen, J.H. and Schellens, J.H. 2010. Bevacizumab. *The Oncologist*. 15, 819.
- Keating, G.M. 2014. Bevacizumab: a review of its use in advanced cancer. *Drugs*. 74, pp.1891-1925.
- Kehoe, S., Hook, J., Nankivell, M., Jayson, G.C., Kitchener, H., Lopes, T., Luesley, D., Perren, T., Bannoo, S. and Mascarenhas, M. 2015. Primary chemotherapy versus primary surgery for newly diagnosed advanced ovarian cancer (CHORUS): an open-label, randomised, controlled, non-inferiority trial. *The Lancet*. 386, pp.249-257.
- Kenny, H.A., Chiang, C.Y., White, E.A., Schryver, E.M., Habis, M., Romero, I.L., Ladanyi, A., Penicka, C.V., George, J. and Matlin, K. 2014. Mesothelial cells promote early ovarian cancer metastasis through fibronectin secretion. *The Journal of Clinical Investigation*. 124, pp.4614-4628.
- Kenny, H.A., Kaur, S., Coussens, L.M. and Lengyel, E. 2008. The initial steps of ovarian cancer cell metastasis are mediated by MMP-2 cleavage of vitronectin and fibronectin. *The Journal of Clinical Investigation*. 118, pp.1367-1379.
- Kessenbrock, K., Plaks, V. and Werb, Z. 2010. Matrix metalloproteinases: regulators of the tumor microenvironment. *Cell*. 141, pp.52-67.
- Khorana, A.A. 2010. Venous thromboembolism and prognosis in cancer. *Thrombosis Research*. 125, pp.490-493.
- Khorana, A.A. 2012. Cancer and coagulation. *American Journal of Hematology*. 87 Suppl 1, S82-7.
- Kindelberger, D.W., Lee, Y., Miron, A., Hirsch, M.S., Feltmate, C., Medeiros, F., Callahan, M. J., Garner, E.O., Gordon, R.W. and Birch, C. 2007. Intraepithelial carcinoma of the fimbria and pelvic serous carcinoma: evidence for a causal relationship. *The American Journal of Surgical Pathology*. 31, pp.161-169.
- Kiss, F., Hevessy, Z., Veszpremi, A., Katona, E., Kiss, C., Vereb, G., Muszbek, L. and Kappelmayer, J.N. 2006. Leukemic lymphoblasts, a novel expression site of coagulation factor XIII subunit A. *Thrombosis and Haemostasis*. 96, pp.176-182.
- Kiss, F., Simon, A., Csathy, L., Hevessy, Z., Katona, E., Kiss, C. and Kappelmayer, J. 2008. A coagulation factor becomes useful in the study of acute leukemias: Studies with blood coagulation factor XIII. *Cytometry Part A*. 73A, pp.194-201.
- Knowles, L.M., Gurski, L.A., Engel, C., Gnarra, J.R., Maranchie, J.K. and Pilch, J. 2013. Integrin $\alpha\beta 3$ and fibronectin upregulate Slug in cancer cells to promote clot invasion and metastasis. *Cancer Research*. 73, pp.6175-6184.
- Koh, S.C., Tham, K.F., Razvi, K., Oei, P.L., Lim, F.K., Roy, A.C. and Prasad, R. 2001. Hemostatic and fibrinolytic status in patients with ovarian cancer and benign

ovarian cysts: could D-dimer and antithrombin III levels be included as prognostic markers for survival outcome? *Clinical and Applied Thrombosis/Hemostasis*. 7, pp.141-148.

- Kohler, H., Ariëns, R.A.S., Whitaker, P. and Grant, P. 1998. A common coding polymorphism in the FXIII A-subunit gene (fxiiiival34leu) affects cross-linking activity. *Thrombosis and Haemostasis*. 80 (04), p.704.
- Kołodziejczyk, J. and Ponczek, M.B. 2013. The role of fibrinogen, fibrin and fibrin (ogen) degradation products (fdps) in tumor progression. *Contemporary Oncology*. 17, 113.
- Komaromi, I., Bagoly, Z. and Muszbek, L. 2011. Factor XIII: novel structural and functional aspects. *Journal of Thrombosis and Haemostasis*. 9, pp.9-20.
- Konecny, G.E., Wang, C., Hamidi, H., Winterhoff, B., Kalli, K.R., Dering, J., Ginther, C., Chen, H.W., Dowdy, S. and Cliby, W. 2014. Prognostic and therapeutic relevance of molecular subtypes in high-grade serous ovarian cancer. *Journal of the National Cancer Institute*. 106.
- Koseki-Kuno, S., Yamakawa, M., Dickneite, G. and Ichinose, A. 2003. Factor XIII A subunit-deficient mice developed severe uterine bleeding events and subsequent spontaneous miscarriages. *Blood*. 102, pp.4410-4412.
- Kuhn, E., Kurman, R.J., Vang, R., Sehdev, A.S., Han, G., Soslow, R., Wang, T.L. and Shih, I.M. 2012. TP53 mutations in serous tubal intraepithelial carcinoma and concurrent pelvic high-grade serous carcinoma—evidence supporting the clonal relationship of the two lesions. *The Journal of Pathology*. 226, pp.421-426.
- Kurman, R.J. and Shih, I.M. 2010. The Origin and pathogenesis of epithelial ovarian cancer—a proposed unifying theory. *The American Journal of Surgical Pathology*. 34, 433.
- Kurman, R.J. and Shih, I.M. 2011. Molecular pathogenesis and extraovarian origin of epithelial ovarian cancer—shifting the paradigm. *Human Pathology*. 42, pp.918-931.
- Kurman, R.J. and Shih, I.M. 2016. The dualistic model of ovarian carcinogenesis: revisited, revised, and expanded. *The American Journal of Pathology*. 186, pp.733-747.
- Laki, K. and Lorand, L. 1948. On the solubility of fibrin clots. *Science*. 108, 280.
- Lawrie, T.A., Winter-Roach, B.A., Heus, P. and Kitchener, H.C. 2015. Adjuvant (post-surgery) chemotherapy for early stage epithelial ovarian cancer. *Cochrane Database of Systematic Reviews*. 2015, Cd004706.
- Ledermann, J.A. and Pujade-Lauraine, E. 2019. Olaparib as maintenance treatment for patients with platinum-sensitive relapsed ovarian cancer. *Therapeutic Advances in Medical Oncology*. 11, 1758835919849753.
- Lee, S.E., Lee, J.H., Ryu, K.W., Nam, B.H., Cho, S.J., Lee, J.Y., Kim, C.G., Choi, I.J., Kook, M.C. and Park, S.R. 2012. Preoperative plasma fibrinogen level is a useful predictor of adjacent organ involvement in patients with advanced gastric cancer. *Journal of Gastric Cancer*. 12, 81.

- Lee, S.H., Suh, I.B., Lee, E.J., Hur, G.Y., Lee, S.Y., Lee, S.Y., Shin, C., Shim, J.J., In, K.H., Kang, K.H., Yoo, S.H. and Kim, J.H. 2013. Relationships of coagulation factor XIII activity with cell-type and stage of non-small cell lung cancer. *Yonsei Medical Journal*. 54, pp.1394-1399.
- Lee, Y., Medeiros, F., Kindelberger, D., Callahan, M.J., Muto, M.G. and Crum, C.P. 2006. Advances in the recognition of tubal intraepithelial carcinoma: applications to cancer screening and the pathogenesis of ovarian cancer. *Advances in Anatomic Pathology*. 13, pp.1-7.
- Leeper, K., Garcia, R., Swisher, E., Goff, B., Greer, B. and Paley, P. 2002. Pathologic findings in prophylactic oophorectomy specimens in high-risk women. *Gynecologic Oncology*. 87, pp.52-56.
- Leitinger, B. and Hohenester, E. 2007. Mammalian collagen receptors. *Matrix Biology*. 26, pp.146-155.
- Lengyel, E. 2010. Ovarian cancer development and metastasis. *American Journal of Pathology*. 177, pp.1053-1064.
- Lenhard, S., Burges, A., Johnson, T., Kirschenhofer, A., Bruns, C., Linke, R. and Friese, K. 2008. Predictive value of PET-CT imaging versus AGO-scoring in patients planned for cytoreductive surgery in recurrent ovarian cancer. *European Journal of Obstetrics & Gynecology and Reproductive Biology*. 140, pp.263-268.
- Letai, A. and Kuter, D.J. 1999. Cancer, coagulation, and anticoagulation. *Oncologist*. 4, pp.443-449.
- Levitan, N., Dowlati, A., Remick, S., Tahsildar, H., Sivinski, L., Beyth, R. and Rimm, A. 1999. Rates of initial and recurrent thromboembolic disease among patients with malignancy versus those without malignancy. *Risk analysis using Medicare claims data. Medicine (Baltimore)*. 78, pp.285-291.
- Lewontin, R. 1988. On measures of gametic disequilibrium. *Genetics*. 120, pp.849-852.
- Li, M., Wang, J., Wang, C., Xia, L., Xu, J., Xie, X. and Lu, W. 2020. Microenvironment remodeled by tumor and stromal cells elevates fibroblast-derived COL1A1 and facilitates ovarian cancer metastasis. *Experimental Cell Research*. 394, 112153.
- Lim, B.C., Ariens, R.A.S., Carter, A.M., Weisel, J.W. and Grant, P.J. 2003. Genetic regulation of fibrin structure and function: complex gene-environment interactions may modulate vascular risk. *The Lancet*. 361, pp.1424-1431.
- Lima, L.G. and Monteiro, R.Q. 2013. Activation of blood coagulation in cancer: implications for tumour progression. *Bioscience Reports*. 33, e00064.
- Linasmitha, V., Pattaraarchachai, J. and Daengdeelert, P. 2004. Prognostic factors for survival of epithelial ovarian cancer. *International Journal of Gynecology & Obstetrics*. 85, pp.66-69.
- Liu, P., Wang, Y., Tong, L., Xu, Y., Zhang, W., Guo, Z. and Ni, H. 2015. Elevated preoperative plasma D-dimer level is a useful predictor of chemoresistance

and poor disease outcome for serous ovarian cancer patients. *Cancer Chemotherapy and Pharmacology*. 76, pp.1163-1171.

- Loewy, A.G., Dunathan, K., Kriel, R. and Wolfinger Jr, H.L.. 1961. Fibrinase. I. Purification of substrate and enzyme. *Journal of Biological Chemistry*. 236, pp.2625-2633.
- Loewy, A.G., Veneziale, C. and Forman, M. 1957. Purification of the factor involved in the formation of urea-insoluble fibrin. *Biochimica et Biophysica Acta*. 26 (3), pp.670-671.
- Lorand, L. 1977. Biochemical functions of transamidating enzymes which crosslink proteins. In *Search and Discovery*. New York: Academic Press, pp.177-193.
- Lóránd, L. 1948. A study on the solubility of fibrin clots in urea. *Hungarica acta physiologica*, 1(6), pp.192-196.
- Lóránd, L. 1950. Fibrin clot: some properties of the "serum factor". *Nature*. 166, pp.694-696.
- LTHT, Leeds Teaching Hospitals NHS Trust. 2021. *Blood Sciences Reference Ranges* [Online]. [Accessed 28th April 2021]. Available from: <https://www.leedsth.nhs.uk/a-z-of-services/pathology/blood-sciences/useful-information-and-links/>
- Lu, K., Zhu, Y., Sheng, L., Liu, L., Shen, L. and Wei, Q. 2011. Serum fibrinogen level predicts the therapeutic response and prognosis in patients with locally advanced rectal cancer. *Hepato-gastroenterology*. 58, pp.1507-1510.
- Lu, P., Weaver, V.M. and Werb, Z. 2012. The extracellular matrix: a dynamic niche in cancer progression. *Journal of Cell Biology*. 196, pp.395-406.
- Luo, Y., Kim, H.S., Kim, M., Lee, M. and Song, Y.S. 2017. Elevated plasma fibrinogen levels and prognosis of epithelial ovarian cancer: a cohort study and meta-analysis. *Gynecologic Oncology*. 28.
- Luvero, D., Milani, A. and Ledermann, J.A. 2014. Treatment options in recurrent ovarian cancer: latest evidence and clinical potential. *Therapeutic Advances in Medical Oncology*. 6, pp.229-239.
- Lyman, G.H. and Khorana, A.A. 2009. Cancer, clots and consensus: new understanding of an old problem. *Journal of Clinical Oncology*. 27, 4821.
- Madsen, C.D., Ferraris, G.M., Andolfo, A., Cunningham, O. and Sidenius, N. 2007. Upar-induced cell adhesion and migration: vitronectin provides the key. *Journal of Cell Biology*. 177, pp.927-39.
- Magwenzi, S., Ajjan, R., Standeven, K., Parapia, L. and Naseem, K. 2011. Factor XIII supports platelet activation and enhances thrombus formation by matrix proteins under flow conditions. *Journal of Thrombosis and Haemostasis*. 9, pp.820-833.
- Malik, G., Knowles, L.M., Dhir, R., Xu, S., Yang, S., Ruoslahti, E. and Pilch, J. 2010. Plasma fibronectin promotes lung metastasis by contributions to fibrin clots and tumor cell invasion. *Cancer Research*. 70, pp.4327-4334.

- Maringe, C., Walters, S., Butler, J., Coleman, M.P., Hacker, N., Hanna, L., Mosgaard, B.J., Nordin, A., Rosen, B., Engholm, G., Gjerstorff, M.L., Hatcher, J., Johannesen, T.B., Mcgahan, C.E., Meechan, D., Middleton, R., Tracey, E., Turner, D., Richards, M.A. and Rachet, B. 2012. Stage at diagnosis and ovarian cancer survival: evidence from the International Cancer Benchmarking Partnership. *Gynecologic Oncology*. 127, pp.75-82.
- Markman, M. and Bookman, M.A. 2000. Second-line treatment of ovarian cancer. *The Oncologist*. 5, pp.26-35.
- Marquez, R.T., Baggerly, K.A., Patterson, A.P., Liu, J., Broaddus, R., Frumovitz, M., Atkinson, E.N., Smith, D.I., Hartmann, L. and Fishman, D. 2005. Patterns of gene expression in different histotypes of epithelial ovarian cancer correlate with those in normal fallopian tube, endometrium, and colon. *Clinical Cancer Research*. 11, pp.6116-6126.
- Mccluggage, W.G. 2011. Morphological subtypes of ovarian carcinoma: a review with emphasis on new developments and pathogenesis. *Pathology*. 43, pp.420-432.
- Mcguire, W.P., Hoskins, W.J., Brady, M.F., Kucera, P.R., Partridge, E.E., Look, K.Y., Clarke-Pearson, D.L. and Davidson, M. 1996. Cyclophosphamide and cisplatin compared with paclitaxel and cisplatin in patients with stage III and stage IV ovarian cancer. *New England Journal of Medicine*. 334, pp.1-6.
- Mckenzie, A.J., Hicks, S.R., Svec, K.V., Naughton, H., Edmunds, Z.L. and Howe, A.K. 2018. The mechanical microenvironment regulates ovarian cancer cell morphology, migration, and spheroid disaggregation. *Scientific Reports*. 8, pp.1-20.
- Merajver, S.D., Pham, T.M., Caduff, R.F., Chen, M., Poy, E.L., Cooney, K.A., Weber, B.L., Collins, F.S., Johnston, C. and Frank, T.S. 1995. Somatic mutations in the BRCA1 gene in sporadic ovarian tumours. *Nature Genetics*. 9, pp.439-443.
- Mezei, Z.A., Katona, É., Kállai, J., Bereczky, Z., Molnár, É., Kovács, B., Ajzner, É., Bagoly, Z., Miklós, T. and Muszbek, L. 2016. Regulation of plasma factor XIII levels in healthy individuals; a major impact by subunit B intron K c.1952+144 C>G polymorphism. *Thrombosis Research*. 148, pp.101-106.
- Mikkola, H., Syrjala, M., Rasi, V., Vahtera, E., Hamalainen, E., Peltonen, L. and Palotie, A. 1994. Deficiency in the A-subunit of coagulation factor XIII: two novel point mutations demonstrate different effects on transcript levels.
- Minig, L., Trimble, E.L. and Colombo, N. 2017. Optimal treatment for women with ovarian cancer. In: Schwab, M. (ed.) *Encyclopedia of cancer*. Berlin, Heidelberg: Springer Berlin Heidelberg.
- Mitchell, J.L., Lionikiene, A.S., Fraser, S.R., Whyte, C.S., Booth, N.A. and Mutch, N.J. 2014. Functional factor XIII-A is exposed on the stimulated platelet surface. *Blood*. 124, pp.3982-3990.
- Mitra, A., Sawada, K., Tiwari, P., Mui, K., Gwin, K. and Lengyel, E. 2011. Ligand-independent activation of c-Met by fibronectin and $\alpha 5 \beta 1$ -integrin regulates ovarian cancer invasion and metastasis. *Oncogene* 30, pp.1566-1576.

- Momenimovahed, Z., Tiznobaik, A., Taheri, S. and Salehiniya, H. 2019. Ovarian cancer in the world: epidemiology and risk factors. *International Journal of Women's Health*. 11, 287.
- Morrissey, C., True, L.D., Roudier, M.P., Coleman, I. M., Hawley, S., Nelson, P.S., Coleman, R., Wang, Y.C., Corey, E. and Lange, P.H. 2008. Differential expression of angiogenesis associated genes in prostate cancer bone, liver and lymph node metastases. *Clinical & Experimental Metastasis*. 25, pp.377-388.
- Mosher, D.F. and Schad, P.E. 1979. Cross-linking of fibronectin to collagen by blood coagulation Factor xiii. *Journal of Clinical Investigation*. 64, pp.781-787.
- Mosmann, T. 1983. Rapid colorimetric assay for cellular growth and survival: application to proliferation and cytotoxicity assays. *Journal of Immunological Methods*. 65, pp.55-63.
- Muszbek, L., Bereczky, Z., Bagoly, Z., Komáromi, I. and Katona, É. 2011. *Factor XIII: A Coagulation Factor With Multiple Plasmatic and Cellular Functions*.
- Myassays.Com. 2021. Internet. Available at: <https://myassays.com/welcome.aspx>: Online data analysis software. [Accessed Last accessed 25/05/2021].
- Nagy, J.A., Meyers, M.S., Mase, E.M., Herzberg, K.T. and Dvorak, H.F. 1995. Pathogenesis of ascites tumor growth: fibrinogen influx and fibrin accumulation in tissues lining the peritoneal cavity. *Cancer Research*. 55, pp.369-375.
- Nemes, Z. and Thomazy, V. 1988. Diagnostic significance of histiocyte-related markers in malignant histiocytosis and true histiocytic lymphoma. *Cancer*. 62, pp.1970-1980.
- Network, C. G. A. R. 2011. Integrated genomic analyses of ovarian carcinoma. *Nature*. 474, 609.
- Ngoka, L.C. 2008. Sample prep for proteomics of breast cancer: proteomics and gene ontology reveal dramatic differences in protein solubilization preferences of radioimmunoprecipitation assay and urea lysis buffers. *Proteome Science*. 6, pp.1-24.
- NICE., National Institute for Care and Health Excellence. 2003. Guidance on the use of paclitaxel in the treatment of ovarian cancer [Online] Technology appraisal guidance TA55. Available from <https://www.nice.org.uk/guidance/ta55>:
- NICE., National Institute for Care and Health Excellence. 2011. Ovarian Cancer: Recognition and Initial Management. [Online] Clinical Guidelines CG122. Available from <https://www.nice.org.uk/guidance/cg122>:
- Nikolajsen, C.L., Dyrland, T.F., Poulsen, E.T., Enghild, J.J. and Scavenius, C. 2014. Coagulation factor xiii substrates in human plasma: identification and incorporation into the clot. *Journal of Biological Chemistry*. 289, pp.6526-6534.
- Nowicka, A., Marini, F.C., Solley, T.N., Elizondo, P.B., Zhang, Y., Sharp, H.J., Broaddus, R., Kolonin, M., Mok, S.C. and Thompson, M.S. 2013. Human

omenta-derived adipose stem cells increase ovarian cancer proliferation, migration, and chemoresistance. *PLOS ONE*. 8, e81859.

- O'shannessy, D.J., Jackson, S.M., Twine, N.C., Hoffman, B.E., Dezso, Z., Agoulnik, S.I. and Somers, E.B. 2013. Gene expression analyses support fallopian tube epithelium as the cell of origin of epithelial ovarian cancer. *International Journal of Molecular Sciences*. 14, pp.13687-13703.
- Östman, A. 2012. The tumor microenvironment controls drug sensitivity. *Nature Medicine*. 18, pp.1332-1334.
- Oswald. 2007. *E.coli electroporation vs chemical transformation*. [Online]. [Accessed 6 June 2021]. Available from: <https://bitesizebio.com/10297/ecoli-electroporation-vs-chemical-transformation/>
- Oudin, M.J. and Weaver, V.M. Physical and chemical gradients in the tumor microenvironment regulate tumor cell invasion, migration, and metastasis. In *Cold Spring Harbor symposia on quantitative biology*, 2016. Cold Spring Harbor Laboratory Press. **81**, pp.189-205.
- Oza, A.M., Cook, A.D., Pfisterer, J., Embleton, A., Ledermann, J.A., Pujade-Lauraine, E., Kristensen, G., Carey, M.S., Beale, P. and Cervantes, A. 2015. Standard chemotherapy with or without bevacizumab for women with newly diagnosed ovarian cancer (ICON7): overall survival results of a phase 3 randomised trial. *The Lancet Oncology*. 16, pp.928-936.
- Ozols, R.F., Bundy, B.N., Greer, B.E., Fowler, J.M., Clarke-Pearson, D., Burger, R.A., Mannel, R.S., Degeest, K., Hartenbach, E.M. and Baergen, R. 2003. Phase III trial of carboplatin and paclitaxel compared with cisplatin and paclitaxel in patients with optimally resected stage III ovarian cancer: a Gynecologic Oncology Group study. *Journal of Clinical Oncology*. 21, pp.3194-3200.
- Palumbo, J.S., Barney, K.A., Blevins, E.A., Shaw, M.A., Mishra, A., Flick, M.J., Kombrinck, K.W., Talmage, K.E., Souri, M., Ichinose, A. and Degen, J.L. 2008. Factor XIII transglutaminase supports hematogenous tumor cell metastasis through a mechanism dependent on natural killer cell function. *Journal of Thrombosis and Haemostasis*. 6, pp.812-819.
- Palumbo, J.S., Kombrinck, K.W., Drew, A.F., Grimes, T.S., Kiser, J.H., Degen, J.L. and Bugge, T.H. 2000. Fibrinogen is an important determinant of the metastatic potential of circulating tumor cells. *Blood*. 96, pp.3302-3309.
- Palumbo, J.S., Potter, J.M., Kaplan, L.S., Talmage, K., Jackson, D.G. and Degen, J.L. 2002. Spontaneous hematogenous and lymphatic metastasis, but not primary tumor growth or angiogenesis, is diminished in fibrinogen-deficient mice. *Cancer Research*. 62, pp.6966-6972.
- Park, J.Y., Kim, D.Y., Suh, D.S., Kim, J.H., Kim, Y.M., Kim, Y.T. and Nam, J.H. 2008. Outcomes of fertility-sparing surgery for invasive epithelial ovarian cancer: oncologic safety and reproductive outcomes. *Gynecologic Oncology*. 110, pp.345-353.
- Pedersen, L.C., Yee, V.C., Bishop, P.D., Letrong, I., Teller, D.C. and Stenkamp, R.E. 1994. Transglutaminase factor-XIII uses proteinase-like catalytic triad to cross-link macromolecules. *Protein Science*. 3, pp.1131-1135.

- Perren, T.J., Swart, A.M., Pfisterer, J., Ledermann, J.A., Pujade-Lauraine, E., Kristensen, G., Carey, M.S., Beale, P., Cervantes, A. and Kurzeder, C. 2011. A phase 3 trial of bevacizumab in ovarian cancer. *New England Journal of Medicine*. 365, pp.2484-2496.
- Petrucci, N., Daly, M.B. and Pal, T. 2016. BRCA1-and BRCA2-associated hereditary breast and ovarian cancer. 1998 September 4 [Updated 2016 December 15]. In: Adam, MP. Ardinger, HH. Pagon, RA. (editors). *GeneReviews® [Internet]*. University of Washington, Seattle; 1993-2021. [Online]. [Accessed 20th June 2021]. Available from: <https://www.ncbi.nlm.nih.gov/sites/books/NBK1247/>.
- Piccart, M.J., Bertelsen, K., James, K., Cassidy, J., Mangioni, C., Simonsen, E., Stuart, G., Kaye, S., Vergote, I. and Blom, R. 2000. Randomized intergroup trial of cisplatin–paclitaxel versus cisplatin–cyclophosphamide in women with advanced epithelial ovarian cancer: three-year results. *Journal of the National Cancer Institute*. 92, pp.699-708.
- Piek, J.M., Verheijen, R.H., Kenemans, P., Massuger, L.F., Bulten, H. and Van Diest, P.J. 2003. BRCA1/2-related ovarian cancers are of tubal origin: a hypothesis. *Gynecologic Oncology*. 90(2), p.491.
- Pignata, S., Scambia, G., Katsaros, D., Gallo, C., Pujade-Lauraine, E., De Placido, S., Bologna, A., Weber, B., Raspagliesi, F. and Panici, P.B. 2014. Carboplatin plus paclitaxel once a week versus every 3 weeks in patients with advanced ovarian cancer (MITO-7): a randomised, multicentre, open-label, phase 3 trial. *The Lancet Oncology*. 15, pp.396-405.
- Pitt-Rivers, R. and Impiombato, F.S. 1968. The binding of sodium dodecyl sulphate to various proteins. *Biochemical Journal*. 109, pp.825-830.
- Polterauer, S., Grimm, C., Seebacher, V., Concin, N., Marth, C., Tomovski, C., Husslein, H., Leipold, H., Hefler-Frischmuth, K., Tempfer, C., Reinthaller, A. and Hefler, L. 2009. Plasma fibrinogen levels and prognosis in patients with ovarian cancer: a multicenter study. *Oncologist*. 14, pp.979-985.
- Porrello, A., Leslie, P.L., Harrison, E.B., Gorentla, B.K., Kattula, S., Ghosh, S.K., Azam, S. H., Holtzhausen, A., Chao, Y.L. and Hayward, M.C. 2018. Factor XIIIa—expressing inflammatory monocytes promote lung squamous cancer through fibrin cross-linking. *Nature Communications*. 9, pp.1-19.
- Prandoni, P., Lensing, A.W., Piccioli, A., Bernardi, E., Simioni, P., Girolami, B., Marchiori, A., Sabbion, P., Prins, M.H., Noventa, F. and Girolami, A. 2002. Recurrent venous thromboembolism and bleeding complications during anticoagulant treatment in patients with cancer and venous thrombosis. *Blood*. 100, pp.3484-3488.
- Prat, J. and FIGO Committee on Gynaecologic Oncology. 2014. Staging classification for cancer of the ovary, fallopian tube, and peritoneum. *International Journal of Gynaecology and Obstetrics*. 124(1), p.1.
- Procyk, R., Bishop, P.D. and Kudryk, B. 1993. Fibrin-recombinant human factor XIII a-subunit association. *Thrombosis Research*. 71, pp.127-138.
- Perren et al. 2011. The New England Journal of Medicine website. In: Protocol, Appendix 14 Translational Research (biomarkers and pharmacogenomics),

pp. 119-121. [Online]. [Accessed 10th June 2021]. Available from: https://www.nejm.org/doi/full/10.1056/nejmoa1103799#article_supplementary_material.

- Przybycin, C.G., Kurman, R.J., Ronnett, B.M., Shih, I.M. and Vang, R. 2010. Are all pelvic (nonuterine) serous carcinomas of tubal origin? *The American Journal of Surgical Pathology*. 34, pp.1407-1416.
- Qayyum, A., Coakley, F.V., Westphalen, A.C., Hricak, H., Okuno, W.T. and Powell, B. 2005. Role of CT and MR imaging in predicting optimal cytoreduction of newly diagnosed primary epithelial ovarian cancer. *Gynecologic Oncology*. 96, pp.301-306.
- Qiu, J., Yu, Y., Fu, Y., Ye, F., Xie, X. and Lu, W. 2012. Preoperative plasma fibrinogen, platelet count and prognosis in epithelial ovarian cancer. *Journal of Obstetrics and Gynaecology Research*. 38, pp.651-657.
- Rath, A., Glibowicka, M., Nadeau, V.G., Chen, G. and Deber, C.M. 2009. Detergent binding explains anomalous SDS-PAGE migration of membrane proteins. *Proceedings of the National Academy of Sciences of the United States of America*. 106, pp.1760-1765.
- Raut, S., Merton, R., Rigsby, P., Muszbek, L., Seitz, R., Ariëns, R., Barrowcliffe, T., Ichinose, A., On Behalf of The ISTH/SSC Factor XIII Subcommittee. and The Factor XIII Standardization Working Party. 2007. A collaborative study to establish the 1st International Standard for factor XIII plasma. *Journal of Thrombosis and Haemostasis*. 5(9), pp.1923-1929.
- Ray-Coquard, I., Morice, P., Lorusso, D., Prat, J., Oaknin, A., Pautier, P., Colombo, N. and ESMO Guideline Committee. 2018. Non-epithelial ovarian cancer: ESMO Clinical Practice Guidelines for diagnosis, treatment and follow-up. *Annals of Oncology*. 29(Suppl 4), iv1-iv18.
- Ray-Coquard, I., Pautier, P., Pignata, S., Pérol, D., González-Martín, A., Berger, R., Fujiwara, K., Vergote, I., Colombo, N. and Mäenpää, J. 2019. Olaparib plus bevacizumab as first-line maintenance in ovarian cancer. *New England Journal of Medicine*. 381, pp.2416-2428.
- Reid, M. B., Gray, C., Fear, J.D. and Bird, C.C. 1986. Immunohistological demonstration of factors xiii^a and xiii^s in reactive and neoplastic fibroblastic and fibro-histiocytic lesions. *Histopathology*. 10, pp.1171-1178.
- Reynolds, T., Butine, M., Visich, J., Gunewardena, K., Macmahon, M., Pederson, S., Bishop, P. and Morton, K. 2005. Safety, pharmacokinetics, and immunogenicity of single-dose rfxiii administration to healthy volunteers. *Journal of Thrombosis and Haemostasis*. 3, pp.922-928.
- Ricciardelli, C. and Rodgers, R.J. Extracellular matrix of ovarian tumors. *Seminars in Reproductive Medicine*. 24(4), pp.270-282.
- Rice, A., Cortes, E., Lachowski, D., Cheung, B., Karim, S., Morton, J. and Del Rio Hernandez, A. 2017. Matrix stiffness induces epithelial–mesenchymal transition and promotes chemoresistance in pancreatic cancer cells. *Oncogenesis*. 6, e352-e352.

- Richardson, V.R., Cordell, P., Standeven, K.F. and Carter, A.M. 2013. Substrates of Factor XIII-A: roles in thrombosis and wound healing. *Clinical Science*. 124, pp.123-37.
- Rieppi, M., Vergani, V., Gatto, C., Zanetta, G., Allavena, P., Taraboletti, G. and Giavazzi, R. 1999. Mesothelial cells induce the motility of human ovarian carcinoma cells. *International Journal of Cancer*. 80, pp.303-307.
- Robbins, K. 1944. A study on the conversion of fibrinogen to fibrin. *American Journal of Physiology*. 142, pp.581-588.
- Ruoslahti, E. and Pierschbacher, M.D. 1987. New perspectives in cell adhesion: RGD and integrins. *Science*. 238, pp.491-497.
- Russo, A., Calò, V., Bruno, L., Rizzo, S., Bazan, V. and Di Fede, G. 2009. Hereditary ovarian cancer. *Critical Reviews in Oncology/Hematology*. 69, pp.28-44.
- Saha, N., Aston, C.E., Low, P.S. and Kamboh, M.I. 2000. Racial and genetic determinants of plasma factor XIII activity. *Genetic Epidemiology*. 19, pp.440-455.
- Sakurai, M., Satoh, T., Matsumoto, K., Michikami, H., Nakamura, Y., Nakao, S., Ochi, H., Onuki, M., Minaguchi, T. and Yoshikawa, H. 2015. High pretreatment plasma D-dimer levels are associated with poor prognosis in patients with ovarian cancer independently of venous thromboembolism and tumor extension. *International Journal of Gynecologic Cancer*. 25(4), pp.593-598.
- Sampson, M.T. and Kakkar, A.K. 2002. Coagulation proteases and human cancer. *Biochemical Society Transactions*. 30, pp.201-207.
- Satpathy, M., Shao, M., Emerson, R., Donner, D.B. and Matei, D. 2009. Tissue transglutaminase regulates matrix metalloproteinase-2 in ovarian cancer by modulating camp-response element-binding protein activity. *Journal of Biological Chemistry*. 284, pp.15390-15399.
- Savant, S.S., Sriramkumar, S. and O'hagan, H.M. 2018. The role of inflammation and inflammatory mediators in the development, progression, metastasis, and chemoresistance of epithelial ovarian cancer. *Cancers*. 10(8), p.251.
- Sawai, Y., Yamanaka, Y. and Nomura, S. 2020. Clinical Significance of Factor XIII Activity and Monocyte-Derived Microparticles in Cancer Patients. *Vascular Health and Risk Management*. 16, pp.103-110.
- Schildkraut, J.M., Schwingl, P.J., Bastos, E., Evanoff, A. and Hughes, C. 1996. Epithelial ovarian cancer risk among women with polycystic ovary syndrome. *Obstetrics & Gynecology*. 88, pp.554-559.
- Schneider, G., Suszynska, M., Kakar, S. and Ratajczak, M.Z. 2016. Vitronectin in the ascites of human ovarian carcinoma acts as a potent chemoattractant for ovarian carcinoma: Implication for metastasis by cancer stem cells. *Journal of Cancer Stem Cell Research*. 4, e1005.
- Hankinson, SE., Danforth, KN. Ovarian cancer. In: Schottenfeld, D. and Fraumeni Jr, J.F. 2006. *Cancer epidemiology and prevention*. Third ed, pp 1013-1026. Oxford University Press.

- Schroeder, V. and Kohler, H.P. 2013. New developments in the area of factor XIII. *Journal of Thrombosis and Haemostasis*. 11, pp.234-244.
- Schroeder, V., Vuissoz, J.M., Cafilisch, A. and Kohler, H.P. 2007. Factor XIII activation peptide is released into plasma upon cleavage by thrombin and shows a different structure compared to its bound form. *Thrombosis and Haemostasis*. 97, pp.890-898.
- Seebacher, V., Polterauer, S., Grimm, C., Husslein, H., Leipold, H., Hefler-Frischmuth, K., Tempfer, C., Reinthaller, A. and Hefler, L. 2010. The prognostic value of plasma fibrinogen levels in patients with endometrial cancer: a multi-centre trial. *British Journal of Cancer*. 102, pp.952-956.
- Seki, H. 1986. [Studies on plasma proteins in normal pregnancy and gynecological malignancy]. *Nihon Sanka Fujinka Gakkai Zasshi*. 38, pp.317-326.
- Sethi, G., Shanmugam, M.K., Ramachandran, L., Kumar, A.P. and Tergaonkar, V. 2012. Multifaceted link between cancer and inflammation. *Bioscience Reports*. **32**(1), pp.1-15.
- Shemirani, A.H., Haramura, G., Bagoly, Z. and Muszbek, L. 2006. The combined effect of fibrin formation and factor XIII A subunit Val34Leu polymorphism on the activation of factor XIII in whole plasma. *Biochimica et Biophysica Acta (BBA)-Proteins and Proteomics*. **1764**(8), pp.1420-1423.
- Shen, D.W., Pouliot, L.M., Hall, M.D. and Gottesman, M.M. 2012. Cisplatin resistance: a cellular self-defense mechanism resulting from multiple epigenetic and genetic changes. *Pharmacological Reviews*. **64**(3), pp.706-721.
- Shen, Y., Shen, R., Ge, L., Zhu, Q. and Li, F. 2012. Fibrillar type I collagen matrices enhance metastasis/invasion of ovarian epithelial cancer via β 1 integrin and PTEN signals. *International Journal of Gynecologic Cancer*. **22**(8), pp.1316-1324.
- Shi, D.Y. and Wang, S.J. 2017. Advances of coagulation factor XIII. *Chinese Medical Journal*. **130**(2), p.219.
- Shih, I.M. and Kurman, R.J. 2004. Ovarian tumorigenesis: a proposed model based on morphological and molecular genetic analysis. *The American Journal of Pathology*. 164, pp.1511-1518.
- Siddik, Z.H. 2003. Cisplatin: mode of cytotoxic action and molecular basis of resistance. *Oncogene*. 22, pp.7265-7279.
- Siebenlist, K.R., Rosenthal, A., Mosesson, M.W., Gohr, C.M., Masuda, I. and Heinkel, D. 2004. Regulation of transglutaminase activity in articular chondrocytes through thrombin receptor-mediated factor XIII synthesis. *Thrombosis and Haemostasis*.
- Simon, A., Bagoly, Z., Hevessy, Z., Csathy, L., Katona, E., Vereb, G., Ujfalusi, A., Szerafin, L., Muszbek, L. and Kappelmayer, J. 2012. Expression of coagulation factor XIII subunit A in acute promyelocytic leukemia. *Cytometry Part B: Clinical Cytometry*. **82**(4), pp.209-216.

- Simpson-Haidaris, P. and Rybarczyk, B. 2001. Tumors and fibrinogen: the role of fibrinogen as an extracellular matrix protein. *Annals of the New York Academy of Sciences*. 936, pp.406-425.
- Singh, S., Akhter, M.S., Dodt, J., Sharma, A., Kaniyappan, S., Yadegari, H., Ivaskevicius, V., Oldenburg, J. and Biswas, A. 2019a. Disruption of Structural Disulfides of Coagulation FXIII-B Subunit; Functional Implications for a Rare Bleeding Disorder. *International Journal of Molecular Sciences*. 20, 1956.
- Singh, S., Akhter, M.S., Dodt, J., Volkens, P., Reuter, A., Reinhart, C., Krettler, C., Oldenburg, J. and Biswas, A. 2019b. Identification of potential novel interacting partners for coagulation factor XIII B (FXIII-B) subunit, a protein associated with a rare bleeding disorder. *International Journal of Molecular Sciences*. 20(11), p. 2682.
- Smoter, M., Bodnar, L., Grala, B., Stec, R., Zieniuk, K., Kozłowski, W. and Szczylik, C. 2013. Tau protein as a potential predictive marker in epithelial ovarian cancer patients treated with paclitaxel/platinum first-line chemotherapy. *Journal of Experimental & Clinical Cancer Research*. 32, pp.1-8.
- Soendergaard, C., Kvist, P.H., Seidelin, J.B. and Nielsen, O.H. 2013. Tissue-regenerating functions of coagulation factor XIII. *Journal of Thrombosis and Haemostasis*. 11, pp.806-816.
- Sourcebioscience, Rochdale, UK. 2021. *Sanger sequencing service* [Online]. [Accessed 25th May 2021]. Available from: <http://www.lifesciences.sourcebioscience.com/genomic-services/sanger-sequencing-service/>
- Souri, M., Osaki, T. and Ichinose, A. 2015. The non-catalytic B subunit of coagulation factor XIII accelerates fibrin cross-linking. *Journal of Biological Chemistry*. 290, pp.12027-12039.
- Sousa, G.F.D., Włodarczyk, S.R. and Monteiro, G. 2014. Carboplatin: molecular mechanisms of action associated with chemoresistance. *Brazilian Journal of Pharmaceutical Sciences*. 50, pp.693-701.
- Soussi, T., Ishioka, C., Claustres, M. and Bérout, C. 2006. Locus-specific mutation databases: pitfalls and good practice based on the p53 experience. *Nature Reviews Cancer*. 6, pp.83-90.
- Ständker, L., Enger, A., Schulz-Knappe, P., Wohn, K.D., Germer, M., Raida, M., Forssmann, W.G. and Preissner, K.T. 1996. Structural and functional characterization of vitronectin-derived RGD-containing peptides from human hemofiltrate. *European Journal of Biochemistry*. 241, pp.557-563.
- Social Science Statistics website. 2021. *Stangroom J. Chi Square Calculator*. [Online]. [Accessed 20th March 2021]. Available from: <https://www.socscistatistics.com/tutorials/chisquare/default.aspx>.
- Stieler, M., Weber, J., Hils, M., Kolb, P., Heine, A., Büchold, C., Pasternack, R. and Klebe, G. 2013. Structure of active coagulation factor XIII triggered by calcium binding: basis for the design of next-generation anticoagulants. *Angewandte Chemie International Edition*. 52, pp.11930-11934.

- Stuart, G.C., Kitchener, H., Bacon, M., Marth, C., Thigpen, T. and Trimble, E. 2011. 2010 Gynecologic Cancer intergroup (GCIG) consensus statement on clinical trials in ovarian cancer. *International Journal of Gynecological Cancer*. 21, pp.750-755.
- Suzuki, R., Toda, H. and Takamura, Y. 1989. Dynamics of blood coagulation factor XIII in ulcerative colitis and preliminary study of the factor XIII concentrate. *Blut*. 59, pp.162-164.
- Tan, T.Z., Miow, Q.H., Huang, R.Y., Wong, M.K., Ye, J., Lau, J.A., Wu, M.C., Bin Abdul Hadi, L.H., Soong, R., Choolani, M., Davidson, B., Nesland, J.M., Wang, L.Z., Matsumura, N., Mandai, M., Konishi, I., Goh, B.C., Chang, J.T., Thiery, J.P. and Mori, S. 2013. Functional genomics identifies five distinct molecular subtypes with clinical relevance and pathways for growth control in epithelial ovarian cancer. *EMBO Molecular Medicine*. 5, pp.1051-1066.
- Tan, T.Z., Yang, H., Ye, J., Low, J., Choolani, M., Tan, D.S., Thiery, J.P. and Huang, R.Y. 2015. CSIOVDB: a microarray gene expression database of epithelial ovarian cancer subtype. *Oncotarget*. 6, pp.43843-43852.
- Tang, L., Liu, K., Wang, J., Wang, C., Zhao, P. and Liu, J. 2010. High preoperative plasma fibrinogen levels are associated with distant metastases and impaired prognosis after curative resection in patients with colorectal cancer. *Journal of Surgical Oncology*. 102, pp.428-432.
- Tangjitgamol, S., Manusirivithaya, S., Laopaiboon, M., Lumbiganon, P. and Bryant, A. 2016. Interval debulking surgery for advanced epithelial ovarian cancer. *Cochrane Database of Systematic Reviews*. John Wiley & Sons, Ltd. 1, pp.1465-1858.
- Taniguchi, M., Ayabe, T., Ashida, T., Fujimoto, Y. and Kohgo, Y. 2002. Genetic and phenotypic polymorphisms of the A subunit of coagulation factor XIII in Japanese population. *Biochemical Genetics*. 40, pp.339-349.
- Tas, F., Kilic, L., Bilgin, E., Keskin, S., Sen, F., Ciftci, R., Yildiz, I. and Yasasever, V. 2013. Clinical and prognostic significance of coagulation assays in advanced epithelial ovarian cancer. *International Journal of Gynecological Cancer*. 23, pp.276-281.
- The Human Protein Atlas website. Factor 13A Tissue Atlas. [Online]. Available at: <https://www.proteinatlas.org/ENSG00000124491-F13A1/tissue>. [Accessed 11th January 2021].
- Thibault, B., Castells, M., Delord, J.P. and Couderc, B. 2014. Ovarian cancer microenvironment: implications for cancer dissemination and chemoresistance acquisition. *Cancer Metastasis Reviews*. 33, pp.17-39.
- Timofeev, J., Galgano, M.T., Stoler, M.H., Lachance, J.A., Modesitt, S.C. and Jazaeri, A.A. 2010. Appendiceal pathology at the time of oophorectomy for ovarian neoplasms. *Obstetrics & Gynecology*. 116, pp.1348-1353.
- Tinholt, M., Sandset, P.M. and Iversen, N. 2016. Polymorphisms of the coagulation system and risk of cancer. *Thrombosis Research*. 140, S49-S54.

- Tothill, R.W., Tinker, A.V., George, J., Brown, R., Fox, S.B., Lade, S., Johnson, D.S., Trivett, M.K., Etemadmoghadam, D. and Locandro, B. 2008. Novel molecular subtypes of serous and endometrioid ovarian cancer linked to clinical outcome. *Clinical Cancer Research*. 14, pp.5198-5208.
- Trimbos, J.B., Parmar, M., Vergote, I., Guthrie, D., Bolis, G., Colombo, N., Vermorken, J.B., Torri, V., Mangioni, C., Pecorelli, S., Lissoni, A. and Swart, A.M. 2003. International Collaborative Ovarian Neoplasm trial 1 and Adjuvant chemotherapy In Ovarian Neoplasm trial: two parallel randomized phase III trials of adjuvant chemotherapy in patients with early-stage ovarian carcinoma. *Journal of the National Cancer Institute*. 95, pp.105-112.
- Tsilidis, K., Allen, N., Key, T., Dossus, L., Lukanova, A., Bakken, K., Lund, E., Fournier, A., Overvad, K. and Hansen, L. 2011. Oral contraceptive use and reproductive factors and risk of ovarian cancer in the European Prospective Investigation into Cancer and Nutrition. *British Journal of Cancer*. 105, pp.1436-1442.
- Tuck, M.K., Chan, D.W., Chia, D., Godwin, A.K., Grizzle, W.E., Krueger, K.E., Rom, W., Sanda, M., Sorbara, L. and Stass, S. 2009. Standard operating procedures for serum and plasma collection: early detection research network consensus statement standard operating procedure integration working group. *Journal of Proteome Research*. 8, pp.113-117.
- Turnock, K., Bulmer, J.N. and Gray, C. 1990. Phenotypic characterization of macrophage subpopulations and localization of factor XIII in the stromal cells of carcinomas. *Histochem J*. 22, pp.661-666.
- Ueki, S., Takagi, J. and Saito, Y. 1996. Dual functions of transglutaminase in novel cell adhesion. *Journal of Cell Science*. **109**(11), pp.2727-2735.
- Unlu, B. and Versteeg, H.H. 2014. Effects of tumor-expressed coagulation factors on cancer progression and venous thrombosis: is there a key factor? *Thrombosis Research*. **133**(2), S76-84.
- Vairaktaris, E., Vassiliou, S., Yapijakis, C., Spyridonidou, S., Vylliotis, A., Derka, S., Nkenke, E., Fourtounis, G., Neukam, F.W. and Patsouris, E. 2007. Increased risk for oral cancer is associated with coagulation factor XIII but not with factor XII. *Oncology Reports*. 18, pp.1537-1543.
- Van Der Burg, M.E., Van Lent, M., Buyse, M., Kobierska, A., Colombo, N., Favalli, G., Lacave, A.J., Nardi, M., Renard, J. and Pecorelli, S. 1995. The effect of debulking surgery after induction chemotherapy on the prognosis in advanced epithelial ovarian cancer. *New England Journal of Medicine*. 332, pp.629-634.
- Van Hylckama Vlieg, A., Komanasin, N., Ariens, R.A., Poort, S.R., Grant, P.J., Bertina, R.M. and Rosendaal, F.R. 2002. Factor XIII Val34Leu polymorphism, factor XIII antigen levels and activity and the risk of deep venous thrombosis. *British Journal of Haematology*. 119, pp.169-175.
- Van Wersch, J.W., Peters, C. and Ubachs, J.M. 1994. Coagulation factor XIII in plasma of patients with benign and malignant gynaecological tumours. *European Journal of Clinical Chemistry and Clinical Biochemistry*. 32, pp.681-684.

- Vang, R., Shih, I.M. and Kurman, R.J. 2009. Ovarian low-grade and high-grade serous carcinoma: pathogenesis, clinicopathologic and molecular biologic features, and diagnostic problems. *Advances in Anatomic Pathology*. 16, 267.
- Vergote, I., Coens, C., Nankivell, M., Kristensen, G.B., Parmar, M.K., Ehlen, T., Jayson, G. C., Johnson, N., Swart, A.M. and Verheijen, R. 2018. Neoadjuvant chemotherapy versus debulking surgery in advanced tubo-ovarian cancers: pooled analysis of individual patient data from the EORTC 55971 and CHORUS trials. *The Lancet Oncology*. 19, pp.1680-1687.
- Vergote, I., Tropé, C.G., Amant, F., Kristensen, G.B., Ehlen, T., Johnson, N., Verheijen, R. H., Van Der Burg, M.E., Lacave, A.J. and Panici, P.B. 2010. Neoadjuvant chemotherapy or primary surgery in stage IIIC or IV ovarian cancer. *New England Journal of Medicine*. 363, pp.943-953.
- Verhaak, R.G., Tamayo, P., Yang, J.Y., Hubbard, D., Zhang, H., Creighton, C.J., Fereday, S., Lawrence, M., Carter, S.L. and Mermel, C.H. 2012. Prognostically relevant gene signatures of high-grade serous ovarian carcinoma. *The Journal of Clinical Investigation*. 123.
- Vilar, R., Fish, R.J., Casini, A. and Neerman-Arbez, M. 2020. Fibrin(ogen) in human disease: both friend and foe. *Haematologica*. 105, pp.284-296.
- Visich, J.E., Zuckerman, L.A., Butine, M.D., Gunewardena, K.A., Wild, R., Morton, K.M. and Reynolds, T.C. 2005. Safety and pharmacokinetics of recombinant factor XIII in healthy volunteers: a randomized placebo-controlled double-blind, multi-dose study. *Thrombosis and Haemostasis*. 94, pp.802-807.
- Vossen, C.Y., Hoffmeister, M., Chang-Claude, J.C., Rosendaal, F.R. and Brenner, H. 2011. Clotting factor gene polymorphisms and colorectal cancer risk. *Journal of Clinical Oncology*. 29, pp.1722-1727.
- Wang, C., Armasu, S.M., Kalli, K.R., Maurer, M.J., Heinzen, E.P., Keeney, G.L., Cliby, W.A., Oberg, A.L., Kaufmann, S.H. and Goode, E.L. 2017. Pooled clustering of high-grade serous ovarian cancer gene expression leads to novel consensus subtypes associated with survival and surgical outcomes. *Clinical Cancer Research*. 23, pp.4077-4085.
- Wang, E., Ngalmé, Y., Panelli, M.C., Nguyen-Jackson, H., Deavers, M., Mueller, P., Hu, W., Savary, C.A., Kobayashi, R. and Freedman, R.S. 2005. Peritoneal and subperitoneal stroma may facilitate regional spread of ovarian cancer. *Clinical Cancer Research*. 11, pp.113-122.
- Wang, J.P. and Hielscher, A. 2017. Fibronectin: how its aberrant expression in tumors may improve therapeutic targeting. *Journal of Cancer*. 8, 674.
- Wang, M., Zhao, J., Zhang, L., Wei, F., Lian, Y., Wu, Y., Gong, Z., Zhang, S., Zhou, J. and Cao, K. 2017. Role of tumor microenvironment in tumorigenesis. *Journal of Cancer*. 8, 761.
- Wang, X., Wang, E., Kavanagh, J. J. and Freedman, R. S. 2005. Ovarian cancer, the coagulation pathway, and inflammation. *Journal of Translational Medicine*. 3, 25.

- Wartiovaara, U., Mikkola, H., Szoke, G., Haramura, G., Karpati, L., Balogh, I., Lassila, R., Muszbek, L. and Palotie, A. 2000. Effect of Val34Leu polymorphism on the activation of the coagulation factor XIII-A. *Thrombosis and Haemostasis*. 84, pp.595-600.
- Weiss, M.S., Metzner, H.J. and Hilgenfeld, R. 1998. Two non-proline cis peptide bonds may be important for factor XIII function. *FEBS Letters*. 423, pp.291-296.
- Wells, P.S., Anderson, J.L., Scarvelis, D.K., Doucette, S.P. and Gagnon, F. 2006. Factor XIII Val34Leu variant is protective against venous thromboembolism: a huge review and meta-analysis. *American Journal of Epidemiology*. 164, pp.101-109.
- Westerlund, A., Hujanen, E., Höyhty, M., Puistola, U. and Turpeenniemi-Hujanen, T. 1997. Ovarian cancer cell invasion is inhibited by paclitaxel. *Clinical & Experimental Metastasis*. 15, pp.318-328.
- White, E.A., Kenny, H.A. and Lengyel, E. 2014. Three-dimensional modeling of ovarian cancer. *Advanced Drug Delivery Reviews*. 79-80, pp.184-92.
- Whittmore, A.S., Harris, R., Itnyre, J. 1992. Characteristics relating to ovarian cancer risk: collaborative analysis of 12 US case-control studies: II. Invasive epithelial ovarian cancers in white women. Collaborative Ovarian Cancer Group. *American Journal of Epidemiology*. **136**(10), pp.1184-1203.
- Wiggins, A.J., Cass, G.K., Bryant, A., Lawrie, T.A. and Morrison, J. 2015. Poly (ADP-ribose) polymerase (PARP) inhibitors for the treatment of ovarian cancer. *Cochrane Database of Systematic Reviews* (5).
- Wilhelm, O., Hafter, R., Copenrath, E., Pflanz, M., Schmitt, M., Babic, R., Linke, R., Gössner, W. and Graeff, H. 1988. Fibrin-fibronectin compounds in human ovarian tumor ascites and their possible relation to the tumor stroma. *Cancer Research*. 48, pp.3507-3514.
- Wilkinson, N., Vroobel, K. and McCluggage, W. 2019. Dataset for histopathological reporting of carcinomas and borderline tumours of the ovaries, fallopian tubes and peritoneum, G079. *Cancer Datasets and Tissue Pathways*. The Royal College of Pathologists website [Online]. [Accessed 15th April 2021]. Available from: <https://www.rcpath.org/profession/guidelines/cancer-datasets-and-tissue-pathways.html>.
- Winter, W.E., 3rd, Maxwell, G.L., Tian, C., Sundborg, M.J., Rose, G.S., Rose, P.G., Rubin, S.C., Muggia, F. and Mcguire, W.P. 2008. Tumor residual after surgical cytoreduction in prediction of clinical outcome in stage IV epithelial ovarian cancer: a Gynecologic Oncology Group Study. *Journal of Clinical Oncology*. 26, pp.83-89.
- Winter-Roach, B.A., Kitchener, H.C. and Dickinson, H.O. 2009. Adjuvant (post-surgery) chemotherapy for early stage epithelial ovarian cancer. *Cochrane Database of Systematic Reviews*. Cd004706.
- Winter-Roach, B.A., Kitchener, H.C. and Lawrie, T.A. 2012. Adjuvant (post-surgery) chemotherapy for early stage epithelial ovarian cancer. *Cochrane Database of Systematic Reviews*. 3, Cd004706.

- Wisén, O. and Gardlund, B. 1988. Hemostasis in Crohn's disease: low factor XIII levels in active disease. *Scandinavian Journal of Gastroenterology*. 23, pp.961-966.
- Wojtukiewicz, M.Z., Rucinska, M., Zacharski, L.R., Kozłowski, L., Zimnoch, L., Piotrowski, Z., Kudryk, B.J. and Kisiel, W. 2001. Localization of blood coagulation factors in situ in pancreatic carcinoma. *Thrombosis and Haemostasis*. 86, pp.1416-1420.
- Wojtukiewicz, M.Z., Zacharski, L.R., Memoli, V.A., Kisiel, W., Kudryk, B.J., Rousseau, S.M. and Stump, D.C. 1990. Malignant melanoma: interaction with coagulation and fibrinolysis pathways in situ. *American Journal of Clinical Pathology*. 93, pp.516-521.
- Wu, J., Fu, Z., Liu, G., Xu, P., Xu, J. and Jia, X. 2017. Clinical significance of plasma D-dimer in ovarian cancer: a meta-analysis. *Medicine*. 96.
- Wu, X., Xue, X., Tang, J., Cheng, X., Tian, W., Jiang, R. and Zang, R. 2013. Evaluation of risk factors for venous thromboembolism in Chinese women with epithelial ovarian cancer. *International Journal of Gynecologic Cancer*. 23.
- Xu, L., He, F., Wang, H., Gao, B., Wu, H. and Zhao, S. 2017. A high plasma D-dimer level predicts poor prognosis in gynecological tumors in East Asia area: a systematic review and meta-analysis. *Oncotarget*. 8, 51551.
- Yamada, Y., Kawaguchi, R., Iwai, K., Niino, E., Morioka, S., Tanase, Y. and Kobayashi, H. 2020. Preoperative plasma D-dimer level is a useful prognostic marker in ovarian cancer. *Journal of Obstetrics and Gynaecology*. 40, pp.102-106.
- Yang, J., Mcnamara, L.E., Gadegaard, N., Alakpa, E.V., Burgess, K.V., Meek, R.D. and Dalby, M.J. 2014. Nanotopographical induction of osteogenesis through adhesion, bone morphogenic protein cosignaling, and regulation of micRNAs. *ACS Nano*. 8, pp.9941-9953.
- Yang, Y., Yang, Y., Yang, J., Zhao, X. and Wei, X. 2020. Tumor microenvironment in ovarian cancer: function and therapeutic strategy. *Frontiers in Cell and Developmental Biology*. 8, 758.
- Yazdian, M., Ataseven, B., Schneider, S., Baert, T., Bommert, M., Traut, A., Du Bois, A. and Harter, P. 2020. The role of factor (f) XIII in patients with advanced epithelial ovarian cancer (EOC) FIGO III/IV. *Geburtshilfe und Frauenheilkunde*. 80, P373.
- Yee, V.C., Le Trong, I., Bishop, P.D., Pedersen, L.C., Stenkamp, R.E. and Teller, D.C. 1996. Structure and function studies of factor xiiiA by x-ray crystallography. *Seminars in Thrombosis and Haemostasis*. 22, pp.377-384.
- Yee, V.C., Pedersen, L.C., Le Trong, I., Bishop, P.D., Stenkamp, R.E. and Teller, D.C. 1994. Three-dimensional structure of a transglutaminase: human blood coagulation factor XIII. *Proceedings of the National Academy of Sciences of the United States of America*. 91, pp.7296-7300.

- Yorifuji, H., Anderson, K., Lynch, G.W., Van De Water, L. and McDonagh, J. 1988. B protein of factor XIII: differentiation between free B and complexed B. *Blood*. **72**(5), pp.1645-50.
- Yousif, N.G. 2014. Fibronectin promotes migration and invasion of ovarian cancer cells through up-regulation of FAK–PI 3 K/A kt pathway. *Cell Biology International*. **38**, pp.85-91.
- Zand, L., Feng, Q., Roskelley, C.D., Leung, P.C. and Auersperg, N. 2003. Differential effects of cellular fibronectin and plasma fibronectin on ovarian cancer cell adhesion, migration, and invasion. *In Vitro Cellular & Developmental Biology-Animal*. **39**, pp.178-182.
- Zhang, Q., Wang, C. and Cliby, W.A. 2019. Cancer-associated stroma significantly contributes to the mesenchymal subtype signature of serous ovarian cancer. *Gynecologic Oncology*. **152**, pp.368-374.
- Zhang, Y., Cao, L., Nguyen, D. and Lu, H. 2016. TP53 mutations in epithelial ovarian cancer. *Translational Cancer Research*. **5**(6), pp.639-649.
- Zheng, H. and Gao, Y.N. 2012. Primary debulking surgery or neoadjuvant chemotherapy followed by interval debulking surgery for patients with advanced ovarian cancer. *Chinese Journal of Cancer Research*. **24**, pp.304-309.